

**ASSESSMENT OF NITROGEN CYCLE PATHWAYS ASSOCIATED WITH
DIFFERENT MAJOR BENTHIC ORGANISMS IN RESPONSE TO
ENVIRONMENTAL CHANGES**

A dissertation by

Yusuf C. El-Khaled

Assessment of nitrogen cycle pathways associated with different major benthic organisms in response to environmental changes

Doctoral Thesis by

Yusuf C. El-Khaled

For the attainment of the academic degree of

Doktor der Naturwissenschaften

– Dr. rer. nat. –

Submitted to the Department of Biology and Chemistry

at the University of Bremen

in March 2021

supervised by Prof. Dr. Christian Wild

Date of Defence: 12.05.2021

Reviewer 1: Prof. Dr. Christian Wild

Reviewer 2: Prof. Dr. Christian R. Voolstra

The present work was carried out from May 2017 until March 2021 at the Center of Environmental Research and Sustainable Technology (UFT), University of Bremen, Germany

The work was financed by the German Research Foundation (DFG, Wi 2677/9-1) and baseline funds from the King Abdullah University of Science and Technology, Thuwal, Saudi Arabia



جامعة الملك عبد الله
للعلوم والتقنية
King Abdullah University of
Science and Technology



Zentrum für
Umweltforschung &
nachhaltige Technologien



DFG
Deutsche
Forschungsgemeinschaft

Dedicated to my mother Ursula

and my brother Ya'qub Yonas

*“Ich vergesse nie die Tage
Da draußen auf dem Meer
Ungewiss und ohne Schlaf
Das hast du nicht verdient
Ich vergesse nie die Tage
Da draußen auf dem Meer
Du warst so oft für mich da
Jetzt bin ich für dich hier“*

– FSF

Abstract

Tropical coral reefs are hotspots of biodiversity, provide important ecosystem services and belong to the most productive ecosystems on earth, although they flourish in oligotrophic, i.e., nutrient-poor waters where nitrogen (N) is scarce. As such, efficient uptake, recycling and removal mechanisms of N by coral reef organisms and substrates, including the key reef ecosystem engineers, the hard corals, are of paramount importance. However, a holistic understanding of microbially performed N cycling is still missing. Previous studies have demonstrated that microbes capable of fixing atmospheric dinitrogen (N₂; diazotrophs) provide bioavailable N to the coral reef organisms. Hypothesised counteracting N-removing mechanisms like denitrification, hence, may help to maintain low N conditions, and ultimately coral (reef) functioning. Hence, N availability in coral reef environments is partly a consequence of the interplay between N₂ fixation and denitrification, but knowledge particularly on denitrification is missing. As coral reefs and their functioning are adapted to oligotrophic environments, environmental alterations such as eutrophication could potentially evoke ecosystem responses, and subsequently, directly affect biogeochemical pathways.

The present thesis aims to extend current knowledge on biogeochemical cycling of N in coral reefs by targeting the following research goals: i) developing a new method to simultaneously determine N₂ fixation and denitrification and quantifying N fluxes *in* and *ex situ*; ii) assessing baseline rates of N₂ fixation and denitrification for major functional groups and assessing their relative importance in intact coral- and degraded algae-dominated reef communities; and iii) investigating the effects of short- and long-term eutrophication on both aforementioned N cycling pathways. Hypothetically, similar to N₂ fixation, denitrification is an active microbially performed N cycling pathway in coral reef organisms and substrates, with eutrophication evoking suppressing and stimulating responses, respectively, of N₂ fixation and denitrification activity. The experimental work consisted of a combination of physiological and molecular tools and was carried out *in situ* and *ex situ* at the central Red Sea.

Methods established during the present dissertation allow the simultaneous quantification of N₂ fixation and denitrification by combining commonly applied acetylene-based incubation methods. Further, community-wide N fluxes were also quantified *in situ* using benthic incubation chambers. Findings of the present thesis reveal that denitrification, like N₂ fixation, is an active pathway in all investigated coral reef substrates and organisms. On an ecosystem level, important N₂ fixers such as turf algae and coral rubble exhibit ~100-fold higher N₂ fixation rates compared to corals, but these substrates are less involved in processing nitrogenous compounds via denitrification. On the other hand, soft corals show 2- to 4-fold higher denitrification rates than turf algae or coral rubble and can thus be characterised as key denitrifiers in reef environments. Extrapolated to coral- and algae-dominated reef areas, turf algae and coral rubble contribute to > 90 % of fixed N in both reef areas, whereas > 50 % of total denitrification was performed by corals in degraded reef areas. *In situ* long-term (8 weeks) eutrophication experiment stimulated both N₂ fixation and denitrification in turf algae, a hard coral and reef sands. Further, a substrate-specific and nutrient concentration-dependant threshold that modulates N₂ fixation and denitrification in coral rubble was observed, as rapid responses in N cycling activities were observed.

In conclusion, using the newly established methods during the thesis, denitrification was identified as an actively performed pathway in coral reef environments. Interestingly and against hypothesis, the effects of eutrophication on N cycling pathways are divergent, with both suppressing and stimulating effects on N_2 fixation and denitrification. Altogether, higher N availability in algae-dominated reefs through high amounts of N_2 fixation may facilitate higher growth rates of reef algae, ultimately resulting in a positive feedback loop (on the budget of bioavailable N), particularly under moderately and realistic nutrient-enriched scenarios. In contrast, coral rubble may inhibit a key role under very eutrophic conditions, as an N-dependant threshold was identified that stimulates denitrification and suppresses N_2 fixation. As such, coral rubble might alleviate excess N from coral reefs via processing N via denitrification. In how far divergent responses of N_2 fixation and denitrification to eutrophication might be further suppressed, counteracted or stimulated due to further anthropogenic stressors such as ocean warming remains to be targeted in future studies. Based on the findings here, future management efforts should ultimately focus on the prevention of local N eutrophication.

Zusammenfassung

Tropische Korallenriffe bieten eine Reihe von wichtigen Ökosystemleistungen. Obwohl sie in oligotrophen, also nährstoffarmen Gewässern vorkommen, in denen gerade Stickstoff (N) rar ist, zählen sie zu den produktivsten Ökosystemen der Erde. Für diese Produktivität sind Mechanismen zentral, die die effiziente Aufnahme, das Recycling und das Entfernen des Ns einzelner Korallenrifforganismen – hierzu zählen unter anderem die Hauptökosystemingenieure ‚Hartkorallen‘ – umsetzen und gewährleisten können. Umfassendes Wissen über den mikrobiellen Stickstoffkreislauf ist jedoch nicht vorhanden. Bisherige Studien haben gezeigt, dass spezielle Mikroben, sog. Diazotrophen, in der Lage sind, atmosphärischen Stickstoff zu fixieren und für weitere Korallenrifforganismen verfügbar zu machen. Vermutete, gegenläufig agierende Prozesse des N-Kreislaufes wie die Denitrifikation könnten dazu beitragen, N aus dem System zu entfernen und so geringe, bevorzugte N-Verfügbarkeit zu gewährleisten. Folglich ist die N-Verfügbarkeit in Korallenriffökosystemen das Resultat des Zusammenspiels von N-Fixierung und Denitrifikation, wobei Wissen und Evidenz speziell über Denitrifikation fehlen. Da Korallenriffe und ihr Funktionieren optimal an nährstoffarme Bedingungen angepasst sind, könnten Umweltveränderungen wie beispielsweise erhöhte Nährstoffeinträge Ökosystemveränderungen hervorrufen und letztlich biogeochemische Prozesse beeinflussen.

Die vorliegende Thesis zielt darauf ab, bestehendes Wissen über biogeochemische Kreisläufe wie den Stickstoffkreislauf in Korallenriffen zu erweitern. Folgende Ziele sind dabei explizit formuliert: i) Simultane Bestimmung von parallel ablaufender N-Fixierung und Denitrifikation sowie das Quantifizieren von N-Prozessen *in* und *ex situ*; ii) Quantifizierung der Basisraten von N-Fixierung und Denitrifikation der Hauptorganismen und –substraten eines Korallenriffs um anhand dessen die relative Wichtigkeit in korallen- und algendominierten Riffbereichen festzulegen; und iii) das Bestimmen der Effekte von Kurz- und Langzeiteutrophierung auf N-Fixierung und Denitrifikation. Mittels einer Kombination aus physiologischen und molekularen Analysewerkzeugen wurden die Effekte von Kurz- und Langzeiteutrophierung auf beide Prozesse in verschiedenen Organismen und Substraten bestimmt. Die experimentelle Arbeit wurde sowohl *in situ* als auch *ex situ* im zentralen Roten Meer durchgeführt.

Die Techniken, die im Rahmen der vorliegenden Dissertation entwickelt wurden, erlauben die zeitgleiche Quantifizierung von N-Fixierung und Denitrifikation. Riffweite Stickstoffflüsse konnten darüber hinaus mit benthischen Kammern *in situ* gemessen werden. Die Ergebnisse der vorliegenden Thesis zeigen, dass Denitrifikation, ähnlich wie die N-Fixierung, ein aktiver Prozess in allen untersuchten Organismen und Substraten ist. Bezogen auf das Ökosystem, weisen Aufwuchsalgen und Korallengeröll ~100x höhere N-Fixierungsraten im Vergleich zu Korallen auf, sind aber gleichzeitig weniger bedeutend im Prozessieren von N via Denitrifikation. Dem stehen Weichkorallen als Hauptdenitrifizierer gegenüber, die zwei- bis vierfach höhere Denitrifikationsraten als Aufwuchsalgen und Korallengeröll aufweisen. Während Aufwuchsalgen und Korallengeröll für > 90 % der N-Fixierung in korallen- und algendominierten Riffbereichen verantwortlich sind, werden > 50% der Gesamtdenitrifikation durch Korallen erzielt. Die Ergebnisse der vorliegenden Arbeit zeigen, dass *in situ* Langzeiteutrophierung (über 8 Wochen) sowohl N-Fixierung als

auch Denitrifikation in Aufwuchsalgen, Hartkorallen und Riffsanden stimuliert. Darüber hinaus wurden direkte Reaktionen von N-Fixierung und Denitrifikation auf Kurzzeiteutrophierung (<12h) in Aufwuchsalgen und Korallengeröll beobachtet. Es konnte gezeigt werden, dass speziell Korallengeröll eine Schlüsselfunktion unter eutrophierten Bedingungen inne haben könnte, da eine N-abhängige Grenze identifiziert werden konnte, die die Denitrifikationsstimulation und N-Fixierungsinaktivität auslöst.

Abschließend lässt sich festhalten, dass anhand der Ergebnisse der vorliegenden Dissertation der Prozess der aktiven ‚Denitrifikation‘ in Korallenriffsystemen identifiziert werden konnte. Weiterhin sind die Effekte von Eutrophierung auf N-Fixierung und Denitrifikation divergent, da sowohl unterdrückende als auch stimulierende Effekte auf beide Prozesse identifiziert worden sind. Alles in allem könnte eine erhöhte N-Fixierung in algendominierten Riffbereichen in einer höheren N-Verfügbarkeit resultieren, die wiederum das Wachstum von Aufwuchsalgen begünstigt. Das ließe sich final als verstärkende Rückkopplungsschleife beschreiben. Diese Schleife ist speziell unter eutrophierten Bedingungen von besonderer Bedeutung, da hierunter sowohl die Stimulation von N-Fixierung als auch Denitrifikation in Aufwuchsalgen, Hartkorallen und Riffsanden beobachtet wurden. Weitere Ergebnisse der vorliegenden Dissertation legen nahe, dass speziell Korallengeröll eine Schlüsselfunktion unter eutrophierten Bedingungen inne haben könnte. Diese Hypothese wird durch eine identifizierte, N-abhängige Grenze gestützt, die die Denitrifikationsstimulation und N-Fixierungsinaktivität auslöst. Sollte diese Grenze überschritten werden, könnte Korallengeröll dazu beitragen, dass überschüssiger N in Korallenriffen über Denitrifikation prozessiert wird. Inwiefern ohnehin schon divergierende Reaktionen von N-Fixierung und Denitrifikation auf Eutrophierung durch weitere Stressoren (z.B. Ozeanerwärmung) verstärkt oder gemildert werden, sollte in zukünftigen Studien untersucht werden. Basierend auf den Ergebnissen der vorliegenden Arbeit sollten zukünftige Managementstrategien darauf abzielen, lokale Eutrophierungsereignisse und -quellen zu verhindern bzw. diese zu regulieren.

Acknowledgements

After completing the present dissertation, I saved this section to be written at the very end. Nevertheless, I am trying to find appropriate words to express my feelings for the people that encouraged me to start, to stand, and finally to finish this journey over the last four years. A whole book that extends the length of this thesis could be written about the importance of all the people I met, worked with and that supported me during my PhD journey.

First off, Christian Wild – thank you for giving me the opportunity to start this research, for believing in me and anticipating outcomes solely a few people believed in. There are many things I have learned from you, most importantly to always look on the bright side of life (and of course that ‘Müller ist Weltklasse’, but that’s another topic). My personal development is, besides the scientific outcomes of the present thesis, the most striking result of the past four years, and it could not have happened without your guidance and your support in every possible way throughout the entire research project.

I would also thank Christian Voolstra for your welcoming and hosting me in Saudi Arabia. I am proud to say that you kicked off my academic and scientific career, and that you allowed me to perform the research that I wanted to do, and to even extend my stay at KAUST despite bureaucratic difficulties. Thank you, Burt Jones, for your support at KAUST as well. I am not exaggerating when I say that the whole PhD thesis would not have been possible without the most amazing team ever (peepz, you know me, I rarely use statements like this...): Flo and Denis, thank you for incubating half of the Abo Shosha reef with me, for your support and for showing how to combine work and passion over the last years. Nils and Claudia, thank you for your inspiration, your patience when taking care of me when I was a klutz at the very start compared to now – how cool is that!? I would like to thank everyone in the former Reef Genomics lab at KAUST, and particularly Håggen and Sabrina, for making me feel welcome, and for making KAUST an unforgettable experience.

I want to express my thanks to my colleagues and friends at the AG Wild from Bremen University. Anna, thanks for being my PhD buddy for more than three years, it leaves a smile on my face when I remember our office talks, shit chats and your support when I was stuck with some statistics. Thank you also, Mr Arjen Tilstra, for being the other half of the nitrogen cycling guys and for your support throughout the last years! I would also explicitly thank Sven Rohde and Ben Kürten for being my mentors within the Glomar programme, for your ideas and feedback during our regular meetings. Thank you, Malik, Simon, Rassil and Nauras for happy chats at work and for your assistance. Finally, a very big thank you goes to Marko Rohlf, Susana Carvalho, Inae Kim-Frommherz and Selma Mezger for agreeing to be panel members for my defence.

My PhD project would not have been the same without the people I met during research stays and conferences. Particularly, thank you Fredi and Felix, Jenny, Rainer and Regina, Andi and Marie for your nice company and for giving me the opportunity to discover new seas abroad...

Die folgenden Worte richten sich an all diejenigen, die über die vergangenen Jahre ein wichtiges Gegengewicht zu meiner Arbeit dargestellt haben. Ohne euch hätte ich diesen Schritt gar nicht erst gewagt, oder wäre nicht an den Punkt gekommen, an dem ich nun stehe. Mein Dank geht an mein Freunde aus meiner Bremer, Oldenburger und niederrheinischen Heimat, ganz besonders an Tammo und Anne (<3), Crison und Sabbel, MaReno, Vanessa und Stievel, die Katzis Joschka und Miriam, Hannes und Clemens, Jänni und Söphiä, Alina, Nico und Peter, Carina, und und und....

Ich möchte mich bei meinen Brüdern Ahmad und Saeed bedanken, dafür, dass ihr die work-life-balance intakt gehalten habt. Danke, dass ihr mich während der letzten Jahre begleitet habt, und dass ihr mich an die positiven Dinge im Leben erinnert habt, als es dringend notwendig war.

أود أن أشكر اشقائي أحمد ملكاوي وسعيد بنا على مساعدتي في الحفاظ على التوازن بين العمل والحياة ، من خلال تسليط الضوء

على الجوانب الإيجابية للحياة عند الضرورة الملحة.

Zu guter Letzt möchte ich meiner Familie danken. Liebe Mama, lieber Ya'qub, liebe Yoshie – ihr habt mich von Anfang bis zum Ende mit Rat, mit teils erhitzten Gemütern, aber stets mit Vertrauen unterstützt und ermutigt. Danke, dass ihr da seid und mich mit eurer Liebe tragt und inspiriert.

Table of contents

V	Abstract
VII	Zusammenfassung
IX	Acknowledgements
XIII	List of publications and manuscripts included in this thesis
XIV	Declaration on the contribution of the candidate to a multi-author article/manuscript which is included as a chapter in the submitted doctoral thesis
17	Chapter 1 General introduction
29	Chapter 2 Simultaneous measurements of dinitrogen fixation and denitrification associated with coral reef substrates: advantages and limitations of a combined acetylene assay
46	Chapter 3 An <i>in situ</i> approach for measuring biogeochemical fluxes in structurally complex benthic communities
70	Chapter 4 Denitrification aligns with N ₂ fixation in Red Sea corals
88	Chapter 5 Relative abundance of nitrogen cycling microbes in coral holobionts reflects environmental nitrate availability
102	Chapter 6 Nitrogen fixation and denitrification activity differ between coral- and algae-dominated Red Sea reefs
130	Chapter 7 Nitrogen eutrophication particularly promotes turf algae in coral reefs of the central Red Sea
152	Chapter 8 <i>In situ</i> eutrophication stimulates dinitrogen fixation and denitrification, and productivity in Red Sea coral reefs
172	Chapter 9 Nutrient pollution enhances productivity and framework dissolution in algae- but not in coral-dominated reef communities
194	Chapter 10 High plasticity of nitrogen fixation and denitrification of common coral reef substrates in response to nitrate availability
210	Chapter 11 General discussion
224	Appendix Supplementary material
225	Supplementary material to Chapter 2
233	Supplementary material to Chapter 3
242	Supplementary material to Chapter 4
248	Supplementary material to Chapter 5
249	Supplementary material to Chapter 6
252	Supplementary material to Chapter 7
254	Supplementary material to Chapter 8

256	Supplementary material to Chapter 9
260	Supplementary material to Chapter 10
262	Versicherung an Eides Statt

List of publications and manuscripts included in this thesis

- El-Khaled YC**, Roth F, Rådecker N, Kharbatia N, Jones BH, Voolstra CR, Wild C (2020) Simultaneous measurements of dinitrogen fixation and denitrification associated with coral reef substrates: advantages and limitations of a combined acetylene assay. *Frontiers in Marine Science* 7: 411. DOI: 10.3389/fmars.2020.00411
- El-Khaled YC**, Roth F, Tilstra A, Rådecker N, Karcher DB, Kürten B, Jones BH, Voolstra CR, Wild C (2020) *In situ* eutrophication stimulates dinitrogen fixation and denitrification, and productivity in Red Sea coral reefs. *Marine Ecology Progress Series* 645: 55-66. DOI: 10.3354/meps13352
- El-Khaled YC**, Roth F, Rådecker N, Tilstra A, Karcher DB, Kürten B, Jones BH, Voolstra CR, Wild C (in review) Nitrogen fixation and denitrification activity differ between coral- and algae-dominated Red Sea reefs. *Scientific Reports*
- El-Khaled YC**, Nafeh R, Roth F, Rådecker N, Karcher DB, Jones BH, Voolstra CR, Wild C (in review) High plasticity of nitrogen fixation and denitrification of common coral reef substrates in response to nitrate availability. *Marine Pollution Bulletin*
- Tilstra A, **El-Khaled YC**, Roth F, Rådecker N, Pogoreutz C, Voolstra CR, Wild C (2019) Denitrification aligns with N₂ fixation in Red Sea corals. *Scientific Reports* 9: 19460. DOI: 10.1038/s41598-019-55408-z
- Roth F, Wild C, Carvalho S, Rådecker N, Voolstra CR, Kürten B, Anlauf H, **El-Khaled YC**, Carolan R, Jones BH (2019) An *in situ* approach for measuring biogeochemical fluxes in structurally complex benthic communities. *Methods in Ecology and Evolution* 10 (5): 712-725. DOI: 10.1111/1365-2435.13625
- Karcher DB, Roth F, Carvalho S, **El-Khaled YC**, Tilstra A, Kürten B, Struck U, Jones BH, Wild C (2020) Nitrogen eutrophication particularly promotes turf algae in coral reefs of the central Red Sea. *PeerJ* 8: e8737. DOI: 10.7717/peerj.8737
- Tilstra A, Roth F, **El-Khaled YC**, Pogoreutz C, Rådecker N, Voolstra CR, Wild C (in review) Relative abundance of nitrogen cycling microbes in coral holobionts reflects environmental nitrate availability. *Royal Society Open Science*
- Roth F, **El-Khaled YC**, Karcher DB, Rådecker N, Carvalho S, Duarte CM, Silva L, Calleja MLL, Moran XAG, Jones BH, Voolstra CR, Wild (in review) Nutrient pollution enhances productivity and framework dissolution in algae- but not in coral-dominated reef communities. *Marine Pollution Bulletin*

Declaration on the contribution of the candidate to a multi-author article/manuscript which is included as a chapter in the submitted doctoral thesis

Contribution of the candidate is given in % of the total work load (up to 100 % for each category)

Chapter 2 | Simultaneous measurements of dinitrogen fixation and denitrification associated with coral reef substrates: advantages and limitations of a combined acetylene assay

Experimental concept and design	100 %
Experimental work and/or acquisition of (experimental data)	100 %
Data analysis and interpretation	75 %
Preparation of figures and tables	100 %
Drafting of the manuscript	75 %

Chapter 3 | An *in situ* approach for measuring biogeochemical fluxes in structurally complex benthic communities

Experimental concept and design	0 %
Experimental work and/or acquisition of (experimental data)	10 %
Data analysis and interpretation	5 %
Preparation of figures and tables	0 %
Drafting of the manuscript	5 %

Chapter 4 | Denitrification aligns with N₂ fixation in Red Sea corals

Experimental concept and design	50 %
Experimental work and/or acquisition of (experimental data)	75 %
Data analysis and interpretation	25 %
Preparation of figures and tables	10 %
Drafting of the manuscript	10 %

Chapter 5 | Relative abundance of nitrogen cycling microbes in coral holobionts reflects environmental nitrate availability

Experimental concept and design	0 %
Experimental work and/or acquisition of (experimental data)	0 %
Data analysis and interpretation	15 %
Preparation of figures and tables	0 %
Drafting of the manuscript	10 %

Chapter 6 | Nitrogen fixation and denitrification activity differ between coral- and algae-dominated Red Sea reefs

Experimental concept and design	100 %
Experimental work and/or acquisition of (experimental data)	100 %
Data analysis and interpretation	80 %
Preparation of figures and tables	90 %
Drafting of the manuscript	100 %

Chapter 7 | Nitrogen eutrophication particularly promotes turf algae in coral reefs of the central Red Sea

Experimental concept and design	10 %
Experimental work and/or acquisition of (experimental data)	20 %
Data analysis and interpretation	10 %
Preparation of figures and tables	20 %
Drafting of the manuscript	10 %

Chapter 8 | *In situ* eutrophication stimulates dinitrogen fixation and denitrification, and productivity in Red Sea coral reefs

Experimental concept and design	80 %
Experimental work and/or acquisition of (experimental data)	100 %
Data analysis and interpretation	100 %
Preparation of figures and tables	95 %
Drafting of the manuscript	100 %

Chapter 9 | Nutrient pollution enhances productivity and framework dissolution in algae- but not in coral-dominated reef communities

Experimental concept and design	30 %
Experimental work and/or acquisition of (experimental data)	30 %
Data analysis and interpretation	50 %
Preparation of figures and tables	5 %
Drafting of the manuscript	20 %

Chapter 10 | High plasticity of nitrogen fixation and denitrification of common coral reef substrates in response to nitrate availability

Experimental concept and design	100 %
Experimental work and/or acquisition of (experimental data)	100 %
Data analysis and interpretation	100 %
Preparation of figures and tables	100 %
Drafting of the manuscript	75 %

Date:

Signature:

Chapter 1

Chapter 1 | General introduction

Yusuf C. El-Khaled^{1*}

¹ Marine Ecology Department, Faculty of Biology and Chemistry, University of Bremen, Germany

*Corresponding author: yek2012@uni-bremen.de

Keywords: Coral Reefs | Nitrogen cycling | Dinitrogen Fixation | Denitrification | Eutrophication

1.1 | Coral Reefs and Nitrogen Cycling

At large, nitrogen (N) is vital for all living organisms and is required for primary production and the production of biomass. Among the key elements required for life (i.e., N, carbon (C), phosphorus, oxygen, and sulphur)¹, N has the greatest total abundance in the environment². Ironically, it is the least accessible for flora and fauna¹. In oligotrophic marine ecosystems such as intact coral reefs, primary production is limited by low amounts of bioavailable N³⁻⁵. Albeit flourishing in nutrient poor, i.e., oligotrophic environments⁶, coral reefs are one of the most diverse and productive ecosystems on the planet. This phenomenon is known as the Darwin's paradox in honour of its first observer⁷. Their extraordinary productivity, thus, relies on the efficient acquisition, retention and disposal of key nutrients; the enigma of high productivity in oligotrophic environments can be explained by the efficient use of available nutrients by coral reef inhabiting organisms and substrates, including their primary ecosystem engineers, the scleractinian corals. The latter build up calcium carbonate skeletons – the main reef framework, which harbours a high biodiversity that contributes to a range of economic and ecological ecosystem services^{8,9}. Scleractinian corals are considered as meta-organisms consisting of the coral host and a wide spectrum of eukaryotic and prokaryotic microorganisms¹⁰, and their formation is commonly termed 'coral holobiont'. These microorganisms, particularly the photosynthetic dinoflagellates of the family Symbiodiniaceae, play an

Box 1 – Dinitrogen Fixation and Denitrification

Dinitrogen (N₂) fixation is the microbially (via diazotrophs) performed conversion of atmospheric N₂ into bioavailable ammonium (NH₄) through the nitrogenase enzyme complex. **Denitrification** is the anaerobic reduction of nitrate and nitrite into atmospheric N₂, including multiple oxidised intermediates such as nitrous oxide, and can be thus considered as an antagonistic pathway to N₂ fixation. Both pathways may be shaped by abiotic parameters: for example, the presence or absence of oxygen may deactivate or activate the dinitrogenase reductase. Further, the availability of bioavailable nitrogen may suppress nitrogenase activity, but stimulate denitrifier activity⁷¹. Phosphorus availability can be correlated either positively⁷² or negatively with N₂ fixation and denitrification⁷³. Additionally, it has been demonstrated that temperature influences denitrifier abundances^{74,75} and the enzymatic activity of nitrogenase^{37,39,52,76}. Whereas N₂ fixation has been demonstrated for hard⁷⁷⁻⁸⁰ and soft corals⁸¹, turf algae⁵², macroalgae^{82,83}, various reef sediment types⁸⁴, sponges⁵², coral rock⁵², coral rubble⁸⁵, etc., denitrification in coral reef environments remained largely untargeted^{20,21,53,55,56,86,87}. Methods to measure both pathways are commonly based on either physiological (e.g., acetylene assays, labelled isotopes)⁸⁸⁻⁹¹ or molecular approaches (e.g., quantification of functional marker genes)^{53,92}.

essential role in providing the coral host with C-rich photosynthates^{11,12}. Translocated photosynthates require additional N supplementation to sustain metabolism and growth¹³, and can a) satisfy the coral hosts' C demand of up to 95 %¹⁴ and b) be used by heterotrophic prokaryotes¹⁵. The relationship between coral hosts and its associated microbes is mutualistic, as C dioxide in return is translocated to the algal symbionts. Further nutrients, such as N or phosphorus, can be acquired via heterotrophic feeding, by an uptake from the water column or/and internal recycling processes^{16,17}. In this context, microbially performed N cycling plays a key role¹⁸: prokaryotic dinitrogen (N₂) fixers (see Box 1) associated with corals and further coral reef organisms, provide *de novo* bioavailable N by converting N₂ into ammonium¹⁹. Biological N₂ fixation can alleviate N limitation for coral reef primary producers¹⁹. One of its antagonistic pathways, i.e., denitrification (see Box 1), may in return remove N in times of high environmental N availability^{20–22}. Coral reefs and their main ecosystem engineers, scleractinian corals, are well adapted to nutrient-poor environments^{12,18}, so that the interplay of both pathways could essentially contribute to maintaining a stable, low N availability and, hence, ecosystem functioning¹⁸.

1.2 | Influence of Environmental Change on Coral Reefs and their N Cycling

Coral reefs have undergone a range of natural disturbances, bleaching events, and crown-of-thorns starfish outbreaks during their geological history²³. Hence, coral reef-associated organisms are adapted to being dynamic, with impacts – at an intermediate level – promoting high species diversity and complexity^{24,25}. However, intensity and frequency of such events has changed, or more precisely: increased. Growing human population, consequently globalisation of markets, congruent developments in agriculture, industries, fisheries and international commerce have lifted the intensity and severity of impacts on a new level²⁶. Due to its main drivers, that aforementioned threats are considered as significant biological and geological forces, the current epoch is termed 'Anthropocene'²⁷.

In the Anthropocene, almost all marine ecosystems worldwide have experienced a range of threats that are relatable to human activities²⁸. These anthropogenic impacts are increasing, *inter alia* due to growing coastal population²⁹. Similarly, coral reefs have been threatened by anthropogenic stressors that can be divided into a) global threats, such as ocean warming and acidification, and b) local threats, such as eutrophication, habitat destruction, sedimentation, and overfishing^{29,30}. Commonly, a combination of global and local threats to coral reefs has ultimately led to rapid decline in live coral cover, with estimations reporting coral cover losses ranging from 30 to 50 % during the 20th century^{31–33}.

Coral reef ecosystems and their functioning rely on a stable, N-limited state^{22,34–36}. However, coral reefs experience seasonal and diel N fluctuations^{37,38}, which potentially shape N₂ fixation activity¹⁹. Further, natural temperature variations may be positively correlated with N₂ fixation potentials^{39–41}, hence increasing corals' N availability with higher water temperature. In how far denitrification, if available in coral reef organisms besides sponges⁴² and marine sediments²⁰, is an active N cycle pathway and functions as a N-relieving mechanism, ultimately maintain a N-limited state in coral reef ecosystems^{22,36}, remains unclear. In the light of climate change, particularly eutrophication, i.e., the introduction of otherwise unavailable N

through agricultural fertiliser runoff, (un-)controlled sewage dumping, aquaculture, etc.^{43,44}, may reshape the biogeochemical cycling in coral reefs. Eutrophication in combination with further stressors, such as prolonged temperature increases, the absence of herbivorous fishes due to overfishing can ultimately lead to phase shifts from intact reefs of hard coral dominance to alternative states of e.g., (macro-) algal dominance^{45–47}. The likelihood of eutrophication events is increasing^{48,49}, however, its effects on coral reef N cycling is largely unknown.

1.3 | Gaps of Knowledge

A holistic understanding of biogeochemical cycles on coral reefs is of paramount interest to understand ecosystem functioning. Whereas N₂ fixation in coral reef organisms and substrates has received much attention in the scientific community over the last decades^{3,19,37,50–52}, knowledge about further N cycling pathways such as denitrification is still in its infancies: denitrification approximations and rates have been demonstrated for biogenic rock^{53,54} and coral reef associated sediments^{20,21,55,56}, but are yet hypothesised for further coral reef organisms and substrates^{57–59}. Furthermore, most studies in the past have focused solely on one of the many N cycling pathways known or on those of similar functionality^{42,56,57,59}, i.e., the reduction to bioavailable N to N₂ by coupled nitrification and denitrification, or from anaerobic ammonium oxidation (ANAMMOX). Antagonistic pathways such as N₂ fixation and denitrification have not been assessed simultaneously for multiple function groups that are associated with coral reefs²⁰. In how far the interplay between these two pathways actually contributes to coral reef ecosystem functioning remains largely untargeted but not of less importance³⁶.

Direct effects of eutrophication on coral reefs and their N cycling have largely been hypothesised^{22,34} or solely demonstrated for coral reef patches²¹, however, ecosystem or multiple organism N flux responses, covering the most dominant benthic functional groups of a common coral reef, have not been investigated yet. Current knowledge is mainly based on a long-term manipulation study in the Great Barrier Reef, where Koop et al. (2001)²¹ reported consistently suppressed N₂ fixation activities and concurrent higher denitrification rates in reef patches under elevated nutrient availability. Nutrient addition resulted in N concentrations far above ambient concentrations (up to 39 µM N) that do not mimic expectable N concentrations associated with eutrophication events^{60–62}. In how far ‘more realistic’ eutrophication scenarios (i.e., lower nutrient concentrations) evoke i) similar or differing N flux responses, ii) differ between coral reef associated functional groups and iii) time-scale depending (short- vs long-term responses) remains to be determined.

Aforementioned shifts in benthic cover from predominantly hard coral cover to (macro-)algae dominance have been observed, described and investigated previously. Although the effects of these phase-shifts on ecosystem services^{8,63–66} and functioning^{67,68} received some attention, Williams & Graham (2019)⁶⁹ emphasise the dimensions of our yet rudimentary understanding of alterations in coral reef functional ecology. Missing knowledge about organism- and substrate-specific denitrification activities, investigations

determining the quantitative and qualitative differences between coral- and algae-dominated reefs regarding their N cycling processes are missing.

1.4 | Aims and Approach

Aims

N is of paramount importance for the functioning of coral reef ecosystems. It is, thus, of particular interest to study biogeochemical fluxes that contribute to the acquisition or disposal of nitrogenous compounds to gain a holistic overview of coral reefs and their functioning under ambient conditions. We aimed to assess the effects of an anthropogenic stressor (eutrophication) on N cycling associated with a range of coral reef associated functional groups. We specifically aimed to answer the following research questions:

1. How can N fluxes be determined simultaneously in coral reef environments? What are suitable techniques to address N and oxygen fluxes *in* and *ex situ*?
2. What are the baseline rates of N₂ fixation and denitrification in the major functional groups, and what is their relative importance regarding intact coral- and degraded algae-dominated reef communities?
3. What are the effects of both short- and long-term eutrophication on coral reef associated functional groups? How does eutrophication alter functioning of coral reef communities?

Approach

All experiments were carried out in the central part of the oligotrophic Red Sea, at whose coast the King Abdullah University of Science and Technology (KAUST) is located. The Red Sea is considered as a 'natural laboratory' due to its various environmental gradients that often reach extreme values⁷⁰, allowing us to study the effects of such environmental parameters, such as temperature, light intensity, (in-) organic nutrient availability, on key N cycling processes. Our approach included the physiological quantification of N₂ fixation and denitrification using acetylene assays, *in situ* quantification of biogeochemical fluxes, molecular quantification of diazotrophs and denitrifiers, quantification of C and N content through elemental and stable isotope analysis, measurements of biotic variables such as oxygen fluxes (C fixation), Symbiodiniaceae cell densities/mitotic indices, monitoring environmental parameters (abiotic variables) including water temperature, water depth, light intensity, salinity, pH, chlorophyll α , and (in-)organic nutrients.

1.5 | Thesis structure and outline

This thesis is composed of 11 chapters with the first and last chapter acting as a general introduction and discussion, respectively. The nine chapters in between consist of already published or submitted manuscripts, and of manuscripts that are intended for publication. All manuscripts included in this thesis contribute to the understanding of N cycling in coral reef environments and address the effects of

environmental change, both natural and anthropogenic, on N₂ fixation and denitrification for a vast range of functional groups associated with coral reefs. More specifically, these nine chapters can be separated into three sections, as follows:

Section 1: Underlying methodology to assess dinitrogen fixation, denitrification and primary productivity

In [Chapter 2](#) we establish a technique that allows the simultaneous quantification of two counteracting N cycle pathways in coral reef environments. This acetylene-based approach consists of a combination of acetylene reduction and acetylene blockage assays, and is utilised to determine both N₂ fixation and denitrification for two coral reef substrates. Its advantages as well as limitations are emphasised in this chapter. [Chapter 3](#) is a protocol to build and use non-invasive, cost-efficient and easy to handle *in situ* incubation chambers that provide reproducible measurements of biogeochemical processes in simple and structurally complex benthic shallow-water communities. These incubation chambers are used to estimate community budgets of photosynthesis and respiration by corals, rock with algae, and carbonate reef sands, which are subsequently compared to budgets extrapolated from conventional *ex situ* single-organism incubations.

Section 2: N₂ fixation and denitrification in current and future coral reef environments

In [Chapter 4](#), denitrification associated with three coral species using molecular and physiological tools was assessed. Here, molecularly obtained results for denitrification matched those of actual denitrification rates that are quantified physiologically. Additionally, other coral associated variables are measured to assess potential relationships with both denitrification and N₂ fixation. In [Chapter 5](#), denitrification in relation to diazotrophy for two Red Sea hard corals is investigated in a seasonal resolution, for which a range of abiotic and biotic variables are monitored. Observed seasonal patterns in denitrification are then related to environmental data. Denitrification in hard corals is just the starting point for a general overview of both N₂ fixation and denitrification in coral reef environments. [Chapter 6](#) provides a holistic overview of N₂ fixation and denitrification activities for the most abundant functional groups of a Red Sea coral reef. Subsequently, benthic cover data is used to extrapolate respective N fluxes to two coral reef scenarios, i.e., a) of coral dominance and b) of algae dominance.

Section 3: Effects of Eutrophication on N₂ fixation and denitrification

To go beyond baseline N cycle assessments (Section 2), a long-term (i.e., 8 weeks) *in situ* eutrophication experiment in a Red Sea coral reef is performed. For this, dissolved inorganic nitrogen concentrations are increased up to 7-fold compared to ambient conditions. In [Chapter 7](#), we examine C and N content of four functional groups (i.e., hard and soft corals, turf algae and reef sediments) using elemental and stable isotope

analyses to assess whether the nitrogen additions to the reef were incorporated into the functional group. In a parallel study (Chapter 8), the effects of *in situ* eutrophication on N₂ fixation and denitrification associated with three functional groups (hard corals, turf algae, and reef sediments) are investigated. Additionally, oxygen fluxes are measured to assess potential relationships with the aforementioned N cycling pathways. We use the *in situ* experiment to address the effect of eutrophication on a range of community-wide biogeochemical functions of intact coral- and degraded algae-dominated reef communities (Chapter 9). Whereas Chapter 7-9 focus on the effect of long-term eutrophication, knowledge about short-term responses of N fluxes is scarce. To this end, we perform a series of short-term incubations with four different nutrient concentrations (i.e., ambient, 1 μM, 5 μM and 10 μM nitrate addition) to investigate the plasticity of N₂ fixation and denitrification in two different coral reef substrates (Chapter 10). Additionally, incubations are performed using different light settings investigating the effect of light and darkness (and hence, oxygen availability and scarcity, respectively) on the aforementioned N cycle fluxes.

1.7 References

1. Galloway, J. N. *et al.* The Nitrogen Cascade. *Bioscience* **53**, 341–356 (2003).
2. Mackenzie, F. T. *Our Changing Planet: An Introduction to Earth System Science and Global Environmental Change*. (1998).
3. Webb, K. L., DuPaul, W. D., Wiebe, W., Sottile, W. & Johannes, R. E. Enewetak (Eniwetok) Atoll: Aspects of the nitrogen cycle on a coral reef. *Limnol. Oceanogr.* **20**, 198–210 (1975).
4. Vitousek, P. M. & Howarth, R. W. Nitrogen limitation on land and in the sea: How can it occur? *Biogeochemistry* **13**, 87–115 (1991).
5. Lesser, M. P. *et al.* Nitrogen fixation by symbiotic cyanobacteria provides a source of nitrogen for the scleractinian coral *Montastraea cavernosa*. *Mar. Ecol. Prog. Ser.* **346**, 143–152 (2007).
6. Odum, H. T. & Odum, E. P. Trophic Structure and Productivity of a Windward Coral Reef Community on Eniwetok Atoll. *Ecol. Monogr.* **25**, 291–320 (1955).
7. Darwin, C. The structure and distribution of coral reefs. in *Smith, Elder* (1842).
8. Moberg, F. & Folke, C. Ecological goods and services of coral reef ecosystems. *Ecol. Econ.* **29**, 215–233 (1999).
9. Wild, C. *et al.* Climate change impedes scleractinian corals as primary reef ecosystem engineers. *Mar. Freshw. Res.* **62**, 205–215 (2011).
10. Rohwer, F., Seguritan, V., Azam, F. & Knowlton, N. Diversity and distribution of coral-associated bacteria. *Mar. Ecol. Prog. Ser.* **243**, 1–10 (2002).
11. Edmunds, P. J. & Spencer Davies, P. An energy budget for *Porites porites* (Scleractinia), growing in a stressed environment. *Coral Reefs* **8**, 37–43 (1989).
12. Muscatine, L. & Porter, J. W. Reef Corals: Mutualistic Symbioses Adapted to Nutrient-Poor Environments. *Bioscience* **27**, 454–460 (1977).
13. Falkowski, P. G., Dubinsky, Z., Muscatine, L. & Porter, J. W. Light and the Bioenergetics of a Symbiotic Coral. *Bioscience* **34**, 705–709 (1984).
14. Muscatine, L. The role of symbiotic algae in carbon and energy flux in coral reefs. in *Coral Reefs* (ed. Dubinsky, Z.) 75–87 (1990).
15. Ferrier-Pagès, C., Gattuso, J. P., Cauwet, G., Jaubert, J. & Allemand, D. Release of dissolved organic carbon and nitrogen by the zooxanthellate coral *Galaxea fascicularis*. *Mar. Ecol. Prog. Ser.* **172**, 265–274 (1998).
16. Muscatine, L. *et al.* Cell-specific density of symbiotic dinoflagellates in tropical anthozoans. *Coral Reefs* **17**, 329–337 (1998).
17. Yellowlees, D., Rees, T. A. V. & Leggat, W. Metabolic interactions between algal symbionts and invertebrate hosts. *Plant, Cell Environ.* **31**, 679–694 (2008).
18. O’Neil, J. M. & Capone, D. G. Nitrogen Cycling in Coral Reef Environments. in *Nitrogen in the Marine Environment* 949–989 (2008). doi:10.1016/B978-0-12-372522-6.00021-9
19. Cardini, U. *et al.* Budget of Primary Production and Dinitrogen Fixation in a Highly Seasonal Red Sea Coral Reef. *Ecosystems* **19**, 771–785 (2016).
20. Capone, D. G., Dunham, S. E., Horrigan, S. G. & Duguay, L. E. Microbial nitrogen transformations in unconsolidated coral reef sediments. *Mar. Ecol. Prog. Ser.* **80**, 75–88 (1992).
21. Koop, K. *et al.* ENCORE: The effect of nutrient enrichment on coral reefs. Synthesis of results and conclusions. *Mar. Pollut. Bull.* **42**, 91–120 (2001).
22. Rådecker, N., Pogoreutz, C., Voolstra, C. R., Wiedenmann, J. & Wild, C. Nitrogen cycling in

- corals: The key to understanding holobiont functioning? *Trends Microbiol.* **23**, 490–497 (2015).
23. Hughes, T. P. & Connell, J. H. Multiple stressors on coral reefs: A long-term perspective. *Limnol. Oceanogr.* **44**, 932–940 (1999).
 24. Connell, J. H. Diversity in tropical rain forests and coral reefs. *Science (80-.)*. **199**, 1302–1310 (1978).
 25. Glynn, P. W. Coral reef bleaching: ecological perspectives. *Coral Reefs* **12**, 1–17 (1993).
 26. Vitousek, P. M. *et al.* Human alteration of the global nitrogen cycle: sources and consequences. *Ecol. Appl.* **7**, 737–750 (1997).
 27. Crutzen, P. J. The ‘Anthropocene’. *Earth Syst. Sci. Anthr.* 13–18 (2006). doi:10.1007/3-540-26590-2_3
 28. Halpern, B. S., Selkoe, K. A., Micheli, F. & Kappel, C. V. Evaluating and ranking the vulnerability of global marine ecosystems to anthropogenic threats. *Conserv. Biol.* **21**, 1301–1315 (2007).
 29. Burke, L., Reytar, K., Spaulding, M. & Perry, A. *Reefs at Risk*. (World Resources Institute, 2011).
 30. Hughes, T. P. *et al.* Climate change, human impacts, and the resilience of coral reefs. *Science* **301**, 929–33 (2003).
 31. Gardner, T. A., Côté, I. M., Gill, J. A., Grant, A. & Watkinson, A. R. Long-term region-wide declines in Caribbean corals. *Science (80-.)*. **301**, 958–960 (2003).
 32. Pandolfi, J. M. *et al.* Global trajectories of the long-term decline of coral reef ecosystems. *Science (80-.)*. **301**, 955–958 (2003).
 33. Carpenter, K. E. *et al.* One-Third of Reef-Building Corals Face Elevated Extinction Risk from Climate Change and Local Impacts. *Science (80-.)*. **321**, 560–563 (2008).
 34. Wiedenmann, J. *et al.* Nutrient enrichment can increase the susceptibility of reef corals to bleaching. *Nat. Clim. Chang.* **3**, 160–164 (2013).
 35. Lapointe, B. E., Brewton, R. A., Herren, L. W., Porter, J. W. & Hu, C. *Nitrogen enrichment, altered stoichiometry, and coral reef decline at Looe Key, Florida Keys, USA: a 3-decade study*. *Marine Biology* **166**, (Springer Berlin Heidelberg, 2019).
 36. O’Neil, J. M. & Capone, D. G. *Nitrogen Cycling in Coral Reef Environments*. *Nitrogen in the Marine Environment* (2008). doi:10.1016/B978-0-12-372522-6.00021-9
 37. Cardini, U. *et al.* Functional significance of dinitrogen fixation in sustaining coral productivity under oligotrophic conditions. *Proc. R. Soc. B Biol. Sci.* **282**, (2015).
 38. Roth, F. *et al.* Coral reef degradation affects the potential for reef recovery after disturbance. *Mar. Environ. Res.* **142**, 48–58 (2018).
 39. Santos, H. F. *et al.* Climate change affects key nitrogen-fixing bacterial populations on coral reefs. *ISME J.* **8**, 2272–2279 (2014).
 40. Cardini, U. *et al.* Microbial dinitrogen fixation in coral holobionts exposed to thermal stress and bleaching. *Environ. Microbiol.* **18**, 2620–2633 (2016).
 41. Cinner, J. Coral reef livelihoods. *Curr. Opin. Environ. Sustain.* **7**, 65–71 (2014).
 42. Hoffmann, F. *et al.* Complex nitrogen cycling in the sponge *Geodia barretti*. *Environ. Microbiol.* **11**, 2228–2243 (2009).
 43. Lapointe, B. E. Nutrient thresholds for bottom-up control of macroalgal blooms on coral reefs in Jamaica and southeast Florida. *Limnol. Oceanogr.* **42**, 1119–1131 (1997).
 44. McManus, J. W. & Polsenberg, J. F. Coral-algal phase shifts on coral reefs: Ecological and environmental aspects. *Prog. Oceanogr.* **60**, 263–279 (2004).

45. Done, T. J. Phase shifts in coral reef communities and their ecological significance. *Hydrobiologia* **247**, 121–132 (1992).
46. Graham, N. A. J., Jennings, S., MacNeil, M. A., Mouillot, D. & Wilson, S. K. Predicting climate-driven regime shifts versus rebound potential in coral reefs. *Nature* **518**, 94–97 (2015).
47. Norström, A. V., Nyström, M., Lokrantz, J. & Folke, C. Alternative states on coral reefs: Beyond coral-macroalgal phase shifts. *Mar. Ecol. Prog. Ser.* **376**, 293–306 (2009).
48. Szmant, A. M. Nutrient Enrichment on Coral Reefs: Is It a Major Cause of Coral Reef Decline? *Estuaries* **25**, 743–766 (2002).
49. Fabricius, K. E. Effects of terrestrial runoff on the ecology of corals and coral reefs: Review and synthesis. *Mar. Pollut. Bull.* **50**, 125–146 (2005).
50. Wiebe, W. J., Johannes, R. E. & Webb, K. L. Nitrogen fixation in a coral reef community. *Science* **188**, 257–259 (1975).
51. Bednarz, V. N. *et al.* Contrasting seasonal responses in dinitrogen fixation between shallow and deep-water colonies of the model coral *Stylophora pistillata* in the northern Red Sea. *PLoS One* **13**, 1–13 (2018).
52. Rix, L. *et al.* Seasonality in dinitrogen fixation and primary productivity by coral reef framework substrates from the northern Red Sea. *Mar. Ecol. Prog. Ser.* **533**, 79–92 (2015).
53. Yuen, Y. S., Yamazaki, S. S., Nakamura, T., Tokuda, G. & Yamasaki, H. Effects of live rock on the reef-building coral *Acropora digitifera* cultured with high levels of nitrogenous compounds. *Aquac. Eng.* **41**, 35–43 (2009).
54. Li, Y. *et al.* Effects of live rock on removal of dissolved inorganic nitrogen in coral aquaria. *Acta Oceanol. Sin.* **36**, 87–94 (2017).
55. Miyajima, T., Suzumura, M., Umezawa, Y. & Koike, I. Microbiological nitrogen transformation in carbonate sediments of a coral-reef lagoon and associated seagrass beds. *Mar. Ecol. Prog. Ser.* **217**, 273–286 (2001).
56. Erler, D. V., Trott, L. A., Alongi, D. M. & Eyre, B. D. Denitrification, anammox and nitrate reduction in sediments of the southern great barrier reef lagoon. *Mar. Ecol. Prog. Ser.* **478**, 57–70 (2013).
57. Yang, S., Sun, W., Zhang, F. & Li, Z. Phylogenetically Diverse Denitrifying and Ammonia-Oxidizing Bacteria in Corals *Alcyonium gracillimum* and *Tubastraea coccinea*. *Mar. Biotechnol.* **15**, 540–551 (2013).
58. Kimes, N. E., Van Nostrand, J. D., Weil, E., Zhou, J. & Morris, P. J. Microbial functional structure of *Montastraea faveolata*, an important Caribbean reef-building coral, differs between healthy and yellow-band diseased colonies. *Environ. Microbiol.* **12**, 541–556 (2010).
59. Siboni, N., Ben-Dov, E., Sivan, A. & Kushmaro, A. Global distribution and diversity of coral-associated Archaea and their possible role in the coral holobiont nitrogen cycle. *Environ. Microbiol.* **10**, 2979–2990 (2008).
60. Loya, Y., Lubinevsky, H., Rosenfeld, M. & Kramarsky-Winter, E. Nutrient enrichment caused by in situ fish farms at Eilat, Red Sea is detrimental to coral reproduction. *Mar. Pollut. Bull.* **49**, 344–353 (2004).
61. Peña-García, D., Ladwig, N., Turki, A. J. & Mudarris, M. S. Input and dispersion of nutrients from the Jeddah Metropolitan Area, Red Sea. *Mar. Pollut. Bull.* **80**, 41–51 (2014).
62. den Haan, J. *et al.* Nitrogen and phosphorus uptake rates of different species from a coral reef community after a nutrient pulse. *Sci. Rep.* **6**, 28821 (2016).
63. White, A. T., Vogt, H. P. & Arin, T. Philippine coral reefs under threat: The economic losses

- caused by reef destruction. *Mar. Pollut. Bull.* **40**, 598–605 (2000).
64. McClanahan, T. R., Hicks, C. C. & Darling, E. S. Malthusian overfishing and efforts to overcome it on Kenyan coral reefs. *Ecol. Appl.* **18**, 1516–1529 (2008).
 65. Nyström, M. *et al.* Confronting Feedbacks of Degraded Marine Ecosystems. *Ecosystems* **15**, 695–710 (2012).
 66. Woodhead, A. J., Hicks, C. C., Norström, A. V., Williams, G. J. & Graham, N. A. J. Coral reef ecosystem services in the Anthropocene. *Funct. Ecol.* **33**, 1023–1034 (2019).
 67. McClanahan, T., Polunin, N. & Done, T. Ecological states and the resilience of coral reefs. *Conserv. Ecol.* **6**, (2002).
 68. Munday, P. L. Habitat loss, resource specialization, and extinction on coral reefs. *Glob. Chang. Biol.* **10**, 1642–1647 (2004).
 69. Williams, G. J. & Graham, N. A. J. Rethinking coral reef functional futures. *Funct. Ecol.* **33**, 942–947 (2019).
 70. Voolstra, C. R. & Berumen, M. L. *Coral Reefs of the Red Sea*. *Red Sea* (2019). doi:10.1007/978-3-030-05802-9
 71. Zumft, W. G. Cell biology and Molecular Basis of Denitrification. *Microbiol. Mol. Biol. Rev.* **61**, 533–616 (1997).
 72. Avşar, C. & Aras, E. S. Quantification of denitrifier genes population size and its relationship with environmental factors. *Arch. Microbiol.* **202**, 1181–1192 (2020).
 73. Li, F. *et al.* Distinct distribution patterns of proteobacterial nirK- and nirS-type denitrifiers in the Yellow River estuary, China. *Can. J. Microbiol.* **63**, (2017).
 74. Szukics, U. *et al.* Nitrifiers and denitrifiers respond rapidly to changed moisture and increasing temperature in a pristine forest soil. *FEMS Microbiol. Ecol.* **72**, 395–406 (2010).
 75. Rasche, F. *et al.* Seasonality and resource availability control bacterial and archaeal communities in soils of a temperate beech forest. *ISME J.* **5**, 389–402 (2011).
 76. Compaoré, J. & Stal, L. J. Effect of temperature on the sensitivity of nitrogenase to oxygen in two heterocystous cyanobacteria. *J. Phycol.* **46**, 1172–1179 (2010).
 77. Pogoreutz, C. *et al.* Nitrogen fixation aligns with nifH abundance and expression in two coral trophic functional groups. *Front. Microbiol.* **8**, 1–7 (2017).
 78. Larkum, A. W. D., Kennedy, I. R. & Muller, W. J. Nitrogen fixation on a coral reef. *Mar. Biol.* **98**, 143–155 (1988).
 79. Shashar, N., Cohen, Y., Loya, Y. & Sar, N. Nitrogen fixation (acetylene reduction) in stony corals - Evidence for coral-bacteria interactions. *Mar. Ecol. Prog. Ser.* **111**, 259–264 (1994).
 80. Williams, W. M., Viner, A. B. & Broughton, W. J. Nitrogen fixation (acetylene reduction) associated with the living coral *Acropora variabilis*. *Mar. Biol.* **94**, 531–535 (1987).
 81. Bednarz, V. N., Cardini, U., Van Hoytema, N., Al-Rshaidat, M. M. D. & Wild, C. Seasonal variation in dinitrogen fixation and oxygen fluxes associated with two dominant zooxanthellate soft corals from the northern Red Sea. *Mar. Ecol. Prog. Ser.* **519**, 141–152 (2015).
 82. Capone, D. G., Taylor, D. L. & Taylor, B. F. Nitrogen fixation (acetylene reduction) associated with macroalgae in a coral-reef community in the Bahamas. *Mar. Biol.* **40**, 29–32 (1977).
 83. Penhale, P. A. & Capone, D. G. Primary productivity and nitrogen fixation in two macroalgae-cyanobacteria associations. *Bull. Mar. Sci.* **31**, 164–169 (1981).
 84. Bednarz, V. N. *et al.* Dinitrogen fixation and primary productivity by carbonate and silicate reef

- sand communities of the Northern Red Sea. *Mar. Ecol. Prog. Ser.* **527**, 47–57 (2015).
85. Davey, M., Holmes, G. & Johnstone, R. High rates of nitrogen fixation (acetylene reduction) on coral skeletons following bleaching mortality. *Coral Reefs* **27**, 227–236 (2008).
 86. Gaidos, E., Rusch, A. & Ilardo, M. Ribosomal tag pyrosequencing of DNA and RNA from benthic coral reef microbiota: Community spatial structure, rare members and nitrogen-cycling guilds. *Environ. Microbiol.* **13**, 1138–1152 (2011).
 87. Rusch, A. & Gaidos, E. Nitrogen-cycling bacteria and archaea in the carbonate sediment of a coral reef. *Geobiology* **11**, 472–484 (2013).
 88. Wilson, S. T., Böttjer, D., Church, M. J. & Karl, D. M. Comparative assessment of nitrogen fixation methodologies, conducted in the oligotrophic north pacific ocean. *Appl. Environ. Microbiol.* **78**, 6516–6523 (2012).
 89. Bednarz, V. N., Grover, R., Maguer, J. F., Fine, M. & Ferrier-Pagès, C. The assimilation of diazotroph-derived nitrogen by scleractinian corals depends on their Metabolic Status. *MBio* **8**, 1–14 (2017).
 90. Grover, R., Ferrier-Pages, C., Maguer, J.-F., Ezzat, L. & Fine, M. Nitrogen fixation in the mucus of Red Sea corals. *J. Exp. Biol.* **217**, 3962–3963 (2014).
 91. Rooks, C. *et al.* Deep-sea sponge grounds as nutrient sinks: Denitrification is common in boreo-Arctic sponges. *Biogeosciences* **17**, 1231–1245 (2020).
 92. Cardini, U. *et al.* Microbial dinitrogen fixation in coral holobionts exposed to thermal stress and bleaching. *Environ. Microbiol.* **18**, 2620–2633 (2016).

Chapter 2

Chapter 2 | Simultaneous measurements of dinitrogen fixation and denitrification associated with coral reef substrates: advantages and limitations of a combined acetylene assay

Yusuf C. El-Khaled^{1*}, Florian Roth^{2,3,4}, Nils Rådecker^{2,5}, Najeh Kharbatia⁶, Burton H. Jones², Christian R. Woolstra^{2,5}, Christian Wild¹

¹Marine Ecology Department, Faculty of Biology and Chemistry, University of Bremen, Bremen, Germany

²Red Sea Research Center, King Abdullah University of Science and Technology (KAUST), Thuwal, Saudi Arabia

³Baltic Sea Centre, Stockholm University, Stockholm, Sweden

⁴Faculty of Biological and Environmental Sciences, Tvärminne Zoological Station, University of Helsinki, Helsinki, Finland

⁵Department of Biology, University of Konstanz, Konstanz, Germany

⁶Analytical Chemistry Core Laboratory (CORE Labs), King Abdullah University of Science and Technology (KAUST), Thuwal, Saudi Arabia

*corresponding author: yek2012@uni-bremen.de

2.1 | Abstract

Nitrogen (N) cycling in coral reefs is of key importance for these oligotrophic ecosystems, but knowledge about its pathways is limited. While dinitrogen (N₂) fixation is comparably well studied, the counteracting denitrification pathway is under-investigated, mainly because of expensive and relatively complex experimental techniques currently available. Here, we combined two established acetylene-based assays to one single setup to determine N₂ fixation and denitrification performed by microbes associated with coral reef substrates/organisms simultaneously. Accumulating target gases (ethylene for N₂ fixation, nitrous oxide for denitrification) were measured in gaseous headspace samples via gas chromatography. We measured N₂ fixation and denitrification rates of two Red Sea coral reef substrates (filamentous turf algae, coral rubble), and demonstrated, for the first time, the co-occurrence of both N cycling processes in both substrates. N₂ fixation rates were up to eight times higher during the light compared to the dark, whereas denitrification rates during dark incubations were stimulated for turf algae and suppressed for coral rubble compared to light incubations. Our results highlight the importance of both substrates in fixing N, but their role in relieving N is potentially divergent. Absolute N₂ fixation rates of the present study correspond with rates reported previously, even though likely underestimated due to an initial lag phase. Denitrification is also presumably underestimated due to incomplete nitrous oxide inhibition and/or substrate limitation. Besides these inherent limitations, we show that a relative comparison of N₂ fixation and denitrification activity between functional groups is possible. Thus, our approach facilitates cost-efficient sample processing in studies interested in comparing relative rates of N₂ fixation and denitrification.

Keywords: Nitrogen cycling | metabolism | gas chromatography | ethylene | nitrous oxide

A modified version of this chapter has been published in *Frontiers in Marine Science* 7:411.

<https://doi.org/10.3389/fmars.2020.00411>

2.2 | Introduction

Nitrogen (N) is one of the primary nutrients critical for the survival of all living organisms. Natural N availability is limited in many ecosystems, while others suffer from eutrophication. Thus, understanding N cycling processes is of paramount interest. Two antagonistic biological processes within the N cycle are of particular importance: (a) the import of new N into the ecosystem via microbes (diazotrophs) capable of converting atmospheric dinitrogen (N_2) into bioavailable forms of N, which is called biological N_2 -fixation, and (b) its counteracting process that removes N from the ecosystem via a reduction of nitrate to N_2 , commonly described as denitrification¹⁻³. Both processes appear in terrestrial and aquatic ecosystems, where N can act as an important factor limiting productivity⁴.

In coral reefs, N cycling is of particular importance as these ecosystems flourish in the oligotrophic waters of the tropics. However, attempts to describe microbial N cycling in coral reef environments are primarily restricted to N_2 fixation to provide information about how coral reefs flourish in nutrient-poor waters and how their N demand is satisfied⁵. Appropriate methods to quantify other pathways are largely missing to date⁶.

N_2 fixation is often quantified by one of two commonly applied methods: labelled isotope tracing techniques^{7,8} or acetylene reduction assays (ARA)^{9,10}. Isotope based techniques can be highly specific in identifying the exact location of N_2 fixation, but they are comparatively expensive and require higher effort to set up, perform and analyse samples. Whereas isotope tracer approaches track the fate of fixed N to the cellular compartments of a target organism/substrate¹¹, acetylene assays measure gross N_2 fixation activities on a “holobiont-wide” level of an organisms/substrate^{8,12,13}. This property is of significance, as coral reef organisms/substrates are considered as holobionts, consisting of the host organism/substrate and all of its associated symbiotic microorganisms¹⁴. The ARA is frequently used due to its comparatively easy handling and cost-effectiveness and has received first attention in the 1960s¹⁵. It makes use of the fact that acetylene acts as an alternative substrate to N_2 , resulting in the preferential reduction of acetylene to ethylene (C_2H_4) instead of N_2 to ammonium by the nitrogenase enzyme (Fig. S2.1). The C_2H_4 evolution is then quantified, e.g., via gas chromatography (GC), as an indirect measurement of N_2 fixation.

Denitrification can be detected using the same methods as described above¹⁶⁻¹⁹. Acetylene assays are carried out as acetylene inhibits the nitrous oxide (N_2O) reductase of denitrifying bacteria, which subsequently results in an accumulation of N_2O (Fig. S2.1)²⁰⁻²². Accumulated N_2O can then be quantified via GC and used as an approximation of denitrification activity.

Denitrification received attention as a mechanism to relieve coral reefs from excessive N only recently, as coral reefs experience and suffer more frequently from anthropogenically N inputs^{23,24}; upcoming studies

should, thus, focus on determining the capacities of coral reef environments to cope both with limited and excessive N by quantifying N₂ fixation and denitrification activities simultaneously²⁵.

In this context, acetylene assays have the potential for detecting both N₂ fixation and denitrification simultaneously. Indeed, both methods have been applied in terrestrial²⁶ and aquatic²⁷ systems. Capone and Montoya (2001)²⁸ already hypothesised a potential simultaneous usage in coral reef environments, but applications on various coral reef organisms and substrates are still missing to date. Comparing multiple functional groups of coral reefs, however, is of key importance, as coral reefs experience regime-shifts that in return alter N cycling patterns that potentially exacerbate or alleviate anthropogenic impacts.

We acknowledge the ongoing scientific debate whether isotope-based approaches or acetylene assays are the methods of choice in order to investigate N cycling pathways. We, therefore, do not compare or discuss both approaches in the present study. Instead, we highlight the application of a combined acetylene-based assay to two common coral reef substrates. We were able to evaluate both process measurements in one single experimental setup and analysis, which we termed COBRA (= combined blockage/reduction acetylene assay). Based on the results of the application, we discuss advantages and limitations as well as its potential use in coral reef science.

2.3 | Materials and Procedures

A complete list of all materials and the equipment used in this protocol as well as a full description of how the acetylene assay was performed can be found in Supplementary Material 2.1 and 2.2, and in Table S2.1.

Collection and Maintenance

Specimens were collected randomly from a semi-exposed area of Abu Shosha reef in the Jeddah region (22°18'15" N, 39°02'56"E) on the west coast of Saudi Arabia in the central Red Sea in March 2018. Turf algae ($n = 5$) and coral rubble fragments ($n = 4$) were selected in order to cover prevailing benthic substrates of the region. Turf algae were defined as dense and flat (<2 cm in height) assemblages of filamentous algae of different species, including small individuals of macroalgae and cyanobacteria. Coral rubble was defined as dislodged parts of framework builders or loose reef rock larger than the sand fraction with its associated microbial community according to Rasser and Riegl (2002)²⁹. All fragments were ~10 cm long and were collected with hammer and chisel from 5 to 6 m water depth. They were immediately transferred to recirculation aquaria on the boat (each filled with 10 L of ambient seawater) and kept until experiments at ambient water temperature and light conditions.

Dinitrogen Fixation and Denitrification Measurements

Incubations were conducted *ex situ* and directly after sample collection (<3 h after collection). N₂ fixation and denitrification incubations were conducted using COBRA according to the steps outlined in detail in Supplementary Material S1. Briefly, all COBRA incubations were conducted in gas-tight 1 L glass chambers, each filled with 800 mL of nutrient-enriched seawater (5 μM NO₃⁻; NO₃⁻ enrichment consisted of previously prepared NaNO₃ stock solution, prepared with MilliQ water and NaNO₃, ≥99.0%, Sigma-Aldrich) and 200 mL headspace (Fig. 2.1). Both incubation water and headspace were 10% acetylene enriched, as a 10% saturation has been successfully applied in acetylene-based assays for the quantification of N₂ fixation^{9,12} and denitrification^{22,30} previously. Nutrient enriched seawater was used, as acetylene inhibits the production of NO₃⁻ in the nitrification pathway^{31,32}. Thus, added NO₃⁻ served as a substrate for denitrification (see section “Limitations” for detailed information). Replicates were arranged in individual incubation chambers, and an additional chamber that was filled exclusively with 5 μM NO₃⁻ enriched seawater as “seawater blank” (Fig. 2.1). Solely one seawater blank was chosen because negligible microbial activity (diazotrophs and hypothetically denitrifiers) in seawater communities was expected according to previous studies^{33–35}. All incubation chambers were placed in a tempered water bath and stirred continuously (500 rpm) to ensure stable measurement conditions for 12 h at *in situ* temperatures (25°C). Dark and light incubations were conducted separately; dark incubations were performed at night in complete darkness. Light incubations were performed with a photon flux of ~200 μM quanta m⁻² s⁻¹. Gaseous samples were taken immediately after starting the incubations (t₀), after 2 h (t₂), 4 h (t₄), 8 h (t₈), and 12 h (t₁₂) and analysed using GC (Agilent 7890A, HP-Plot/Q column, helium pulsed discharge detector) via manual injection. N₂ fixation and denitrification were quantified by changes in gas concentrations according to equations 2–6 outlined in Supplementary Material S2.1. Besides start and end concentrations, two different intervals were selected as basis for the rate calculations, particularly t₄–t₁₂ for N₂ fixation and t₀–t₄ for denitrification activity. Finally, concentrations were corrected for the seawater blank signal, related to incubation volume and normalized to the surface area of the substrates (Tables S2.2, S2.3). Surface areas for turf algae and coral rubble fragments were calculated using cloud-based 3D models of samples (Autodesk Remake v19.1.1.2)^{36,37}.

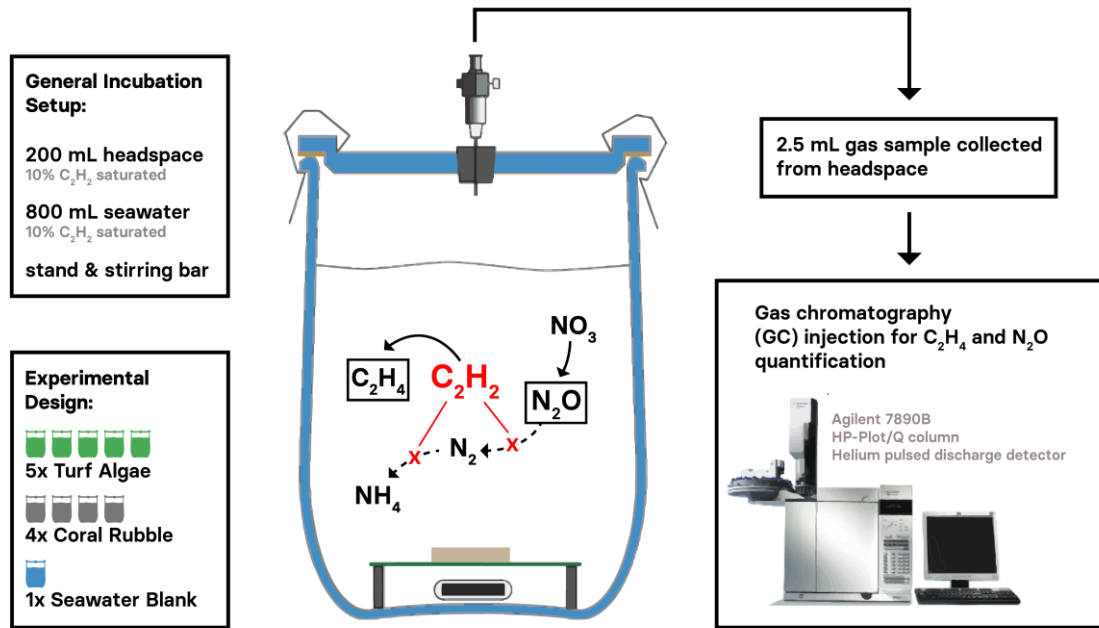


Figure 2.1 | Experimental design and general setup of the CORBA (= Combined Reduction/Blockage Acetylene assay) to simultaneously measure dinitrogen (N_2) fixation and denitrification in environmental samples. The two target gases ethylene and nitrous oxide accumulate (framed C_2H_4 and N_2O , resp.) as provided acetylene (C_2H_2) is (a) preferentially reduced to C_2H_4 instead of N_2 to ammonium (NH_4), and (b) inhibiting the evolution of in the N_2 gas at the N_2O -stage. Gaseous samples can be analysed using gas chromatography.

Calibration

A concentration series of C_2H_4 (Abdullah Hashim Industrial Gases & Equipment Co. Ltd. Specialty Gases Center, 19.6 ppm in balanced air; 210 ppm in balanced air) and N_2O (Air Liquide, 199.6 ppm in balanced Helium) was prepared by diluting commercial standards to desired standard concentrations. Standards covered the expected ranges of 0–210 ppm for C_2H_4 and 0–2 ppm for N_2O , respectively, and were injected manually into the GC. For the C_2H_4 calibration curve, standards with known concentrations of 210, 105, 52.5, 21, 20, 10, 5, 2, 1, and 0 ppm were measured in duplicates. The same was done for the N_2O calibration curve, where standards with known concentrations of 2, 1, 0.5, 0.2 ppm, and 0 ppm were injected.

Statistical Analysis

The statistical analysis was performed using Sigmaplot 12 (Systat software, v12.0). A two-way analysis of variance (ANOVA) with factors “substrates” and “sampling time” was performed. In case of $p < 0.05$, a *post hoc* test (Tukey HSD) was performed to check for significant differences between substrates and sampling times. Significance level was set at $\alpha = 0.05$.

2.4 | Results

Limits of detection (LOD), obtained from duplicate measurements of prepared standard samples, were 0.3 ppm for both target gases (Fig. S2.2). Standard curves showed high linearity for both target gases (linear regressions; $R^2 > 0.99$; $p < 0.0001$, $F > 800$; Fig. S2.2).

Concentrations for both C_2H_4 and N_2O in seawater blank incubations over the incubation time of 12 h were stable (Fig. S2.3). Production of C_2H_4 (as a proxy for N_2 fixation) and N_2O (as a proxy for denitrification) were measured in both dark and light conditions (Fig. 2.2, Tables S2.2, S2.3). Statistical analysis identified “time” as a significant factor in both processes and regardless of light availability (Table S2.4). C_2H_4 evolution was measured in both substrates and was higher in light compared to dark incubations. Overall, C_2H_4 increased over time, with an initial lag phase in the first 4 h of incubation. Consequently, N_2 fixation rates calculated discounting the initial lag phase were one third higher than rates resulting from start-end concentrations (Table 1.1).

N_2O evolution was detected for turf algae and coral rubble, with turf algae showing significantly higher amounts of N_2O after 2, 8, and 12 h incubation time regardless of light availability (Table S2.5). For both substrates, the highest amounts of N_2O were measured after 4 h of incubation. Unlike to C_2H_4 evolution, no initial lag phase was observed. In contrast, N_2O only increased in the first 4 h and remained stable or decreased afterward. Turf algae denitrification rates were higher in dark than those for coral rubble, but similar when incubated in light (Table 2.1). Denitrification rates obtained from the first 4 h of incubation were up to 8 times higher than those resulting from start-end concentrations (Table 2.1).

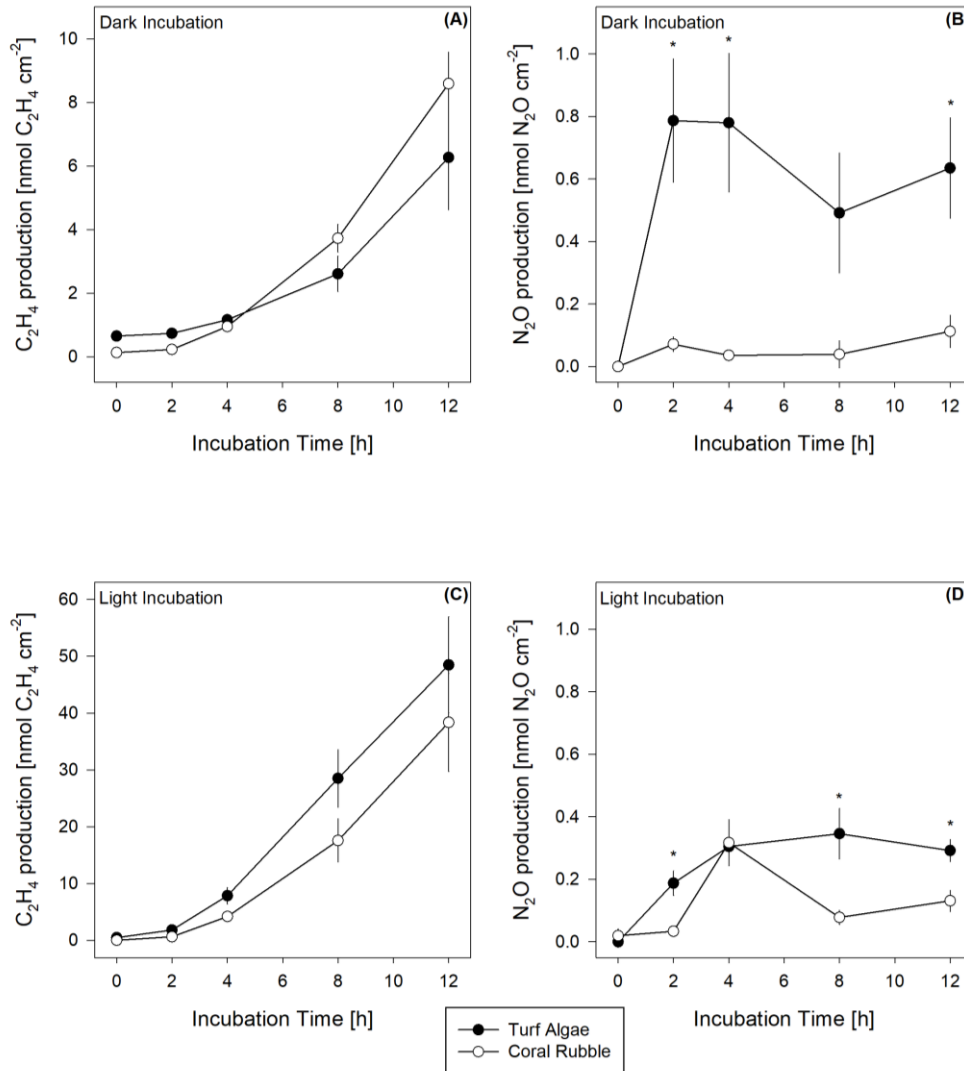


Figure 2.2 | Ethylene (C₂H₄) production as a proxy for N₂ fixation (**A,C**) and nitrous oxide (N₂O) production as a proxy for denitrification (**B,D**) in turf algae (n = 5) and coral rubble (n = 4) in dark (top graphs) and light (bottom graphs) incubation over time. Asterisks indicate significant differences (p < 0.05) between both substrates. Note: Different scales for C₂H₄ concentrations.

Table 2.1 | N₂ fixation (nmol N₂ cm⁻² h⁻¹) and denitrification (nmol N₂O cm⁻² h⁻¹) rates/potentials in turf algae and coral rubble. Rates are obtained from varying sampling times (in squared brackets) to highlight underestimations when solely start/end values are used to generate N₂ fixation and denitrification rates. Dark incubation rates are highlighted in grey colour, light incubation rates are highlighted in white colour. All N₂ fixation rates were converted with a conservative conversion factor of 4:1 (C₂H₄:N₂), according to Mulholland et al. (2004). Values are presented in mean ± SE.

	N ₂ fixation [t ₀ - t ₁₂]	N ₂ fixation [t ₄ - t ₁₂]	Denitrification [t ₀ -t ₁₂]	Denitrification [t ₀ -t ₄]
Turf Algae	0.12 ± 0.03	0.16 ± 0.05	0.05 ± 0.01	0.19 ± 0.06
Coral Rubble	0.18 ± 0.02	0.24 ± 0.03	0.01 ± 0.00	0.01 ± 0.00
Turf Algae	1.00 ± 0.17	1.27 ± 0.22	0.02 ± 0.00	0.08 ± 0.00
Coral Rubble	0.80 ± 0.18	1.07 ± 0.24	0.01 ± 0.00	0.08 ± 0.02

2.5 | Discussion

Dinitrogen Fixation and Denitrification Measurements

In the present study, we were able to demonstrate the co-occurrence of N₂ fixation and denitrification in turf algae and coral rubble for the first time. The simultaneous presence of these antinomic processes has been detected in coral reef associated sediments¹⁶ and microbial mats³⁸ before. Potentially, both pathways can be carried out by the same microbes³⁹ and are indirectly linked by their similar environmental requirements⁴⁰. Absolute N₂ fixation rates (i.e., calculated based on sampling points t₀ and t₁₂) measured in the present study were in the same range for turf algae⁴¹ and coral rubble³⁵, who also obtained N₂ fixation rates via acetylene-based assays (Table 2.2). Potentially, the similarity of rates of both substrates was due to a similar associated microbial composition on the substrates in terms of ecological niche and thus N₂ fixation activity. To the best of our knowledge, this was the first study to quantify rates of denitrification in coral rubble and turf algae, and, thus, no comparison to previous reports is possible.

Table 2.2 | N₂ fixation (nmol N₂ cm⁻² h⁻¹) and denitrification (nmol N₂O cm⁻² h⁻¹) rates of turf algae and coral rubble in comparison with values reported from other coral reef areas worldwide acquired via acetylene assays. Rates of the presented study were obtained from mean values from t₀ and t₁₂ sampling times of both dark and light incubations to demonstrate comparability though being ultimately underestimated. All N₂ fixation rates were converted with a conservative conversion factor of 4:1 (C₂H₄:N₂), according to Mulholland et al. (2004)¹². Values are presented in mean ± SE. GBR = Great Barrier Reef, Australia. n.d.a.= no data available.

N ₂ fixation	Denitrification	Location	Reference
Turf algae			
0.56 ± 0.10	0.04 ± 0.01	Central Red Sea	Present study
0.44 ± 0.04*	n.d.a.	Northern Red Sea	Rix et al. (2015) ⁴¹
Coral rubble			
0.49 ± 0.10	0.01 ± 0.00	Central Red Sea	Present study
1.00 ± 0.25	n.d.a.	GBR	Davey et al. (2008) ⁴²
0.58 ± 0.20*	n.d.a.	Northern Red Sea	Cardini et al. (2016) ³⁵
0.90 – 4.00	n.d.a.	GBR	Larkum (1988) ⁴³
0.74 – 5.70	n.d.a.	GBR	Larkum et al. (1988) ⁴⁴

*winter season

Interestingly, both substrates showed stimulated N_2 fixation during light compared to dark incubations. denitrification activity was similar in both substrates during light incubations, whereas dark incubations showed suppressed denitrification activity in coral rubble but stimulated denitrification in turf algae (Table 2.1). Nitrogenase, the key enzyme performing N_2 fixation, is extremely sensitive to oxygen⁴⁵, and N_2 fixation is generally considered as an anaerobic process⁴⁶. Likewise, denitrification is also an anaerobic process⁴⁷. Both incubations (dark and light) were started with freshly collected seawater containing natural, ambient oxygen concentrations, which likely increased during light and decreased during dark incubations due to photosynthesis or respiration^{35,41,48}. The occurrence of both anaerobic processes despite the presence of oxygen (i.e., during light) indicates that both N_2 fixation and denitrification may be spatially separated from oxygen evolution in both substrates, or that the involved diazotrophs and denitrifiers are capable of performing N_2 fixation and denitrification, resp., in the presence of oxygen^{49–52}. Furthermore, aerobic conditions promote nitrification⁵³, i.e., the oxidation from ammonium to nitrite and NO_3^- , which serves as a substrate for denitrification⁵⁴. However, in how far photosynthesis and respiration affected N_2 fixation and denitrification activities in both substrates in the present study remains speculative. Synoptically, the method aids to reveal interesting N cycling patterns. This emphasises the general applicability of the combined technique for the quantification of N_2 fixation rates, yet revealing interesting patterns for both N cycling pathways.

Our findings revealed increasing C_2H_4 concentrations over the total incubation time of 12 h with an initial lag phase in the first 4 h, which is shorter than reported before^{55–57}. Considering start (t_0) and end (t_{12}) concentrations will thus result in an underestimation of N_2 fixation rates (Table 2.1). However, N_2 fixation rates based on start/end concentrations are comparable to previous studies that have applied standard acetylene reduction assays (Table 2.2), indicating that COBRA still provides sufficient information to go beyond relative comparisons between functional groups but also allowing comparative analysis with other studies. Nevertheless, the most accurate rates are derived by omitting the initial lag phase when calculating rates and considering sampling points t_4 and t_{12} instead.

In the case of N_2O rates, we revealed higher N_2O rates obtained from the first 4 h incubation time (Table 2.1). This leads to the suggestion of a short sampling interval to identify denitrification potentials (i.e., t_0 and t_4). The detected maximum after 4 h likely reflects an incomplete blockage of the denitrification pathway⁵⁸. A depletion of accumulated N_2O gas concentrations via denitrifying bacteria is likely due to reduced denitrification inactivity as NO_3^- substrate has been consumed (see next section). However, our findings reveal a significant difference in accumulated N_2O after 12 h between turf algae and coral rubble fragments, despite a decrease in N_2O concentrations after 4 h. As a result, we recommend short sampling intervals but

also conclude that even over 12 h incubation time, a relative comparison between different functional groups may be possible as long as methodological limitations (e.g., substrate availability) are considered.

Altogether, we recommend performing incubations for 12 h, with sampling points at t_0 , t_4 , and t_{12} . If feasible with regard to costs and workload, we suggest a higher temporal resolution (i.e., more sampling points) to achieve rates that are potentially more precise. By all means, the temporal resolution chosen in the present study enables calculations for most reliable N_2 fixation (from t_4 until t_{12}) rates and denitrification (from t_0 until t_4) potentials. In case that solely start- and end-measurements can be performed (from t_0 until t_{12}), we conclude that a) the rates measured with the COBRA still allow comparisons with other studies in case of N_2 fixation (Table 2.2); and b) COBRA provides sufficient information about the relative importance by accounting for relative changes in rates across substrates in case of denitrification activity, even though both N cycling pathways may be underestimated.

Limitations

Acetylene assays have faced criticism in the last decades. Limitations of acetylene assays have been reviewed extensively in Giller (1987)⁵⁹, Groffman et al. (2006)⁶, and Wilson et al. (2012)¹¹. Reported restraints are of general nature and cannot be directly related to a combination of both acetylene reduction and inhibition as in the presented setup here. Thus, we focus on methodological limitations that are important to consider for the interpretation of relative rather than absolute rates⁶.

Firstly, Oremland and Capone (1988)³² observed an unspecific inhibitory effect of acetylene on other N cycling pathways, as acetylene inhibits the formation of NO_3^- via the nitrification pathway. This can ultimately result in an underestimation of denitrification^{6,31,60,61}, as there is a close coupling of both nitrification and denitrification (i.e., the production of NO_3^- via nitrification serves as a substrate for denitrification). This is particularly the case in oligotrophic systems, where NO_3^- may be a limiting factor for denitrification⁶². Hence, to preclude substrate limitation, incubations with NO_3^- addition, as used in this study, can aid maintaining denitrification activity in the absence of nitrification^{38,62,63}. However, the results obtained with COBRA and nutrient addition reflect, thus, a denitrification potential rather than actual denitrification rates, as artificially increased substrate availability drives denitrification above natural occurring rates. A potential side effect of added NO_3^- on N_2 fixation activity should be addressed in future studies. Theoretically, with the addition of NO_3^- , an energetically more cost-efficient alternative N source (i.e., through assimilation) is provided, as compared to N_2 fixation⁶⁴. The preferential NO_3^- assimilation potentially results in lower N_2 fixation rates. Yet, there is both evidence for the inhibition of N_2 fixation by

the availability of NO_3^- and counterproof that N_2 fixation occurs with substantial rates in the presence of up to $30 \mu\text{M NO}_3^-$.⁶⁵

A time-dependent incomplete inhibition of N_2O through the presence of acetylene has been discussed before^{6,58}. An incomplete inhibition and a subsequent N_2O reduction in the presence of acetylene can, thus, result in an incorrect estimation of total denitrification. Yu et al. (2010)⁵⁸ have reported incomplete inhibitions after ≥ 24 h. Our results indicate that observed patterns of decreasing N_2O concentrations after > 4 h incubation time potentially occur due to an incomplete blockage. Possibly, substrate depletion during the incubation time also lead to decreasing N_2O concentrations after > 4 h of incubation time, as NO_3^- a) is potentially used as a substrate for denitrification⁵⁴ or) may be assimilated immediately by turf algae⁶⁶ and potentially also by coral rubble. It remains unclear if saturating the incubation chamber with $>10\%$ acetylene will result in a complete inhibition.

Advantages and Use in Research

Generally, acetylene assays are applied as indirect approaches to identify N_2 fixation as well as denitrification. Despite their limitations (see above), they have provided N_2 fixation and denitrification rate quantifications and estimates for many aquatic systems.

We could demonstrate that a combination of both approaches (i.e., acetylene reduction and acetylene blockage assay) can be performed simultaneously. Both assays have been performed separately over a wide range of aquatic substrates and organisms before^{35,67}. As no changes in the basic setup have been carried out here, we hypothesize that the here presented approach (similar to commonly applied acetylene assays) can be used as a versatile method for organisms and substrates of various aquatic environments.

By using COBRA, the number of samples and measuring time is halved, as only one gaseous sample and consequently, only one sample run is required to detect both target gases. In addition, we were able to measure four gaseous headspace samples per hour using either manual or autosampler injection (see Supplementary Material 2.1, 2.2), whereby the autosampler has the capacity to measure 71 samples within < 18 h. Overall, the high sample throughput enables the generation of profound datasets in a minimum of time, with the possibility to receive a high temporal resolution with multiple functional groups of a targeted coral environment. This opens the door to a deeper understanding of temporal and spatial patterns of N_2 fixation and denitrification across various substrates and organisms and their associated microbial community.

Previous acetylene-based investigations mostly used flame ionization detectors for N_2 fixation quantification and either electron capture or thermal conductivity detectors for denitrification detection^{28,38,63,68}. The latter

have a high sensitivity for N₂O but are also prone to interference from other compounds^{28,69}. In the present study, we used a helium pulsed discharge ionization detector. This detector is up to 500 times more sensitive than the thermal conductivity sensor and up to 50 times more sensitive than the flame ionization detector^{70,71}. Owing to the use of only one single and very sensitive detector⁶⁹ only one type of carrier gas was required for one sample run. This leads to a reduction in costs, time, storage, and usage of further gases.

In the future, unprecedented dramatic environmental changes will be a major challenge for life in the earth's oceans⁷². Thus, research will undoubtedly focus on understanding and predicting the effects of climate change and other anthropogenic pressures on marine ecosystems and their organisms^{73–75}. Special emphasis will be laid on the effects of environmental change on marine microbial communities, which act as the major drivers of elemental transformations of terrestrial and marine biogeochemical cycles^{76,77}. N cycling is one of the most important biogeochemical cycles, and, as such, changes in N availability (through eutrophication) will likely evoke physiological and metabolic responses in coral reef organisms/substrates. Their study is paramount for understanding N cycling from a species to ecosystem level with knowledge of a changing environment⁷⁸. Eutrophication, as well as ocean warming and acidification, belong to the mainly discussed and assessed threats. These can easily be implemented in the COBRA by adjusting incubation parameters, e.g., temperature, nutrient availability and pH, or a combination of such. Hence, the described N cycling pathways can be investigated in an anthropogenically influenced system that simulates conditions comparable to common anthropogenic stressor scenarios. As investigations on the effects of climate change have become a major scientific interest, the opportunities to include them in the here presented technique underline its potential.

2.6 | Acknowledgments

We are grateful to Arjen Tilstra, Rodrigo Villalobos, João Cúrdia, and Denis B. Karcher for support during fieldwork. Many thanks also to Söphiä Tobler, Rainer Willhaus, and Jan Krause for their help in developing the figures. Further, we would like to thank the editor as well as the two reviewers for their constructive comments on the manuscript.

2.7 | References

1. Vitousek, P. M. *et al.* Human alteration of the global nitrogen cycle: sources and consequences. *Ecol. Appl.* **7**, 737–750 (1997).
2. Gruber, N. & Sarmiento, J. L. *Large-scale biogeochemical-physical interactions in elemental cycles. THE SEA: Biological-Physical Interactions in the Oceans* **12**, (2002).
3. Jickells, T. D. & Weston, K. *Nitrogen Cycle - External Cycling: Losses and Gains. Treatise on Estuarine and Coastal Science* **5**, (Elsevier Inc., 2012).
4. Lesser, M. P. *et al.* Nitrogen fixation by symbiotic cyanobacteria provides a source of nitrogen for the scleractinian coral *Montastraea cavernosa*. *Mar. Ecol. Prog. Ser.* **346**, 143–152 (2007).
5. Neil, J. M. O. & Capone, D. G. *Nitrogen Cycling in Coral Reef Environments.* (2008). doi:10.1016/B978-0-12-372522-6.00021-9
6. Groffman, P. M. *et al.* Methods for Measuring Denitrification: Diverse Approaches to a Difficult Problem. *Ecol. Appl.* **16**, 2091–2122 (2006).
7. Montoya, J. P., Voss, M., Kahler, P. & Capone, D. G. A Simple, High-Precision, High-Sensitivity Tracer Assay for N₂ Fixation. *Appl. Environ. Microbiol.* **62**, 986–993 (1996).
8. Grover, R., Ferrier-Pages, C., Maguer, J.-F., Ezzat, L. & Fine, M. Nitrogen fixation in the mucus of Red Sea corals. *J. Exp. Biol.* **217**, 3962–3963 (2014).
9. Pogoreutz, C. *et al.* Nitrogen fixation aligns with nifH abundance and expression in two coral trophic functional groups. *Front. Microbiol.* **8**, 1–7 (2017).
10. Tilstra, A. *et al.* Seasonality affects dinitrogen fixation associated with two common macroalgae from a coral reef in the northern Red Sea. *Mar. Ecol. Prog. Ser.* **575**, 69–80 (2017).
11. Wilson, S. T., Böttjer, D., Church, M. J. & Karl, D. M. Comparative assessment of nitrogen fixation methodologies, conducted in the oligotrophic north pacific ocean. *Appl. Environ. Microbiol.* **78**, 6516–6523 (2012).
12. Mulholland, M. R., Bronk, D. A. & Capone, D. G. Dinitrogen fixation and release of ammonium and dissolved organic nitrogen by *Trichodesmium* IMS101. *Aquat. Microb. Ecol.* **37**, 85–94 (2004).
13. Mohr, W., Großkopf, T., Wallace, D. W. R. & LaRoche, J. Methodological underestimation of oceanic nitrogen fixation rates. *PLoS One* **5**, 1–7 (2010).
14. Rosenberg, E., Koren, O., Reshef, L., Efrony, R. & Zilber-Rosenberg, I. The role of microorganisms in coral health, disease and evolution. *Nat. Rev. Microbiol.* **5**, 355–362 (2007).
15. Hardy, R. W. F., Holsten, R. D., Jackson, E. K. & Burns, R. C. The acetylene - ethylene assay for N₂ fixation: laboratory and field evaluation. *Plant Physiol.* **43**, 1185–1207 (1968).
16. Koop, K. *et al.* ENCORE: The effect of nutrient enrichment on coral reefs. Synthesis of results and conclusions. *Mar. Pollut. Bull.* **42**, 91–120 (2001).
17. Groffman, P. M. *et al.* Methods for Measuring Denitrification : *Ecol. Appl.* **16**, 2091–2122 (2006).
18. Hoffmann, F. *et al.* Complex nitrogen cycling in the sponge *Geodia barretti*. *Environ. Microbiol.* **11**, 2228–2243 (2009).
19. Myrstener, M., Jonsson, A. & Bergström, A. K. The effects of temperature and resource availability on denitrification and relative N₂O production in boreal lake sediments. *J. Environ. Sci.* **47**, 82–90 (2016).
20. Fedorova, R. I., Milekhina, E. I. & Il'Yukhina, N. I. Evaluation of the method of 'gas metabolism' for detecting extraterrestrial life. Identification of nitrogen-fixation microorganisms. *Izv. Akad. Nauk SSSR Ser. Biol.* **6**, 797–806 (1973).

21. Balderston, W. L., Sherr, B. & Payne, W. J. Blockage By Acetylene of Nitrous-Oxide Reduction in *Pseudomonas-Perfectomarinus*. *Appl. Environ. Microbiol.* **31**, 504–508 (1976).
22. Yoshinari, T. & Knowles, R. Acetylene Inhibition of Nitrous Oxide Reduction by Denitrifying Bacteria. *Biochem. Biophys. Res. Commun.* **69**, 705–710 (1976).
23. Halpern, B. S. *et al.* A Global Map of Human Impact on Marine Ecosystems. *Science (80-.)*. **319**, 948–952 (2008).
24. Smith, V. H. & Schindler, D. W. Eutrophication science: where do we go from here? *Trends Ecol. Evol.* **24**, 201–207 (2009).
25. Rådecker, N., Pogoreutz, C., Voolstra, C. R., Wiedenmann, J. & Wild, C. Nitrogen cycling in corals: The key to understanding holobiont functioning? *Trends Microbiol.* **23**, 490–497 (2015).
26. Yoshinari, T., Hynes, R. & Knowles, R. Acetylene inhibition of nitrous oxide reduction and measurement of denitrification and nitrogen fixation in soil. *Soil Biol. Biochem.* **9**, 177–183 (1977).
27. Bertics, V. J., Sohm, J. A., Magnabosco, C. & Ziebis, W. Denitrification and Nitrogen Fixation Dynamics in the Area Surrounding an Individual Ghost Shrimp (*Neotrypaea californiensis*) Burrow System. *Appl. Environ. Microbiol.* **78**, 3864–3872 (2012).
28. Capone, D. G. & Montoya, J. P. Nitrogen Fixation and Denitrification. *Methods Microbiol.* **30**, 501–515 (2001).
29. Rasser, M. W. & Riegl, B. Holocene coral reef rubble and its binding agents. *Coral Reefs* **21**, 57–72 (2002).
30. Shrewsbury, L. H., Smith, J. L., Huggins, D. R., Carpenter-Boggs, L. & Reardon, C. L. Denitrifier abundance has a greater influence on denitrification rates at larger landscape scales but is a lesser driver than environmental variables. *Soil Biol. Biochem.* **103**, 221–231 (2016).
31. Hynes, R. K. & Knowles, R. Inhibition by acetylene of ammonia oxidation in *Nitrosomonas europaea*. *FEMS Microbiol. Lett.* **4**, 319–321 (1978).
32. Oremland, R. S. & Capone, D. G. Use of ‘Specific’ Inhibitors in Biogeochemistry and Microbial Ecology. *Adv. Microbi. Ecol.* 285–383 (1988). doi:10.1007/978-1-4684-5409-3_8
33. Foster, R. A., Paytan, A. & Zehr, J. P. Seasonality of N₂ fixation and nifH gene diversity in the Gulf of Aqaba (Red Sea). *Limnol. Oceanogr.* **54**, 219–233 (2009).
34. Bednarz, V. N., Cardini, U., Van Hoytema, N., Al-Rshaidat, M. M. D. & Wild, C. Seasonal variation in dinitrogen fixation and oxygen fluxes associated with two dominant zooxanthellate soft corals from the northern Red Sea. *Mar. Ecol. Prog. Ser.* **519**, 141–152 (2015).
35. Cardini, U. *et al.* Budget of Primary Production and Dinitrogen Fixation in a Highly Seasonal Red Sea Coral Reef. *Ecosystems* **19**, 771–785 (2016).
36. Lavy, A. *et al.* A quick, easy and non-intrusive method for underwater volume and surface area evaluation of benthic organisms by 3D computer modelling. *Methods Ecol. Evol.* **6**, 521–531 (2015).
37. Gutierrez-Heredia, L., Benzoni, F., Murphy, E. & Reynaud, E. G. End to End Digitisation and Analysis of Three-Dimensional Coral Models, from Communities to Corallites. *PLoS One* **11**, e0149641 (2016).
38. Joye, S. B. & Paerl, H. W. Contemporaneous nitrogen fixation and denitrification in intertidal microbial mats: rapid response to runoff events. *Mar. Ecol. Prog. Ser.* **94**, 267–274 (1993).
39. Bothe, H., Klein, B., Stephan, M. P. & Döbereiner, J. Transformations of inorganic nitrogen by *Azospirillum* spp. *Arch. Microbiol.* **130**, 96–100 (1981).
40. Tilstra, A. *et al.* Denitrification Aligns with N₂ Fixation in Red Sea Corals. *Sci. Rep.* **9**, 19460 (2019).
41. Rix, L. *et al.* Seasonality in dinitrogen fixation and primary productivity by coral reef framework

- substrates from the northern Red Sea. *Mar. Ecol. Prog. Ser.* **533**, 79–92 (2015).
42. Davey, M., Holmes, G. & Johnstone, R. High rates of nitrogen fixation (acetylene reduction) on coral skeletons following bleaching mortality. *Coral Reefs* **27**, 227–236 (2008).
 43. Larkum, A. W. D. High rates of nitrogen fixation on coral skeletons after predation by the crown of thorns starfish *Acanthaster planci*. *Mar. Biol.* **97**, 503–506 (1988).
 44. Larkum, A. W. D., Kennedy, I. R. & Muller, W. J. Nitrogen fixation on a coral reef. *Mar. Biol.* **98**, 143–155 (1988).
 45. Robson, R. L. & Postgate, J. R. Oxygen and Hydrogen in Biological Nitrogen Fixation. *Annu. Rev. Microbiol.* **34**, 183–207 (1980).
 46. Compaoré, J. & Stal, L. J. Effect of temperature on the sensitivity of nitrogenase to oxygen in two heterocystous cyanobacteria. *J. Phycol.* **46**, 1172–1179 (2010).
 47. Zumft, W. G. Cell biology and Molecular Basis of Denitrification. *Microbiol. Mol. Biol. Rev.* **61**, 533–616 (1997).
 48. Mague, T. H., Weare, N. M. & Holm-Hansen, O. Nitrogen fixation in the North Pacific Ocean. *Mar. Biol.* **24**, 109–119 (1974).
 49. Lloyd, D., Boddy, L. & Davies, K. J. P. Persistence of bacterial denitrification capacity under aerobic conditions: The rule rather than the exception. *FEMS Microbiol. Lett.* **45**, 185–190 (1987).
 50. Berman-Frank, I. *et al.* Segregation of nitrogen fixation and oxygenic photosynthesis in the marine cyanobacterium *Trichodesmium*. *Science (80-.)*. **294**, 1534–1537 (2001).
 51. Silvennoinen, H., Liikanen, A., Torssonen, J., Stange, C. F. & Martikainen, P. J. Denitrification and N₂O effluxes in the Bothnian Bay (northern Baltic Sea) river sediments as affected by temperature under different oxygen concentrations. *Biogeochemistry* **88**, 63–72 (2008).
 52. Bednarz, V. N. *et al.* Contrasting seasonal responses in dinitrogen fixation between shallow and deep-water colonies of the model coral *Stylophora pistillata* in the northern Red Sea. *PLoS One* **13**, e0199022 (2018).
 53. Rysgaard, S. *et al.* Oxygen regulation of nitrification and denitrification in sediments. *Limnol. Oceanogr.* **39**, 1643–1652 (1994).
 54. Devol, A. H. *Denitrification Including Anammox. Nitrogen in the Marine Environment* (2008). doi:10.1016/B978-0-12-372522-6.00006-2
 55. Patriquin, D. G. & McClung, C. R. Nitrogen Accretion, and the Nature and Possible Significance of N₂ Fixation (Acetylene Reduction) in a Nova Scotian *Spartina alterniflora* Stand. *Mar. Biol.* **47**, 227–242 (1978).
 56. Williams, W. M., Viner, A. B. & Broughton, W. J. Nitrogen fixation (acetylene reduction) associated with the living coral *Acropora variabilis*. *Mar. Biol.* **94**, 531–535 (1987).
 57. Shieh, W. Y. & Lin, Y. M. Nitrogen fixation (acetylene reduction) associated with the zoanthid *Palythoa tuberculosa* Esper. *J. Exp. Mar. Bio. Ecol.* **163**, 31–41 (1992).
 58. Yu, K., Seo, D. C. & Delaune, R. D. Incomplete acetylene inhibition of nitrous oxide reduction in potential denitrification assay as revealed by using ¹⁵N-Nitrate tracer. *Commun. Soil Sci. Plant Anal.* **41**, 2201–2210 (2010).
 59. Giller, K. E. Use and abuse of the acetylene reduction assay for measurement of ‘associative’ nitrogen fixation. *Soil Biol. Biochem.* **19**, 783–784 (1987).
 60. Jenkins, M. C. & Kemp, W. M. The coupling of nitrification and denitrification in two estuarine sediments. *Limnol. Oceanogr.* **29**, 609–619 (1984).
 61. Seitzinger, S. Denitrification and Nitrification Rates in Aquatic Sediments. in *Handbook of Methods in*

- Aquatic Microbiol. Ecology* (eds. Kemp, P. F., Sherr, B. F., Sherr, E. B. & Cole, J. J.) 633–641 (1993).
62. Miyajima, T., Suzumura, M., Umezawa, Y. & Koike, I. Microbiological nitrogen transformation in carbonate sediments of a coral-reef lagoon and associated seagrass beds. *Mar. Ecol. Prog. Ser.* **217**, 273–286 (2001).
 63. Haines, J. R., Atlas, R. M., Griffiths, R. P., Morita, R. Y. & Sea, B. Denitrification and Nitrogen Fixation in Alaskan Continental Shelf Sediments. **41**, 412–421 (1981).
 64. Falkowski, P. G. *Enzymology of Nitrogen Assimilation. Nitrogen in the Marine Environment* (ACADEMIC PRESS, INC., 1983). doi:10.1016/b978-0-12-160280-2.50031-6
 65. Knapp, A. N. The sensitivity of marine N₂ fixation to dissolved inorganic nitrogen. *Front. Microbiol.* **3**, 374 (2012).
 66. den Haan, J. *et al.* Nitrogen and phosphorus uptake rates of different species from a coral reef community after a nutrient pulse. *Sci. Rep.* **6**, 28821 (2016).
 67. Olson, J. B., Steppe, T. F., Litaker, R. W. & Paerl, H. W. N₂-fixing microbial consortia associated with the ice cover of Lake Bonney, Antarctica. *Microb. Ecol.* **36**, 231–238 (1998).
 68. Capone, D. G., Dunham, S. E., Horrigan, S. G. & Duguay, L. E. Microbial nitrogen transformations in unconsolidated coral reef sediments. *Mar. Ecol. Prog. Ser.* **80**, 75–88 (1992).
 69. Roberge, M. T., Finley, J. W., Lukaski, H. C. & Borgerding, A. J. Evaluation of the pulsed discharge helium ionization detector for the analysis of hydrogen and methane in breath. *J. Chromatogr. A* **1027**, 19–23 (2004).
 70. Woo, J.-C., Moon, D.-M. & Kawaguchi, H. Design and Characterization of a Helium-Discharge Ionization Detector for Gas Chromatography. *Anal. Sci.* **12**, 195–200 (1996).
 71. Hunter, M. C. *et al.* The use of the helium ionization detector for gas chromatographic monitoring of trace atmospheric components. *HRC J. High Resolut. Chromatogr.* **21**, 75–80 (1998).
 72. Harnik, P. G. *et al.* Extinctions in ancient and modern seas. *Trends Ecol. Evol.* **27**, 608–617 (2012).
 73. Bijma, J., Pörtner, H. O., Yesson, C. & Rogers, A. D. Climate change and the oceans - What does the future hold? *Mar. Pollut. Bull.* **74**, 495–505 (2013).
 74. Pandolfi, J. M., Connolly, S. R., Marshall, D. J. & Cohen, A. L. Projecting coral reef futures under global warming and ocean acidification. *Science (80-.)*. **333**, 418–422 (2011).
 75. Runge, J. A. *et al.* End of the century CO₂ concentrations do not have a negative effect on vital rates of *Calanus finmarchicus*, an ecologically critical planktonic species in North Atlantic ecosystems. *ICES J. Mar. Sci.* **73**, 937–950 (2016).
 76. Gruber, N. & Galloway, J. N. An Earth-system perspective of the global nitrogen cycle. *Nature* **451**, 293–296 (2008).
 77. Gruber, N. Warming up, turning sour, losing breath: Ocean biogeochemistry under global change. *Philos. Trans. R. Soc. A Math. Phys. Eng. Sci.* **369**, 1980–1996 (2011).
 78. Cardini, U., Bednarz, V. N., Foster, R. A. & Wild, C. Benthic N₂ fixation in coral reefs and the potential effects of human-induced environmental change. *Ecol. Evol.* **4**, 1706–1727 (2014).

Chapter 3

Chapter 3 | An in situ approach for measuring biogeochemical fluxes in structurally complex benthic communities

Florian Roth^{1*}, Christian Wild², Susana Carvalho¹, Nils Rådecker¹, Christian R. Voolstra¹, Benjamin Kürten¹, Holger Anlauf¹, **Yusuf C. El-Khaled**², Ronan Carolan³ & Burton H. Jones¹

¹ King Abdullah University of Science and Technology (KAUST), Red Sea Research Center, Thuwal 23955-6900, Saudi Arabia

² University of Bremen, Faculty of Biology and Chemistry, Marine Ecology Department, 28369 Bremen, Germany

³ King Abdullah University of Science and Technology (KAUST), Core Labs, Thuwal 23955-6900, Saudi Arabia

*Corresponding author: florian.roth@kaust.edu.sa

3.1 | Abstract

I) The exchange of energy and nutrients are integral components of ecological functions of benthic shallow-water ecosystems and are directly dependent on *in situ* environmental conditions. Traditional laboratory experiments cannot account for the multidimensionality of interacting processes when assessing metabolic rates and biogeochemical fluxes of structurally complex benthic communities. Current *in situ* chamber systems are expensive, limited in their functionality, and the deployment is often restricted to planar habitats (e.g., sediments or seagrass meadows) only.

II) To overcome these constraints, we describe a protocol to build and use non-invasive, cost-effective, and easy to handle *in situ* incubation chambers that provide reproducible measurements of biogeochemical processes in simple and structurally complex benthic shallow-water communities. Photogrammetry tools account for the structural complexity of benthic communities, enabling to calculate accurate community fluxes. We tested the performance of the system in laboratory assays and various benthic habitats (i.e., algae growing on rock, coral assemblages, sediments, and seagrass meadows). In addition, we estimated community budgets of photosynthesis and respiration by corals, rock with algae, and carbonate sediments, which were subsequently compared to budgets extrapolated from conventional *ex situ* single-organism incubations.

III) The tests highlight the transparency (> 90% light transmission) of the chambers and minimal water exchange with the surrounding medium on most substrates. Linear dissolved oxygen fluxes in dependence to incubation time showed sufficient mixing of the water by circulation pumps and no organismal stress response. The comparison to single-organism incubations showed that *ex situ* measurements might overestimate community-wide net primary production and underestimate respiration and gross photosynthesis by 20 – 90%.

IV) The proposed protocol overcomes the paucity of observational and manipulative studies that can be performed in *in situ* native habitats, thus producing widely-applicable and realistic assessments on the

community level. Importantly, the tool provides a standardized approach to compare community functions across a wide range of benthic habitats. We identify multiple experimental strategies, including the manipulation of stressors/factors, and discuss how the method may be implemented in a variety of aquatic studies.

Keywords: Respiratory chambers | Incubations | Photogrammetry | 3D models | Field-based measurements | Community budgets

A modified version of this chapter has been published in *Methods in Ecology and Evolution* 10 (5)

<https://doi.org/10.1111/2041-210X.13151>

3.2 | Introduction

Anthropogenic environmental change is rapidly transforming the community composition, structure, and functioning of coastal and estuarine benthic shallow-water ecosystems on a global scale¹. Processes such as primary production, calcification, organic matter (OM) remineralization, and nutrient cycling are important indicators of ecosystem status, health, and alteration²⁻⁴. However, the complexity of interactions underlying these processes requires a holistic assessment with accurate measurements of community metabolism and biogeochemical fluxes⁵. Consequently, community-wide and standardized measurements of biogeochemical properties of benthic communities are a prerequisite for ecosystem management⁶. However, obtaining such data has proven challenging.

Currently, metabolic rates and element cycling processes of various benthic communities are mainly derived from experimental studies conducted in aquaria or mesocosm systems⁷⁻¹¹. In such studies, benthic communities are reconstructed *ex situ* according to information gathered during benthic field surveys. Mesocosms (continuous flow or static) provide a unique way to measure biogeochemical exchange rates under controlled conditions. These traditional methods, however, are seldom capable of accommodating the complexity and variability of natural systems¹². Moreover, substrates and individual organisms must be actively removed and incubated *ex situ*, making this process destructive and prone to experimental artifacts. Additionally, community measurements in *ex situ* flumes and mesocosms are extremely costly, and few laboratories are capable of accommodating the complexities of natural systems.

Most community-wide *in situ* measurements of metabolic and biogeochemical processes have generally quantified spatial geochemical changes in the water column using the Eulerian¹³ or Lagrangian¹⁴ flow respirometry technique. These methods involve measuring the upstream-downstream changes of the chemical properties in a parcel of water in a unidirectional flow field. This approach has difficulties to accurately tracking the movement of water parcels due to the complex topography of many habitats, resulting in a significant margin of error¹⁵. Moreover, water must have sufficient contact time with the substrate for its chemistry to be affected by processes of interest, limiting the resolution of geochemical measurements¹⁶.

Enclosure experiments (*ex situ* or *in situ*) associated with benthic shallow-water systems have often utilized small (< 4 L volume, usually only 1 L) incubation chambers¹⁷⁻¹⁹. These chambers effectively isolate a limited volume of water over individual organisms, enabling short-term incubation experiments. While providing valuable measurements of processes associated with individual organisms, community-wide responses cannot be achieved. Nonetheless, single-organism incubations are the foremost approach to extrapolate responses of representative taxa of a known habitat to community-wide budgets²⁰⁻²².

In recent years, larger *in situ* incubations chambers (5 – 120 L volume) have been used across different benthic shallow-water habitats²³⁻²⁵. These chambers enclose both the underlying substrate and overlying water to assess areal rates of production and uptake by quantifying temporal changes in the overlying water chemistry. They provide a non-invasive technique that better reflects the ambient conditions, nevertheless,

these studies have often been restricted to plain two-dimensional (2D) habitats, such as sediments^{24–26} or seagrass meadows²⁷. Here, fluxes could simply be related to the covered seafloor area and the known water volume of the chamber.

The application of such systems has been notably absent for communities with structurally complex, three-dimensional (3D) structures (e.g., rocky beds, oyster banks, or coral reef habitats). Photosynthesis, calcification, and OM cycling, however, are all examples of processes affected by the volume and surface area of the organisms, yet no tools have been available to quantify these variables *in situ* non-intrusively. Previous that measured community processes on intertidal rocks²⁸ or coral reefs^{29,30} considered the 2D area of the seafloor alone; hence, results may have a large margin of uncertainty.

Given the above, a reliable, versatile, and widely reproducible method for assessing the biogeochemical functioning of benthic shallow-water communities in their natural environment is lacking. To address these challenges, we developed an end-to-end *in situ* incubation protocol that aims at measuring biogeochemical fluxes associated with whole benthic communities. The technique can be applied across a wide range of benthic shallow-water habitats, from simple (e.g., sediments) to complex (e.g., corals or rocky beds). We inform on material selection and construction processes to build cost-effective and easy to handle *in situ* chambers made from ridged polymethyl methacrylate cylinders. Combined with recent advances in computer-assisted photogrammetry, this approach offers a new way for accurately measuring all biogeochemical fluxes in a non-intrusive manner. We present data from laboratory tests, field incubations, and, subsequently, compare our results to data from a commonly applied protocol of estimating community budgets from incubations of single organisms. Lastly, we discuss how the method may be implemented in a variety of marine and aquatic ecological studies that include standard and manipulative experimental approaches.

3.3 Material and Methods

Construction of Benthic Incubation Chambers

Benthic chambers were constructed from 5 mm thick polymethyl methacrylate (PMMA) cylinders (diameter: 0.50 m, height: 0.39 m) with a removable, gas-tight lid of the same material (0.40 m total height) (Fig. 3.1; additionally, see Supplementary Material to Chapter 3 for a detailed overview of all parts required for the construction, prices, and vendors, as well as detailed design and assembly schematics in Fig. S3.1 – S3.3). The size was chosen to accommodate large communities with rigid features while still being easily handled by divers. The chambers are open at the bottom to be mounted over natural benthic communities. On soft-bottom substrates, the chambers are inserted into the ground down to 5 cm to seal off the incubation medium from the surrounding seawater. On hard-bottom substrates, where the chambers cannot be inserted into the ground, wide (20 cm) PVC skirts (Table S3.1) attached 5 cm above the base are used to minimize water intrusions. The lid-top can be fastened onto the chamber using M5 x 0.8 mm wing-head

PVC bolts (Table S3.1). A silicone O-ring (Table S3.1) sits in a gland to create a gas-tight seal between chamber and lid. Once mounted correctly, the chambers enclose a theoretical volume of 66.8 to 76.7 L of water (depending on the depth of insertion into the ground) and cover 0.2 m² of the seafloor.

Due to their flat surface, lids can be easily modified to accommodate measurement and sampling requirements for the desired experiment. In the setup presented here, all chambers were equipped with autonomous recording dissolved oxygen (DO) sensors (HOBO U26, Onset Computer Corporation, Cape Cod, USA; precision 0.02 mg L⁻¹, accuracy \pm 2%, automatic temperature and pressure compensated and salinity corrected), and HOBO Pendant® light loggers (Onset Computer Corporation, Cape Cod, USA).

Furthermore, the chambers were equipped with two sampling ports: 1) One one-way stopcock female to male luer-lock (Table S3.1); 2) one stopcock 3/4 inch with barbed hose adapter (Table S3.1). Among others, these sampling ports offer the possibility for controlled sampling of many biological and chemical variables, such dissolved organic carbon (DOC), dissolved inorganic nutrients, dissolved inorganic carbon (DIC), total alkalinity (TA), bacterial or viral samples.

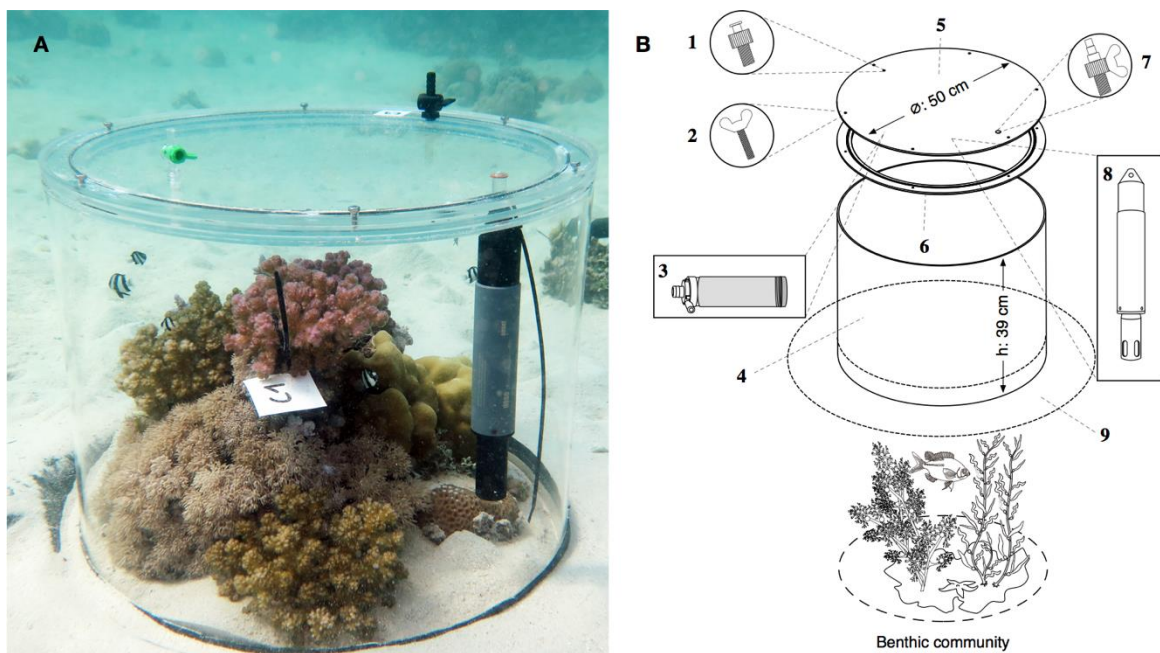


Figure 3.1 | Benthic incubation chamber deployed *in situ* over a natural coral reef community (A), and general layout of the chamber (B). (1) One one-way stopcock female to male luer-lock; (2) Six wing-head bolts to fasten lid; (3) Adjustable flow control circulation pump; (4) Main chamber body made from polymethyl methacrylate cylinders (50 cm diameter, 39 cm height); (5) Removable lid made from polymethyl methacrylate (0.5 cm thickness); (6) O-ring; (7) Stopcock 3/4 inch with hose barb adapter; (8) Temperature and dissolved oxygen recorder (HOBO U26); (9) PVC skirt. Note: The circulation pump in A is behind the tubular oxygen sensor.

All chambers were equipped with individual water circulation pumps to ensure that withdrawn water samples for later analysis are representative of the entire volume and to avoid the development of chemical gradients (Fig. S3.4). An adjustable flow control further allowed to mimic hydrodynamic conditions under ambient conditions. For this, 6 V DC motors (300 mA, 2 W) with a magnetic impeller (Table S3.1) were

powered by four 1.5 V AA mignon cells (2600 mAh) (Table S3.1). A low voltage pulse-width modulation (PMW) speed controller (Table S3.1) enables step-less controllable flow rates of 0.2 – 2 L min⁻¹. All electronic parts were encapsulated in a PVC tube (40 mm inner diameter, 150 mm length) (Table S3.1) with the pump on one end, and with a screw cap and a silicone O-ring (Table S3.1) at the back. The screw cap allows easy access to the electronics to exchange batteries, switching on/off of pumps, and to conduct maintenance works. The pump at the front end was secured and sealed off with non-toxic marine grade epoxy resin (Table S3.1).

General Procedures: Chamber Deployment, Water Sampling, and Cleaning

Chamber Deployment

The chambers can be deployed easily by two people either snorkeling or SCUBA diving depending on the study site. Chambers are first installed without their lids for easier maneuverability and to minimize pressure and wave-induced disturbance to the benthic substrate. The 39 cm-high chambers are carefully positioned over the benthic community of interest, and pushed into the sediment to a depth of 5 cm, thus enclosing a 34 cm high water column. The wide PVC skirts attached to the chambers are placed onto the substrate and weighed down by a heavy chain, rocks or rubble to further prevent water exchange. If the substrate does not allow to insert the chamber fully, the PVC skirt will sufficiently isolate the chamber from the surrounding water (see results of leakage testing below). At least one hour time should be given to let sediments settle before proceeding. Subsequently, the lid, equipped with pumps and sensors, is fitted to the chamber and secured in place with six wing-head bolts. The incubations start by closing the chambers' lid and sampling ports.

Water Sampling

Water samples for water chemistry parameters (e.g., DOC, DIC, DIN, TA, etc.) or other biological variables (e.g., eDNA) can be withdrawn from one of the two sampling ports at any time of the incubation. Small water samples can be withdrawn with syringes from the luer-lock valve. Larger volumes of water can be withdrawn from the barbed stopcock. We recommend opening both sampling ports when withdrawing a water sample to avoid a reduced pressure inside the chamber and to replace the withdrawn volume of water by water from outside the chamber rather than by sediment pore water. Considering that 200 mL of water is sufficient for the concurrent measurement of inorganic nutrients, TA, DIC, DOC, and fluorescent dissolved OM, a water exchange during sampling of 0.26% is negligible. Further, the dilution of the water body inside the chambers with surrounding seawater can be easily corrected for mathematically. Additionally, the two sampling ports are positioned opposite of each other on the lid, reducing the risk of sampling water from the inlet valve given sufficient mixing by the pumps.

Cleaning Procedures

After field deployment, the incubation chambers can be rinsed with fresh water. Wing-head screws, valves, and other attached parts can be removed and cleaned separately. All materials of the presented set-up can be washed with 4% HCl solution if necessary (e.g., for reliable DOC measurements). We recommend rinsing with deionized water before long-term storage.

Considerations for Calculating Accurate Community Fluxes

Surface Area and Volume Quantification of Structurally Complex Habitats

To evaluate physiological and biogeochemical processes of complex habitats, it is crucial to determine the volume and surface area of the enclosed benthic communities. Here, we quantified the 3D surface area and volume of a community in a chamber by photogrammetric techniques involving computer modelling discussed in Lavy et al. (2015)³¹ and Gutierrez-Heredia et al. (2016)³². The use of cloud computing and the availability of freeware make this tool widely accessible. Briefly, ~100 digital photographs are taken *in situ* from multiple angles of each community with a digital camera with an underwater housing (Fig. 3.2A). Using the software ReCap® (Autodesk Inc.), raw pictures can be uploaded into a cloud-based interface for further processing, thereby reducing the computational requirements of the users' machine. ReCap® automatically produces a digital 3D model from the photographs that can be downloaded within one hour and opened with the software interface. The colored model can be used for the determination of the community composition (Fig. 3.2B). From the mesh model (Fig. 3.2C), the 3D surface area and volume are calculated using internal tools of the same software.

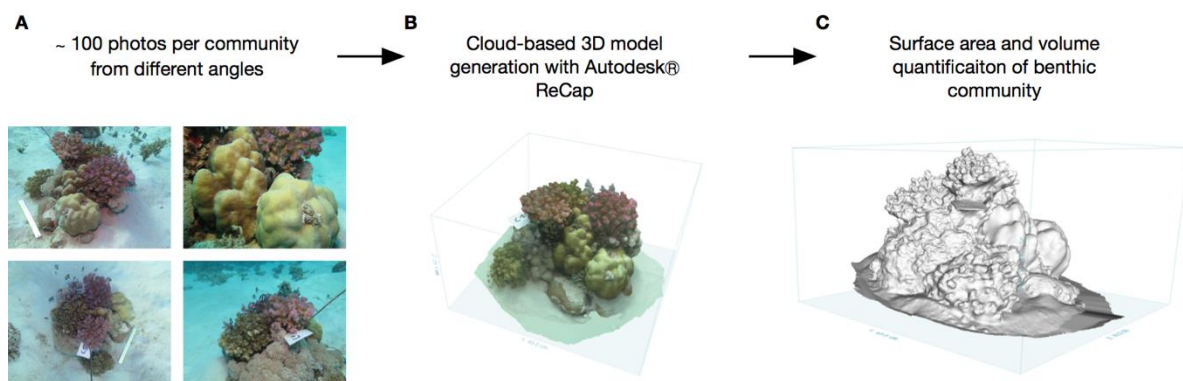


Figure 3.2 | Simplified workflow to generate 3D models for the assessment of community structure, surface area and volume of structurally complex benthic communities. **(A)** Around 100 photos are taken of the benthic community from different angles with a simple underwater digital camera (i.e., Canon PowerShot G12). **(B)** Pictures are uploaded for a cloud-based 3D model generation with the software ReCap® (Autodesk Inc.). Colored 3D models based on pictures are used for assessments of community structure and composition. **(C)** Software-integrated tools enable surface area and volume quantification.

The exact water volume (V) in each chamber during an incubation is calculated by subtracting the measured community volume (V_C) as well as the volume occupied by the sensors (V_S) and the pump (V_P) from the theoretical volume (V_T) enclosed by the chamber above the sediment line:

$$V = V_T - V_C - V_S - V_P$$

Calculating Community Fluxes from Discrete Water Samples and Continuous Measurements

Community fluxes of water chemistry parameters can be calculated from discrete water samples or from continuous measurements by sensors (e.g., dissolved oxygen loggers). All fluxes should be normalized to incubation water volume (V ; in L), incubation duration (I_T ; in h), and the surface area (SA ; in m^2) of the enclosed benthic community. Community fluxes for water chemistry variable (Var) can be calculated from discrete start-end point sampling as:

$$Var(t) = \left[\frac{(\Delta Var) \cdot V}{I_T \cdot SA} \right]$$

For variables that can be continuously measured (e.g., dissolved oxygen) community fluxes of monotonic metabolic processes (e.g., photosynthesis and respiration) can be calculated from linear regressions. Here, the slope (m) of a linear regression is used to calculate flux-rates as:

$$Var(t) = \left[\frac{m \cdot V}{SA} \right]$$

As full time series are often non-linear at times (e.g., the rate of O_2 initially decelerates as the organisms equilibrate after handling), calculations using the full time series can result in underestimating metabolic rates. Truncating the data to exclude these non-linearities manually is subjective and difficult to reproduce. Therefore, we recommend using the “LoLinR” package for R³³, which provides a flexible toolkit to implement local linear regression techniques to estimate biological rates from linear and non-linear time series data. Local linear regressions enhance the accuracy by estimating the slope of a linear subset of the time series as defined by linearity metrics underpinning the function (details in Olito et al. (2017)³³).

Performance Tests on Various Substrates under Laboratory and *In Situ* Conditions

Laboratory Assays for Leakage Testing and Light Transmission

To ensure that a watertight seal can be created around benthic communities, chambers were secured on different substrates in 200 L holding tanks in the laboratory according to the protocol above. Six replicate chambers were placed on coarse reef sand (1 – 3 mm grain size) and six on coarse rock/rubble pieces (~5 cm), respectively. After closing the chambers, red food color dye Allura Red (Red 40) was injected into the chambers via the luer-lock valve. All chambers were equipped with temperature-, light- and DO-loggers and the circulation pumps were switched on to simulate field deployment conditions. An initial 50 mL aliquot of water was withdrawn from each chamber and from the surrounding tank water (background control) using a syringe for initial concentrations. Each chamber was then left in the holding tank for 6 h before another water sample was collected from inside the chamber and the surrounding water. A Trilogy Laboratory Fluorometer with an absorbance module (Trilogy 7200-050) was used to measure the absorbance of light at 504 nm by each sample to determine if any dye had transferred from inside the chambers to the surrounding tank water. A series of volumetric dilutions made from a stock solution of known Allura Red concentrations (seven-point calibration) was used to determine the concentration of Allura Red in a sample.

Light transmission through 0.5 mm thick polymethyl methacrylate cylinders was tested with a LAMBDA 1050 UV/Vis/NIR Spectrophotometer (PerkinElmer) at 1 nm interval from 250 nm – 750 nm wavelength. In addition, light transmission was assessed *in situ* by comparing the data from light loggers deployed inside and outside of the chambers (details are described in the supplementary material to Chapter 3).

Incubations of Simple and Structurally Complex Benthic Substrates

To validate the versatility of the system on various substrates and conditions, incubations for DO production measurements were carried out on: a) hard-bottom communities: i.e., algae growing over a reef framework at 5 m water depth; b) hard-bottom communities on sand: i.e., assemblages of coral colonies on sand at 5 m water depth; c) carbonate sands at 5 m water depth in a reef lagoon; and d) mixed species seagrass meadows at 1.5 m water depth. In addition, to sensitize for the correct use of the chambers (i.e., activation of pumps, securing chambers with weights), we carried out incubations of coral colonies on sand with and without an active circulation pump system, and incubations of mixed species seagrass meadows at 1.5 m water depth under high wave-conditions with and without additional weights to secure the incubation chambers on the substrate. All incubations were performed concurring to the protocol above. Incubations lasted for 90 – 120 minutes. Incubations of different communities were carried out during different seasons in 2017, and absolute values should, therefore, not be compared. As any stress response from the organisms, water intrusions from the surrounding medium, or non-sufficient mixing by the pumps results in non-linear DO production rates, the ‘quality’ of the incubations was assessed by evaluating the linearity of DO fluxes

corrected for background seawater metabolism and normalized to community surface area. For this, the overall linearity in DO production of each incubation was tested by Pearson correlations of the full time series. In addition, we quantified the number of data points (given in % of the total number of data points of the full time series) that met the model assumptions for the local linear regressions. As recommended by the model developers, model assumptions are met if 20% of the data points follow a strictly linear trend. Hence, selected model parameters were $\alpha = 0.2$, with a linearity metric = $L\%$ ³³.

Case Study: Coral Reef Community Budgets of Primary Production and Comparison to *Ex Situ* Single-Organism Incubations

To illustrate the applicability over simple (i.e., sediments) and structurally complex (i.e., coral- and algae) communities, we conducted a case study at a coral reef in the Central Red Sea. Field tests were carried out at Abu Shosha reef located on the west coast of Saudi Arabia (22°18'16.3"N; 39°02'57.7"E) in July 2017. The reef is characterized by a patchwork of coral- and algae-dominated communities that are distributed on an area of coarse carbonate reef sand at a water depth of 4 – 7 m. For the incubations, four coral-dominated communities surrounded by sediment (> 40% coral cover, but less than 10% algal cover), four rocky communities overgrown by heterogeneous assemblages of algae surrounded by sediment (hereafter ‘algae-dominated’; > 40% algae, but less than 10% coral cover), and carbonate sediments (hereafter ‘sediments’) were selected haphazardly with a minimum distance of 3 m. All communities were incubated for measurements of net primary production (NPP) and respiration (R) according to the protocol above (detailed procedures for the case study can be found in the supplementary material). To estimate gross primary production (GPP), each R measurement was added to its corresponding NPP measurement ($NPP + |R| = GPP$), assuming that respiration rates in the light were equal to those derived from dark incubations (covered chambers) during the day³⁴. O₂ fluxes were converted into carbon (C) fluxes assuming a theoretical molar ratio of CO₂:O₂ = 1³⁵. For comparison with other benthic systems and methods, resulting contributions were expressed in mmol C m⁻² h⁻¹.

Subsequently, *in situ* community measurements were compared to *ex situ* community budgets estimated from single-organism incubations – a commonly applied technique to measure community budgets of structurally complex habitats, such as coral reefs. Community budgets from single organism incubations were estimated by an adapted protocol from Cardini et al. (2016)²¹. The details for the *ex situ* incubations are described in the supplementary material. Briefly, organisms representing the dominant functional components from benthic chambers during *in situ* incubations were incubated individually for NPP, R and GPP rates in the laboratory. Afterwards, *ex situ* fluxes of single-organism incubations were extrapolated to the metabolism in *in situ* chambers, considering the specific 3D area covered by the respective functional groups from the chambers’ communities and the volume of seawater included in the chambers.

3.4 Results

Leakage Testing

No significant difference between start ($1.32 \pm 0.05 \mu\text{mol L}^{-1}$) and end ($1.25 \pm 0.04 \mu\text{mol L}^{-1}$) concentration of Allura Red dye inside the incubation chambers was detected on coarse reef sands (mean concentrations reduced by 5.3 % within six hours; two-tailed t-test: p | t | = 0.2722) (Fig. 3.3). On rock/rubble, the concentration of Allura Red was significantly reduced by 12.4 % within six hours (from 1.37 ± 0.04 to $1.20 \pm 0.03 \mu\text{mol L}^{-1}$, respectively; two-tailed t-test: p | t | = 0.0057), indicating minimal water exchange under laboratory conditions (Fig. 3.3).

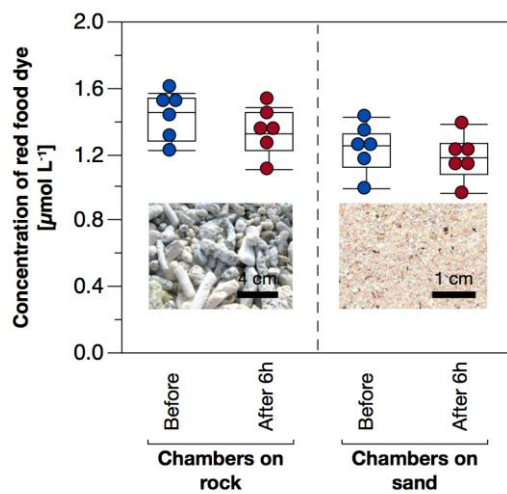


Figure 3.3 | Leakage test of incubation chambers on different substrates. Six replicate chambers each were placed in large holding tanks on rock/rubble pieces (~5 cm) and coarse reef sand (1 – 3 mm), and red food dye was injected into the chambers. The concentrations of Allura Red dye (determined by absorbance of light at 504 nm) was measured from samples in the chambers after adding the dye (referred to as 'Before') and after 6 hours of incubation (referred to as 'After 6h'). Boxplots showing the median (line across a box), quartiles (upper and lower bounds of each box) and extremes (upper and lower whisker). The ends of the whisker are set at $1.5 \times \text{IQR}$ above the third quartile (Q3) and $1.5 \times \text{IQR}$ below the first quartile (Q1). Scale bars are given in each picture.

Light

Spectral analysis showed a light transmission through the chamber material averaging 92% within PAR (photosynthetic active radiation; 400-700 nm) (Fig. 3.4A), while light within the UV range was attenuated (16% and 1% transmission for UVA and UVB, respectively). During field deployment, on average 9.4% reduced light availability within PAR was measured (90.6% transmission) for incubation chambers compared to outside of the chambers at the same time and water depth (Fig. 3.4B).

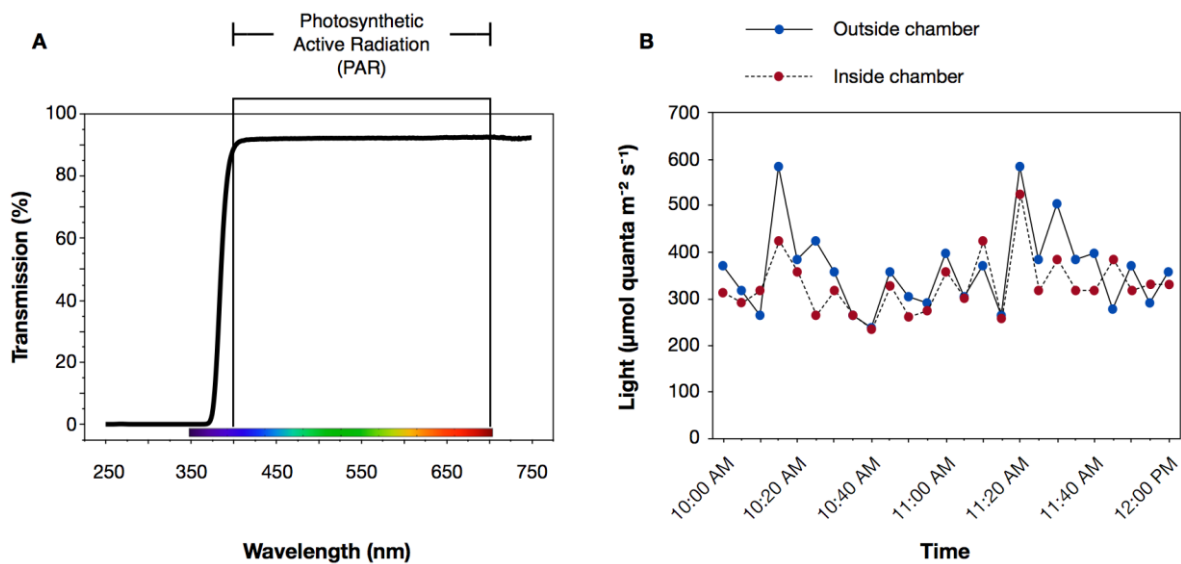


Figure 3.4 | Spectral transparency of benthic incubation chambers. (A) Transmittance of the polymethyl methacrylate material (0.5 mm thickness) measured with a spectrophotometer (UV-2450, Shimadzu Corporation) at a 1 nm wavelength interval. (B) Simultaneous measurements of light (photosynthetic active radiation spectra) inside and outside of one incubation chamber deployed at 5 m water depth in June 2017.

Incubations of Hard-Bottom and Soft-Bottom Communities

Incubations of both structurally complex (i.e., ‘rocks with algae’ and ‘corals on sand’) and simple (i.e., ‘carbonate reef sediments’ and ‘seagrasses’) habitats revealed a production of DO over time (Fig. 3.5A). Incubation chambers that were deployed on hard-bottom substrates (i.e., rocks with algae) had detectable water intrusions from outside the chamber, resulting in an average linearity of the DO production of $r^2 = 0.916 \pm 0.032$ (Pearson correlation; $n = 4$), where 20 – 48 % of the data points could be included in the local linear regressions by the LolinR function. Incubations that took place on sediments (i.e., corals on sand, carbonate sediments, and seagrasses), showed a more linear DO production ($r^2 = 0.994 \pm 0.002$; Pearson correlation; $n = 12$), where 51 – 90 % of the data points could be included in the local linear regressions.

Incubations of coral-dominated communities on sand with and without active circulation pumps highlighted the necessity of the pumps in mixing the water column within the chambers (Fig. 3.5B). The lack of active circulation pumps resulted in non-linear DO production ($r^2 = 0.721 \pm 0.114$; Pearson correlation; $n = 3$), where only 15 – 22 % of the data points could be included in the local linear regressions. In contrast, sufficient water circulation with active pumps resulted in a linear DO production ($r^2 = 0.997 \pm 0.002$; Pearson correlation; $n = 4$), where 58 – 88 % of the data points could be included in the local linear regressions.

In an intertidal habitat with high wave action, chambers without additional weights on the PVC skirts were shaken by the water movement, resulting in a non-linear DO production ($r^2 = 0.689 \pm 0.211$; Pearson correlation; $n = 4$; < 20 – 50 % of the data points included in local linear regressions) due to water intrusions

(Fig. 3.5C). In contrast, 5 kg heavy chains on the PVC skirts secured the chambers sufficiently onto the substrates, resulting in linear DO production rates ($r^2 = 0.982 \pm 0.009$; Pearson correlation; $n = 4$; 41 – 84 % of the data points included in local linear regressions).

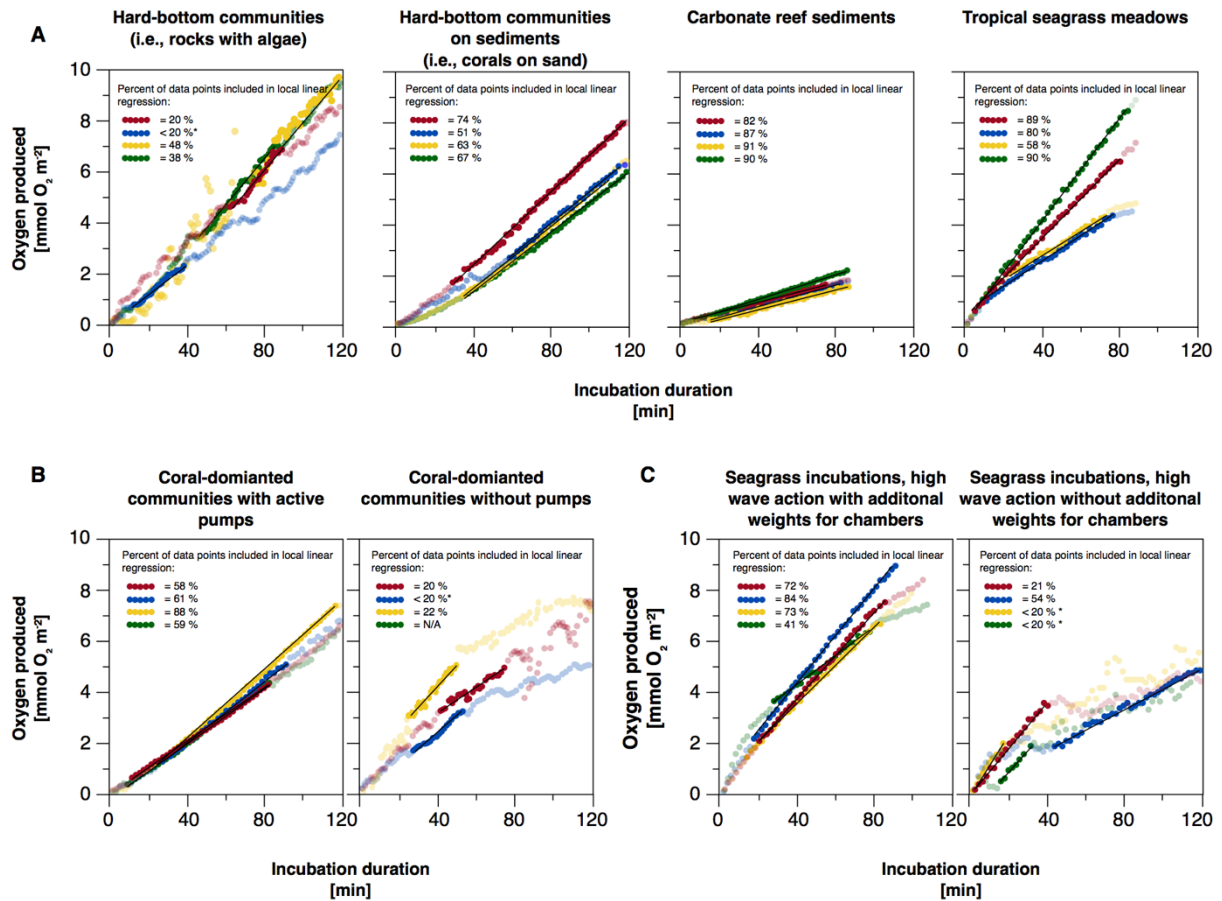


Figure 3.5 | Dissolved oxygen production during incubations of various substrates (A), with/without active circulation pumps (B), and under high wave action in an intertidal zone with/without additional weights (C). Shown is the production of dissolved oxygen over time (incubation periods ranging from 90 to 120 minutes), corrected for seawater background metabolism and normalized to the surface area of the incubated substrate. Points of different colors represent independent replicate incubations of the respective substrate. Opaque points with lines (●, ●, ●, and ●) represent data points of incubations that were included by the “LoLinR” package for R (Olito et al., 2017)³³ in a local linear regression for dissolved oxygen calculations. The amount of points included in the local linear regression is given in percent in each plot. As recommended by Olito et al. (2017)³³, an asterisk indicates that less than 20% of the data points followed a linear trend, hence model assumptions were not met. Transparent points (●, ●, ●, and ●) represent all data point of the respective incubation that did not follow a linear trend.

Community-Wide Budgets for Photosynthesis and Respiration in Coral Reef Habitats

In situ incubations revealed a significant difference between benthic coral reef habitats (i.e., *coral-dominated* vs. *algae-dominated* vs. *sediments*) for NPP, R and GPP (Fig. 3.6A; detailed statistical test results in Table S3.3 of the supplementary material). Algae-dominated communities exhibited 3- and 9-fold higher NPP rates ($8.99 \pm 1.18 \text{ mmol C m}^{-2} \text{ h}^{-1}$) compared to coral-dominated communities and sediments, respectively (3.29

± 0.23 and 0.98 ± 0.41 mmol C m⁻² h⁻¹), while respiration rates were 90% higher in algae-dominated communities (-6.46 ± 0.32 mmol C m⁻² h⁻¹) compared to both coral-dominated communities and sediments (-3.37 ± 0.26 mmol C m⁻² h⁻¹, and -3.40 ± 0.31 mmol C m⁻² h⁻¹, respectively). This resulted in 2.3-fold higher GPP values (15.45 ± 1.32 mmol C m⁻² h⁻¹) of algae-dominated communities, compared to communities dominated by corals (6.65 ± 0.47 mmol C m⁻² h⁻¹) and 3.5-fold higher GPP values as compared to sediments (4.38 ± 0.15 mmol C m⁻² h⁻¹).

We assessed the performance of *in situ* incubations by monitoring that the temporal patterns of DO concentrations remained linear during incubations. The average correlation coefficient from all light incubations was $r^2 = 0.996 \pm 0.002$ (Pearson correlation; $n = 12$; $p < 0.0001$ in all cases) and $r^2 = 0.991 \pm 0.004$ (Pearson correlation; $n = 12$; $p < 0.0001$ in all cases) for all dark incubations, with 73 – 90 % and 69 – 91 % of the data points included in the local linear regressions, respectively. In an exemplary chamber with a coral-dominated community, DO increased from 5.12 to 7.84 mg L⁻¹ during the light showing a highly linear relationship (Pearson correlation: $r^2 = 0.997$, $p < 0.0001$) to the incubation time (Fig. 3.6B). Further, the water temperature inside the chamber increased slightly by 0.4 °C during the incubation (from 32.0 to 32.4 °C. In contrast, during the 2 h dark incubation of the same community, DO decreased from 5.00 to 2.02 mg L⁻¹ within 2 h (Pearson correlation: $r^2 = 0.993$, $p < 0.0001$) (Fig. 6C). The water temperature remained stable (31.9 °C before and after the incubation).

Comparison of *In Situ* and *Ex Situ* Estimates of Community-Wide Oxygen Fluxes

The comparison of community oxygen fluxes between *in situ* and *ex situ* incubations revealed significant differences between these methods (Fig 3.6; detailed statistical test results in Table S3.3 of the supplementary material). Community fluxes derived from *ex situ* incubations showed significantly lower R rates for each of the three habitats compared to *in situ* incubations (25, 62, and 92% lower for coral, algae, and sediments, respectively). Further, *ex situ* incubations overestimated NPP by 35% in the case of coral-dominated communities, and by 82% in sediments. While GPP among the two methods was similar in coral-dominated communities, it was underestimated by *ex situ* incubations by > 50% both in algae and sediments. As a consequence, *ex situ* extrapolations were not able to resolve differences in community metabolism between algae and coral-dominated communities.

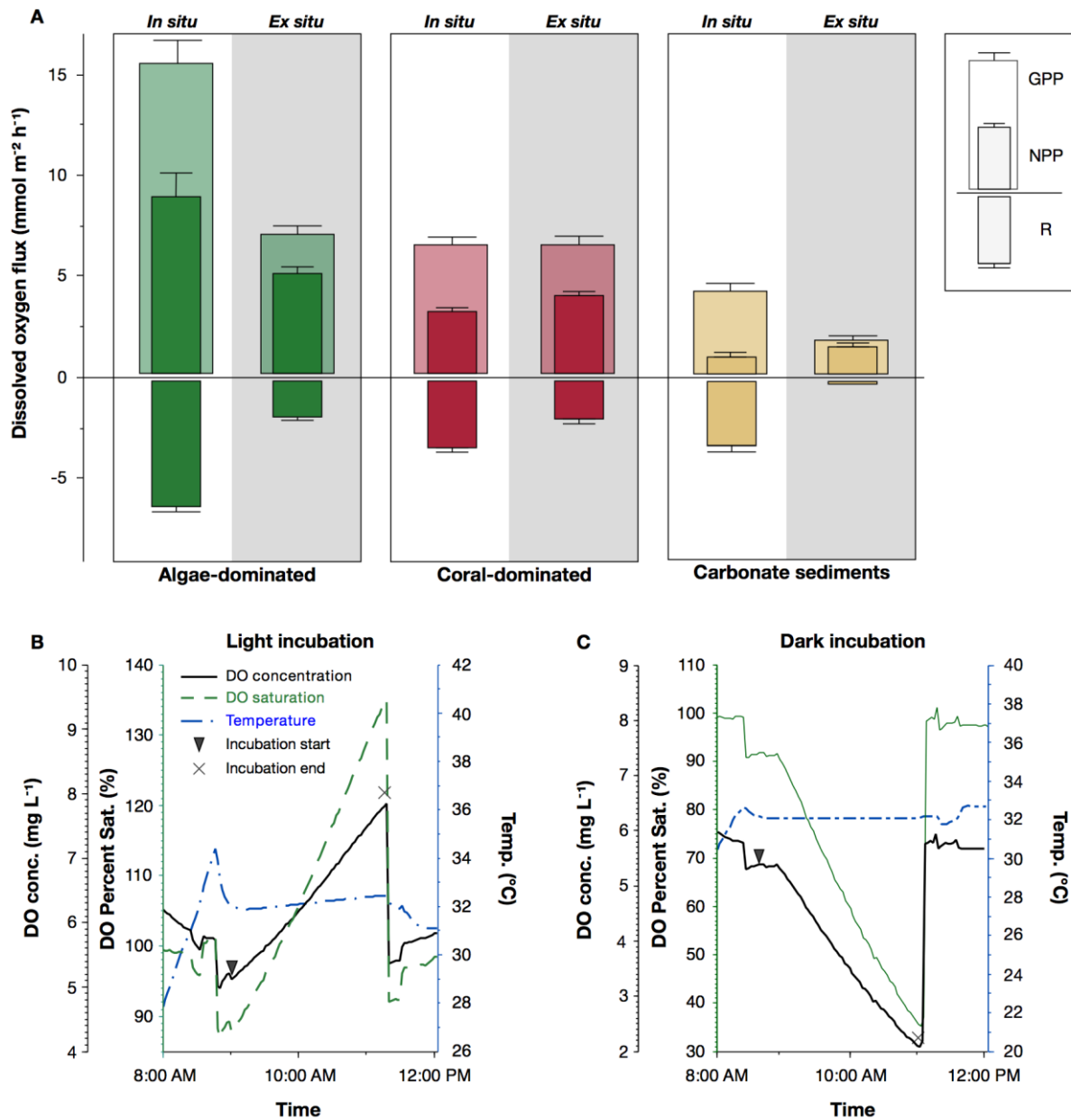


Figure 3.6 | Community budgets of dissolved oxygen fluxes from *in situ* benthic chamber incubations and *ex situ* single organism measurements of algae- and coral-dominated reef habitats and carbonate reef sediments. Community fluxes of dissolved oxygen (DO) of the respective native communities (*in situ*) and estimated budgets from single-organism incubations (*ex situ*) (A). Sensor readings of DO and temperature (Temp.) during two-hour light (B) and dark (C) incubations of one representative coral-dominated community. GPP = Gross primary production; NPP = Net primary production; R = Respiration; DO conc. = Dissolved oxygen concentration; DO Percent Sat. = Dissolved oxygen percent saturation. Values of (A) are given as means ($n = 4$) \pm standard error.

3.5 Discussion

Most marine and aquatic ecosystems are presently under threat due to the combined effects of anthropogenic perturbations³. Understanding and predicting the responses of these ecosystems to stress requires considering processes across all levels of biological organization⁶. While current knowledge is

advancing rapidly on scales ranging from molecular to whole-organism levels, our understanding of responses of whole communities in their natural environment is limited due to logistical and methodological constraints. In particular, measuring responses of communities with complex, three-dimensional structures is challenging, as many biogeochemical variables are affected by the volume and surface area of the organisms, with no tools available to quantify, non-intrusively, these variables *in situ*. Thus, it is crucial to develop a tool to accurately assess biogeochemical processes central to the ecological success of structurally complex benthic communities *in situ*. We have demonstrated that reliable and reproducible metabolic data can be generated using a combination of freely accessible photogrammetry tools and low-cost, easily deployable incubations chambers.

Advantages of the new *In Situ* Chamber Incubation Method

A major advantage of the here-described protocol is the ability to measure metabolic and biogeochemical processes in various benthic habitats, with both simple and complex structures. In the existing literature, a multitude of *in situ* incubation chambers are presented. Especially abundant are systems for the incubation of bare sediments^{24–26} or seagrass meadows²⁷, while approaches targeting hard-bottom communities (e.g., coral assemblages or rocks with algae) are scarce^{28,30}. In addition, most chambers are purpose-built for one specific study and community type, limiting the ability to compare ecosystem functions across a wide range of benthic habitats.

Both the laboratory and field assays demonstrated that the here-presented system could be deployed successfully on sediments, seagrass meadows, rocky habitats and coral assemblages – some of the most conspicuous benthic shallow water habitats³⁶. Thereby, a combination of hardware features and the post-processing of data renders the approach extremely versatile. The use of PMMA cylinders offers multiple advantages, such as that they are commercially available in large sizes and at low costs. Particularly hard-bottom communities (e.g., branching coral colonies) require chambers that are large enough to be mounted over rigid features (e.g., coral branches). The size of 50 cm diameter and 40 cm height has, thereby, proven more versatile over systems using small chambers that cover less surface area^{27,37}, or dome-shaped chambers³⁸ that are restricted in their height in the peripheries. The removable lid maintains the good maneuverability underwater that, usually, goes along with smaller devices only³⁰. As the chambers are constructed entirely from PMMA, incubated communities are not subjected to shading by opaque materials (e.g., as used for frames in Haas et al. (2013)³⁹ for stabilization), and the light transmission (90 – 92% within the PAR spectrum) exceeds values reported for flexible systems made from polyvinyl chloride¹⁷. Thereby, the risks to underestimate processes related to photosynthesis are reduced. In addition, PMMA is durable and can be acid-washed, as needed for precise measurements of DOC and related compounds. The large, rigid and level surfaces of the chambers allow easy customization, permitting multiple sensors and additional device or sampling port attachments that can promote to use the system for numerous experimental strategies. As such, the dual two-way-valve mechanism supports additions and removals of small and large amounts of water to be made to and from the chambers without disturbance of the incubation.

A major consideration when deploying benthic chambers is the mixing of the enclosed water. Despite its importance, water circulation systems are often disregarded as the individual power supply and a water-tight encapsulation is deemed challenging. We present custom-made, rechargeable pumps that ensure constant mixing within the chambers. The water movement simulates as closely as possible the hydrodynamic conditions of the undisturbed benthic substrate and ensures that water phase measurements reflect the average conditions inside the chamber. The correct alignment of the pump's outflow and the adjustable flow control creates a unidirectional current flow in round chambers, resulting in a radial pressure gradient that simulates sediment percolation as generated by natural boundary flow-topography interactions^{40–42}.

Besides the hardware, one of the most important features of the here-presented approach is the use of cloud-based photogrammetry tools. The freely available software enables, for the first time, non-intrusive assessments of the composition, volume and surface area of benthic communities^{31,32}. This step is essential to relate changes in the water chemistry to the benthic community of interest and to make results widely comparable across regions and ecosystems.

Lastly, an important advantage of the system is that all materials required to build the incubation chambers are commercially available online at relatively low cost (~ 250 USD per chamber – including pumps, excluding sensors) (Table S3.1). In combination with minimal construction efforts (i.e., simple drilling, gluing, etc.) and an available protocol, the system can be used with high replication and at high temporal and spatial resolution without the need for costly infrastructure during deployment and sampling. Thereby, the system can increase the sampling scale of *in situ* measurements and facilitates precise, standardized flux measurements across many different benthic habitats.

Lessons Learned from Pilot Deployments

The field deployment of the autonomous operating chambers provided *in situ* metabolic data from various benthic shallow-water habitats. The chambers performed consistently when deployed on soft-bottom substrates. On sediments and seagrass meadows, community-wide DO production rates were highly linear over time, and no significant water intrusions were detected. The large PVC skirts around the chambers maintained a good seal from the surrounding water on most substrates. Yet, the linearity of DO fluxes was slightly reduced as some water intrusions were detected on rocky substrates, despite that reliable DO production rates were calculated by local linear regressions. For future considerations, we recommend additional soft edges (e.g., thick closed-cell polystyrene foam) at the bottom of the chambers that, if compressed, fill irregularities in the substrate, forming a good seal between the rock and chamber²⁸. DO production rates during field tests were not linear when the circulation pumps were either switched off (indicator for stratification within the chambers) or when chambers were not secured to the substrates with weights in an intertidal habitat with strong waves (indicator for water intrusions). These tests highlight that special attention should be paid to use and deploy the chambers correctly to achieve reliable measurements. All incubations had in common that the rate of O₂ production initially decelerates as the organisms

equilibrate after handling and closing the chambers. Thereby, the use of the *LolinR* package for local linear regressions offers the advantage to use non-linear time-series data for calculating monotonic metabolic processes³³. We further highlight the importance of including continuous monitoring of variables (e.g., dissolved oxygen). Such measurements allow identifying of seawater intrusions and improper mixing in the chambers, thereby inform on possible confounding factors for other non-continuously monitored variables. If sensors for continuous measurements cannot be used for a variable of interest, water samples should be taken after an initial equilibration period of 10 – 20 minutes.

We highlight the versatility of the chambers in a case study calculating community-wide photosynthesis and respiration budgets of different coral reef communities of the Central Red Sea. The standardized protocol enabled a direct comparison between structurally complex (i.e., coral- and algae-dominated reef communities) and more simple, planar (i.e., sediments) habitats. Thereby, oxygen fluxes of sediments were in the same order of magnitude to previous studies from the Red Sea⁴³ and elsewhere⁴¹ that used small (5 – 6 L) stirred benthic chambers. A direct comparison to values derived from *in situ* incubations of complex habitats (i.e., coral- and algae-dominated communities) is not possible, as no comparable approach has been applied before. Consequently, we related resulting oxygen fluxes from our *in situ* approach to estimated community budgets from *ex situ* single-organisms incubations from the same reef. While in the same order of magnitude, an apparent trend was detected: Community budgets from *ex situ* single-organism incubations, as a conventional technique, tended to overestimate NPP, while community-wide R and GPP rates were underestimated by up to 90%. This tendency is also evident when comparing our findings to previous coral reef community budgets from single-organism incubations^{20,21}. Using this traditional *ex situ* approach, communities may be disturbed, and cryptic habitats, and particularly cracks and crevices within the reef matrix are not considered. Hence, studies of benthic fluxes in the natural environment result in more realistic estimates, since cryptic habitats encompass about 60-75% of the total surface area of the reef⁴⁴. The organisms inhabiting the cryptic spaces (e.g., sponges, bryozoans, and tunicates) are generally not included in *ex situ* budgets, however, they metabolize organic matter in the order of 15-30 % of the gross production of a coral reef^{45,46}.

During all experiments, all system components proved extremely reliable. Importantly, the “plug and play” design of system enabled two divers to deploy up to eight chambers and to start the incubations within 45 min of dive time. An additional dive time of around 5 – 10 min will allow taking a sufficient number of pictures from each community for a later 3D model generation.

Before the final experimental application of chambers, the users should identify the optimal incubation time, and biomass to water volume ratio, to avoid anoxic or hypoxic conditions during incubations of communities of interest. Hence, due to the large size of the selected coral reef communities of the case study, incubations were already terminated after two hours. At this time, the O₂ saturation in the chambers reached values of 135 % during light, and 35 % during dark incubations. The black PVC sleeves for each chamber provided a way to measure dark respiration rates during the day, that can be considered similar to respiration rates during the night³⁴. Sleeves are not needed for respiration measurements during the night.

Limitations of Benthic *In Situ* Incubations

Overall, no direct limitations regarding deployment, replication, and reproducibility of *in situ* incubations were observed during our field testing. However, some general limitations with benthic chambers include: (i) Depending on the size of the community relative to the water volume, measurements can only be conducted for a few hours out of the day, making daily rates challenging to obtain. Longer incubations would require replacing the seawater periodically to maintain natural conditions (e.g., as in Tait & Schiel (2010)²⁸); (ii) Although the chambers are among the largest currently available, size constraints still limit incubations to relatively small assemblages, and results may not necessarily reflect all aspects of fully sized communities; (iii) PMMA effectively removes most UV radiation, hence, the chambers possibly affect measured rates of photosynthesis for very shallow waters, where UV may inhibit some photosynthetic processes; (iv) Some environments may be too energetic for using enclosures or do not enable to achieve a good isolation of the water. Additional weights, soft edges on the bottom and more extended PVC flaps on the sides may improve the sealing on hard substrates. We recommend the execution of a leakage-test when using the chambers in a new location/type of substrate; and (v) Large incubation chambers provide important information about community-wide metabolic and biogeochemical fluxes, however, individual incubations may be necessary to complement ecological information about the contribution of a particular group or taxa to the community functioning.

Potential Use in Marine and Aquatic Research

Although this study focused on tropical benthic shallow-water communities, the method can easily be applied to any benthic community of interest that is accessible from land or within the limits of a scientific diving operation. As a descriptive tool at the community level, the chambers offer a new way to achieve reliable data of biogeochemical functioning in response to natural and anthropogenic changes, as synergistic and antagonistic interactions between organisms are not considered when organisms are incubated separately. We highlight the possibility to measure multiple parameters simultaneously (through sensors and water sampling) that can help linking responses that have often been assessed independently only, or where high species diversity and biotic interactions shape ecosystem functions.

Importantly, the presented approach can easily be used in experimental and manipulative strategies to quantify community functional responses to relevant global and local disturbances. While not pursued in the initial construction phase, the large rigid surfaces and the individual power supply of each chamber can support additional accessories, such as peristaltic dosing pumps, immersion heaters or pH flow feed-back control systems as applied previously^{47,48}. These developments should not be considered as a limitation to the existing approach but rather highlight the advantages of such an adaptable system.

Lastly, flux measurements with benthic chambers can provide a practical tool in quantifying gas (e.g., methane, nitrous oxide, carbon dioxide) emissions from, and carbon sequestration capacity by (known as 'blue carbon') highly productive benthic ecosystems (e.g., seagrass meadows or algal beds) (reviewed in

Fourqurean et al. (2017)⁴⁹). This information may be critical for assessing the capacity these ecosystems have for mitigating climate change ^{50,51}.

Conclusion

The here-presented incubation chambers offer an easy and cost-effective sampling solution that overcomes some challenges of conventional respirometry chambers. By allowing non-destructive, *in situ* metabolic and biogeochemical analysis of both simple and structurally complex benthic communities, the presented chambers offer a versatile platform for novel applications and experimental strategies. Measuring the effects of community interactions underlying benthic-pelagic biogeochemical processes may rapidly advance our understanding of ecosystem functioning and complement findings from aquaria and mesocosm studies. In doing so, the platform can transcend the boundaries of current research in multiple directions: a) Providing a standardized method that can be applied across multiple habitats; b) Measuring the response of whole communities, rather than from isolated organisms; c) Overcoming the shortage of observational and manipulative studies carried out directly in the field, thus producing widely-applicable and realistic findings; and c) Enhancing our mechanistic understanding of how environmental drivers modulate particular processes across different habitats.

3.6 Acknowledgments

We are grateful to the personnel from the King Abdullah University of Science and Technology (KAUST) Coastal and Marine Resources Core Lab for logistical support. The authors would also like to thank Luis Ribeiro da Silva, Rodrigo Villalobos and João Cúrdia who helped during fieldwork. We thank Fatima Mamhud, Vincent Saderne, and Ute Langner for the help with seagrass incubations. This work was supported by KAUST baseline funding to BHJ.

3.8 References

1. Harley, C. D. G. *et al.* The impacts of climate change in coastal marine systems. *Ecol. Lett.* **9**, 228–241 (2006).
2. Lotze, H. K. *et al.* Depletion, degradation, and recovery potential of estuaries and coastal seas. *Science (80-.)*. **312**, 1806–1809 (2006).
3. Halpern, B. S. *et al.* A Global Map of Human Impact on Marine Ecosystems. *Science (80-.)*. **319**, 948–952 (2008).
4. Cloern, J. E. *et al.* Human activities and climate variability drive fast-paced change across the world's estuarine-coastal ecosystems. *Glob. Chang. Biol.* **22**, 513–529 (2016).
5. Griffiths, J. R. *et al.* The importance of benthic-pelagic coupling for marine ecosystem functioning in a changing world. *Glob. Chang. Biol.* **23**, 2179–2196 (2017).
6. Brierley, A. S. & Kingsford, M. J. Impacts of Climate Change on Marine Organisms and Ecosystems. *Curr. Biol.* **19**, R602–R614 (2009).
7. Russell, B. D., Thompson, J. A. I., Falkenberg, L. J. & Connell, S. D. Synergistic effects of climate change and local stressors: CO₂ and nutrient-driven change in subtidal rocky habitats. *Glob. Chang. Biol.* **15**, 2153–2162 (2009).
8. Comeau, S., Carpenter, R. C., Lantz, C. A. & Edmunds, P. J. Ocean acidification accelerates dissolution of experimental coral reef communities. *Biogeosciences* **12**, 365–372 (2015).
9. Althea, F. P. M. & Duffy, J. E. Foundation species identity and trophic complexity affect experimental seagrass communities. *Mar. Ecol. Prog. Ser.* **556**, 105–121 (2016).
10. Wagenhoff, A., Lange, K., Townsend, C. R. & Matthaei, C. D. Patterns of benthic algae and cyanobacteria along twin-stressor gradients of nutrients and fine sediment: a stream mesocosm experiment. *Freshw. Biol.* **58**, 1849–1863 (2013).
11. Bellworthy, J. & Fine, M. The Red Sea Simulator: A high-precision climate change mesocosm with automated monitoring for the long-term study of coral reef organisms. *Limnol. Oceanogr. Methods* **16**, 367–375 (2018).
12. Riebesell, U., Fabry, V. J., Hansson, L. & Gattuso, J.-P. *Guide to Best Practices in Ocean Acidification Research and Data Reporting. Report of international research workshop on best practices for ocean acidification research (19-21 November 2008 in Kiel, Germany)* (2010). doi:10.2777/58454
13. Falter, J. L., Lowe, R. J., Atkinson, M. J., Monismith, S. G. & Schar, D. W. Continuous measurements of net production over a shallow reef community using a modified Eulerian approach. *J. Geophys. Res. Ocean.* **113**, 1–14 (2008).
14. Gattuso, J. P., Pichon, M., Delesalle, B., Canon, C. & Frankignoulle, M. Carbon fluxes in coral reefs. I. Lagrangian measurement of community metabolism and resulting air-sea CO₂disequilibrium. *Mar. Ecol. Prog. Ser.* **145**, 109–121 (1996).
15. Shaw, E. C., Phinn, S. R., Tilbrook, B. & Steven, A. Comparability of Slack Water and Lagrangian Flow Respirometry Methods for Community Metabolic Measurements. *PLoS One* **9**, e112161 (2014).
16. Monsen, N. E., Cloern, J. E., Lucas, L. V. & Monismith, S. G. A comment on the use of flushing time, residence time, and age as transport time scales. *Limnol. Oceanogr.* **47**, 1545–1553 (2002).
17. Camp, E. F. *et al.* The 'Flexi-Chamber': A novel cost-effective in situ respirometry chamber for coral physiological measurements. *PLoS One* **10**, 1–21 (2015).
18. Sawall, Y., Al-Sofyani, A., Banguera-Hinestroza, E. & Voolstra, C. R. Spatio-temporal analyses of Symbiodinium physiology of the coral *Pocillopora verrucosa* along large-scale nutrient and temperature gradients in the Red Sea. *PLoS One* **9**, 1–12 (2014).

19. Ferrier-Pagès, C. *et al.* In situ assessment of the daily primary production of the temperate symbiotic coral *Cladocora caespitosa*. *Limnol. Oceanogr.* **58**, 1409–1418 (2013).
20. Naumann, M. S., Jantzen, C., Haas, A. F., Iglesias-Prieto, R. & Wild, C. Benthic primary production budget of a Caribbean reef lagoon (Puerto Morelos, Mexico). *PLoS One* **8**, (2013).
21. Cardini, U. *et al.* Budget of Primary Production and Dinitrogen Fixation in a Highly Seasonal Red Sea Coral Reef. *Ecosystems* **19**, 771–785 (2016).
22. Eidens, C. *et al.* Benthic primary production in an upwelling-influenced coral reef, Colombian Caribbean. *PeerJ* **2**, e554 (2014).
23. Hughes, D. J., Atkinson, R. J. A. & Ansell, A. D. A field test of the effects of megafaunal burrows on benthic chamber measurements of sediment-water solute fluxes. *Mar. Ecol. Prog. Ser.* **195**, 189–199 (2000).
24. L’Helguen, S. *et al.* A novel approach using the ¹⁵N tracer technique and benthic chambers to determine ammonium fluxes at the sediment-water interface and its application in a back-reef zone on Reunion Island (Indian Ocean). *J. Exp. Mar. Bio. Ecol.* **452**, 143–151 (2014).
25. Tengberg, A. *et al.* Benthic chamber and profiling landers in oceanography—a review of design, technical solutions and functioning. *Prog. Oceanogr.* **35**, 253–294 (1995).
26. Rasheed, M., Wild, C., Jantzen, C. & Badran, M. Mineralization of particulate organic matter derived from coral-reef organisms in reef sediments of the Gulf of Aqaba. *Chem. Ecol.* **22**, 13–20 (2006).
27. Silva, J., Santos, R., Calleja, M. L. & Duarte, C. M. Submerged versus air-exposed intertidal macrophyte productivity: From physiological to community-level assessments. *J. Exp. Mar. Bio. Ecol.* **317**, 87–95 (2005).
28. Tait, L. W. & Schiel, D. R. Primary productivity of intertidal macroalgal assemblages: Comparison of laboratory and in situ photorespirometry. *Mar. Ecol. Prog. Ser.* **416**, 115–125 (2010).
29. Yates, K. K. & Halley, R. B. Measuring coral reef community metabolism using new benthic chamber technology. *Coral Reefs* **22**, 247–255 (2003).
30. Haas, A. F. *et al.* Influence of coral and algal exudates on microbially mediated reef metabolism. *PeerJ* **1**, e108 (2013).
31. Lavy, A. *et al.* A quick, easy and non-intrusive method for underwater volume and surface area evaluation of benthic organisms by 3D computer modelling. *Methods Ecol. Evol.* **6**, 521–531 (2015).
32. Gutierrez-Heredia, L., Benzoni, F., Murphy, E. & Reynaud, E. G. End to End Digitisation and Analysis of Three-Dimensional Coral Models, from Communities to Corallites. *PLoS One* **11**, e0149641 (2016).
33. Olito, C., White, C. R., Marshall, D. J. & Barneche, D. R. Estimating monotonic rates from biological data using local linear regression. *J. Exp. Biol.* jeb.148775 (2017). doi:10.1242/jeb.148775
34. Bidwell, R. G. S. Photosynthesis and light and dark respiration in freshwater algae. *Can. J. Bot.* **55**, 809–818 (1977).
35. Clavier, J., Boucher, G. & Garrigue, C. Benthic respiratory and photosynthetic quotients in a tropical lagoon. *Life Sci.* **317**, 937–942 (1994).
36. Diaz, R. J., Solan, M. & Valente, R. M. A review of approaches for classifying benthic habitats and evaluating habitat quality. *J. Environ. Manage.* **73**, 165–181 (2004).
37. Migné, A., Trigui, R. J., Davoult, D. & Desroy, N. Benthic metabolism over the emersion - immersion alternation in sands colonized by the invasive Manila clam *Ruditapes philippinarum*. *Estuar. Coast. Shelf Sci.* **200**, 371–379 (2018).

38. Smith, R. L., Böhlke, J. K., Repert, D. A. & Hart, C. P. Nitrification and denitrification in a midwestern stream containing high nitrate: In situ assessment using tracers in dome-shaped incubation chambers. *Biogeochemistry* **96**, 189–208 (2009).
39. Haas, A. F. *et al.* Influence of coral and algal exudates on microbially mediated reef metabolism. *PeerJ* **2013**, 1–28 (2013).
40. Glud, R. N., Forster, S. & Huettel, M. Influence of radial pressure gradients on solute exchange in stirred benthic chambers. *Mar. Ecol. Prog. Ser.* **141**, 303–311 (1996).
41. Rasheed, M., Wild, C., Franke, U. & Huettel, M. Benthic photosynthesis and oxygen consumption in permeable carbonate sediments at Heron Island, Great Barrier Reef, Australia. *Estuar. Coast. Shelf Sci.* **59**, 139–150 (2004).
42. Huettel, M. & Rusch, A. Transport and degradation of phytoplankton in permeable sediment. *Limnol. Oceanogr.* **45**, 534–549 (2000).
43. Wild, C. *et al.* Coral sand O₂ uptake and pelagic-benthic coupling in a subtropical fringing reef, Aqaba, Red Sea. *Aquat. Biol.* **6**, 133–142 (2009).
44. Richter, C. & Wunsch, M. Cavity-dwelling suspension feeders in coral reefs - A new link in reef trophodynamics. *Mar. Ecol. Prog. Ser.* **188**, 105–116 (1999).
45. Maldonado, M., Ribes, M. & van Duyl, F. C. *Nutrient Fluxes Through Sponges. Biology, Budgets, and Ecological Implications. Advances in Marine Biology* **62**, (Elsevier Ltd., 2012).
46. de Jongh, F. & Van Duyl, F. C. The Impact of Suspension Feeders in Cryptic Habitats on the Trophodynamics of Coral Reefs. *Methods* (2004).
47. Marker, M. *et al.* The coral proto - free ocean carbon enrichment system (CP-FOCE): Engineering and development. in *OCEANS'10 IEEE SYDNEY* 1–10 (IEEE, 2010). doi:10.1109/OCEANSSYD.2010.5603603
48. Kline, D. I., Kuntz, N. M., Breitbart, M., Knowlton, N. & Rohwer, F. Role of elevated organic carbon levels and microbial activity in coral mortality. *Mar. Ecol. Prog. Ser.* **314**, 119–125 (2006).
49. Fourqurean, J. W. *et al.* Coastal Blue Carbon. *Habitat Conserv.* 860 (2017).
50. Yarbro, L. A. & Carlson, P. R. Community oxygen and nutrient fluxes in seagrass beds of Florida Bay, USA. *Estuaries and Coasts* **31**, 877–897 (2008).
51. McGlathery, K. J., Anderson, I. C. & Tyler, A. C. Magnitude and variability of benthic and pelagic metabolism in a temperate coastal lagoon. *Mar. Ecol. Prog. Ser.* **216**, 1–15 (2001).
52. Roth, F. *et al.* Data from: An in situ approach for measuring biogeochemical fluxes in structurally complex benthic communities. *Methods Ecol. Evol.* (2019). doi:https://doi.org/10.5061/dryad.80c1rq2

Chapter 4

Chapter 4 | Denitrification aligns with N₂ fixation in Red Sea corals

Arjen Tilstra^{1*}, Yusuf C. El-Khaled¹, Florian Roth², Nils Rådecker², Claudia Pogoreutz², Christian R. Woolstra^{2,3}, Christian Wild¹

¹ Marine Ecology Department, Faculty of Biology and Chemistry, University of Bremen, Bremen, Germany

² Red Sea Research Center, Division of Biological and Environmental Science and Engineering, King Abdullah University of Science and Technology, Thuwal, Saudi Arabia

³ Department of Biology, University of Konstanz, Konstanz, Germany

* Corresponding author: tilstra@uni-bremen.de

4.1 | Abstract

Denitrification may potentially alleviate excess nitrogen (N) availability in coral holobionts to maintain a favourable N to phosphorous ratio in the coral tissue, however, little is known about the activity of denitrifiers. The present study used the *nirS* marker gene as a proxy for denitrification potential along with measurements of denitrification rates in a comparative taxonomic framework from the Red Sea: *Acropora hemprichii*, *Millepora dichotoma*, and *Pleuractis granulosa*. Relative *nirS* gene copy numbers associated with the tissues of these common corals were assessed and compared with denitrification rates on the holobiont level. In addition, dinitrogen (N₂) fixation rates, Symbiodiniaceae cell density, and oxygen evolution were assessed to provide an environmental context for denitrification. Findings revealed that relative abundances of the *nirS* gene were 16– and 17–fold higher in *A. hemprichii* compared to *M. dichotoma* and *P. granulosa*, respectively. In concordance, highest denitrification rates were measured in *A. hemprichii*, followed by *M. dichotoma* and *P. granulosa*. Denitrification rates were positively correlated with N₂ fixation rates and Symbiodiniaceae cell densities. Our results suggest that denitrification may counterbalance the N input from N₂ fixation in the coral holobiont, and we hypothesize that these processes may be limited by photosynthates released by the Symbiodiniaceae.

Keywords: Coral reefs | diazotrophy | nitrogen cycling | Anthozoa | Hydrozoa | Symbiodiniaceae

A modified version of this chapter has been published in *Scientific Reports* 9(1)

<https://doi.org/10.1038/s41598-019-55408-z>

4.2 | Introduction

Corals are holobionts consisting of the coral host and a diverse microbiome composed of Symbiodiniaceae (i.e., endosymbiotic dinoflagellates capable of photosynthesis), and prokaryotes, i.e. bacteria and archaea, among other microbes¹. Complex symbiotic interactions within these holobionts render corals mixotrophic, that is they can obtain nutrients through both autotrophic and heterotrophic means^{2–4}. The endosymbiotic dinoflagellates, belonging to the family Symbiodiniaceae⁵, provide the coral with a substantial part of their metabolic energy via autotrophy in the form of photosynthetically fixed carbon (C)⁶. In return, the Symbiodiniaceae require nutrients from the coral host, e.g. nitrogen (N) and phosphorous (P), which can be obtained via heterotrophic feeding or by uptake from the water column and/or internal (re)cycling^{7,8}.

The involvement of prokaryotes in holobiont nutrient cycling has received increasing attention in recent years. Diazotrophs in particular (microbes capable of fixing atmospheric dinitrogen (N₂)) ubiquitously occur in corals^{9–11} and are recognized as an important source of N for holobiont productivity^{12–16}. Diazotrophs can provide the holobiont with bioavailable N in the form of ammonium, a preferred N source for Symbiodiniaceae^{17–19}, in particular in times of N scarcity¹¹.

Excess (microbial) input of bioavailable N into the coral holobiont can potentially lead to a misbalance of the N:P ratio, i.e. a shift from N towards P limitation, thereby increasing bleaching susceptibility^{14,20,21}. Previously, it was hypothesized that the activity of other N-cycling microbes could alleviate coral holobionts from nutrient stress via the removal of nitrogenous compounds²². Indeed, ammonium oxidizing (i.e. nitrifying) and nitrate reducing (i.e. denitrifying) prokaryotes occur ubiquitously on coral reefs^{23–27}, including coral holobionts^{22,28,29}. The denitrification pathway in particular may be important for holobiont functioning as it effectively removes bioavailable N. Here, nitrate is reduced to atmospheric N₂ via the activity of four main enzymes, i.e. nitrate reductase (converting nitrate to nitrite), nitrite reductase (converting nitrite to nitric oxide), nitric oxide reductase (converting nitric oxide to nitrous oxide), and nitrous oxide reductase (converting nitrous oxide to N₂) (Fig. 4.1)^{30,31}. While Symbiodiniaceae cells are considered a major N sink in the coral holobiont³², excess N could potentially be removed by denitrifying microbes to help maintain an N-limited state¹⁴. However, whether removal of excess N via denitrification contributes to holobiont functioning and health remains poorly understood.

Recently, Pogoreutz *et al.*¹⁰ demonstrated that N₂ fixation rates may not only be species-specific, but align with relative gene copy numbers and expression of the *nifH* gene. This pattern was linked to heterotrophic capacity of the investigated corals. However, it is unknown how these patterns of N₂ fixation activity ultimately relate to other N-cycling processes, i.e. denitrification, within the coral holobiont. The present study thus aimed to answer (i) whether patterns of denitrification are coral species-specific; (ii) whether relative abundances of the *nirS* gene (denitrification potential) can be related to denitrification rates; and (iii) whether denitrification aligns with other biological variables within the coral holobiont, specifically N₂ fixation, photosynthesis, and cell density of Symbiodiniaceae. These questions were answered in a comparative taxonomic framework of three common Red Sea coral species. Relative gene copy numbers of the *nirS* gene, which encodes for a nitrite reductase containing cytochrome *cd*₁, were assessed by qPCR to serve as a proxy for denitrification potential of coral tissue-associated prokaryotes. Relative quantification

of *nirS* gene copy numbers was achieved by referencing against the ITS2 region of Symbiodiniaceae. Denitrification and N₂ fixation rates were quantified indirectly using a COmbined Blockage/Reduction Acetylene (COBRA) assay³³. Finally, Symbiodiniaceae cell densities were manually counted and photosynthesis was assessed by measuring O₂ fluxes.

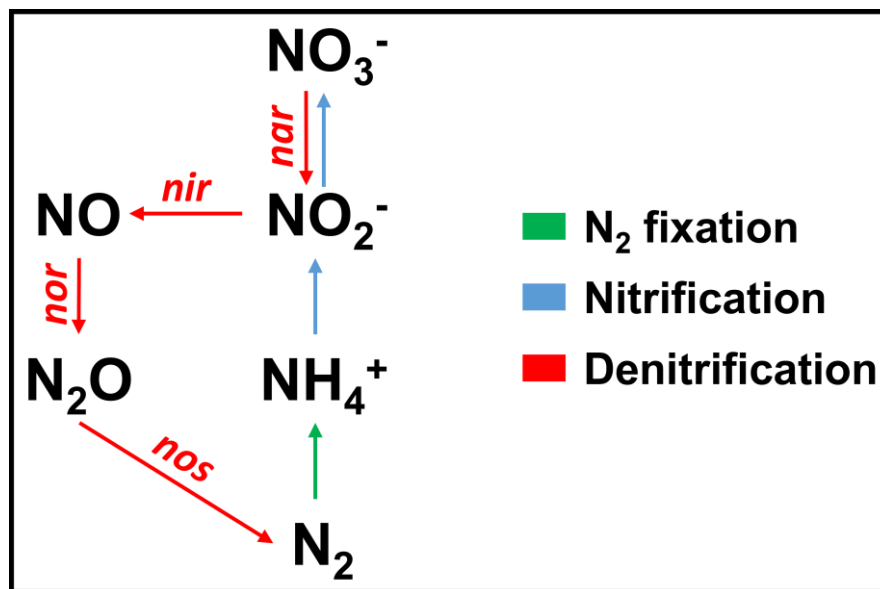


Figure 4.1 | Schematic representation of three major pathways involved in nitrogen cycling, including the four gene clusters responsible for denitrification. N₂ = atmospheric nitrogen, NH₄⁺ = ammonium, NO₂⁻ = nitrite, NO₃⁻ = nitrate, NO = nitric oxide, N₂O = nitrous oxide, *nar* = gene cluster for nitrate reductase, *nir* = gene cluster for nitrite reductase, *nor* = gene cluster for nitric oxide reductase, *nos* = gene cluster for nitrous oxide reductase.

4.3 | Materials and Methods

Sample Collection, Aquarium Facilities, and Maintenance

This study was conducted at the King Abdullah University of Science and Technology (KAUST) in Saudi Arabia. Three common coral species were selected (Fig. 4.2A) and collected at approx. 5 m water depth at the semi-exposed side of the inshore reef Abu Shosha (N22°18'15", E39°02'56") located in the Saudi Arabian central Red Sea in November 2017; specifically, the acroporid coral *Acropora hemprichii* ($n = 4$ colonies), the hydrozoan *Millepora dichotoma* ($n = 4$ colonies), and the fungiid coral *Pleauractis granulosa* ($n = 8$ polyps). Coral colonies of the same species were sampled at least 10 m apart to account for genetic diversity. After collection, the corals were transferred to recirculation aquaria filled with reef water on the vessel, and subsequently transported to the wet lab facility of the Coastal and Marine Resources (CMOR) Core Lab at KAUST. The branching corals *A. hemprichii* and *M. dichotoma* were immediately fragmented into two fragments of similar size each. Fragments were distributed into four independent replicate 150 L flow-through tanks, i.e. each tank held two distinct fragments of each branching coral species (see Fig. S4.1). Individual polyps of *P. granulosa* were not fragmented and distributed randomly over the four tanks. Fragments/polyps were left to acclimate for two weeks prior to the start of measurements. All tanks were continuously supplied with sediment-filtered seawater (flow through rate 300 L h⁻¹) from inshore

reefs located 1.5 km off KAUST with the following parameters: temperature 27 °C, salinity 40 PSU, and dissolved oxygen (O₂) 6.4 mg O₂ L⁻¹. All fragments were exposed to a photon flux of ~150 μmol m⁻² s⁻¹³⁴ on a 12:12 h light/dark cycle. Corals were kept in nutrient-rich seawater (nitrate ~3 μM, phosphate ~0.40 μM) to stimulate denitrification response in coral holobionts^{35–37}. For each measurement, one fragment/polyp of each species per tank was taken, avoiding sampling fragments that originated from the same colony. This resulted in four fragments/polyps per species from four different colonies for each measurement (see Fig. S4.1).

DNA Extraction and Relative Quantification of the *nirS* Gene via Quantitative PCR (qPCR)

Quantitative PCR was used to quantify relative gene copy numbers of the *nirS* gene as a proxy for abundance of denitrifying prokaryotes in the coral tissues, i.e. denitrification potential. To this end, the coral tissue was removed from the skeleton by airblasting with RNase free water and pressurized air using a sterilized airbrush (Agora-Tec GmbH, Schmalkalden, Germany). For *P. granulosa*, tissue was blasted off from both top and bottom surfaces and was pooled subsequently. The resulting tissue slurries were homogenized using an Ultra Turrax (for approx. 20 s) and stored at -20 °C until further processing. Total DNA was extracted from 100 μL of tissue slurry using the Qiagen DNeasy Plant Mini Kit (Qiagen, Germany) according to manufacturer's instructions. DNA extraction yields were determined using a NanoDrop 2000C spectrophotometer (Thermo Fisher Scientific, Waltham, MA, USA). DNA concentrations were adjusted to 2 ng μL⁻¹ and stored at -20 °C until further processing.

qPCR assays were performed in technical triplicates for each coral fragment or polyp. Each assay contained 9 μL reaction mixture and 1 μL DNA template. Reaction mixture contained Platinum SYBR Green qPCR Master Mix (Invitrogen, Carlsbad, CA, United States), 0.2 μL of each primer (10 μM, see below and details of primer assessment in the Supplementary Methods to Chapter 4), 0.2 μL of ROX dye and 3.4 μL of RNase-free water. Negative controls (i.e., reactions consisting of only qPCR reagents and nuclease-free water without any DNA added) were included in the assay in technical triplicates to account for potential laboratory and kit contamination. The relative number of *nirS* gene copies (i.e. relative abundance of denitrifiers) was determined by normalization against the multi copy gene marker ITS2 of Symbiodiniaceae as previously used for the normalization of *nifH* gene copy numbers in a comparative taxonomic coral framework¹⁰. A total of 18 primers covering all main enzymes in the denitrification pathway (Fig. 4.1) were tested for this study and yielded ten primer pairs that produced PCR products in the suggested size range (see details of primer assessment in the Supplementary Methods to Chapter 4). Temperature gradient PCRs were applied (from 51 °C to 62 °C) to assess the optimal annealing temperature of every primer pair (see details of primer assessment in the Supplementary Methods to Chapter 4). Due to substantial differences in amplification performance of primer pairs, we selected a primer pair for *nirS* which encodes for a nitrite reductase containing cytochrome *cd1* as the target gene. For the amplification of *nirS*, the primers cd3aF 5'-GTSAACG TSAAGGARACSGG-3' and R3cd 5'-GASTTCGGRTGSGTCTTGA-3' were used³⁸. This primer pair was previously found to perform well with DNA from other marine templates, such as

coral rock²⁴, marine sediments³⁹, as well as environmental samples from intertidal zones⁴⁰, and terrestrial ecosystems^{41–43}. To amplify the ITS2 region of Symbiodiniaceae the primers SYM_VAR_5.8S2 5'–GAAT^TGCGAAGACTCCGTGAACC–3' and SYM_VAR_REV 5'–CGGGTTCWCTTGTGTGACTTCATGC–3' were used⁴⁴. The thermal cycling protocol used for the amplification of both target genes was 50 °C for 2 min, 95 °C for 2 min, 50 cycles of 95 °C for 30 s, 51 °C for 1 min, 72 °C for 1 min, and a final 72 °C extension cycle for 2 min. Amplification specificity was determined by adding a dissociation step. All assays were performed on the ABI 7900HT Fast Real–Time PCR System (Applied Biosystems, CA, USA). Standard calibration curves were run simultaneously covering 5 orders of magnitude (10³–10⁷ copies of template per assay for the ITS2 and *nirS* gene). The qPCR efficiency (E) of both primer pairs was 84 % and 86 %, respectively, calculated according to the equation $E = [10^{(-1/\text{slope})} - 1]$. Relative fold change of *nirS* gene copies were calculated as $2^{(-\Delta\Delta Ct)}$ against ITS2 Ct values using *P. granulosa* samples as the reference.

Throback *et al.*⁴⁵ assessed a range of *nirS* primer pairs and concluded that the primer pair used in the present study (i.e. cd3aF and R3cd) had the largest range and worked best for *nirS* gene assessments. Currently, there are no optimal universal primers for the amplification of the *nirS* gene available⁴⁶. Any quantification of *nirS* abundances is hence biased by the primer pair used and its suitability strongly depends on the phylogenetic diversity of the template. Thus, while the primer combination used here shows a high coverage of 67 % of known *nirS* diversity⁴⁶, our results can only provide an approximation of the relative abundance of denitrifying bacteria across samples until more (meta)genomic data for coral–associated denitrifiers are available.

Denitrification and N₂ Fixation Measurements

To measure denitrification and N₂ fixation rates simultaneously, we incubated corals using a COBRA assay, as described in El–Khaled *et al.*³³. Of note, acetylene inhibits the production of nitrate in the nitrification pathway^{47,48}. As nitrate serves as a substrate for denitrification, the inhibition of nitrification may thus result in an underestimation of denitrification rates. To compensate for such effects, nutrient–rich incubation water was used to preclude substrate limitation^{35–37}.

Briefly, incubations were conducted in gas–tight 1 L glass chambers, each filled with 800 mL of nutrient–rich sediment–filtered seawater (DIN = ~3 µM, phosphate = ~0.40 µM) and a 200 mL gas headspace. Both incubation water and headspace were enriched with 10% acetylene. Each chamber contained a single *A. hemprichii* or *M. dichotoma* fragment or *P. granulosa* polyp. Incubations of four biological replicates per species were performed (see Fig. S4.1), and three additional chambers without corals served as controls to correct for planktonic background metabolism. During the 24 h incubations, chambers were submersed in a temperature–controlled water bath and constantly stirred (500 rpm) to create a constant water motion and homogenous environment (27 °C, 12:12 h dark/light cycle, photon flux of ~150 µmol m⁻² s⁻¹). Nitrous oxide (N₂O; as a proxy for denitrification) and ethylene (C₂H₄; as a proxy for N₂ fixation) concentrations were quantified by gas chromatography and helium pulsed discharge detection (Agilent 7890B GC system with HP–Plot/Q column, lower detection limit for both target gases was 0.3 ppm). To

facilitate comparisons of both N-cycling processes, N₂O and C₂H₄ production rates were converted into N production using molar ratios of N₂O:N₂ = 1 and C₂H₄:N₂ = 3⁴⁹, and multiplying by 2 to convert N₂ to N, resulting in rates of nmol N cm⁻² d⁻¹. Gas concentrations were normalized to coral surface area, which was calculated using cloud-based 3D models of samples (Autodesk Remake v19.1.1.2)^{50,51}.

Symbiodiniaceae Cell Density

Tissue slurry for DNA extraction was also used to obtain cell densities of Symbiodiniaceae (see Fig. S4.1). Symbiodiniaceae cell densities were obtained by manual counts of homogenized aliquots of 20 μL, which were diluted 5 times, using a Neubauer-improved hemocytometer on a light microscope with HD camera (Zeiss, Germany). Resulting photographs were analysed using the Cell Counter Notice in ImageJ software (National Institutes of Health, USA). Cell counts for each individual were done in duplicates and subsequently averaged. Finally, cell counts were normalized to coral surface area to obtain cell densities of Symbiodiniaceae for each fragment or polyp.

O₂ Fluxes

Net photosynthesis (P_n) and dark respiration (R) were assessed from O₂ evolution/depletion measurements with the same fragments/polyps 2 days prior to using them for denitrification and N₂ fixation rate measurements. Corals were incubated for 2 h in individual gas-tight 1 L glass chambers, filled with nutrient-rich sediment-filtered seawater (DIN = ~3 μM, phosphate = ~0.40 μM). Each chamber contained a single *A. hemprichii* or *M. dichotoma* fragment or *P. granulosa* polyp. Incubations of four biological replicates per species were performed (see Fig. S4.1), and three additional chambers without corals served as controls to correct for planktonic background metabolism. During the incubations, chambers were submersed in a temperature-controlled water bath (kept at 27 °C) and constantly stirred (500 rpm) to create a continuous water motion and homogenous environment. Light incubations for P_n were performed under a photon flux of ~150 μmol m⁻² s⁻¹. R was obtained by incubating in complete darkness. O₂ concentrations were measured at the start and end of the respective incubation period using an optical oxygen multiprobe (WTW, Germany). O₂ concentrations at the start of the incubation were subtracted from O₂ concentrations at the end, corrected for controls and normalized to incubation time and surface area of the corals. R is presented as a negative rate. Finally, gross photosynthesis (P_g) was calculated as the difference between P_n and R as follows: $P_g = (P_n) - (R)$.

Statistical Analyses

Data were analysed using non-parametric permutational multivariate analysis of variance (PERMANOVA) using PRIMER-E version 6 software⁵² with the PERMANOVA+ add on⁵³. To test for differences in relative *nirS* gene copy numbers, denitrification rates, N₂ fixation rates, Symbiodiniaceae cell densities and O₂ fluxes between species, 1-factorial PERMANOVAs were performed, based on Bray-Curtis similarities of square-root transformed data. Therefore, Type III (partial) sum of squares was used with unrestricted

permutation of raw data (999 permutations), and PERMANOVA pairwise tests with parallel Monte Carlo tests were carried out when significant differences were found.

Differences between denitrification and N₂ fixation rates within each coral species were assessed using SigmaPlot 12.0 (Systat software). T-tests were performed for normally distributed data and Mann–Whitney U tests were performed when data were not normally distributed.

Additionally, to identify the biological variable (single trial variable) and combination of biological variables (multiple trial variables) that “best explains” the denitrification rate pattern of the coral samples, a Biota and/or Environment matching routine (BIOENV) was performed with 999 permutations based on Spearman Rank correlations. A distance-based linear model (DistLM) using a step-wise selection procedure with AICc as a selection criterion was used to calculate the explanatory power of correlating biological variables^{52,54}. Finally, the same BIOENV and DistLM routine was performed for N₂ fixation rates of the coral samples.

As *P. granulosa* consisted of four individual polyps per measurement (no technical replicates originating from the same polyp), data for each variable were averaged and used as a single data point in analyses unless the same individuals were used (see Fig. S4.1). All values are given as mean ± SE.

4.4 | Results

Relative Abundances of the *nirS* Gene and Denitrification Rates

The qPCR confirmed the presence of the *nirS* gene in the tissues of all investigated corals (Fig. 4.2A and Fig. 4.2B). *Acropora hemprichii* exhibited significantly higher relative *nirS* gene copy numbers compared to *M. dichotoma* (~16-fold; pair-wise PERMANOVA, $t = 3.82, p = 0.015$) and *P. granulosa* (~17-fold; pair-wise PERMANOVA, $t = 3.25, p = 0.029$). A similar pattern was found for denitrification rates (Fig. 4.2C). *Acropora hemprichii* exhibited the highest denitrification rates ($\sim 0.38 \pm 0.13$ nmol N cm⁻² d⁻¹), followed by *M. dichotoma* ($\sim 0.17 \pm 0.10$ nmol N cm⁻² d⁻¹) and *P. granulosa* ($\sim 0.05 \pm 0.02$ nmol N cm⁻² d⁻¹). Denitrification rates in *A. hemprichii* were significantly different from those in *P. granulosa* (pair-wise PERMANOVA, $t = 2.75, p = 0.036$), but not those measured in *M. dichotoma* (pair-wise PERMANOVA, $t = 1.31, p = 0.237$). Finally, denitrification rates in *M. dichotoma* were not significantly different from those in *P. granulosa* (pair-wise PERMANOVA, $t = 1.23, p = 0.264$).

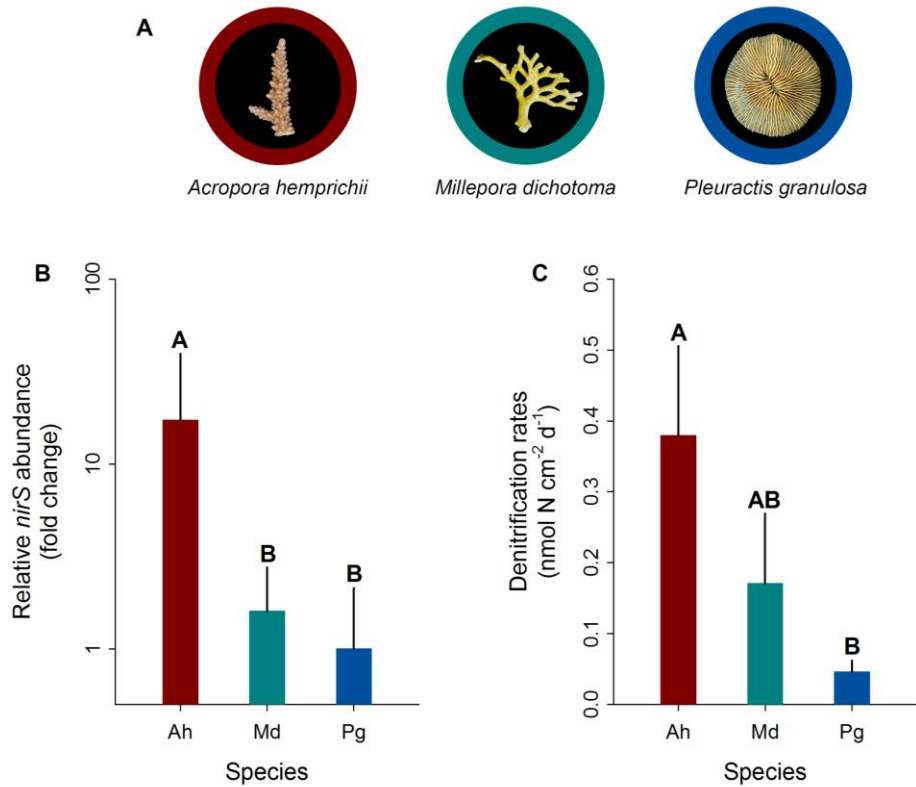


Figure 4.2 | Relative *nirS* gene copy numbers and rates of denitrification associated with three Red Sea coral species. **(A)** Representative photographs of investigated species, **(B)** fold changes in relative *nirS* gene copy numbers normalized to ITS2 copy numbers as measured by quantitative PCR, and **(C)** denitrification rates measured indirectly via the combined blockage/reduction acetylene assay (COBRA-assay). Ah = *A. hemprichii*, Md = *M. dichotoma*, and Pg = *P. granulosa*. Fold changes were calculated in relation to *P. granulosa*; bars indicate the mean; error bars indicate upper confidence intervals (+ 1 SE); $n = 4$ per species, except Ah and Pg in **(B)** ($n = 3$). Different letters above error bars indicate statistically significant differences between groups within each figure (pair-wise PERMANOVAs, $p < 0.05$).

N₂ fixation, Symbiodiniaceae Cell Density and O₂ Fluxes

N₂ fixation rates were highest in *M. dichotoma* (0.23 ± 0.11 nmol N cm⁻² d⁻¹), followed by *A. hemprichii* (0.21 ± 0.12 nmol N cm⁻² d⁻¹), and lowest in *P. granulosa* (0.04 ± 0.03 nmol N cm⁻² d⁻¹) (Fig. 4.3A). Due to high biological variation in the samples, these differences between coral species were not significant (Fig. 4.3A).

Cell densities of Symbiodiniaceae were significantly higher in *A. hemprichii* ($0.86 \pm 0.15 \times 10^6$ cells cm⁻²) compared to *M. dichotoma* ($0.10 \pm 0.02 \times 10^6$ cells cm⁻²; pair-wise PERMANOVA, $t = 6.86$, $p < 0.001$) and *P. granulosa* ($0.13 \pm 0.03 \times 10^6$ cells cm⁻²; pair-wise PERMANOVA, $t = 5.03$, $p = 0.003$) (Fig. 4.3B). Cell densities of Symbiodiniaceae in *M. dichotoma* and *P. granulosa* did not differ significantly (Fig. 4.3B).

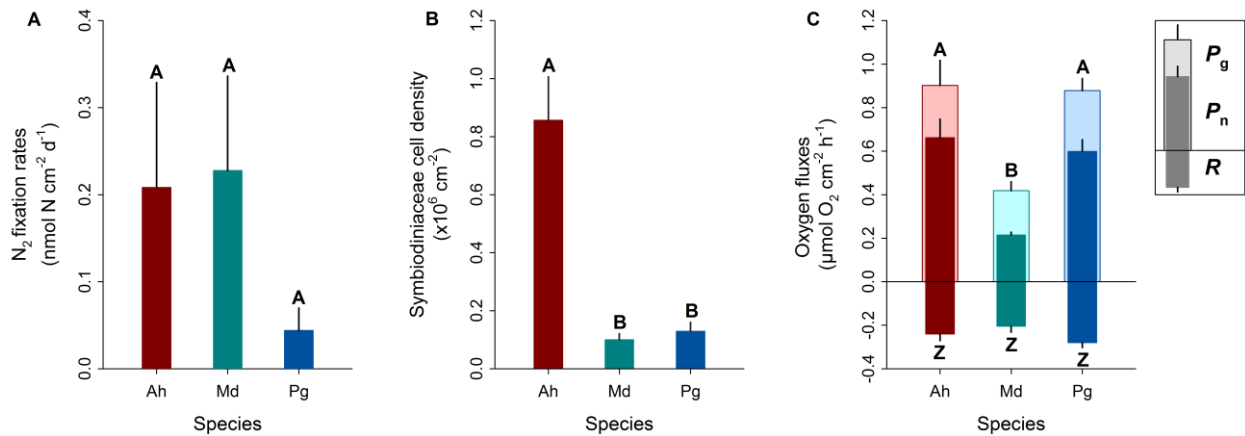


Figure 4.3 | Biological variables of three Red Sea corals. **(A)** N₂ fixation rates measured indirectly using a COBRA assay, **(B)** Symbiodiniaceae cell densities, and **(C)** oxygen fluxes. Ah = *Acropora hemprichii*, Md = *Millepora dichotoma*, and Pg = *Pleurodictis granulosa*. P_g = gross photosynthesis, P_n = net photosynthesis, R = dark respiration. Bars indicate the mean; error bars indicate upper confidence intervals (+1 SE); n = 4 per species. Different letters above error bars indicate statistically significant differences within each plot (pair-wise PERMANOVAs, p < 0.05); differences in **(C)** apply to both P_g and P_n.

Significantly lower P_n was found for *M. dichotoma* ($0.21 \pm 0.01 \mu\text{mol O}_2 \text{ cm}^{-2} \text{ h}^{-1}$) compared to that of *A. hemprichii* ($0.66 \pm 0.09 \mu\text{mol O}_2 \text{ cm}^{-2} \text{ h}^{-1}$; pair-wise PERMANOVA, t = 6.55, p = 0.002) and that of *P. granulosa* ($0.60 \pm 0.05 \mu\text{mol O}_2 \text{ cm}^{-2} \text{ h}^{-1}$; pair-wise PERMANOVA, t = 8.95, p < 0.001) (Fig. 4.3C). The same pattern was found for P_g; *M. dichotoma* exhibited significantly lower P_g ($0.42 \pm 0.04 \mu\text{mol O}_2 \text{ cm}^{-2} \text{ h}^{-1}$) than that of *A. hemprichii* ($0.90 \pm 0.12 \mu\text{mol O}_2 \text{ cm}^{-2} \text{ h}^{-1}$; pair-wise PERMANOVA, t = 4.14, p = 0.007) and that of *P. granulosa* ($0.88 \pm 0.06 \mu\text{mol O}_2 \text{ cm}^{-2} \text{ h}^{-1}$; pair-wise PERMANOVA, t = 6.21, p = 0.002) (Fig. 4.3C). No significant differences were found for R between species (PERMANOVA, Pseudo-F = 1.73, p = 0.243) (Fig. 4.3C).

Comparison of Denitrification Rates and N₂ fixation Rates

No significant differences were found between denitrification and N₂ fixation rates for either species (T-test, p > 0.05; Fig. 4.4).

Correlation Analyses

The biological variable that best explained the denitrification rates was N₂ fixation (BIOENV, r = 0.654, p = 0.004). The combination of biological variables that explained denitrification rates best were N₂ fixation and Symbiodiniaceae cell density (BIOENV, r = 0.592, p = 0.002). Indeed, 85.6% of the variation in denitrification rates could be explained by N₂ fixation and Symbiodiniaceae cell density (DistLM). The biological variable that best explained the N₂ fixation rates was denitrification (BIOENV, r = 0.651, p = 0.006). The combination of biological variables that explained N₂ fixation best were denitrification and Symbiodiniaceae cell density (BIOENV, r = 0.342, p = 0.046). Indeed, 82.9% of the

variation in N₂ fixation rates could be explained by denitrification and Symbiodiniaceae cell density (DistLM).

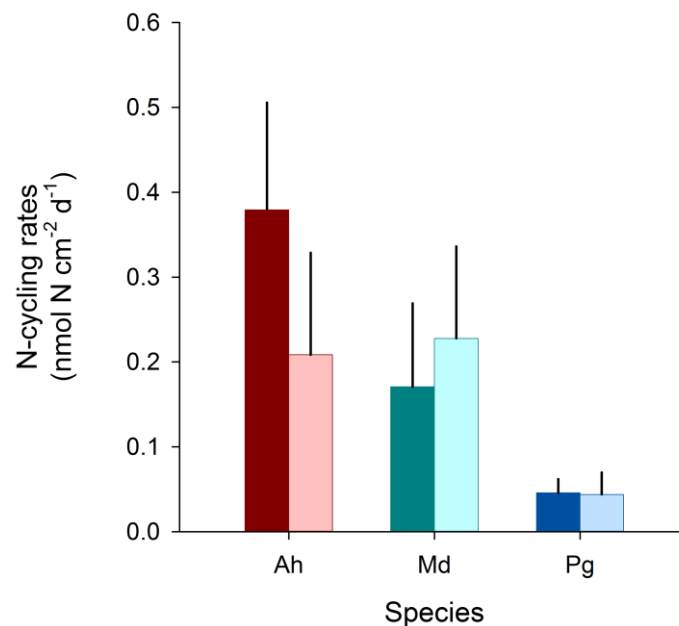


Figure 4.4 | Comparison of denitrification rates and N₂ fixation rates of three Red Sea coral species. Ah = *Acropora hemprichii*, Md = *Millepora dichotoma*, and Pg = *Pleuraetis granulosa*. Bars indicate the mean; error bars indicate upper confidence intervals (+1 SE); dark bars represent denitrification rates; light bars represent N₂ fixation rates; $n = 4$ per species.

4.5 | Discussion

Despite the importance of N as a key nutrient for the metabolism of symbiotic corals⁵⁵, relatively little is known about the removal of N by microbes in the internal N-cycling of coral holobionts^{12,14}. Here, we assessed relative abundances of coral tissue-associated denitrifiers (using relative gene copy numbers of the *nirS* gene as a proxy), as well as denitrification and N₂ fixation rates on the holobiont level in a comparative taxonomic framework using three common Red Sea corals. Our results suggest that denitrification is an active N-cycling pathway in coral holobionts and may be linked with diazotroph activity and Symbiodiniaceae cell density, the interplay of which may have important implications for coral holobiont nutrient cycling.

It was previously hypothesized that coral associated N-cycling microbes may have a capacity to alleviate nutrient stress via the removal of bioavailable N^{14,22,28,29}. While the community structure and phylogenetic diversity of denitrifying microbes have been previously assessed in a soft and a hard coral²⁹, we here present the first study to link relative coral tissue-associated abundances of denitrifying prokaryotes with denitrification rates. Our findings highlight that denitrification may play a role in removing bioavailable N from the coral holobiont. The contribution and hence potential functional importance of denitrification may depend on the host species.

In the present study, the highest relative *nirS* gene copy numbers were found in *A. hemprichii*, while lower relative numbers were observed in *M. dichotoma* and *P. granulosa*. The patterns in relative abundance of the *nirS* gene obtained through qPCR were largely reflected in denitrification rates measured using a COBRA assay. As such, these data suggest that relative *nirS* gene abundance may be a suitable proxy of denitrification potential in corals. Small deviations in the patterns observed for both measurements may be potentially explained by a) differences in the community composition of denitrifying microbes; fungi involved in N metabolism may be present in coral holobionts⁵⁶ and likely lack a (homologous) *nirS* gene⁵⁷, by b) the multi-copy nature of the ITS2^{58,59}; by relating *nirS* to ITS2, the relative abundances of *nirS* genes could potentially be underestimated, and by c) the potential presence of denitrifying microbes in the coral skeleton^{29,60–62}.

The present study identified a positive correlation between denitrification and N₂ fixation activity across the three Red Sea coral species investigated. As such, denitrification may have the capacity to counterbalance N input from N₂ fixation in coral holobionts. We here propose that these processes may be indirectly linked by their similar environmental requirements and constraints.

Denitrification as well as N₂ fixation are anaerobic processes^{31,63}. However, in the present study, no relationship was found between O₂ fluxes and denitrification and N₂ fixation rates. This strongly suggests that the activity of these anaerobic processes may be spatially or temporally separated from O₂ evolution in the coral holobiont, or that the involved N-cycling prokaryotes are capable of supporting these processes in the presence of O₂^{64–67}. In addition to anaerobic conditions, most denitrifiers and diazotrophs require organic C as their energy source, i.e. are heterotrophic^{9,43,68,69}. Besides the uptake of organic C from the water column⁷⁰ and heterotrophic feeding by the coral host, the Symbiodiniaceae are the main source of C-rich photosynthates within the holobiont⁷¹. Notably, the present study showed a positive correlation between denitrification rates with N₂ fixation combined with Symbiodiniaceae cell density. In addition, a positive correlation was also shown for N₂ fixation, namely with denitrification combined with Symbiodiniaceae cell density. This suggest that the heterotrophic prokaryotes of both N-cycling pathways may rely partially on Symbiodiniaceae for obtaining organic C for respiration. As such, the correlation of denitrification and N₂ fixation may be the result of a shared organic C limitation within the holobiont¹⁴. However, a potential functional relationship between N-cycling prokaryotes and phototrophic Symbiodiniaceae remains yet to be determined.

The observed positive correlation between the two N-cycling pathways, i.e. denitrification and N₂ fixation, may have important implications for the general understanding of nutrient cycling within coral holobionts, and hence our understanding of coral ecology. In a stable healthy holobiont, N input from N₂ fixation may be compensated for by N removal via denitrification. As such, the activity of these two processes should be interpreted in relation to each other to understand their overall effect on holobiont N availability, and hence nutrient dynamics.

Environmental stress may directly affect the equilibrium of these processes, as both eutrophication and the increase in sea surface temperatures directly affect N-cycling within the coral holobiont¹⁴. Increases in inorganic N availability may lead to a reduction of diazotroph activity in coral holobionts due to the so

called “ammonia switch-off”⁷², which is evidenced by negative correlations between N availability and N₂ fixation for both planktonic and benthic diazotrophs^{73–75}. Denitrification, on the one hand, may even be stimulated by increased nitrate availability³¹. This hypothesized interplay of denitrification and N₂ fixation would hence allow coral holobionts to effectively remove excessive N¹⁴.

Increased sea surface temperatures, on the other hand, may directly stimulate N₂ fixation⁷⁶. While the environmental drivers for stimulated N₂ fixation activity are not fully resolved yet, increased diazotrophy may affect holobiont functioning if not compensated for by denitrification activity¹⁰. However, with increasing water temperature, Symbiodiniaceae may retain more photosynthates for their own metabolism⁷⁷, potentially limiting organic C availability not only for the coral host, but also for heterotrophic microbes, including denitrifiers. Thus, microbial N-cycling may be more important in highly autotrophic coral holobionts, as they rely more on the Symbiodiniaceae for organic C and may be more susceptible to potential nutrient imbalances due to e.g. increased diazotrophic activity¹⁰. Indeed, the capacity for heterotrophic feeding has been linked to having a lower susceptibility to warming^{78–81} and eutrophication⁸². However, besides the potential ability to remove bioavailable N from the coral holobiont, the role of denitrifiers under (non-)stressful scenarios remains speculative at this point. Thus, future research could focus on several aspects to disentangle a potential role of denitrification in the context of microbial N-cycling within coral holobionts by (a) identifying the spatial niche that denitrifiers occupy and in which abundances; (b) identifying the denitrifiers’ primary energy source(s) under regular and stressed (e.g. eutrophic or warming) conditions; (c) by quantifying and assessing the interplay of denitrification with other N-cycling processes (potentially) ubiquitous in coral holobionts, e.g. N₂ fixation, nitrification and ANAMMOX, through molecular, physiological and/or isotope analyses; and (d) how the interplay of N-cycling processes in the coral holobiont is altered in global change scenarios.

4.6 | Acknowledgments

We thank KAUST CMOR staff and boat crews for their support with diving operations. Financial support was provided by KAUST baseline funds to CRV and the German Research Foundation (DFG) grant Wi 2677/9–1 to CW.

4.7 | References

1. Rohwer, F., Seguritan, V., Azam, F. & Knowlton, N. Diversity and distribution of coral-associated bacteria. *Mar. Ecol. Prog. Ser.* **243**, 1–10 (2002).
2. Furla, P. *et al.* The symbiotic anthozoan: A physiological chimera between alga and animal. *Integr. Comp. Biol.* **45**, 595–604 (2005).
3. Rahav, O., Dubinsky, Z., Achituv, Y. & Falkowski, P. G. Ammonium metabolism in the zooxanthellate coral, *Stylophora pistillata*. *Proc. R. Soc.* **337**, 325–337 (1989).
4. Houlbrèque, F. & Ferrier-Pagès, C. Heterotrophy in tropical scleractinian corals. *Biol. Rev.* **84**, 1–17 (2009).
5. LaJeunesse, T. C. *et al.* Systematic revision of Symbiodiniaceae highlights the antiquity and diversity of coral endosymbionts. *Curr. Biol.* **28**, 2570–2580.e6 (2018).
6. Muscatine, L. & Porter, J. W. Reef corals: mutualistic symbioses adapted to nutrient-poor environments. *Bioscience* **27**, 454–460 (1977).
7. Muscatine, L. *et al.* Cell-specific density of symbiotic dinoflagellates in tropical anthozoans. *Coral Reefs* **17**, 329–337 (1998).
8. Yellowlees, D., Rees, T. A. V. & Leggat, W. Metabolic interactions between algal symbionts and invertebrate hosts. *Plant, Cell Environ.* **31**, 679–694 (2008).
9. Lema, K. A., Willis, B. L. & Bourne, D. G. Corals form characteristic associations with symbiotic nitrogen-fixing bacteria. *Appl. Environ. Microbiol.* **78**, 3136–3144 (2012).
10. Pogoreutz, C. *et al.* Nitrogen fixation aligns with *nifH* abundance and expression in two coral trophic functional groups. *Front. Microbiol.* **8**, 1187 (2017).
11. Cardini, U. *et al.* Functional significance of dinitrogen fixation in sustaining coral productivity under oligotrophic conditions. *Proc. R. Soc. B Biol. Sci.* **282**, 20152257 (2015).
12. Benavides, M. *et al.* Diazotrophs: a non-negligible source of nitrogen for the tropical coral *Stylophora pistillata*. *J. Exp. Biol.* **219**, 2608–2612 (2016).
13. Benavides, M., Bednarz, V. N. & Ferrier-Pagès, C. Diazotrophs: Overlooked key players within the coral symbiosis and tropical reef ecosystems? *Front. Mar. Sci.* **4**, (2017).
14. Rådecker, N., Pogoreutz, C., Voolstra, C. R., Wiedenmann, J. & Wild, C. Nitrogen cycling in corals: the key to understanding holobiont functioning? *Trends Microbiol.* **23**, 490–497 (2015).
15. Lesser, M. P. *et al.* Nitrogen fixation by symbiotic cyanobacteria provides a source of nitrogen for the scleractinian coral *Montastraea cavernosa*. *Mar. Ecol. Prog. Ser.* **346**, 143–152 (2007).
16. Robbins, S. J. *et al.* A genomic view of the reef-building coral *Porites lutea* and its microbial symbionts. *Nat. Microbiol.* (2019). doi:10.1038/s41564-019-0532-4
17. Muller-Parker, G. & D’Elia, C. F. Interactions between corals and their symbiotic algae. *Life Death Coral Reefs* **5**, 96–113 (1997).
18. Taguchi, S. & Kinzie III, R. A. Growth of zooxanthellae in culture with two nitrogen sources. *Mar. Biol.* **138**, 149–155 (2001).
19. Grover, R., Maguer, J.-F., Allemand, D. & Ferrier-Pagès, C. Nitrate uptake in the scleractinian coral *Stylophora pistillata*. *Limnol. Oceanogr.* **48**, 2266–2274 (2003).

20. Wiedenmann, J. *et al.* Nutrient enrichment can increase the susceptibility of reef corals to bleaching. *Nat. Clim. Chang.* **3**, 160–164 (2013).
21. Pogoreutz, C. *et al.* Sugar enrichment provides evidence for a role of nitrogen fixation in coral bleaching. *Glob. Chang. Biol.* **23**, 3838–3848 (2017).
22. Siboni, N., Ben-Dov, E., Sivan, A. & Kushmaro, A. Global distribution and diversity of coral-associated *Archaea* and their possible role in the coral holobiont nitrogen cycle. *Environ. Microbiol.* **10**, 2979–2990 (2008).
23. Sobolev, D., Boyett, M. R. & Cruz-Rivera, E. Detection of ammonia-oxidizing *Bacteria* and *Archaea* within coral reef cyanobacterial mats. *J. Oceanogr.* **69**, 591–600 (2013).
24. Yuen, Y. S., Yamazaki, S. S., Nakamura, T., Tokuda, G. & Yamasaki, H. Effects of live rock on the reef-building coral *Acropora digitifera* cultured with high levels of nitrogenous compounds. *Aquac. Eng.* **41**, 35–43 (2009).
25. Capone, D. G., Dunham, S. E., Horrigan, S. G. & Duguay, L. E. Microbial nitrogen transformations in unconsolidated coral reef sediments. *Mar. Ecol. Prog. Ser.* **80**, 75–88 (1992).
26. Gaidos, E., Rusch, A. & Ilardo, M. Ribosomal tag pyrosequencing of DNA and RNA from benthic coral reef microbiota: community spatial structure, rare members and nitrogen-cycling guilds. *Environ. Microbiol.* **13**, 1138–1152 (2011).
27. Rusch, A. & Gaidos, E. Nitrogen-cycling bacteria and archaea in the carbonate sediment of a coral reef. *Geobiology* **11**, 472–484 (2013).
28. Kimes, N. E., Van Nostrand, J. D., Weil, E., Zhou, J. & Morris, P. J. Microbial functional structure of *Montastraea faveolata*, an important Caribbean reef-building coral, differs between healthy and yellow-band diseased colonies. *Environ. Microbiol.* **12**, 541–556 (2010).
29. Yang, S., Sun, W., Zhang, F. & Li, Z. Phylogenetically diverse denitrifying and ammonia-oxidizing bacteria in corals *Alcyonium gracillimum* and *Tubastraea coccinea*. *Mar. Biotechnol.* **15**, 540–551 (2013).
30. Jetten, M. S. M. The microbial nitrogen cycle. *Environ. Microbiol.* **10**, 2903–2909 (2008).
31. Zumft, W. G. Cell biology and molecular basis of denitrification. *Microbiol. Mol. Biol. Rev.* **61**, 533–616 (1997).
32. Pernice, M. *et al.* A single-cell view of ammonium assimilation in coral-dinoflagellate symbiosis. *ISME J.* **6**, 1314–1324 (2012).
33. El-Khaled, Y. *et al.* Combined Acetylene Blockage and Reduction Assay (COBRA) for Dinitrogen Fixation and Denitrification Estimation. *Protocols.io* (2019). doi:10.17504/protocols.io.9ith4en
34. Roth, F. *et al.* Coral reef degradation affects the potential for reef recovery after disturbance. *Mar. Environ. Res.* **142**, 48–58 (2018).
35. Haines, J. R., Atlas, R. M., Griffiths, R. P. & Morita, R. Y. Denitrification and nitrogen fixation in Alaskan continental shelf sediments. *Appl. Environ. Microbiol.* **41**, 412–21 (1981).
36. Joye, S. B. & Paerl, H. W. Contemporaneous nitrogen fixation and denitrification in intertidal microbial mats: rapid response to runoff events. *Mar. Ecol. Prog. Ser.* **94**, 267–274 (1993).
37. Miyajima, T., Suzumura, M., Umezawa, Y. & Koike, I. Microbiological nitrogen transformation in carbonate sediments of a coral-reef lagoon and associated seagrass beds. *Mar. Ecol. Prog. Ser.* **217**, 273–286 (2001).

38. Michotey, V., Méjean, V. & Bonin, P. Comparison of methods for quantification of cytochrome cd1-denitrifying bacteria in environmental marine samples. *Appl. Environ. Microbiol.* **66**, 1564–1571 (2000).
39. Nakano, M., Shimizu, Y., Okumura, H., Sugahara, I. & Maeda, H. Construction of a consortium comprising ammonia-oxidizing bacteria and denitrifying bacteria isolated from marine sediment. *Biocontrol Sci.* **13**, 73–89 (2008).
40. Dini-Andreote, F., Brossi, M. J. L., van Elsas, J. D. & Salles, J. F. Reconstructing the genetic potential of the microbially-mediated nitrogen cycle in a salt marsh ecosystem. *Front. Microbiol.* **7**, 902 (2016).
41. Jung, J. *et al.* Change in gene abundance in the nitrogen biogeochemical cycle with temperature and nitrogen addition in Antarctic soils. *Res. Microbiol.* **162**, 1018–1026 (2011).
42. Jung, J., Yeom, J., Han, J., Kim, J. & Park, W. Seasonal changes in nitrogen-cycle gene abundances and in bacterial communities in acidic forest soils. *J. Microbiol.* **50**, 365–373 (2012).
43. Chen, S. *et al.* Organic carbon availability limiting microbial denitrification in the deep vadose zone. *Environ. Microbiol.* **20**, 980–992 (2018).
44. Hume, B. C. C. *et al.* An improved primer set and amplification protocol with increased specificity and sensitivity targeting the *Symbiodinium* ITS2 region. *PeerJ* **6**, e4816 (2018).
45. Throbäck, I. N., Enwall, K., Jarvis, Å. & Hallin, S. Reassessing PCR primers targeting *nirS*, *nirK* and *nosZ* genes for community surveys of denitrifying bacteria with DGGE. *FEMS Microbiol. Ecol.* **49**, 401–417 (2004).
46. Bonilla-Rosso, G., Wittorf, L., Jones, C. M. & Hallin, S. Design and evaluation of primers targeting genes encoding NO-forming nitrite reductases: Implications for ecological inference of denitrifying communities. *Sci. Rep.* **6**, 1–8 (2016).
47. Hynes, R. K. & Knowles, R. Inhibition by acetylene of ammonia oxidation in *Nitrosomonas europaea*. *FEMS Microbiol. Lett.* **4**, 319–321 (1978).
48. Oremland, R. S. & Capone, D. G. Use of “specific” inhibitors in biogeochemistry and microbial ecology. in *Advances in Microbial Ecology* 285–383 (Springer, 1988). doi:10.1007/978-1-4684-5409-3_8
49. Hardy, R. W. F., Holsten, R. D., Jackson, E. K. & Burns, R. C. The acetylene - ethylene assay for N₂ fixation: laboratory and field evaluation. *Plant Physiol.* **43**, 1185–1207 (1968).
50. Lavy, A. *et al.* A quick, easy and non-intrusive method for underwater volume and surface area evaluation of benthic organisms by 3D computer modelling. *Methods Ecol. Evol.* **6**, 521–531 (2015).
51. Gutierrez-Heredia, L., Benzoni, F., Murphy, E. & Reynaud, E. G. End to end digitisation and analysis of three-dimensional coral models, from communities to corallites. *PLoS One* **11**, e0149641 (2016).
52. Clarke, K. R. & Gorley, R. N. PRIMER v6: Users Manual/Tutorial. 1–192 (2006).
53. Anderson, M. J. A new method for non parametric multivariate analysis of variance. *Austral Ecol.* **26**, 32–46 (2001).
54. Anderson, M. J., Gorley, R. N. & KR, C. *PERMANOVA + for PRIMER: Guide to software and statistical methods.* (2008).
55. Béraud, E., Gevaert, F., Rottier, C. & Ferrier-Pagès, C. The response of the scleractinian coral *Turbinaria reniformis* to thermal stress depends on the nitrogen status of the coral holobiont. *J. Exp.*

- Biol.* **216**, 2665–2674 (2013).
56. Wegley, L., Edwards, R., Rodriguez-Brito, B., Liu, H. & Rohwer, F. Metagenomic analysis of the microbial community associated with the coral *Porites astreoides*. *Environ. Microbiol.* **9**, 2707–2719 (2007).
 57. Shoun, H., Fushinobu, S., Jiang, L., Kim, S.-W. & Wakagi, T. Fungal denitrification and nitric oxide reductase cytochrome P450nor. *Philos. Trans. R. Soc. B Biol. Sci.* **367**, 1186–1194 (2012).
 58. Arif, C. *et al.* Assessing *Symbiodinium* diversity in scleractinian corals via next-generation sequencing-based genotyping of the ITS2 rDNA region. *Mol. Ecol.* **23**, 4418–4433 (2014).
 59. LaJeunesse, T. C. Diversity and community structure of symbiotic dinoflagellates from Caribbean coral reefs. *Mar. Biol.* **141**, 387–400 (2002).
 60. Marcelino, V. R., van Oppen, M. J. H. & Verbruggen, H. Highly structured prokaryote communities exist within the skeleton of coral colonies. *ISME J.* **12**, 300–303 (2018).
 61. Yang, S.-H. *et al.* Metagenomic, phylogenetic, and functional characterization of predominant endolithic green sulfur bacteria in the coral *Isopora palifera*. *Microbiome* **7**, 3 (2019).
 62. Pernice, M. *et al.* Down to the bone : the role of overlooked endolithic microbiomes in reef coral health. *ISME J.* (2019). doi:10.1038/s41396-019-0548-z
 63. Compaoré, J. & Stal, L. J. Effect of temperature on the sensitivity of nitrogenase to oxygen in two heterocystous cyanobacteria. *J. Phycol.* **46**, 1172–1179 (2010).
 64. Silvennoinen, H., Liikanen, A., Torssonen, J., Stange, C. F. & Martikainen, P. J. Denitrification and N₂O effluxes in the Bothnian Bay (northern Baltic Sea) river sediments as affected by temperature under different oxygen concentrations. *Biogeochemistry* **88**, 63–72 (2008).
 65. Lloyd, D., Boddy, L. & Davies, K. J. P. Persistence of bacterial denitrification capacity under aerobic conditions: the rule rather than the exception. *FEMS Microbiol. Ecol.* **45**, 185–190 (1987).
 66. Berman-Frank, I. *et al.* Segregation of nitrogen fixation and oxygenic photosynthesis in the marine cyanobacterium *Trichodesmium*. *Science (80-)*. **294**, 1534–1537 (2001).
 67. Bednarz, V. N. *et al.* Contrasting seasonal responses in dinitrogen fixation between shallow and deep-water colonies of the model coral *Stylophora pistillata* in the northern Red Sea. *PLoS One* **13**, e0199022 (2018).
 68. Her, J.-J. & Huang, J.-S. Influences of carbon source and C/N ratio on nitrate/nitrite denitrification and carbon breakthrough. *Bioresour. Technol.* **54**, 45–51 (1995).
 69. Olson, N. D., Ainsworth, T. D., Gates, R. D. & Takabayashi, M. Diazotrophic bacteria associated with Hawaiian *Montipora* corals: Diversity and abundance in correlation with symbiotic dinoflagellates. *J. Exp. Mar. Bio. Ecol.* **371**, 140–146 (2009).
 70. Sorokin, Y. I. On the feeding of some scleractinian corals with bacteria and dissolved organic matter. *Limnol. Oceanogr.* **18**, 380–385 (1973).
 71. Falkowski, P. G., Dubinsky, Z., Muscatine, L. & Porter, J. W. Light and the bioenergetics of a symbiotic coral. *Bioscience* **34**, 705–709 (1984).
 72. Kessler, P. S., Daniel, C. & Leigh, J. A. Ammonia switch-off of nitrogen fixation in the methanogenic archaeon *Methanococcus maripaludis*: mechanistic features and requirement for the novel GlnB homologues, Nif1 and Nif2. *J. Bacteriol.* **183**, 882–889 (2001).

73. Tilstra, A. *et al.* Effects of water column mixing and stratification on planktonic primary production and dinitrogen fixation on a northern Red Sea coral reef. *Front. Microbiol.* **9**, 2351 (2018).
74. Bednarz, V. N., Cardini, U., van Hoytema, N., Al-Rshaidat, M. M. D. & Wild, C. Seasonal variation in dinitrogen fixation and oxygen fluxes associated with two dominant zooxanthellate soft corals from the northern Red Sea. *Mar. Ecol. Prog. Ser.* **519**, 141–152 (2015).
75. Rix, L. *et al.* Seasonality in dinitrogen fixation and primary productivity by coral reef framework substrates from the northern Red Sea. *Mar. Ecol. Prog. Ser.* **533**, 79–92 (2015).
76. Santos, H. F. *et al.* Climate change affects key nitrogen-fixing bacterial populations on coral reefs. *ISME J.* **8**, 2272–2279 (2014).
77. Baker, D. M., Freeman, C. J., Wong, J. C. Y., Fogel, M. L. & Knowlton, N. Climate change promotes parasitism in a coral symbiosis. *ISME J.* **12**, 921–930 (2018).
78. McClanahan, T. R., Baird, A. H., Marshall, P. A. & Toscano, M. A. Comparing bleaching and mortality responses of hard corals between southern Kenya and the Great Barrier Reef, Australia. *Mar. Pollut. Bull.* **48**, 327–335 (2004).
79. Tremblay, P., Gori, A., Maguer, J. F., Hoogenboom, M. & Ferrier-Pagès, C. Heterotrophy promotes the re-establishment of photosynthate translocation in a symbiotic coral after heat stress. *Sci. Rep.* **6**, (2016).
80. Wooldridge, S. A. Formalising a mechanistic linkage between heterotrophic feeding and thermal bleaching resistance. *Coral Reefs* **33**, 1131–1136 (2014).
81. Grottoli, A. G., Rodrigues, L. J. & Palardy, J. E. Heterotrophic plasticity and resilience in bleached corals. *Nature* **440**, 1186–1189 (2006).
82. Seemann, J. *et al.* Importance of heterotrophic adaptations of corals to maintain energy reserves. *Proc. 12th Int. Coral Reef Symp.* 9–13 (2012)

Chapter 5

Chapter 5 | Evidence for dynamic environmental control of coral holobiont nitrogen cycling

Arjen Tölstra^{1*}, Florian Roth^{2,3,4}, Yusuf C. El-Khaled¹, Claudia Pogoreutz^{2,5}, Nils Rådecker^{2,5,6}, Christian R. Voolstra^{2,5*}, Christian Wild¹

¹ Marine Ecology Department, Faculty of Biology and Chemistry, University of Bremen, Bremen, Germany

² Red Sea Research Center, King Abdullah University of Science and Technology, Thuwal, Kingdom of Saudi Arabia

³ Baltic Sea Centre, Stockholm University, Stockholm, Sweden

⁴ Tvärminne Zoological Station, Faculty of Biological and Environmental Sciences, University of Helsinki, Helsinki, Finland

⁵ Department of Biology, University of Konstanz, Konstanz, Germany

⁶ Laboratory for Biological Geochemistry, School of Architecture, Civil and Environmental Engineering, École Polytechnique Fédérale de Lausanne (EPFL), Lausanne, Switzerland

* Corresponding authors: tolstra@uni-bremen.de & chris.voolstra@gmail.com

5.1 | Abstract

Recent research suggests nitrogen (N) cycling microbes are important for coral holobiont functioning. In particular, coral holobionts may acquire novel bioavailable N via prokaryotic dinitrogen (N₂) fixation or remove excess N via denitrification activity. However, our understanding of environmental drivers on these processes *in hospite* remains limited. Employing the strong seasonality of the central Red Sea, this study assessed the effects of environmental parameters on the proportional abundances of N-cycling microbes associated with *Acropora hemprichii* and *Stylophora pistillata*. Specifically, we quantified changes in the relative ratio between *nirS* and *nifH* gene copy numbers, as a proxy for seasonal shifts in denitrification and N₂ fixation potential in corals, respectively. In addition, we assessed coral-tissue associated Symbiodiniaceae cell densities and monitored environmental parameters to provide a biotic and environmental context, respectively. Ratios of *nirS* to *nifH* gene copy numbers revealed similar seasonal patterns in both coral species, with ratios closely following patterns in environmental N availability. As Symbiodiniaceae cell densities also aligned with environmental N availability, the seasonal shifts in *nirS* to *nifH* gene ratios are likely driven by N availability in the coral holobiont. Thereby, our results suggest that N-cycling in coral holobionts likely dynamically adjusts to environmental conditions by increasing and/or decreasing denitrification and N₂ fixation potential according to environmental N availability. Microbial N-cycling may, thus, extenuate the effects of changes in environmental N availability on coral holobionts and support maintenance of the coral – Symbiodiniaceae symbiosis.

Keywords: Coral reefs | nitrogen cycling | Scleractinia | seasonality | denitrification | dinitrogen fixation

A modified version of this chapter has been submitted to *Royal Society Open Science* and is currently in review

5.2 | Introduction

The oligotrophic nature of coral reefs requires an efficient use and recycling of the available nutrients within the ecosystem, including their main engineers, scleractinian corals. As such, corals consist not simply of the animal host alone, but additionally harbour a diverse range of eukaryotic and prokaryotic microorganisms¹, rendering it so-called “holobiont”. Many of these coral associated microorganisms aid in nutrient (re)cycling^{2,3}. Nitrogen (N) is an essential macro nutrient, the availability of which often being the controlling factor for primary production (i.e. the fixation of inorganic carbon [CO₂] through photosynthesis) in coral holobionts^{4,5}. Despite the importance of N for coral holobionts, *in hospite* limitation of N is crucial for maintaining the symbiosis between the coral animal (as the host) and the photosynthetic algal symbionts of the family Symbiodiniaceae⁶. Translocation of photosynthates (derived from Symbiodiniaceae), i.e. the main supply of organic C for the coral host⁷, is optimal when Symbiodiniaceae are N limited^{8–10}. The interruption of N limitation may thus lead to the cessation of photosynthate translocation, which may ultimately lead to the breakdown of the coral/Symbiodiniaceae symbiosis due to increased bleaching susceptibility^{9,11,12}. Thus, the cycling of N is critical for understanding coral holobiont functioning⁹.

Environmental availability of N is known to fluctuate in coral reef environments. This may include natural fluctuations, e.g. seasonality in N availability^{13–15}, as well as anthropogenic N input¹⁶. In this sense, coral-associated microbes, in particular prokaryotes may play an integral role in coral holobiont N cycling. On the one hand, diazotrophs, prokaryotes capable of fixing atmospheric dinitrogen (N₂), may provide the coral holobiont with de novo bioavailable N in the form of ammonium in times of environmental N scarcity^{17–19}. On the other hand, microbes capable of denitrification, i.e. the chemical reduction of nitrate to N₂, may play a putative role in alleviating the coral holobiont from excess N²⁰. In that sense, it was hypothesized that high denitrification rates may maintain N limitation for Symbiodiniaceae, and, as a result, may potentially support the functioning of the coral/Symbiodiniaceae symbiosis^{9,11}. To this end, the presence of denitrifiers in coral holobionts was first reported in the late 2000s^{21,22} and Tilstra et al.²⁰ recently demonstrated that denitrification indeed constitutes an active metabolic pathway present in coral holobionts from the oligotrophic central Red Sea.

Taken together, microbial N cycling has the potential to increase or reduce N availability for the coral holobiont. However, our understanding of how abiotic and biotic factors affect nitrogen cycling properties in corals remains poorly understood. Making use of the pronounced seasonality of the Red Sea, the present study aimed to (i) assess patterns in the abundance of denitrifiers (approximated via *nirS* gene copy numbers) in relation to diazotrophs (approximated via *nifH* gene copy numbers) in a seasonal resolution (from herein referred to as *nirS* to *nifH* gene ratios); and (ii) identify environmental parameters potentially driving the observed seasonal patterns. Due to the potential stimulating or suppressing effects of DIN on denitrification²³ and diazotrophy^{24–27}, respectively, we hypothesized that the seasonal patterns of *nirS* to *nifH* gene ratios in coral holobionts would be mostly affected by dissolved inorganic N (DIN), i.e. nitrate, nitrite, and/or ammonium concentrations.

5.3 | Materials and Methods

Sample Collection

Two common species of hard coral, i.e. *Acropora hemprichii* (Acroporidae) and *Stylophora pistillata* (Pocilloporidae), were collected over four seasons (Fig. 5.1A). Corals were collected at approx. 5 m water depth at the semi-exposed side of the inshore reef Abu Shosha (N22°18'15", E39°02'56") located in the Saudi Arabian central Red Sea between April 2017 and January 2018: April 2017 sampling (spring), August 2017 (summer), November 2017 (fall), and January 2018 (winter). During each season, eight fragments of each coral species were collected from spatially separated colonies (> 10 m) to ensure genetic diversity. Immediately after collection, fragments were flash frozen in liquid nitrogen aboard the research vessel. Subsequently, fragments were transported to the laboratories of the King Abdullah University of Science and Technology and stored at -80 °C until further processing.

DNA Extraction and Quantitative PCR (qPCR)

Quantitative PCRs were carried out according to Tilstra et al.²⁰. Briefly, relative copy numbers of the functional genes *nirS* and *nifH* were used as a proxy for denitrification and diazotrophy, respectively, as implemented previously^{19,20,28}. To this end, coral tissues were separated from the skeleton by pressurized air. DNA was extracted from 100 µL of the resulting tissue slurry using the Qiagen DNeasy Plant Mini Kit (Qiagen, Germany) according to the manufacturer's instructions. Extracted DNA was of varying quality and amplification was not possible in some samples resulting in varying levels of replicates for each species and season.

qPCR assays were performed in triplicates for each biological replicate (i.e., coral fragment). Each assay contained 9 µL reaction mixture and 1 µL DNA template (input adjusted to approx. 3 ng DNA µL⁻¹). Reaction mixture contained 5 µL Platinum SYBR Green qPCR Master Mix (Invitrogen, Carlsbad, CA, United States), 0.2 µL of each primer (10 µM), 0.2 µL of ROX dye and 3.4 µL of RNase-free water. *NirS* to *nifH* gene ratios were determined by normalizing against the *nifH* gene (see Table 5.1 for primers used). The thermal cycling protocol was 50 °C for 2 min, 95 °C for 2 min, 50 cycles of 95 °C for 30 s, 51 °C for 1 min, 72 °C for 1 min and a 72 °C extension cycle for 2 min. Amplification specificity was determined by adding a dissociation step (melting curve analysis). All assays were performed on the ABI 7900HT Fast Real-Time PCR System (Applied Biosystems, CA, USA). Standard calibration curves were run simultaneously covering 8 orders of magnitude (10¹–10⁸ copies of template per assay each for the *nirS* and *nifH* gene). The qPCR efficiency (E) of the primer pairs was 86 % and 87 %, respectively, calculated according to the equation $E = [10^{(-1/\text{slope})} - 1]$. *NirS* to *nifH* gene ratios were calculated as $2^{(-\Delta\Delta C_t)}$ against *nifH* Ct values using the season with the lowest relative abundances as the reference²⁹.

Table 5.1 | Selected primers used for amplification

Target gene	Primer	Nucleotide sequence (5' → 3')	Reference
		G TSAACG TSAAGGARACSG	
<i>nirS</i>	cd3aF	G	Michotey et al. ³⁰
	R3cd	GASTTCGGRTGSGTCTTGA	
<i>nifH</i>	F2	TGYGAYCCIAAIGCIGA	Gaby and Buckley ³¹
	R6	TCIGGIGARATGATGGC	

Symbiodiniaceae Cell Density

An aliquot of the tissue slurry used for DNA extraction was used to obtain cell densities of Symbiodiniaceae. Tissue slurry aliquots were homogenized, diluted at a ratio of 5:1, and Symbiodiniaceae cells were subsequently counted using a Neubauer–improved hemocytometer on a light microscope with HD camera (Zeiss, Germany). Resulting photographs were analyzed using the Cell Counter Notice in ImageJ software (National Institutes of Health, USA). Cell counts for tissue slurries for each individual coral were done in duplicates and subsequently averaged. Finally, to obtain cell densities of Symbiodiniaceae per unit area of coral tissue, cell counts were normalized to coral surface area, which was calculated using cloud–based 3D models of samples (Autodesk Remake v19.1.1.2)^{32,33}.

Environmental Parameters

Environmental data, i.e. temperature, light intensity (photosynthetically active radiation [PAR = 400–700 nm], salinity, dissolved oxygen, nitrate, nitrite, ammonium, dissolved inorganic phosphorus (DIP = [phosphate]), and dissolved organic carbon (DOC), were described and published previously in Roth et al.¹⁴ and were reanalysed for the purpose of the present study.

Temperature was measured continuously with data loggers (Onset HOBO Water Temperature Pro v2 Data Logger – U22–001; accuracy: ± 0.21 °C) one month prior and within the month of sampling on a 30 min interval. Light availability (lux) was measured with data loggers (Onset HOBO Pendant UA– 002–64; spectral detection range 150–1200 nm) for three full days every month and converted to photosynthetically active radiation (PAR = 400–700 nm) using a conversion factor of 51.8. Salinity was measured for three full days every month using a conductivity measuring cell (TetraCon®, 925, WTW, accuracy: ± 0.5 % of value, internal conversion to salinity). Dissolved oxygen (DO) was quantified on 2 days within the month of sampling by taking the average of eight autonomous recording DO and temperature sensors (HOBO U26; temperature corrected and salinity adjusted) that were deployed at 5 m water depth within a radius of 50 m of the sampling site. Seawater samples were taken in triplicates at the sampling site on three days during each month, i.e. one month prior to sampling and the month of sampling, to measure (in)organic nutrients. Nitrate, nitrite and DIP were measured photometrically, while ammonium was measured fluorometrically. DIN:DIP ratios were calculated, where DIN = [nitrate] + [nitrite] + [ammonium]. Subsamples for dissolved organic carbon (DOC) were filtered through 0.2 μ m Millipore® polycarbonate filters into pre–combusted

(450°C, 4.5 h) acid-washed amber glass vials (Wheaton) with Teflon-lined lids, and samples were subsequently acidified with H₃PO₄ until reaching a pH 1 – 2. Samples were kept in the dark at 4 °C until further analysis by high-temperature catalytic oxidation (HTCO) using a total organic carbon analyzer (Shimadzu, TOC-L). To monitor the accuracy of DOC concentration measurements, we used reference material of deep-sea carbon (42 – 45 μmol C L⁻¹) and low carbon water (1 – 2 μmol C L⁻¹).

Statistical Analyses

To assess seasonality, data were analyzed using non-parametric permutational multivariate analysis of variance (PERMANOVA) using PRIMER-E version 6 software³⁴ with the PERMANOVA+ add on³⁵. To test for differences in *nirS* and *nifH* gene ratios and Symbiodiniaceae cell densities between seasons, 2-factorial PERMANOVAs were performed with season and coral species as main factors, while 1-factorial PERMANOVAs were performed with season as a main factor for environmental parameters, based on Bray-Curtis similarities of square-root transformed data. Type III (partial) sum of squares were therefore used with unrestricted permutation of raw data (999 permutations), and PERMANOVA pairwise tests with parallel Monte Carlo tests were carried out when significant differences were found.

Pearson Product-Moment Correlation tests were performed to identify correlations between *nirS* to *nifH* gene ratios, Symbiodiniaceae cell density and environmental variables. Salinity and nitrite were omitted from the analyses as differences were assumed to have no ecological significance. Finally, linear regression analysis was used to assess a potential statistical relationship between *nirS* to *nifH* gene ratios and Symbiodiniaceae cell density over all seasons. All values are given as mean ± SE.

5.4 | Results

NirS to *nifH* Gene Ratios

Lowest *nirS* to *nifH* gene ratios were observed during the spring season, hence gene ratios for other seasons were calculated as fold changes in relation to spring (Fig. 5.1B). In the summer, gene ratios increased ~2-fold for both species, while they increased ~11-fold during the fall for *A. hemprichii* and ~52-fold for *S. pistillata* (Fig. 5.1B). During winter, gene ratios were ~5-fold higher in *A. hemprichii* compared to spring (no data available for *S. pistillata* for this season) (Fig. 5.1B). Due to strong variation there were no significant differences found between seasons for *A. hemprichii*. For *S. pistillata* gene ratios were higher during fall compared to spring (pair-wise PERMANOVA, $t = 2.83$, $p = 0.038$). There was no interactive effect of season and species on gene ratios (PERMANOVA, pseudo-F = 0.14, $p = 0.877$; Table S5.1). However, there was an effect of season (PERMANOVA, pseudo-F = 3.04, $p = 0.039$; Table S5.1) and species (PERMANOVA, pseudo-F = 6.11, $p = 0.019$; Table S5.1) on gene ratios. Indeed, gene ratios were higher during fall compared to spring (pair-wise PERMANOVA, $t = 3.12$, $p = 0.013$) and summer (pair-wise PERMANOVA, $t = 2.45$, $p = 0.024$).

Symbiodiniaceae Cell Density

Cell densities of Symbiodiniaceae varied more strongly between seasons in *A. hemprichii* compared to *S.*

pistillata (Table S5.1; Fig. 5.1C). Cell densities for *A. hemprichii* were lowest in spring ($0.31 \pm 0.03 \times 10^6$ cells cm^{-2}) and significantly increased during summer ($0.56 \pm 0.05 \times 10^6$ cells cm^{-2} ; pair-wise PERMANOVA, $t = 4.14$, $p < 0.001$) (Fig. 5.1C). Subsequently, cell densities significantly increased in fall ($0.78 \pm 0.06 \times 10^6$ cells cm^{-2} ; pair-wise PERMANOVA, $t = 2.69$, $p = 0.014$), but returned to densities similar to summer, during winter ($0.59 \pm 0.10 \times 10^6$ cells cm^{-2}) (Fig. 5.1C). Cell densities of Symbiodiniaceae in tissues of *S. pistillata* were similar during spring, summer and winter (0.53 ± 0.07 , 0.52 ± 0.08 , $0.50 \pm 0.04 \times 10^6$ cells cm^{-2} , respectively) (Fig. 5.1C). However, densities during fall were significantly higher compared to the other seasons ($0.73 \pm 0.06 \times 10^6$ cells cm^{-2} ; pair-wise PERMANOVA, $p < 0.05$) (Fig. 5.1C).

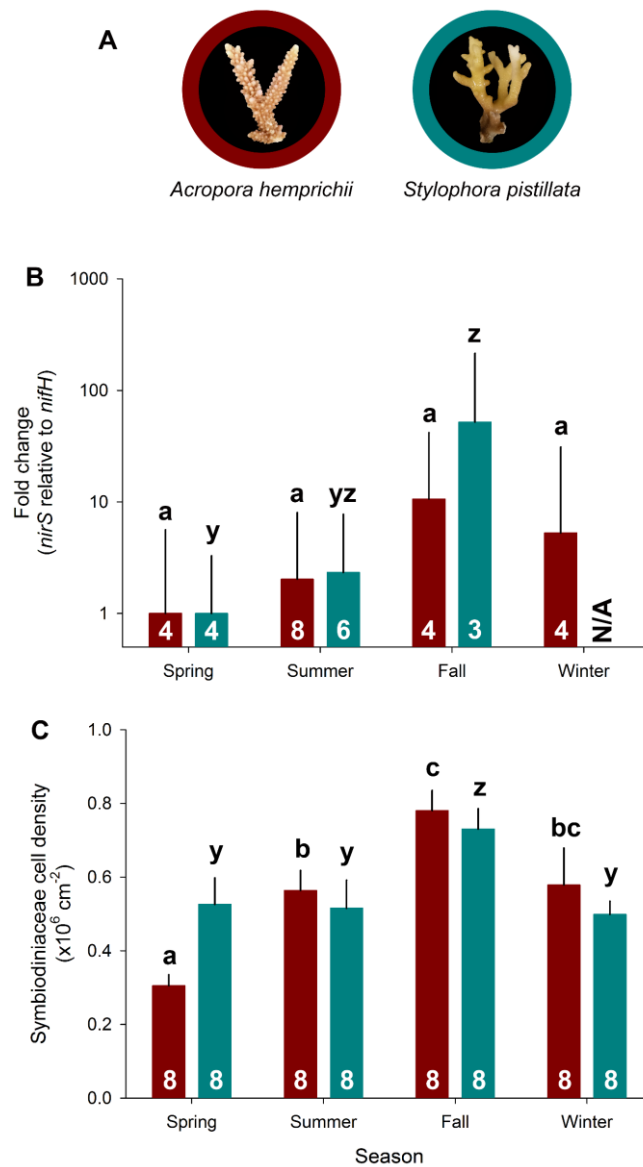


Figure 5.1 | Patterns of *nirS* to *nijH* gene ratios and Symbiodiniaceae cell densities associated with two Red Sea hard coral species across four seasons. **(A)** Representative photographs of investigated species, **(B)** Fold change of *nirS* to *nijH* gene ratios, **(C)** Symbiodiniaceae cell densities. Fold changes were calculated in relation to spring, during which both species exhibited the lowest *nirS* to *nijH* gene ratios; bars indicate the mean; error bars indicate upper confidence intervals (+ 1 SE). Numbers in the bars represent the sample size (n). Different letters above error bars indicate statistically significant differences per species between seasons within each plot (pair-wise PERMANOVA, $p < 0.05$). N/A = not available.

Environmental Parameters

Several environmental parameters exhibited marked seasonal fluctuations (Fig. 5.2). Temperature and PAR increased from spring to the summer season when both parameters were at their highest (31.99 ± 0.01 °C and 573 ± 13 $\mu\text{mol m}^{-2} \text{s}^{-1}$, respectively) (Fig. 5.2A and Fig. 5.2B). Dissolved oxygen was lowest in summer (5.26 ± 0.05 mg L⁻¹) and highest in winter (6.44 ± 0.03 mg L⁻¹) (Fig. 5.2C). Nitrate was highest during the fall season (0.93 ± 0.02 μM) and lowest during the spring season (0.30 ± 0.05 μM) (Fig. 5.2D). Nitrite remained stable throughout all seasons (0.045 ± 0.005 μM) (Fig. 5.2E). Ammonium was highest during summer (0.19 ± 0.03 μM) (Fig. 5.2F). DIN followed the same pattern as nitrate being highest during the fall season (1.11 ± 0.03 μM) and lowest during the spring season (0.46 ± 0.08 μM) (Fig. 5.2G). DIP was stable from spring until fall but decreased during winter (0.08 ± 0.01 μM) (Fig. 5.2H). Salinity remained relatively stable throughout the period of study (39.85 ± 0.015 PSU) (Fig. 5.2I). DOC followed the same seasonal pattern as temperature, being highest in summer (77.36 ± 0.47 μM) and lowest in spring (67.44 ± 0.27 μM) and winter (68.99 ± 0.77 μM) (Fig. 5.2).

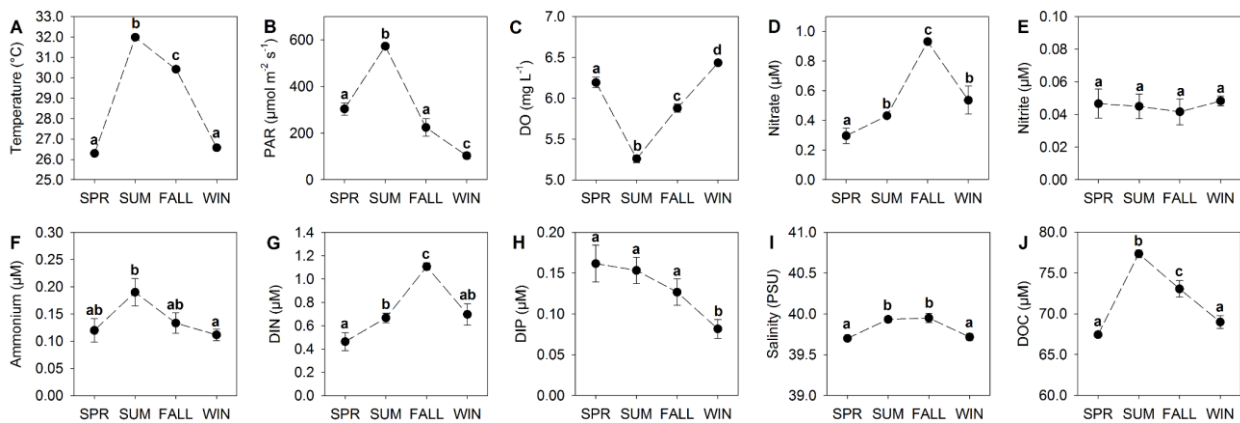


Figure 5.2 | Means (\pm S.E.) of environmental parameters measured over four seasons. **(A)** Temperature, **(B)** Photosynthetically Active Radiation (PAR), **(C)** dissolved oxygen (DO), **(D)** nitrate, **(E)** nitrite, **(F)** ammonium, **(G)** Dissolved Inorganic Nitrogen (DIN = [nitrate] + [nitrite] + [ammonium]), **(H)** Dissolved Inorganic Phosphorus (DIP = [phosphate]), **(I)** salinity, **(J)** Dissolved Organic Carbon (DOC). Different letters above error bars indicate significant differences between seasons within each plot ($p < 0.05$). SPR = spring; SUM = summer; WIN = winter. Data were extracted from Roth et al.¹⁴ and re-analysed for the purpose of this study.

Correlation analyses

Due to the lack of a significant interaction between season and species *nirS* to *nifH* gene ratios (Table S5.1), data for both species were pooled for correlation analyses.

The strongest correlation for both species' *nirS* to *nifH* gene ratios was with nitrate (Pearson Product–Moment Correlation, $r = 0.463$, $p = 0.007$; Fig. 5.3A; Table S5.2). Symbiodiniaceae cell densities also correlated strongest with nitrate for both *A. hemprichii* (Pearson Product–Moment Correlation, $r = 0.649$, $p < 0.001$; Fig. 5.3B; Table S5.2) and *S. pistillata* (Pearson Product–Moment Correlation, $r = 0.446$, $p = 0.011$; Fig. 5.3C; Table S5.2).

No relationship was found between *nirS* to *nifH* gene ratios and Symbiodiniaceae cell densities for *A.*

bemprichii (linear regression, $F = 1.35$, $r^2 = 0.07$, $p = 0.260$) and *S. pistillata* (linear regression, $F = 2.21$, $r^2 = 0.17$, $p = 0.165$).

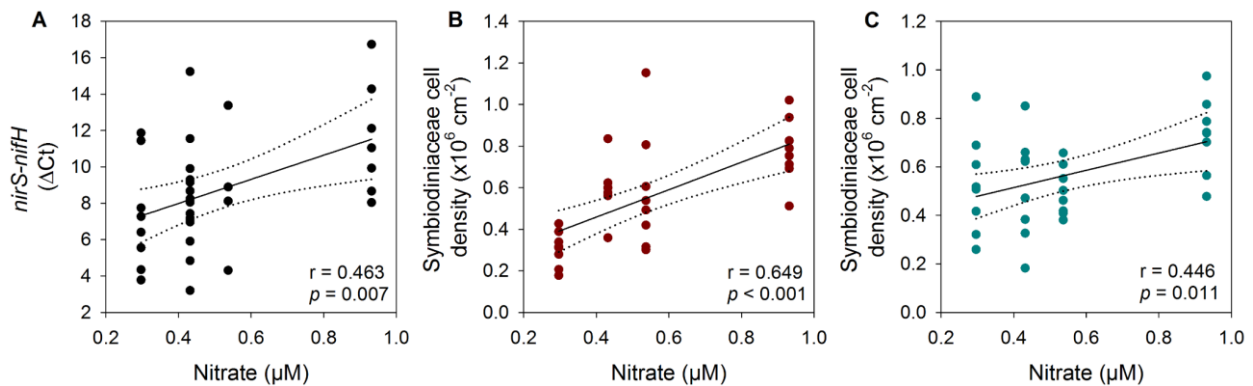


Figure 5.3 | Pearson Product–Moment Correlation analyses for (A) ΔCt of *nirS–nifH* against environmental nitrate concentrations pooled for both coral species, and cell densities of Symbiodiniaceae against environmental nitrate concentrations for (B) *Acropora bemprichii* and (C) *Stylophora pistillata*. r = Pearson coefficient. Dotted lines represent 95% confidence intervals.

5.5 | Discussion

Coral associated microbial N cycling still remains an understudied, but potentially very important part of coral holobiont functioning as it may be a source or sink of bioavailable N^0 . Here, we assessed the proportional dynamics of two antagonistic N–cycling pathways, i.e. denitrification and diazotrophy, in two common central Red Sea coral species (Fig. 5.1A) in a seasonal resolution. To this end, proportional abundances of the functional marker gene *nirS*, as a proxy for denitrification²⁰, were calculated in relation to the functional marker gene *nifH*, as a proxy for diazotrophy¹⁹ (Fig. 5.1B). Importantly, the *nirS* to *nifH* gene ratios presented in this study are not based on absolute, but relative abundances of each respective marker gene. Consequently, the here presented approach does not allow for any conclusion regarding the absolute abundance of marker genes, or, ultimately, absolute abundances of either denitrifiers or diazotrophs. Rather, changes in the ratio may be interpreted as a proxy for a shift in the relative abundance of denitrifying in relation to N_2 –fixing prokaryotes. In this light, increasing ratios may reflect an increase in denitrifying microbes and/or a decrease in N_2 –fixing microbes and vice versa. Using this approach, we were able to reveal the seasonal dynamics of microbial nitrogen cycling in Red Sea corals.

Seasonal Patterns and Environmental Drivers of Denitrification and N_2 Fixation Potential in Corals

The *nirS* to *nifH* gene ratios followed a very similar pattern in both coral species across seasons (Fig. 5.1B). Fall was characterized by the highest and spring by the lowest *nirS* to *nifH* gene ratios in both species. While we did not provide measurements of pathway activity in the present study, relative gene abundances of both marker genes (i.e. *nirS* and *nifH*) were previously shown to align with denitrification and N_2 fixation rates, respectively^{19,20}. Consequently, the observed patterns of *nirS* to *nifH* gene ratios will likely translate into similar seasonal patterns for associated denitrification to N_2 fixation activities. In this light, the similarity of

the seasonal patterns found in both coral species suggests that the functional niche occupied by different N-cycling microbes may be very similar and highly responsive to changing environmental conditions.

Among all investigated environmental parameters, nitrate (the biggest contributor to DIN throughout all four investigated seasons; Fig. S5.1) and DIN concentrations showed the strongest correlation with relative *nirS* to *nifH* gene ratios across coral species (Table S5.2). As the substrate for denitrifiers, nitrate may directly stimulate denitrification activity²³. Likewise, increased nitrate and/or ammonium concentrations have been shown to depress diazotroph activity^{24–27}. The observed patterns in relative *nirS* to *nifH* gene ratios may, thus, be the direct consequence of increased environmental N availability in the coral holobiont.

The notion of seasonally changing N availability driving patterns in ratios of prokaryotic N cycling functional groups within coral holobionts is corroborated by the patterns of Symbiodiniaceae cell densities observed in both coral species. Similar to *nirS* to *nifH* gene ratios, Symbiodiniaceae cell densities exhibited strong seasonal differences that positively correlated with environmental nitrate and DIN concentrations (Fig. 5.3B and Fig. 5.3C, Table S5.2). As Symbiodiniaceae population densities are known to be governed by N availability in the stable coral–algae symbiosis^{36,37}, this suggests that environmental N availability was closely linked with N availability within the coral holobiont in the present study as previously observed in ex situ studies^{38–40}.

Dynamics of N-Cycling Microbes as a Buffer against Seasonal Changes in Environmental N Availability?

Limited N availability is critical to coral holobiont functioning as it limits population growth of Symbiodiniaceae *in hospite* and maintains high rates of translocation of photosynthetic carbon (C) to the host^{8–10,41}. Seasonal or anthropogenically driven increases in environmental N availability may consequently stimulate Symbiodiniaceae proliferation, thereby disrupting or reducing organic C translocation to the host, ultimately posing a threat to overall coral holobiont functioning^{11,42}. Yet, coral holobionts manage to thrive in highly dynamic environments with considerable temporal and spatial variations in N availability^{13–15}. The positive correlation of Symbiodiniaceae densities and environmental N availability in the present study suggests that the coral hosts may not have been able to fully maintain stable N availability within the holobiont. In this light, the observed increase in relative *nirS* to *nifH* gene ratios with increasing N availability, suggests an increase in denitrifying prokaryotes, likely reflecting a beneficial role of N cycling microbes in regulating N availability within the holobiont. During periods of low N availability (e.g., spring), low relative *nirS* to *nifH* gene ratios likely implies reduced denitrification and increased N fixation activity. Likewise, during periods of high N availability (e.g., fall), high relative *nirS* to *nifH* gene ratios likely reflect increased denitrification and reduced N fixation activity. If indeed translatable to corresponding prokaryotic activity, the observed dynamics in functional N cycling gene ratios may, thus, directly support coral holobiont functioning⁹. Specifically, the interplay of denitrifiers and N₂-fixers may support the removal of excess N during times of excess N availability, whilst providing access to new bioavailable N in times of low environmental N availability^{9,17}. Whilst these processes may evidently have been insufficient to the stabilization of N availability within the holobiont as shown in the present study, they may be directly assisting the coral host in regulating Symbiodiniaceae populations.

Future Research Directions

The present study adds to a rapidly growing body of research highlighting the functional importance of N cycling microbes in coral holobiont functioning. Deciphering the interactions between N-cyclers and other coral holobiont members promises to advance our understanding of coral holobiont functioning in light of environmental conditions and anthropogenically-driven change. Whilst combined molecular (sequencing, real-time PCR) and physiological approaches haven proven powerful tools to study N-cycling properties of coral holobionts, future studies should aim to address the localization of the main microbial players along with an accurate quantification of metabolic interactions with other holobiont members. In this light, fluorescence *in situ* hybridization (FISH) as well as nanoscale secondary ion mass spectrometry (NanoSIMS) techniques may allow for an integrated and functional understanding of metabolic interactions in light of their localization within the coral holobiont.

5.6 | Acknowledgements

We thank KAUST CMOR staff and boat crews for their support with diving operations. Financial support was provided by KAUST baseline funds to C.R. Voolstra and the German Research Foundation (DFG) grant Wi 2677/9-1 to C. Wild.

5.7 | References

1. Rohwer, F., Seguritan, V., Azam, F. & Knowlton, N. Diversity and distribution of coral-associated bacteria. *Mar. Ecol. Prog. Ser.* **243**, 1–10 (2002).
2. Falkowski, P. G., Dubinsky, Z., Muscatine, L. & Porter, J. W. Light and the bioenergetics of a symbiotic coral. *Bioscience* **34**, 705–709 (1984).
3. Hernandez-Agreda, A., Leggat, W., Bongaerts, P., Herrera, C. & Ainsworth, T. D. Rethinking the coral microbiome: simplicity exists within a diverse microbial biosphere. *MBio* **9**, e00812-18 (2018).
4. Falkowski, P. G. Evolution of the nitrogen cycle and its influence on the biological sequestration of CO₂ in the ocean. *Nature* **387**, 272–275 (1997).
5. Wang, J. T. & Douglas, A. E. Essential amino acid synthesis and nitrogen recycling in an alga-invertebrate symbiosis. *Mar. Biol.* **135**, 219–222 (1999).
6. LaJeunesse, T. C. *et al.* Systematic revision of Symbiodiniaceae highlights the antiquity and diversity of coral endosymbionts. *Curr. Biol.* **28**, 2570-2580.e6 (2018).
7. Muscatine, L. The role of symbiotic algae in carbon and energy flux in reef corals. in *Coral Reefs* (ed. Dubinsky, Z.) 75–87 (Elsevier, 1990).
8. Béraud, E., Gevaert, F., Rottier, C. & Ferrier-Pagès, C. The response of the scleractinian coral *Turbinaria reniformis* to thermal stress depends on the nitrogen status of the coral holobiont. *J. Exp. Biol.* **216**, 2665–2674 (2013).
9. Rädecker, N., Pogoreutz, C., Voolstra, C. R., Wiedenmann, J. & Wild, C. Nitrogen cycling in corals: the key to understanding holobiont functioning? *Trends Microbiol.* **23**, 490–497 (2015).
10. Dubinsky, Z. & Stambler, N. Marine pollution and coral reefs. *Glob. Chang. Biol.* **2**, 511–526 (1996).
11. Pogoreutz, C. *et al.* Sugar enrichment provides evidence for a role of nitrogen fixation in coral bleaching. *Glob. Chang. Biol.* **23**, 3838–3848 (2017).
12. Wiedenmann, J. *et al.* Nutrient enrichment can increase the susceptibility of reef corals to bleaching. *Nat. Clim. Chang.* **3**, 160–164 (2013).
13. Tilstra, A. *et al.* Seasonality affects dinitrogen fixation associated with two common macroalgae from a coral reef in the northern Red Sea. *Mar. Ecol. Prog. Ser.* **575**, 69–80 (2017).
14. Roth, F. *et al.* Coral reef degradation affects the potential for reef recovery after disturbance. *Mar. Environ. Res.* **142**, 48–58 (2018).
15. D'Angelo, C., Wiedenmann, J. & Angelo, C. D. Impacts of nutrient enrichment on coral reefs: New perspectives and implications for coastal management and reef survival. *Curr. Opin. Environ. Sustain.* **7**, 82–93 (2014).
16. Lapointe, B. E., Brewton, R. A., Herren, L. W., Porter, J. W. & Hu, C. *Nitrogen enrichment, altered stoichiometry, and coral reef decline at Looe Key, Florida Keys, USA: a 3-decade study.* *Marine Biology* vol. 166 (Springer Berlin Heidelberg, 2019).
17. Cardini, U. *et al.* Functional significance of dinitrogen fixation in sustaining coral productivity under oligotrophic conditions. *Proc. R. Soc. B Biol. Sci.* **282**, 20152257 (2015).
18. Lema, K. A., Willis, B. L. & Bourne, D. G. Corals form characteristic associations with symbiotic nitrogen-fixing bacteria. *Appl. Environ. Microbiol.* **78**, 3136–3144 (2012).
19. Pogoreutz, C. *et al.* Nitrogen fixation aligns with *nifH* abundance and expression in two coral trophic functional groups. *Front. Microbiol.* **8**, 1187 (2017).
20. Tilstra, A. *et al.* Denitrification aligns with N₂ fixation in Red Sea corals. *Sci. Rep.* **9**, 19460 (2019).
21. Siboni, N., Ben-Dov, E., Sivan, A. & Kushmaro, A. Global distribution and diversity of coral-

- associated *Archaea* and their possible role in the coral holobiont nitrogen cycle. *Environ. Microbiol.* **10**, 2979–2990 (2008).
22. Kimes, N. E., Van Nostrand, J. D., Weil, E., Zhou, J. & Morris, P. J. Microbial functional structure of *Montastraea faveolata*, an important Caribbean reef-building coral, differs between healthy and yellow-band diseased colonies. *Environ. Microbiol.* **12**, 541–556 (2010).
 23. Zumft, W. G. Cell biology and molecular basis of denitrification. *Microbiol. Mol. Biol. Rev.* **61**, 533–616 (1997).
 24. Koop, K. *et al.* ENCORE: The effect of nutrient enrichment on coral reefs. Synthesis of results and conclusions. *Mar. Pollut. Bull.* **42**, 91–120 (2001).
 25. Cardini, U., Bednarz, V. N., Foster, R. A. & Wild, C. Benthic N₂ fixation in coral reefs and the potential effects of human-induced environmental change. *Ecol. Evol.* **4**, 1706–1727 (2014).
 26. Fay, P. Oxygen relations of nitrogen fixation in cyanobacteria. *Microbiol. Rev.* **56**, 340–73 (1992).
 27. Knapp, A. N. The sensitivity of marine N₂ fixation to dissolved inorganic nitrogen. *Front. Microbiol.* **3**, 374 (2012).
 28. Tilstra, A. *et al.* Relative diazotroph abundance in symbiotic Red Sea corals decreases with water depth. *Front. Mar. Sci.* **6**, 372 (2019).
 29. Pfaffl, M. W. A new mathematical model for relative quantification in real-time RT–PCR. *Nucleic Acids Res.* **29**, e45 (2001).
 30. Michotey, V., Méjean, V. & Bonin, P. Comparison of methods for quantification of cytochrome cd1-denitrifying bacteria in environmental marine samples. *Appl. Environ. Microbiol.* **66**, 1564–1571 (2000).
 31. Gaby, J. C. & Buckley, D. H. A comprehensive evaluation of PCR primers to amplify the *nifH* gene of nitrogenase. *PLoS One* **7**, e42149 (2012).
 32. Lavy, A. *et al.* A quick, easy and non-intrusive method for underwater volume and surface area evaluation of benthic organisms by 3D computer modelling. *Methods Ecol. Evol.* **6**, 521–531 (2015).
 33. Gutierrez-Heredia, L., Benzoni, F., Murphy, E. & Reynaud, E. G. End to end digitisation and analysis of three-dimensional coral models, from communities to corallites. *PLoS One* **11**, e0149641 (2016).
 34. Clarke, K. R. & Gorley, R. N. PRIMER v6: Users Manual/Tutorial. 1–192 (2006).
 35. Anderson, M. J. A new method for non parametric multivariate analysis of variance. *Austral Ecol.* **26**, 32–46 (2001).
 36. Falkowski, P. G., Dubinsky, Z., Muscatine, L. & McCloskey, L. Population control in symbiotic corals - Ammonium ions and organic materials maintain the density of zooxanthellae. *Bioscience* **43**, 606–611 (1993).
 37. Xiang, T. *et al.* Symbiont population control by host-symbiont metabolic interaction in Symbiodiniaceae-cnidarian associations. *Nat. Commun.* **11**, 108 (2020).
 38. Grover, R., Maguer, J. F., Allemand, D. & Ferrier-Pages, C. Urea uptake by the scleractinian coral *Stylophora pistillata*. *J Exp Mar Biol Ecol* **332**, 216–225 (2006).
 39. Grover, R., Maguer, J.-F., Allemand, D. & Ferrier-Pagès, C. Nitrate uptake in the scleractinian coral *Stylophora pistillata*. *Limnol. Oceanogr.* **48**, 2266–2274 (2003).
 40. Grover, R., Maguer, J.-F., Vaganay, S. R.- & S, C. F.-P. Uptake of ammonium by the scleractinian coral *Stylophora pistillata*: Effect of feeding, light, and ammonium concentrations. *Limnol. Oceanogr.* **47**, 782–790 (2002).
 41. Krueger, T. *et al.* Intracellular competition for nitrogen controls dinoflagellate population density in

corals. *Proc. R. Soc. B* **287**, 20200049 (2020).

42. Vega Thurber, R. L. *et al.* Chronic nutrient enrichment increases prevalence and severity of coral disease and bleaching. *Glob. Chang. Biol.* **20**, 544–554 (2014).

Chapter 6

Chapter 6 | Nitrogen fixation and denitrification activity differ between coral- and algae-dominated Red Sea reefs

Yusuf C. El-Khaled^{1*}, Florian Roth^{2,3,4}, Nils Rådecker^{2,5,6}, Arjen Tilstra¹, Denis B. Karcher^{1,7}, Benjamin Kürten^{2,8}, Burton H. Jones², Christian R. Woolstra^{2,5}, Christian Wild¹

¹Marine Ecology Department, Faculty of Biology and Chemistry, University of Bremen, 28359 Bremen, Germany

²Red Sea Research Center, King Abdullah University of Science and Technology (KAUST), 23995 Thuwal, Saudi-Arabia

³Baltic Sea Centre, Stockholm University, 10691 Stockholm, Sweden

⁴Faculty of Biological and Environmental Sciences, Tvärminne Zoological Station, University of Helsinki, 00014 Helsinki, Finland

⁵Department of Biology, University of Konstanz, 78457 Konstanz, Germany

⁶Laboratory for Biological Geochemistry, School of Architecture, Civil and Environmental Engineering, Ecole Polytechnique Fédérale de Lausanne (EPFL), CH-1015 Lausanne, Switzerland

⁷Australian National Centre for the Public Awareness of Science, Australian National University, ACT 2601 Canberra, Australia

⁸Jülich Research Centre GmbH, Project Management Jülich, 18069 Rostock, Germany

*corresponding author: yek2012@uni-bremen.de

6.1 | Abstract

Coral reefs experience phase shifts from coral- to algae-dominated benthic communities, which could affect the interplay between processes introducing and removing bioavailable nitrogen. However, the magnitude of such processes, i.e., dinitrogen (N₂) fixation and denitrification, respectively, and their response to phase shifts remains unknown in coral reefs. We assessed both processes for the dominant species of six benthic categories (hard and soft corals, turf algae, coral rubble, biogenic rock, reef sands), accounting for > 98 % of the benthic of a central Red Sea coral reef. Rates were extrapolated to the relative benthic cover of the studied organisms in co-occurring coral- and algae-dominated areas of the same reef. In general, benthic categories with high N₂ fixation exhibited low denitrification activity. Extrapolated to the respective reef area, turf algae and coral rubble accounted for > 90 % of overall N₂ fixation, whereas corals contributed to more than half of reef denitrification. Total N₂ fixation was twice as high in algae- compared to coral-dominated areas, whereas denitrification was similar. We conclude that algae-dominated reefs promote new nitrogen inputs through enhanced N₂ fixation and residual denitrification. The subsequent increased nitrogen availability could support net productivity, resulting in a positive feedback loop that increases the competitive advantage of algae over corals in phase-shifted reefs.

Keywords: Dinitrogen Fixation | Denitrification | Diazotrophy | Nutrient Cycling | Biogeochemical Cycling | Red Sea | Nitrogen Budget | Metabolism | Coral Reefs

A modified version of this chapter has been submitted to *Scientific Reports* and is currently in review

6.2 | Introduction

Nitrogen (N) is vital for all living organisms and is required for primary production and the production of biomass. Among the key elements required for life (i.e., N, carbon, phosphorus [P], oxygen and sulphur ¹), N in the form of dinitrogen (N₂) gas has the greatest total abundance in the environment ². Ironically, however, N₂ gas is the least accessible for flora and fauna ¹. In oligotrophic marine ecosystems such as coral reefs, primary production is limited by low amounts of bioavailable N forms such as ammonium (NH₄⁺) or nitrate³⁻⁵. Yet, coral reefs belong to the most productive ecosystems on earth and are regarded as oases in an oceanic desert ⁶⁻⁸. In this context, microbial N cycling plays a key role by introducing, recycling and removing N from coral reefs⁹. Particularly, biological dinitrogen (N₂) fixation, i.e., the conversion of atmospheric N₂ into bioavailable NH₄⁺ by prokaryotic microbes (diazotrophs), can alleviate N limitation for coral reef primary producers ¹⁰. In addition, the recycling of *de novo* bioavailable N via nitrification^{4,11} may serve as a mechanism to prevent the loss of N¹². In contrast, denitrification (i.e., the conversion of nitrate to atmospheric N₂ by microbes) may remove bioavailable N in times of high environmental N availability ¹²⁻¹⁴. Likewise, fixed N can be transformed into atmospheric N₂ via anaerobic ammonium oxidation (ANAMMOX), a pathway functioning as an additional N removing mechanism in coral reef sponges¹⁵, and hypothetically in further coral reef associated organisms¹⁶. Whereas N influxes to coral reefs via N₂ fixation are comparably well-studied ^{10,17,18}, knowledge about N efflux via denitrification is limited for coral reef substrates (such as reef sediments) ^{13,14}, and just starting to be generated for coral reef organisms (e.g., hard corals) ¹⁹⁻²². Corals reefs and their main ecosystem engineers, scleractinian corals, are adapted to nutrient-poor environments ^{23,24}, so that both the import of bioavailable N via N₂ fixation as well as the removal via denitrification may essentially contribute to maintaining a stable, low N availability and, hence, ecosystem functioning ²³. Further N cycling processes are hypothesised to help flourishing in aforementioned low N environments. For example, nitrification, i.e., the oxidation of NH₄⁺ to nitrite and nitrate, has been measured in coral reef environments^{4,25}, and may function as an internal recycling mechanism with nitrate serving as a substrate for coupled denitrification¹⁶.

Coral reefs not only belong to one of the most productive but also to the most threatened ecosystems on the planet. Global and local change associated stressors such as ocean warming and acidification ^{26,27}, eutrophication ²⁸, and overfishing ²⁹ undermine the health of coral reefs and can eventually lead to coral mass mortality ³⁰. The remaining coral skeletons offer substrates ³¹⁻³³ for fast-growing, highly competitive algae assemblages ³⁴, which may lead to a transition from coral-dominated to algae-dominated reef states. Due to the stability of these novel communities, these transitions have been interpreted as phase-shifts ³⁵⁻³⁷. Although the effects of these phase-shifts on ecosystem services ³⁸⁻⁴² and functioning ^{43,44} have received some attention, Williams & Graham (2019)⁴⁵ emphasise our yet rudimentary understanding of alterations in coral reef functional ecology. Although we already observe different ecosystem states (e.g., coral-dominated or alternative states on coral reefs)⁴⁶, our knowledge about their functioning is still in its infancy. Additionally, functioning likely differs between coral- and algae-dominated communities ^{47,48}.

N cycling is critical for the stability of coral reef ecosystems; however, it has not been investigated yet how gain (via N₂ fixation) and loss (via denitrification) terms of bioavailable N differ quantitatively between coral- and algae-dominated reef states. For this study, we hypothesised differences between coral- and algae-dominated reef states in the amount of total fixed and denitrified N, based on differences in N₂ fixation and denitrification activities of different benthic categories^{10,49,50} and due to an altered reef community structure associated with phase-shifts. Further, we hypothesised that N cycling processes may have the potential to amplify and catalyse phase-shifts through the proliferation of turf algae as prominent N₂ fixers⁵¹. The role of denitrification in reef communities is mostly unknown, as well as the interplay of both N₂ fixation and denitrification in coral- and algae-dominated reefs. Understanding N cycling patterns in baseline scenarios (i.e., coral-dominated) and alternative reef states (i.e., algae-dominated) is, hence, of paramount interest to gain a holistic understanding of these dynamic systems, which then can be used as a basis to address, elaborate, and expand future management strategies.

In the present study, we carried out acetylene-based incubations i) to identify the key players that import and/or remove nitrogenous compounds into/from the reef system; and ii) to provide a relative budget for two counteracting N cycling processes (i.e., N₂ fixation and denitrification) in a comparative framework that covers the main species of six key benthic categories that together account for > 98 % of the benthic cover on a central Red Sea coral reef with two distinct reef areas.

6.3 | Material and Methods

Study Site and Benthic Community Composition

The Abu Shosha reef in the Jeddah Region (22° 18' 15" N, 39° 02' 56" E) on the west coast of Saudi Arabia in the central Red Sea was chosen due to the co-occurrence of both coral- (i.e., > 40 % hard coral cover) and algae (< 15 % hard coral cover, > 40 % turf algae cover) dominated areas within the same reef (Fig. S6.1)⁵². Both areas are approx. 50 m² in size, were located at the same water depth (~ 5 m) and were solely used as a base for relating the respective N cycling rates to the reef area. Specimens were sampled from the total reef area (see next paragraph). The selected reef displays a small-scale heterogeneity of communities in varying degrees of community composition with both target reef areas being less than 30 m apart from each other.

Benthic community composition of the Abu Shosha reef was determined for an earlier study⁵² by photo quadrats¹³³, providing a two-dimensional (2D) planar reef coverage of each benthic category. Briefly, a PVC quadrat (50 x 50 cm², 0.25 m²) was randomly placed on the reef surface (12 x in coral-dominated area, 10 x in the algae-dominated area), and a photograph was taken from approx. 1 m distance to the substrate. Photographs were then analysed with the software Coral Point Count with Excel extension (CPCe) 4.1¹³⁴. With the help of the software, 48 randomly located points were overlaid on the photographs, resulting in 576 and 480, respectively, data points per study area. The underlying benthos for each data point was determined to the lowest possible taxon. The major benthic categories of the investigated reef were (Fig.

6.1): filamentous turf algal assemblages (hereafter termed turf algae), coral rubble, soft coral (i.e., *Xenia* sp.), biogenic coral rock (hereafter termed biogenic rock), carbonate reef sands (hereafter termed reef sands), hard corals, macroalgae, and the giant clams (*Tridacna* sp.). Hard corals were identified to the genus level. Turf communities consisted of a heterogeneous assemblage of different filamentous algae and cyanobacteria. Examples from the Northern Red Sea have shown that turf algae, as defined for the present study, account for the highest fraction (up to 90%) of benthic algal cover¹³⁵. Areas of bare coral rock, that were not covered with any of the other benthic categories but associated with endolithic algae and crustose coralline algae were defined as biogenic coral rock¹³⁶ (hereafter termed biogenic rock). Coral rubble was defined as dislodged parts of framework builders with its associated microbial community according to Rasser and Riegl (2002)¹²⁸.

Sample Collection and Maintenance

All benthic categories, i.e. hard corals *Pocillopora verrucosa* (n = 5), *Acropora hemprichii* (n = 4), *Stylophora pistillata* (n = 4), soft coral of the *Xenia* genus (n = 5), biogenic rock (n = 5), coral rubble (n = 4), reef sands (n = 5) and turf algae (n = 5), were collected randomly from the overall reef area (i.e., regardless whether from coral- or algae-dominated areas; Fig. 6.1 – Step 1) and immediately incubated after sampling in March 2018. Due to feasibility, the three most abundant hard coral species were chosen as they represent the most abundant species of the Abo Shosha reef. To increase readability and comprehensiveness, we refer to “hard corals” from here on. The aforementioned benthic categories were selected as they comprised more than 98 % of the benthic cover in both coral- and algae-dominated parts of the reef⁵². Where necessary, fragments were collected with hammer and chisel. *P. verrucosa*, *A. hemprichii*, *S. pistillata* and turf algae fragments (limestone covered with turf-algae) were approx. 10 cm long. Hard coral fragments were sampled from different coral colonies (> 10 m distance between each other) to account for genetic diversity. Individual coral colonies of *Xenia* sp. were collected with a small piece of anchoring rock (< 0.5 cm diameter) to prevent tissue damage. Reef sands were sampled using a Petri dish (polystyrene, 5.5 cm diameter, 1.4 cm depth) which was pushed carefully into the sand. Reef sands were then fixed to the dish from underneath so that upper sand “cores” with a max. sediment depth of 14 mm were sampled, covering a similar depth as reported previously^{10,59}. All fragments and Petri dishes containing reef sand samples were immediately transferred to recirculation aquaria on the boat after sampling, each filled with ambient seawater. Fragments of *P. verrucosa*, *Xenia* sp., turf algae, coral rubble, biogenic rock as well as sediment samples were kept at ambient water temperature and light conditions until the experimental incubations started within 3 h after sampling. For *P. verrucosa*, it has been demonstrated successfully that freshly collected fragments can be utilised for physiological quantifications¹³⁷. Fragments of *A. hemprichii* and *S. pistillata* were sampled two weeks prior all other specimens. After being transferred to the wet lab facilities of the Coastal and Marine Resources (CMOR) Core Lab at KAUST, fragments were distributed randomly into four independent replicate 150 L flow-through tanks (flow-through rate 300 L h⁻¹) for two weeks to allow for acclimation and healing of tissue damage. Each aquarium was constantly supplied with ambient, sediment-filtered reef water

from inshore reefs located 1.5 km off KAUST, and ambient light conditions, i.e., a photon flux of $\sim 200 \mu\text{M}$ quanta $\text{m}^{-2} \text{s}^{-1}$, representing the daytime average photon flux of the studied reef and water depth during this period of the year.

Nitrogen Cycle Fluxes

Incubations were performed using a COmbined Blockage/Reduction Acetylene assay (hereafter COBRA; Fig. 6.1 – Step 2) modified after El-Khaled and others (2020)⁷⁷. Briefly, COBRA incubations were performed in gastight 1 L glass chambers (800 mL seawater + 200 mL headspace). As acetylene inhibits the production of nitrate via nitrification^{138,139}, seawater (ambient NO_3 concentrations ranged between 0.09 and $0.34 \mu\text{M}$)^{22,140} was supplemented with nitrate to a final concentration of $5 \mu\text{M}$ as a substrate for the denitrification pathway to counteract substrate limitation (see supplementary material 6.5). Incubations with nitrate amended seawater have been performed successfully in previous studies^{141–143}. Potentially, the addition of nitrate suppresses N_2 fixation¹⁴⁴, particularly as nitrate uptake has been reported for various benthic categories^{145,146}. Theoretically, this could alter microbial functioning of benthic categories, as the acquisition of N via uptake is less cost-intensive¹⁴⁷. However, persistent N_2 fixation rates in the presence of nitrate of up to $30 \mu\text{M}$ have been reported¹⁴⁷. Furthermore, El-Khaled and others (2020)⁷⁷ conclude that the technique provides sufficient information about the relative importance of different benthic categories by accounting for relative changes in N cycling rates (both N_2 fixation and denitrification). COBRA provides denitrification “potentials” as artificially provided nitrate during the incubations drives denitrification above natural levels⁷⁷. Acetylene was added to both incubation water and headspace at a concentration of 10 %. This saturated acetylene concentration in the gastight incubation chambers leads to the preferential reduction of acetylene to ethylene (C_2H_4) instead of N_2 to NH_4 by the key enzyme nitrogenase^{148,149}. Moreover, acetylene blocks the nitrous oxide (N_2O) reductase activity in the denitrification pathway leading to an accumulation of N_2O ^{150,151}. Replicate samples were incubated and two additional chambers without specimens served as controls to correct for planktonic background activity. All incubations lasted for 24 h with a 12:12 h dark/light cycle and a photon flux of $\sim 200 \mu\text{M}$ quanta $\text{m}^{-2} \text{s}^{-1}$, representing the daytime average photon flux of the studied reef and water depth during this period of the year. Incubation chambers were submerged in a temperature-controlled water bath at 27°C (resembling the ambient seawater temperature measured at the reef in 5 m depth during sampling) and constantly stirred (500 rpm) to ensure sufficient exchange between the water body and headspace. Gas samples were taken at the start (t_0) and the end (t_{24}) of each incubation, and analysed targeting C_2H_4 (as a proxy for N_2 fixation) and N_2O (as a proxy for denitrification) by gas chromatography and helium pulsed discharge detector (Agilent 7890B GC system with HP-Plot/Q column, lower detection limits for both target gases were 0.3 ppm). Results were normalised to incubation time, corrected for the seawater control signal, related to incubation volume, and normalised to the surface area of the organisms/substrates. Surface areas of incubated organisms/substrates were determined photometrically using cloud-based 3D models (Autodesk Remake v19.1.1.2)^{152,153} of *P. verrucosa*, *A. hemprichii*, *S. pistillata*, *Xenia* sp., biogenic rock, coral rubble and turf algae fragments. Reef sand

surface areas were calculated using dimensions of Petri dishes that were utilised for sand core sampling (surface area = $\pi * \text{radius}^2$). Notably, sediment depth and, hence, oxygenation status as well as pore-water movement through the sediment matrix affect the biogeochemical cycling, with potentially higher N cycling activity due to anaerobic milieus provided in deeper sand layers⁶⁵. Oxygen fluxes were quantified parallel with identical benthic categories to validate that neither hypoxia nor hyperoxia (conditions that, e.g., are detrimental to organisms evoking alteration of physiological responses) conditions occurred during N cycling incubations¹⁵⁴. We refer to supplementary material 6.6 for further information.

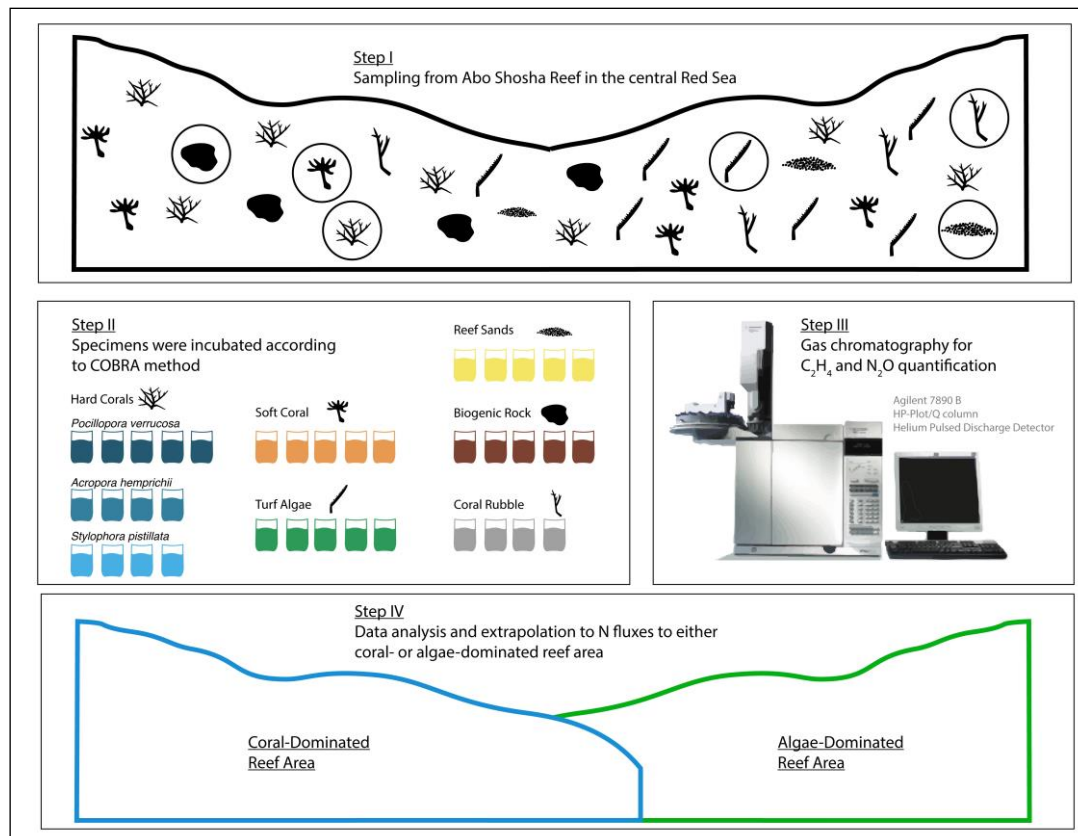


Figure 6.1 | Stepwise illustration of sampling, data acquisition and analysis. Step I illustrates sampling of specimens randomly from the overall reef area (i.e., regardless of coral- or algae-dominated area). Afterwards (step II), all specimens were incubated according to the COBRA method⁷⁷ with the displayed replication. Gas samples were taken for ethylene (C₂H₄) and nitrous oxide (N₂O) measurements via gas chromatography (step III) for N cycling rate quantifications. Obtained data were used for extrapolation to N fluxes to either coral- or algae-dominated reef areas (step IV).

Data Treatment of Nitrogen Fluxes

Production rates of C₂H₄ and N₂O were converted to N fluxes using conservative molar ratios of N₂O:N₂ = 1 and C₂H₄:N₂ = 4¹⁵⁵. Obtained individual rates were presented as fold change relative to mean rates of hard corals for each respective benthic category that was collected randomly from the overall reef area (Fig. 6.3A, 6.3B). Extrapolations for total fixed or removed N (via N₂ fixation and denitrification, respectively) were performed according to formulas in supplementary material 6.7. Briefly, rates were extrapolated by multiplication according to reef benthos 3D area considering the respective 2D to 3D conversion factor

(Table S6.3, according to Cardini and others (2016)¹⁰). Then, these benthic category-specific rates were used to account for the relative cover (i.e., 2D planar coverage obtained from cover assessments described previously) of each benthic category in the respective reef area (i.e., coral- and algae-dominated, resp.), which provides cumulative N fluxes related to 3D reef area (Fig. 6.5; expressed as fixed or denitrified $\mu\text{mol N m}^{-2}$ benthos 3D area d^{-1} , resp.).

Statistical Analysis

Statistical analyses were performed using Primer-E v6¹⁵⁶ with the PERMANOVA+ extension¹⁵⁷. Differences in the N cycling processes among benthic categories were tested for significance using permutational analysis of variance (PERMANOVA) on a Bray-Curtis similarity matrix of square-root transformed data. In case significant differences occurred, pairwise t-tests with parallel Monte Carlo tests were performed. Type III (partial) sum of squares was used with an unrestricted permutation of raw data (999 permutations). Unless mentioned otherwise, hard coral data consists of pooled replicates of the three investigated hard coral species (i.e., *P. verrucosa*, *A. hemprichii*, *S. pistillata*) of which mean rates and standard error of means were calculated. Normality (Shapiro-Wilk test) and differences between benthic categories coverage in both reef areas (e.g., hard coral cover in coral-dominated versus hard coral cover in algae-dominated areas) were tested using SigmaPlot (Version 12.0). Two-tailed t-tests were used if data were distributed normally whereas Mann-Whitney-Rank-sum tests were used if data were not normally distributed. Differences in the benthic composition among reef areas (i.e., coral vs. algae-dominated) were visualised using a principal coordinate analysis (PCO). Total fixed and removed N in both reef areas was calculated based on the sum of means of extrapolated rates/potentials of individual benthic categories and the respective standard propagated error, with Friedman's aligned rank test checking for significant differences among respective reef areas (using R v4.0.4¹⁵⁸ with the interface Rstudio v1.0.153¹⁵⁹). A one-way analysis of similarities (ANOSIM; 999 permutations) was used to describe the dissimilarities between both reef areas. Furthermore, a distance-based linear model (DistLM; 999 permutations) using a step-wise selection procedure with AICc as a selection criterion was used to calculate which benthic category(ies) coverage explained visualised dissimilarities best^{156,157}.

Limitations

Typical budget uncertainties include i) deviations from theoretical molar ratios (i.e., $\text{N}_2\text{O}:\text{N}_2$ and $\text{C}_2\text{H}_4:\text{N}_2$) in different benthic categories (Wilson and others (2012) and references therein¹⁶⁰), ii) methodological underestimation of N cycle processes^{77,161,162}, iii) environmental alterations by benthic categories as an effect of benthic primary productivity¹¹⁶, iv) underestimations of N cycling rates for benthic categories that could not be assessed in their entirety such as reef sands, and v) reef-wide underestimations/omission of metabolic processes in cryptic habitats, such as cracks and crevices within the natural reef matrix, that harbour specific

organisms (e.g., sponges, bryozoan, and tunicates). These organisms are generally not included in ex situ budget derivations. Nevertheless, the results of the present study are comparable to reefs of similar character and structural complexity. However, N cycling activity may vary substantially in reefs of differing structure, with more/fewer cracks and crevices in the reef matrix with inhabiting species that can remarkably contribute to metabolic processes in coral reefs ^{163,164}.

Furthermore, all specimens were sampled randomly from the overall reef area, thus, disregarding potential differences in the microbial communities of benthic categories. These differences are likely to occur between coral- or algae-dominated reef areas ¹¹⁶, and may influence N cycling processes. However, potential effects of differences in the microbial communities of benthic categories that originate in dependence of their origin in the reef, are rather insignificant as they would not allow for identification of differences in N cycling activities between benthic categories. Hence, we assume that shifts in the community composition are likely more relevant for the overall N fluxes than changes of N cycling activities within single benthic categories.

We, thus, consider the major results of the present study as solid and reliable, especially as the investigated benthic categories of investigated species cover > 98 % in both reef areas so that we consider discussed and presented data as conservative estimates. Furthermore, aforementioned underestimation of N fluxes result from initial lag phases in the evolution of C₂H₄^{61,77}, and from potential incomplete blockages of the denitrification pathway¹⁶¹. Due to potential underestimations of both N₂ fixation and denitrification, we, thus, refrained from directly comparing both pathways.

6.4 Results

Benthic Community Composition

Two distinct reef community states characterised by contrasting relative cover of benthic categories were identified (Fig. 6.2A, Fig. S6.1) and pre-defined as “algae-” and “coral-dominated reef areas” (according to Roth and others (2018)⁵²). A detailed overview of the benthic communities is attached as Table S6.1. Briefly, algae-dominated areas displayed approximately twice as much turf algae-cover compared to coral-dominated areas (Mann-Whitney U $p = 0.007$), whereas hard coral cover was 3-fold lower (Mann-Whitney U $p < 0.001$). Pre-defined differentiation between algae- and coral-dominated reef areas were confirmed visually by Principle Coordinate Analysis (PCO, Fig. 6.2B) and ANOSIM ($R = 0.605$, $p = 0.001$). Hard corals and turf algae were the major drivers of separation and explained 64.2 % of the dissimilarities between reef areas (DistLM).

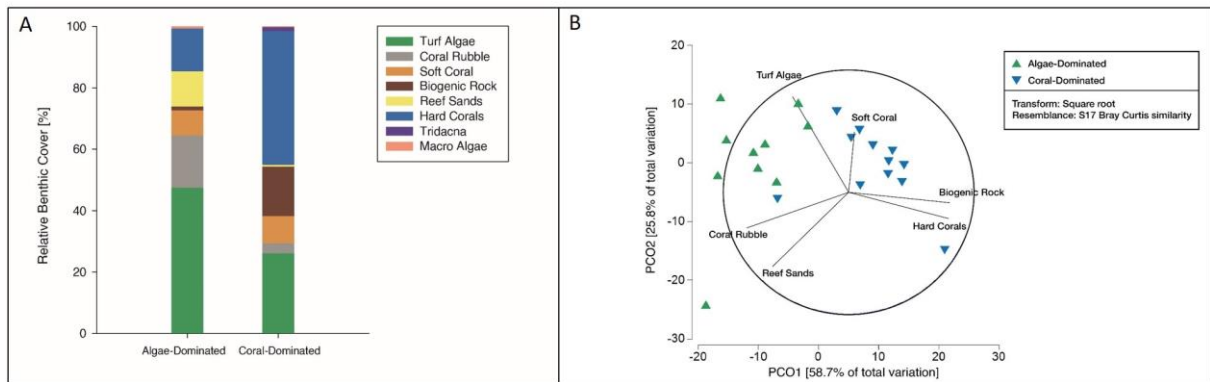


Figure 6.2 | (A) Relative benthic cover in algae- and coral-dominated areas. Benthic cover data is presented as mean proportional cover of major benthic categories assessed by photo quadrats ($n = 10$ in algae-dominated areas, $n = 12$ in coral-dominated areas). Adapted from Roth and others (2018). **(B)** Principle Coordinate Analysis (PCO) of benthic community cover at the algae-dominated (green) and coral-dominated (blue) areas. Vector overlay shows correlations > 0.4 based on Pearson ranking, green triangles display replicates of algae-dominated areas ($n = 10$), blue triangles display replicates of coral-dominated areas ($n = 12$).

Nitrogen Fluxes of Individual Benthic Categories

Turf algae and coral rubble showed highest N_2 fixation rates per substrate surface area, being approximately 5 to 6-fold higher than those of biogenic rock, 10 to 12-fold higher than reef sands, ~ 32 to 39-fold higher than soft coral, and approximately two orders of magnitude higher than hard corals (Fig. 6.3A, Table 6.1 and S6.2).

Due to nitrate addition during incubations, we present denitrification as potentials instead of rates (see Method section). The soft coral displayed the highest denitrification activity, being 3- to 4-fold higher than that of reef sands, biogenic rock and coral rubble, and 6-fold higher than denitrification potentials of hard corals and turf algae (Fig. 6.3B, Table 6.1 and S6.2). Among hard corals (i.e., data above comprised the average potentials across *P. verrucosa*, *A. hemprichii*, and *S. pistillata*), *A. hemprichii* showed the highest denitrification potential that was 5-fold higher than that of *P. verrucosa* (pair-wise PERMANOVA $t = 3.407$, $p = 0.01$) and 26-fold higher than *S. pistillata* (pair-wise PERMANOVA $t = 5.696$, $p < 0.001$).

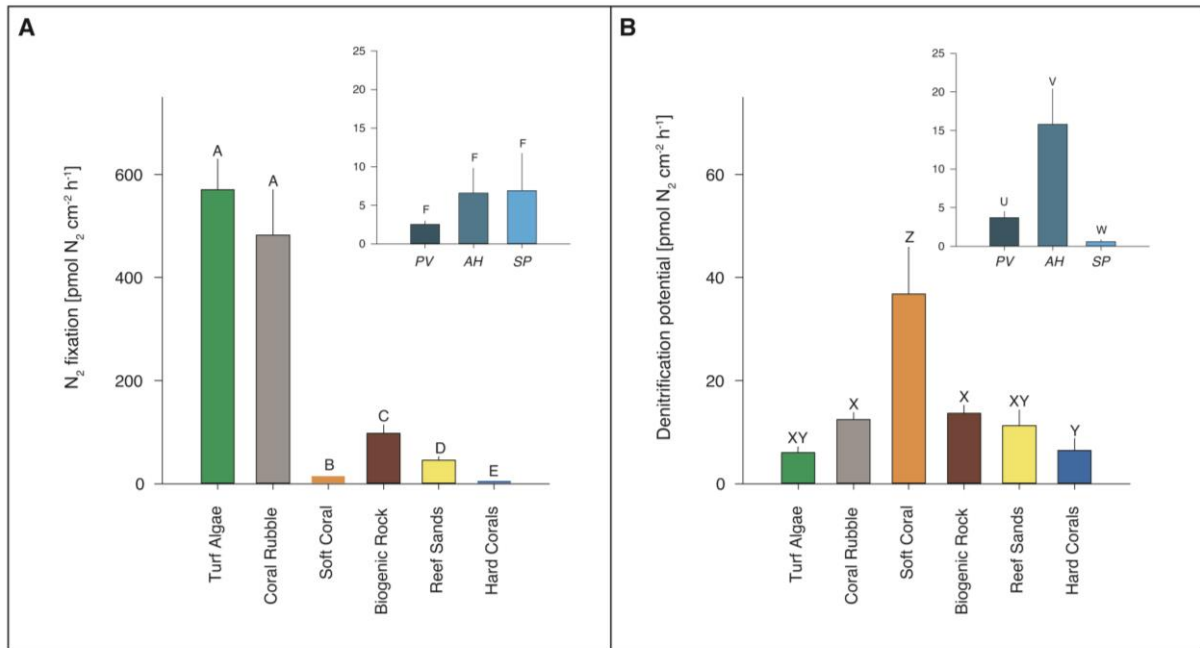


Figure 6.3 | Dinitrogen (N₂) fixation rates **(A)** and denitrification potentials **(B)** of investigated benthic categories and hard coral species. Organisms and substrates (turf algae n = 5, coral rubble n = 4, soft coral n = 5, biogenic rock n = 5, reef sands n = 5, hard corals n = 13) were sampled randomly from both reef areas. Rates and potentials for hard corals consist of mean values of *P. verrucosa* (PV, n = 5), *A. hemprichii* (AH, n = 4), *S. pistillata* (SP, n = 4). Letters above bars indicate significant differences if different, or non-significance if shared. Y-Axis labels for imbedded hard coral data plots are analogue to respective N₂ fixation rate or denitrification potential plot. Note different scales for N₂ fixation and denitrification.

Table 6.1 | Results of permutational analysis of variance (PERMANOVA) and subsequent pair-wise tests for N₂ fixation (highlighted in salmon) and denitrification (highlighted in blue) in all benthic categories. Significant p-values in bold. Top: t-values; bottom: p-values.

	Turf Algae	Coral Rubble	Soft Coral	Biogenic Rock	Reef Sands	Hard Corals	
Turf Algae		0.882	8.793	6.774	10.773	7.439	DINITROGEN FIXATION
Coral Rubble	3.044 0.015		6.913 0.001	4.690 0.004	7.463 0.001	6.362 0.001	
Soft Coral	4.395 0.005	2.608 0.032		4.637 0.001	3.299 0.003	2.374 0.030	
Biogenic Rock	3.551 0.004	0.474 0.661	2.623 0.027		2.550 0.031	5.501 0.001	
Reef Sands	1.344 0.211	0.764 0.454	2.643 0.023	1.056 0.318		4.651 0.001	
Hard Corals	0.944 0.360	2.601 0.047	3.585 0.002	2.434 0.015	1.643 0.111		
	DENITRIFICATION						

Nitrogen Fluxes in Different Benthic Categories Referred to Reef Areas

We used individual rates/potentials of N₂ fixation and denitrification from all measured organisms and substrates (see Table S6.2) to calculate budgets for communities of the assessed reef areas dominated either by corals or turf algae. Cumulated fixed N was 2-fold higher in the algae-dominated compared to the coral-dominated area (Friedman's aligned rank test $p = 0.24$), whereas denitrification was similar (Friedman's aligned rank test $p = 0.19$; Fig. 6.4). Turf algae assemblages contributed most to N₂ fixation in both algae-dominated (70.2 %) and coral-dominated areas (79.8 %), followed by coral rubble (28.4 % in algae-dominated and 11.3 % in coral-dominated area, respectively; Fig. 6.5). In contrast, hard and soft corals combined accounted for 75.5 % and 52.4 % of denitrification activity in coral- and algae-dominated areas, respectively (Fig. 6.5).

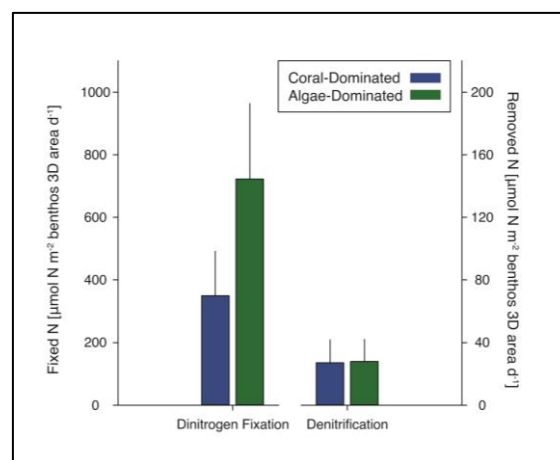


Figure 6.4 | Total fixed (via dinitrogen fixation) and removed N (via denitrification) in both reef areas (calculated as sum of means of extrapolated rates of individual benthic categories \pm standard propagated error; according to supplementary material supplementary material 6.3; no significant differences were observed by applying Friedman's aligned rank test).

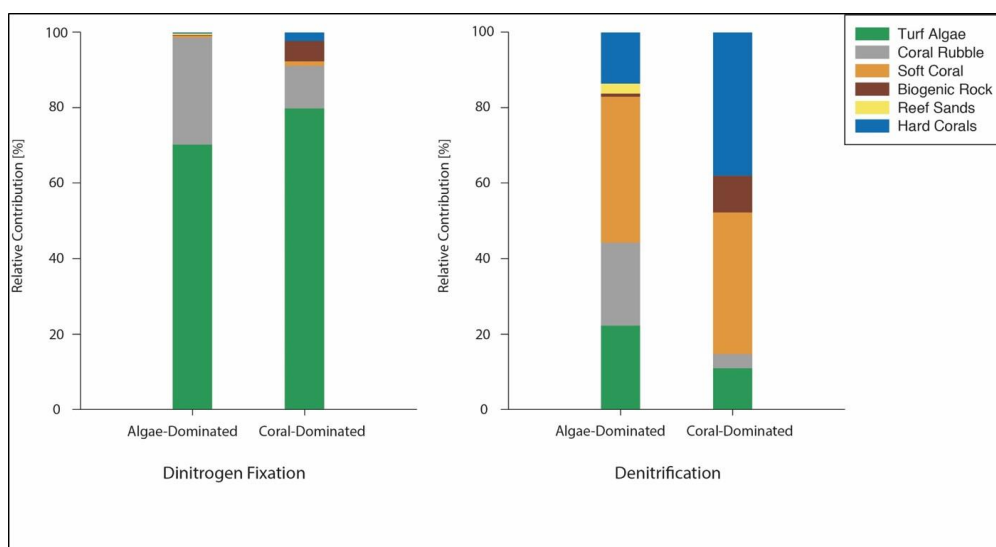


Figure 6.5 | Relative contribution of studied benthic categories to total dinitrogen fixation and total denitrification in coral- and algae-dominated reef areas.

6.5 | Discussion

Stable and low N availability is of central importance to the health and resilience of coral holobionts^{12,53}, and consequently, of coral reef ecosystems in general²³. Thus, processes that introduce or remove bioavailable N, such as N₂ fixation and denitrification, respectively, may play a key role in the functioning of coral reefs²³. Our study is – to the best of our knowledge – the first to provide a comparative overview of denitrification activities of major coral reef related benthic categories. By investigating two N cycling process, we were able to extend previous work of Cardini and others (2016)¹⁰, who showed a link between reef-wide primary production and N₂ fixation. We related benthic category-specific N₂ fixation rates and denitrification potentials (per 2D substrate surface area, Table S6.2) to their relative contribution on a 3D level (Table S6.3), and likewise extrapolated metabolic processes to both coral- and algae dominated reef communities (per 3D benthos surface area, Fig. 6.4, Table S6.1). This may be of particular importance, as algal dominance on coral reefs will likely increase as a consequence of frequently occurring mass coral bleaching events^{54,55} and reduced time available for recovery⁵⁶ that diminish the return to coral-dominated reef states⁵⁷.

N₂ Fixation and Denitrification by Key Benthic Categories on Coral Reefs

Individual N₂ fixation rates of benthic categories are in line^{10,21,49,50,58} or lower^{10,59,60} than rates reported in previous studies (see Table 6.2) from the Red Sea that were obtained with similar measurement techniques (i.e., acetylene-based assays) and sampling intervals (t_0 and t_{24}). Slightly lower N₂ fixation rates in the present study may a) be due to an underestimation caused by an initial lag phase associated with acetylene-based assays^{61,62} (see limitations), which was omitted from rate calculations of other studies⁶⁰ but included here; or b) due varying to sampling times: benthic categories of the present study were incubated in March 2018, which together with measured environmental background parameters^{22,63} belongs to the winter season. It has been demonstrated that N₂ fixation activity in winter is generally lower than in summer^{10,50,64}, which hypothetically explains lower N₂ fixation rates of the present study compared to previously reported rates (see Table 6.2). In how far seasonality affects denitrification potentials of the investigated benthic categories, remains to be determined.

Our results suggest a clear distinction between key benthic categories, in which the most active N₂-fixers showed lowest denitrification potentials and *vice versa*. Turf algae and coral rubble were identified as the largest N₂-fixers confirming previous findings by Cardini and others (2016)¹⁰; however, they play a minor role in reducing N availability via denitrification. Reef sands, as active sites of microbial N transformations in coral reefs¹⁴, play only a marginal role in both N₂ fixation and denitrification in the present study, compared to the other benthic categories. Potentially, comparatively low N₂ fixation and denitrification activity in reef sands of the present study is due to well-oxygenated top sediment layers⁶⁵ thwarting these rather anaerobic processes^{66,67}. Even though reef sand N cycling rates are likely underestimated in the

studied reef areas (as top layers were sampled; see limitations section), they solely cover a minor fraction of the benthic cover.

Table 6.2 | N₂ fixation rates (nmol N₂ cm⁻² h⁻¹) of investigated benthic categories in comparison with values reported from other coral reef areas worldwide acquired via acetylene-based assays. All N₂ fixation rates were converted with a conservative conversion factor of 4:1 (C₂H₄:N₂) according to Mulholland and others (2004)¹⁵⁵. Values are presented in mean ± SE.

N₂ fixation	Location	Reference
<u>Turf algae</u>		
0.57 ± 0.05	Central Red Sea	Present study
0.44 ± 0.04*	Northern Red Sea	Rix and others (2015) ⁵⁰
2.31 ± 0.09**	Northern Red Sea	Shashar and others (1994) ⁶⁰
<u>Coral rubble</u>		
0.48 ± 0.09	Central Red Sea	Present study
1.00 ± 0.25	Great Barrier Reef, Australia	Davey and others (2008) ⁷⁸
0.58 ± 0.20*	Northern Red Sea	Cardini and other (2016) ¹⁰
0.90 – 4.00	Great Barrier Reef, Australia	Larkum (1988) ⁷⁹
0.74 – 5.70	Great Barrier Reef, Australia	Larkum and other (1988) ¹⁸
13.86 ± 4.11**	Northern Red Sea	Shashar and others (1994) ⁶⁰
<u>Soft Coral (<i>Xenia</i> sp.)</u>		
0.014 ± 0.004	Central Red Sea	Present study
0.003 ± 0.000*	Northern Red Sea	Bednarz and others (2015) ⁴⁹
<u>Biogenic Rock</u>		
0.098 ± 0.016	Central Red Sea	Present study
0.112 ± 0.038*	Northern Red Sea	Rix and others (2015) ⁵⁰
0.13 ± 0.01**	Northern Red Sea	Shashar and others (1994) ⁶⁰
<u>Reef Sands</u>		
0.046 ± 0.006	Central Red Sea	Present study
0.296 ± 0.067*	Northern Red Sea	Bednarz and others (2015) ⁵⁹
4.88 ± 1.38**	Northern Red Sea	Shashar and others (1994) ⁶⁰
<u>Hard Corals</u>		
0.005 ± 0.002	Central Red Sea	Present study
0.000 – 0.003	Central Red Sea	Pogoreutz and others (2017) ⁵⁸
0.012 ± 0.003*	Northern Red Sea	Cardini and others (2016) ¹⁰
0.016 ± 0.087	Central Red Sea	Tilstra and others (2019) ²¹
0.988 ± 0.211**	Northern Red Sea	Shashar and others (1994) ⁶⁰

* winter season; **summer season

From an ecological perspective, turf algae are pioneers³⁴ and opportunists^{69,70}, which can form extensive mats even under oligotrophic conditions^{71,72}. Furthermore, they can rapidly take-over bare substrate due to high growth rates^{34,69,73,74}. The high N demand needed to fuel metabolism and biomass production in filamentous turf algae can, to a large extent, be satisfied by high N₂-fixing activities^{34,50,75,76}. A recent study shows that accumulated N in the form of turf algal biomass can be exported to the wider reef³⁴. N₂ fixation activities of coral rubble are similar to those of turf algae, which confirms findings of a recent study⁷⁷. Coral rubble N₂ fixation activity measured here is in the range of previous studies^{78,79} and may, thus, be driven by microbial communities inhabiting coral rubble surfaces, as suggested by Davey and others (2008)⁷⁸, who observed significantly higher N₂ fixation activity in coral rubble compared to living hard corals.

Among all benthic categories, corals (both hard and soft corals) showed lowest N₂ fixation activities, being in a similar range^{10,49,80} or significantly lower⁶⁰ than rates measured previously with acetylene reduction techniques. Lower N₂ fixation rates for hard corals of the present study may have occurred due to a phosphate limitation of N₂ fixation^{13,81,82}, as phosphate concentrations in the seawater were comparatively low ranging between 0.06 and 0.07 μM ^{22,63}. Additionally, discrepancies could also result from differing surface area determination techniques used here and in other studies before. Previous studies determined the surface area of investigated benthic categories, such as hard corals, using aluminium foil method⁸³ or advanced geometry^{50,59}, but potentially lack accuracy⁸⁴ and, hence, potentially underestimates the surface area of hard corals and, thus, overestimates N fluxes. The soft coral displayed highest denitrification activity. The interplay of N₂ fixation and denitrification, favouring low internal N availability, may be vital for the stability between the coral host and the associated photosynthetic algal endosymbiont of the family Symbiodiniaceae (sensu Rädercker and others (2015))¹². Low N₂ fixation and comparatively high denitrification activity may promote the host's control over symbiotic algae⁸⁵ by keeping N availability desirably limited^{5,86}. As such, seasonal fluctuations (Tilstra and others, in review) or environmental stressors like eutrophication or ocean warming may influence both processes¹², leading to shifts from N to P or another micronutrient (e.g., iron) limitation^{87–89}, which can result in a breakdown of the coral-Symbiodiniaceae symbiosis⁸⁸. Furthermore, Tilstra and others (2019)²¹ hypothesised a negative correlation between heterotrophic capacity and denitrification activity in coral holobionts. Hard coral species used in the present study are considered as autotrophic corals^{90–93}, with differences in their autotrophic capacity might drive different observed denitrification potentials (Fig. 6.3B). This link may extend to soft corals as the investigated soft coral of the family Xenidae is a functional autotroph⁹⁴ with a low heterotrophic capacity, which could explain the observation of comparatively high denitrification activity. As such, denitrification is an anaerobic process. Potentially, observed denitrification potential differences among the hard coral species and *Xenia* sp. occurred due to their different capacity in releasing and producing mucus^{68,95}, with thick mucus layers favouring high anaerobic potentials that might facilitate denitrification⁹⁵. It has been demonstrated recently, that soft coral mucus does not provide a favourable habitat for associated diazotrophs⁶⁸, which in return could explain observed comparatively low N₂ fixation rates.

Implications for Coral- and Algae-Dominated Reefs

Extrapolated reef-wide fixed N via N₂ fixation of both coral- and algae-dominated reef areas (350.01 ± 97.87 and $722.91 \pm 241.26 \mu\text{mol N m}^{-2} \text{d}^{-1}$, respectively; Fig. 6.4) is in line with previously calculated reef-wide N₂ fixation budgets of Larkum and others (1988)¹⁸ and Cardini and others (2016)¹⁰, who have reported an annual average N₂ fixation activity of 156-1330 $\mu\text{mol N m}^{-2} \text{d}^{-1}$ and $546 \pm 69 \mu\text{mol N m}^{-2} \text{d}^{-1}$, respectively.

At the community level, the relative contribution of key benthic categories varied when compared to N fluxes related to substrate surface area. Together, turf algae and coral rubble represent 91 % of overall N₂ fixation in coral-dominated and 99 % in algae-dominated reef areas. Hard and soft corals are key players in coral-dominated reef areas, in which both benthic categories together account for 52 % of benthic cover (in the investigated Abo Shosha reef area) and contributed equally to the 78 % of overall denitrification. This is surprising, as both benthic categories showed lowest (hard corals) or highest (soft coral) denitrification activity. While all investigated hard coral species showed similar N₂ fixation patterns, findings regarding their denitrifying activity showed a large variability (Fig 6.3). Based on our results, we hypothesise that reefs with a higher *Acropora hemprichii* cover (compared to *Stylophora pistillata* or *Pocillopora verrucosa*) display higher capacities to remove bioavailable N via denitrification and could, thus, be more resilient to higher N availability than those of *S. pistillata* or *P. verrucosa* dominance. However, we have solely considered a small selection of hard corals with a branching morphology that are considered as autotrophs⁹⁰⁻⁹³. It remains speculative how other hard coral species, such as those of mounding and plating morphologies, or heterotrophic corals^{96,97} with different mass transfer characteristics^{98,99} contribute to potential reef resilience.

Besides being most abundant in coral-dominated areas, hard corals (especially branching hard corals, represented by the species selected in the present study) contribute most to the three-dimensional structure (i.e., spatial complexity or rugosity) of coral reef ecosystems¹⁰⁰⁻¹⁰², which increases the relative importance of hard corals for N₂ fixation and particularly denitrification in both reef areas in the present study. A reduction of hard coral cover and, thus, spatial complexity (i.e., a loss of cryptic 3D area) also leads to a reduced contribution to overall denitrification (Fig 6.5), even though denitrification potentials for hard corals are similar to those of reef sands and turf algae when related to 2D substrate surface area (Fig. 6.3). Even in the algae-dominated reef area, both hard and soft corals still contributed to more than 50 % of overall denitrification (Fig. 6.5), despite covering only ~ 22 % of the seafloor. The mentioned reduction or loss of spatial complexity is commonly associated with coral-phase shifts¹⁰³. Whereas the importance of structural complexity and consequences of its loss in coral reefs has been recognised on multi-fold levels before, e.g., on fish communities¹⁰³⁻¹⁰⁶, invertebrate diversity^{107,108} and ecosystem services^{42,101,109,110}, our data suggest substantial consequences on N cycling dynamics. The most striking result is the difference in total N import via N₂ fixation in both reef states, besides changes in the relative contribution of denitrifying corals in the respective reef areas. Turf algae were identified as key N₂-fixers and their higher abundance in benthic coverage leads to a 100 % increase of N₂ fixation in algae-dominated compared to coral-dominated areas (Fig. 6.4). At the same time, denitrification, a process that may alleviate coral reef environments from

excess N^{12-15,21} remained stable in the algae-dominated part of the reef. It remains target of future studies to evolve the role of ANAMMOX in coral reefs, but hypothetically, ANAMMOX is vital to remove bioavailable N from coral reef environments¹⁶. However, key ANAMMOX-performing players have not been identified in coral reefs yet, nor were they included in the present study (see limitations). Nevertheless, a higher N availability (i.e., higher fixed N inputs with stable denitrification activity) in algae-dominated reefs could have multiple consequences resulting in a positive feedback loop. Higher N accumulation could promote algae to proliferate in nutrient-poor waters by relieving N limitation^{111,112}, similarly as eutrophication promotes turf proliferation in coral reefs⁶³. This can result in high abundances of benthic algae that in turn deter herbivorous fish that successively control algal proliferation by grazing¹¹³. Jessen and Wild (2013)¹¹⁴ have described this feedback loop before, and we here append that excess N can either be further utilised for growth or metabolism, and that increased N availability can result in a higher release of algal exudates such as dissolved organic nitrogen (DON)¹¹⁵ from benthic algae during active growth or decomposition. Ultimately, this feedback loop could turn a reef from a previously net sink of DON into a DON source¹⁷.

Implications for Alternative Reef States

In the present study, we evaluated two distinct reef communities and the implications of their varying benthic composition. Microbial communities associated with the benthic categories are likely to not only vary between coral- and algae-dominated reefs¹¹⁶, but also between investigated benthic categories¹¹⁷⁻¹¹⁹. Varying microbial communities and their interactions might have implications for N₂ fixation and denitrification activities, but were not considered in the present study (see limitations), and should, thus, be investigated in future studies.

Discontinuous shifts¹²⁰, shifts of varying intensity¹²¹, or community shifts from reefs dominated by corals to assemblages other than benthic (turf) algae have been reported (reviewed in Norström and others (2009))⁴⁶. These alternative reef states, besides the shifts to algae-dominated reefs, can be of corallimorpharian, sponge, ascidian or soft coral dominance⁴⁶. Particularly soft coral dominance is common in the Red Sea^{122,123} and other regions such as Taiwan, East Pacific¹²⁴ and at the Great Barrier Reef, Australia¹²⁵, where the soft coral genus *Xenia* attains as much as 80 % of benthic cover after disturbance^{46,126}. Moreover, climate change associated stressors such as ocean acidification might induce community shifts from hard to soft coral dominance¹²⁷. Bednarz and others (2015)⁴⁹ propose that soft corals may become an important player in N cycling due to their increasing dominance in benthic cover in the northern Red Sea. Based on the results of the present study, we carefully speculate that a high soft coral cover may alleviate degraded reefs, or reefs in a transitional state, from excessive N. To which extent *Xenia* sp., as the main denitrifying organism, can contribute to decelerate coral reef degradation remains to be determined in future studies. Hypothetically, N limitation can be exacerbated in *Xenia* sp. dominated reef areas, as more N is removed via denitrification than in hard coral or algae-reef dominated areas. This hypothesis is

supported by findings of Pupier and others (2019)⁶⁸, who suggest a significant decrease in N₂ fixation and subsequent N limitation in soft coral-dominated reefs.

Coral rubble-dominated areas, particularly reef flats, can be the result of fragmentation and erosion processes of nearby reef areas such as leeward slopes, resulting in mobile fragments that are unsuitable for coral colonisation¹²⁸. Findings of the present study confirm previous hypotheses, in which the potential of coral rubble as highly active N₂-fixers can aggravate N influxes to a destroyed or vulnerable reef^{53,78}. At the same time, our findings indicate that the denitrifying capacity of rubble-dominated reefs is presumably lower than in intact coral-dominated areas (i.e., due to lower structural complexity and relatively lower denitrification activity compared to soft corals), which leads us to the conclusion that this reef state will compound N influxes on an ecosystem level so that N likely accumulates.

We demonstrated that N influxes via N₂ fixation could lead to an aggregation of N in algae-dominated communities, while differences regarding the bioavailable N removal via denitrification could not be observed between coral- and algae-dominated reef areas. Potentially, N₂ fixation rates^{10,50,59} as well as denitrification potentials (Tilstra and others, unpubl. data) experience seasonal fluctuations, that might cause feedback responses in the extrapolated fixed or removed N. The range of these feedback responses remains to be determined.

Further N cycling processes in coral reefs including anaerobic ammonium oxidation (ANAMMOX, transformation of fixed NH₄⁺ and NO₂⁻ to elemental N₂) that potentially alleviate systems from N^{129,130}, have been identified in coral microbiomes¹³¹ and coral-reef sponges¹⁵. The extent to which ANAMMOX can serve as a N removal process in shifting reefs, remains to be determined. Further, cryptic habitats in coral reefs harbouring high abundances of sponges¹³² may reduce bioavailable N via ANAMMOX, and should be prioritised in future studies as they were not considered in the present study (see limitations). Stressor-induced phase shifts and, therewith, loss of structural complexity, i.e., cryptic habitats, remain subject to future studies about these important players in the biogeochemical cycling of N.

6.6 | Acknowledgements

We are grateful to Rodrigo Villalobos and João Cúrdia for their support during fieldwork. Many thanks also to Carina Kitir, Söphiä Tobler and Jän Krause for their support in developing the figures, as well as to Najeh Kharbatia for technical support with GC.

6.7 | References

1. Galloway, J. N. *et al.* The Nitrogen Cascade. *Bioscience* **53**, 341–356 (2003).
2. Mackenzie, F. T. *Our Changing Planet: An Introduction to Earth System Science and Global Environmental Change*. (1998).
3. Vitousek, P. M. & Howarth, R. W. Nitrogen limitation on land and in the sea: How can it occur? *Biogeochemistry* **13**, 87–115 (1991).
4. Webb, K. L., DuPaul, W. D., Wiebe, W., Sottile, W. & Johannes, R. E. Enewetak (Eniwetok) Atoll: Aspects of the nitrogen cycle on a coral reef. *Limnol. Oceanogr.* **20**, 198–210 (1975).
5. Lesser, M. P. *et al.* Nitrogen fixation by symbiotic cyanobacteria provides a source of nitrogen for the scleractinian coral *Montastraea cavernosa*. *Mar. Ecol. Prog. Ser.* **346**, 143–152 (2007).
6. Hoegh-Guldberg, O. Environmental and economic importance of the world's coral reefs. *Mar. Freshw. Res.* **50**, 839–866 (1999).
7. Bell, P. R. F. Eutrophication and coral reefs-some examples in the Great Barrier Reef lagoon. *Water Res.* **26**, 553–568 (1992).
8. Sorokin, Y. I. Microbiological Aspects of the Productivity of Coral Reefs. in *Biology and Geology of Coral Reefs* (eds. Jones, O. A. & Endean, R.) 17–46 (ACADEMIC PRESS, INC., 1973).
9. O'Neil, J. M. & Capone, D. G. Nitrogen Cycling in Coral Reef Environments. in *Nitrogen in the Marine Environment* 949–989 (2008). doi:10.1016/B978-0-12-372522-6.00021-9
10. Cardini, U. *et al.* Budget of Primary Production and Dinitrogen Fixation in a Highly Seasonal Red Sea Coral Reef. *Ecosystems* **19**, 771–785 (2016).
11. Scheffers, S. R., Nieuwland, G., Bak, R. P. M. & Van Duyl, F. C. Removal of bacteria and nutrient dynamics within the coral reef framework of Curaçao (Netherlands Antilles). *Coral Reefs* **23**, 413–422 (2004).
12. Rådecker, N., Pogoreutz, C., Voolstra, C. R., Wiedenmann, J. & Wild, C. Nitrogen cycling in corals: The key to understanding holobiont functioning? *Trends Microbiol.* **23**, 490–497 (2015).
13. Koop, K. *et al.* ENCORE: The effect of nutrient enrichment on coral reefs. Synthesis of results and conclusions. *Mar. Pollut. Bull.* **42**, 91–120 (2001).
14. Capone, D. G., Dunham, S. E., Horrigan, S. G. & Duguay, L. E. Microbial nitrogen transformations in unconsolidated coral reef sediments. *Mar. Ecol. Prog. Ser.* **80**, 75–88 (1992).
15. Hoffmann, F. *et al.* Complex nitrogen cycling in the sponge *Geodia barretti*. *Environ. Microbiol.* **11**, 2228–2243 (2009).
16. Rådecker, N., Pogoreutz, C., Voolstra, C. R., Wiedenmann, J. & Wild, C. Nitrogen cycling in corals: The key to understanding holobiont functioning? *Trends Microbiol.* **23**, 490–497 (2015).
17. Wiebe, W. J., Johannes, R. E. & Webb, K. L. Nitrogen fixation in a coral reef community. *Science* **188**, 257–259 (1975).
18. Larkum, A. W. D., Kennedy, I. R. & Muller, W. J. Nitrogen fixation on a coral reef. *Mar.*

- Biol.* **98**, 143–155 (1988).
19. Kimes, N. E., Van Nostrand, J. D., Weil, E., Zhou, J. & Morris, P. J. Microbial functional structure of *Montastraea faveolata*, an important Caribbean reef-building coral, differs between healthy and yellow-band diseased colonies. *Environ. Microbiol.* **12**, 541–556 (2010).
 20. Yang, S., Sun, W., Zhang, F. & Li, Z. Phylogenetically Diverse Denitrifying and Ammonia-Oxidizing Bacteria in Corals *Alcyonium gracillimum* and *Tubastraea coccinea*. *Mar. Biotechnol.* **15**, 540–551 (2013).
 21. Tilstra, A. *et al.* Denitrification Aligns with N₂ Fixation in Red Sea Corals. *Sci. Rep.* **9**, 19460 (2019).
 22. El-Khaled, Y. *et al.* In situ eutrophication stimulates dinitrogen fixation, denitrification, and productivity in Red Sea coral reefs. *Mar. Ecol. Prog. Ser.* **645**, 55–66 (2020).
 23. O’Neil, J. M. & Capone, D. G. *Nitrogen Cycling in Coral Reef Environments. Nitrogen in the Marine Environment* (2008). doi:10.1016/B978-0-12-372522-6.00021-9
 24. Muscatine, L. & Porter, J. W. Reef Corals: Mutualistic Symbioses Adapted to Nutrient-Poor Environments. *Bioscience* **27**, 454–460 (1977).
 25. Mohideen Wafar, S. W. and J. J. D. Nitrification in reef corals. *Limnol. Oceanogr.* **35**, 725–730 (1990).
 26. Pandolfi, J. M., Connolly, S. R., Marshall, D. J. & Cohen, A. L. Projecting coral reef futures under global warming and ocean acidification. *Science* (80-.). **333**, 418–422 (2011).
 27. Hughes, T. P. *et al.* Coral reefs in the Anthropocene. *Nature* **546**, 82–90 (2017).
 28. Fabricius, K. E. Factors Determining the Resilience of Coral Reefs to Eutrophication: A Review and Conceptual Model. in *Coral Reefs: An Ecosystem in Transition* (eds. Dubinsky, Z. & Stambler, N.) 493–505 (2011). doi:10.1007/978-94-007-0114-4_28
 29. Bellwood, D. R., Hughes, T. P., Folke, C. & Nyström, M. Confronting the coral reef crisis. *Nature* **429**, 827–833 (2004).
 30. Lapointe, B. E., Brewton, R. A., Herren, L. W., Porter, J. W. & Hu, C. *Nitrogen enrichment, altered stoichiometry, and coral reef decline at Looe Key, Florida Keys, USA: a 3-decade study. Marine Biology* **166**, (Springer Berlin Heidelberg, 2019).
 31. Hughes, T. P. *et al.* Phase Shifts, Herbivory, and the Resilience of Coral Reefs to Climate Change. *Curr. Biol.* **17**, 360–365 (2007).
 32. Williams, I. D., Polunin, N. V. C. & Hendrick, V. J. Limits to grazing by herbivorous fishes and the impact of low coral cover on macroalgal abundance on a coral reef in Belize. *Mar. Ecol. Prog. Ser.* **222**, 187–196 (2001).
 33. Mumby, P. J., Hastings, A. & Edwards, H. J. Thresholds and the resilience of Caribbean coral reefs. *Nature* **450**, 98–101 (2007).
 34. Roth, F. *et al.* High rates of carbon and dinitrogen fixation suggest a critical role of benthic pioneer communities in the energy and nutrient dynamics of coral reefs. *Funct. Ecol.* (2020). doi:10.1111/1365-2435.13625
 35. Done, T. J. Phase shifts in coral reef communities and their ecological significance. *Hydrobiologia* **247**, 121–132 (1992).
 36. Hughes, T. P. Catastrophes, phase shifts, and large-scale degradation of a Caribbean coral

- reef. *Science (80-.)*. **265**, 1547–1551 (1994).
37. McManus, J. W. & Polsenberg, J. F. Coral-algal phase shifts on coral reefs: Ecological and environmental aspects. *Prog. Oceanogr.* **60**, 263–279 (2004).
 38. Moberg, F. & Folke, C. Ecological goods and services of coral reef ecosystems. *Ecol. Econ.* **29**, 215–233 (1999).
 39. White, A. T., Vogt, H. P. & Arin, T. Philippine coral reefs under threat: The economic losses caused by reef destruction. *Mar. Pollut. Bull.* **40**, 598–605 (2000).
 40. McClanahan, T. R., Hicks, C. C. & Darling, E. S. Malthusian overfishing and efforts to overcome it on Kenyan coral reefs. *Ecol. Appl.* **18**, 1516–1529 (2008).
 41. Nyström, M. *et al.* Confronting Feedbacks of Degraded Marine Ecosystems. *Ecosystems* **15**, 695–710 (2012).
 42. Woodhead, A. J., Hicks, C. C., Norström, A. V., Williams, G. J. & Graham, N. A. J. Coral reef ecosystem services in the Anthropocene. *Funct. Ecol.* **33**, 1023–1034 (2019).
 43. McClanahan, T., Polunin, N. & Done, T. Ecological states and the resilience of coral reefs. *Conserv. Ecol.* **6**, (2002).
 44. Munday, P. L. Habitat loss, resource specialization, and extinction on coral reefs. *Glob. Chang. Biol.* **10**, 1642–1647 (2004).
 45. Williams, G. J. & Graham, N. A. J. Rethinking coral reef functional futures. *Funct. Ecol.* **33**, 942–947 (2019).
 46. Norström, A. V., Nyström, M., Lokrantz, J. & Folke, C. Alternative states on coral reefs: Beyond coral-macroalgal phase shifts. *Mar. Ecol. Prog. Ser.* **376**, 293–306 (2009).
 47. Brandl, S. J. *et al.* Coral reef ecosystem functioning: eight core processes and the role of biodiversity. *Front. Ecol. Environ.* **17**, 445–454 (2019).
 48. Roth, F. *et al.* High summer temperatures amplify functional differences between coral- and algae-dominated reef communities. *Ecology* (2020). doi:10.1002/ecy.3226
 49. Bednarz, V. N., Cardini, U., Van Hoytema, N., Al-Rshaidat, M. M. D. & Wild, C. Seasonal variation in dinitrogen fixation and oxygen fluxes associated with two dominant zooxanthellate soft corals from the northern Red Sea. *Mar. Ecol. Prog. Ser.* **519**, 141–152 (2015).
 50. Rix, L. *et al.* Seasonality in dinitrogen fixation and primary productivity by coral reef framework substrates from the northern Red Sea. *Mar. Ecol. Prog. Ser.* **533**, 79–92 (2015).
 51. den Haan, J. *et al.* Nitrogen fixation rates in algal turf communities of a degraded versus less degraded coral reef. *Coral Reefs* **33**, 1003–1015 (2014).
 52. Roth, F. *et al.* Coral reef degradation affects the potential for reef recovery after disturbance. *Mar. Environ. Res.* **142**, 48–58 (2018).
 53. Holmes, G. & Johnstone, R. W. The role of coral mortality in nitrogen dynamics on coral reefs. *J. Exp. Mar. Bio. Ecol.* **387**, 1–8 (2010).
 54. Hoegh-Guldberg, O. *et al.* Coral Reefs Under Rapid Climate Change and Ocean Acidification. *Science (80-.)*. **318**, 1737–1742 (2007).
 55. Van Hooidonk, R. *et al.* Local-scale projections of coral reef futures and implications of the Paris Agreement. *Sci. Rep.* **6**, 1–8 (2016).

56. Osborne, K. *et al.* Delayed coral recovery in a warming ocean. *Glob. Chang. Biol.* **23**, 3869–3881 (2017).
57. Graham, N. A. J., Jennings, S., MacNeil, M. A., Mouillot, D. & Wilson, S. K. Predicting climate-driven regime shifts versus rebound potential in coral reefs. *Nature* **518**, 94–97 (2015).
58. Pogoreutz, C. *et al.* Sugar enrichment provides evidence for a role of nitrogen fixation in coral bleaching. *Glob. Chang. Biol.* **23**, 3838–3848 (2017).
59. Bednarz, V. N. *et al.* Dinitrogen fixation and primary productivity by carbonate and silicate reef sand communities of the Northern Red Sea. *Mar. Ecol. Prog. Ser.* **527**, 47–57 (2015).
60. Shashar, N., Feldstein, T., Cohen, Y. & Loya, Y. Nitrogen fixation (acetylene reduction) on a coral reef. *Coral Reefs* **13**, 171–174 (1994).
61. Patriquin, D. G. & McClung, C. R. Nitrogen Accretion, and the Nature and Possible Significance of N₂ Fixation (Acetylene Reduction) in a Nova Scotian *Spartina alterniflora* Stand. *Mar. Biol.* **47**, 227–242 (1978).
62. Shieh, W. Y. & Lin, Y. M. Nitrogen fixation (acetylene reduction) associated with the zoanthid *Palythoa tuberculosa* Esper. *J. Exp. Mar. Bio. Ecol.* **163**, 31–41 (1992).
63. Karcher, D. B. *et al.* Nitrogen eutrophication particularly promotes turf algae in coral reefs of the central Red Sea. *PeerJ* **8**, e8737 (2020).
64. Bednarz, V. N. *et al.* Contrasting seasonal responses in dinitrogen fixation between shallow and deep-water colonies of the model coral *Stylophora pistillata* in the northern Red Sea. *PLoS One* **13**, 1–13 (2018).
65. Schöttner, S. *et al.* Drivers of bacterial diversity dynamics in permeable carbonate and silicate coral reef sands from the Red Sea. *Environ. Microbiol.* **13**, 1815–1826 (2011).
66. Zumft, W. G. Cell biology and Molecular Basis of Denitrification. *Microbiol. Mol. Biol. Rev.* **61**, 533–616 (1997).
67. Compaoré, J. & Stal, L. J. Effect of temperature on the sensitivity of nitrogenase to oxygen in two heterocystous cyanobacteria. *J. Phycol.* **46**, 1172–1179 (2010).
68. Pupier, C. A. *et al.* Divergent capacity of scleractinian and soft corals to assimilate and transfer diazotrophically derived nitrogen to the reef environment. *Front. Microbiol.* **10**, (2019).
69. Littler, M. & Littler, D. The Nature of Turf and Boring Algae and Their Interactions on Reefs. *Smithson. Contrib. to Mar. Sci.* 213–217 (2013).
70. Rosenberg, G. & Ramus, J. Uptake of inorganic nitrogen and seaweed surface area: Volume ratios. *Aquat. Bot.* **19**, 65–72 (1984).
71. Fong, P., Rudnicki, R. & Zedler, J. B. *Algal community response to nitrogen and phosphorus loading in experimental mesocosms: Management recommendations for southern California lagoons.* (1987).
72. Fong, C. R., Gaynus, C. J. & Carpenter, R. C. Complex interactions among stressors evolve over time to drive shifts from short turfs to macroalgae on tropical reefs. *Ecosphere* **11**, (2020).
73. Roth, F., Stuhldreier, I., Sánchez-Noguera, C., Morales-Ramírez, T. & Wild, C. Effects of simulated overfishing on the succession of benthic algae and invertebrates in an upwelling-influenced coral reef of Pacific Costa Rica. *J. Exp. Mar. Bio. Ecol.* **468**, 55–66 (2015).

74. Stuhldreier, I., Bastian, P., Schönig, E. & Wild, C. Effects of simulated eutrophication and overfishing on algae and invertebrate settlement in a coral reef of Koh Phangan, Gulf of Thailand. *Mar. Pollut. Bull.* **92**, 35–44 (2015).
75. Yamamuro, M., Kayanne, H. & Minagawa, M. Carbon and nitrogen stable isotopes of primary producers in coral reef ecosystems. *Limnol. Oceanogr.* **40**, 617–621 (1995).
76. Tilstra, A. *et al.* Seasonality affects dinitrogen fixation associated with two common macroalgae from a coral reef in the northern Red Sea. *Mar. Ecol. Prog. Ser.* **575**, 69–80 (2017).
77. El-Khaled, Y. C. *et al.* Simultaneous Measurements of Dinitrogen Fixation and Denitrification Associated With Coral Reef Substrates : Advantages and Limitations of a Combined Acetylene Assay. *Front. Mar. Sci.* **7**, 411 (2020).
78. Davey, M., Holmes, G. & Johnstone, R. High rates of nitrogen fixation (acetylene reduction) on coral skeletons following bleaching mortality. *Coral Reefs* **27**, 227–236 (2008).
79. Larkum, A. W. D. High rates of nitrogen fixation on coral skeletons after predation by the crown of thorns starfish *Acanthaster planci*. *Mar. Biol.* **97**, 503–506 (1988).
80. Pogoreutz, C. *et al.* Nitrogen fixation aligns with nifH abundance and expression in two coral trophic functional groups. *Front. Microbiol.* **8**, 1–7 (2017).
81. Arrigo, K. K. Marine microorganisms and global nutrient cycles. *Nature* **437**, 349–355 (2004).
82. Mills, M. M., Ridame, C., Davey, M., La Roche, J. & Geider, R. J. Iron and phosphorus co-limit nitrogen fixation in the eastern tropical North Atlantic. *Nature* **429**, 292–294 (2004).
83. Porter, J. W., Muscatine, L., Dubinsky, Z. & Falkowski, P. G. Primary production and photoadaptation in light- and shade-adapted colonies of the symbiotic coral, *Stylophora pistillata*. *Proc. R. Soc. London. Ser. B. Biol. Sci.* **222**, 161–180 (1984).
84. Veal, C. J., Holmes, G., Nunez, M., Hoegh-Guldberg, O. & Osborn, J. A comparative study of methods for surface area and three dimensional shape measurement of coral skeletons. *Limnol. Oceanogr. Methods* **8**, 241–253 (2010).
85. Falkowski, P. P. G., Dubinsky, Z., Muscatine, L. & McCloskey, L. Population Control in Symbiotic Corals. *Bioscience* **43**, 606–611 (1993).
86. Eyre, B. D., Glud, R. N. & Patten, N. Mass coral spawning: A natural large-scale nutrient addition experiment. *Limnol. Oceanogr.* **53**, 997–1013 (2008).
87. D'Angelo, C. & Wiedenmann, J. Impacts of nutrient enrichment on coral reefs: New perspectives and implications for coastal management and reef survival. *Curr. Opin. Environ. Sustain.* **7**, 82–93 (2014).
88. Wiedenmann, J. *et al.* Nutrient enrichment can increase the susceptibility of reef corals to bleaching. *Nat. Clim. Chang.* **3**, 160–164 (2013).
89. Ferrier-Pagès, C., Godinot, C., D'Angelo, C., Wiedenmann, J. & Grover, R. Phosphorus metabolism of reef organisms with algal symbionts. *Ecol. Monogr.* **86**, 262–277 (2016).
90. Muscatine, L., Falkowski, P. G., Porter, J. W. & Dubinsky, Z. Fate of photosynthetic fixed carbon in light- and shade-adapted colonies of the symbiotic coral *Stylophora pistillata*. *Proc. R. Soc. B Biol. Sci.* **222**, 181–202 (1984).
91. Conti-Jerpe, I. E. *et al.* Trophic strategy and bleaching resistance in reef-building corals. *Sci.*

- Adv.* **6**, (2020).
92. Houlbrèque, F. & Ferrier-Pagès, C. Heterotrophy in tropical scleractinian corals. *Biol. Rev.* **84**, 1–17 (2009).
 93. Muscatine, L., Porter, J. W. & Kaplan, I. R. Resource partitioning by reef corals as determined from stable isotope composition. *Pacific Sci.* **48**, 304–312 (1994).
 94. Schlichter, D., Svoboda, A. & Kremer, B. P. Functional autotrophy of *Heteroxenia fuscescens* (Anthozoa: Alcyonaria): carbon assimilation and translocation of photosynthates from symbionts to host. *Mar. Biol.* **78**, 29–38 (1983).
 95. Babbin, A. R. *et al.* Discovery and quantification of anaerobic nitrogen metabolisms among oxygenated tropical stony corals. *ISME J.* (2020). doi:10.1038/s41396-020-00845-2
 96. Pogoreutz, C. *et al.* Nitrogen fixation aligns with nifH abundance and expression in two coral trophic functional groups. *Front. Microbiol.* **8**, 1–7 (2017).
 97. Muscatine, L. The role of symbiotic algae in carbon and energy flux in coral reefs. in *Coral Reefs* (ed. Dubinsky, Z.) 75–87 (1990).
 98. van Woesik, R., Irikawa, A., Anzai, R. & Nakamura, T. Effects of coral colony morphologies on mass transfer and susceptibility to thermal stress. *Coral Reefs* **31**, 633–639 (2012).
 99. Patterson, M. R. & Sebens, K. P. Forced convection modulates gas exchange in cnidarians. *Proc. Natl. Acad. Sci. U. S. A.* **86**, 8833–8836 (1989).
 100. Jones, C. G., Lawton, J. H. & Shachak, M. Organisms as Ecosystem Engineers. *Oikos* **69**, 373 (1994).
 101. Graham, N. A. J. & Nash, K. L. The importance of structural complexity in coral reef ecosystems. *Coral Reefs* **32**, 315–326 (2013).
 102. Hughes, T. P. *et al.* Climate change, human impacts, and the resilience of coral reefs. *Science* **301**, 929–33 (2003).
 103. Graham, N. A. J. *et al.* Dynamic fragility of oceanic coral reef ecosystems. *Proc. Natl. Acad. Sci. U. S. A.* **103**, 8425–8429 (2006).
 104. Sano, M., Shimizu, M. & Nose, Y. Long-term effects of destruction of hermatypic corals by *Acanthaster plana* infestation on reef fish communities at Iriomote Island, Japan. *Mar. Ecol. Prog. Ser.* **37**, 191–199 (1987).
 105. Lindahl, U., Öhman, M. C. & Schelten, C. K. The 1997/1998 mass mortality of corals: Effects on fish communities on a Tanzanian coral reef. *Mar. Pollut. Bull.* **42**, 127–131 (2001).
 106. Jones, G. P., McCormick, M. I., Srinivasan, M. & Eagle, J. V. Coral decline threatens fish biodiversity in marine reserves. *Proc. Natl. Acad. Sci. U. S. A.* **101**, 8251–8253 (2004).
 107. Idjadi, J. A. & Edmunds, P. J. Scleractinian corals as facilitators for other invertebrates on a Caribbean reef. *Mar. Ecol. Prog. Ser.* **319**, 117–127 (2006).
 108. Bracewell, S. A., Clark, G. F. & Johnston, E. L. Habitat complexity effects on diversity and abundance differ with latitude: an experimental study over 20 degrees. *Ecology* **99**, 1964–1974 (2018).
 109. Cinner, J. E. *et al.* Linking Social and Ecological Systems to Sustain Coral Reef Fisheries.

- Curr. Biol.* **19**, 206–212 (2009).
110. Sheppard, C., Dixon, D. J., Gourlay, M., Sheppard, A. & Payet, R. Coral mortality increases wave energy reaching shores protected by reef flats: Examples from the Seychelles. *Estuar. Coast. Shelf Sci.* **64**, 223–234 (2005).
 111. Adey, W. H. & Goertemiller, T. Coral reef algal turfs: master producers in nutrient poor seas. *Phycologia* **26**, 374–386 (1987).
 112. Fong, P. & Paul, V. J. Coral Reef Algae. in *Coral Reefs: An Ecosystem in Transition* (eds. Dubinsky, Z. & Stambler, N.) 241–272 (Springer, Dordrecht, 2011). doi:10.1007/978-94-007-0114-4_17
 113. Hoey, A. S. & Bellwood, D. R. Suppression of herbivory by macroalgal density: A critical feedback on coral reefs? *Ecol. Lett.* **14**, 267–273 (2011).
 114. Jessen, C. & Wild, C. Herbivory effects on benthic algal composition and growth on a coral reef flat in the Egyptian Red Sea. *Mar. Ecol. Prog. Ser.* **476**, 9–21 (2013).
 115. Haas, A. F. & Wild, C. Composition analysis of organic matter released by cosmopolitan coral reef-associated green algae. *Aquat. Biol.* **10**, 131–138 (2010).
 116. Haas, A. F. *et al.* Influence of coral and algal exudates on microbially mediated reef metabolism. *PeerJ* **2013**, 1–28 (2013).
 117. Roach, T. N. F. *et al.* A multiomic analysis of in situ coral-turf algal interactions. *Proc. Natl. Acad. Sci. U. S. A.* **117**, 13588–13595 (2020).
 118. van Oppen, M. J. H. & Blackall, L. L. Coral microbiome dynamics, functions and design in a changing world. *Nat. Rev. Microbiol.* **17**, 557–567 (2019).
 119. Liang, J. *et al.* Distinct bacterial communities associated with massive and branching scleractinian corals and potential linkages to coral susceptibility to thermal or cold stress. *Front. Microbiol.* **8**, 1–10 (2017).
 120. Fung, T., Seymour, R. M. & Johnson, C. R. Alternative stable states and phase shifts in coral reefs under anthropogenic stress. *Ecology* **92**, 967–982 (2011).
 121. Bruno, J. F., Sweatman, H., Precht, W. F., Selig, E. R. & Schutte, V. G. W. Assessing evidence of phase shifts from coral to macroalgal dominance on coral reefs. *Ecology* **90**, 1478–1484 (2009).
 122. Tilot, V., Leujak, W., Ormond, R. F. G., Ashworth, J. A. & Mabrouk, A. Monitoring of South Sinai coral reefs: influence of natural and anthropogenic factors. *Aquat. Conserv. Mar. Freshw. Ecosyst.* (2008). doi:10.1002/aqc.942
 123. Riegl, B. & Piller, W. E. Coral frameworks revisited—reefs and coral carpets in the northern Red Sea. *Coral Reefs* **18**, 241–253 (1999).
 124. Benayahu, Y., Jeng, M. S., Perkol-Finkel, S. & Dai, C. F. Soft corals (Octocorallia: Alcyonacea) from Southern Taiwan. II. Species diversity and distributional patterns. *Zool. Stud.* **43**, 548–560 (2004).
 125. Ninio, R., Meekan, M., Done, T. & Sweatman, H. Temporal patterns in coral assemblages on the Great Barrier Reef from local to large spatial scales. *Mar. Ecol. Prog. Ser.* **194**, 65–74 (2000).
 126. Fox, H. E., Pet, J. S., Dahuri, R. & Caldwell, R. L. Recovery in rubble fields: Long-term impacts of blast fishing. *Mar. Pollut. Bull.* **46**, 1024–1031 (2003).

127. Inoue, S., Kayanne, H., Yamamoto, S. & Kurihara, H. Spatial community shift from hard to soft corals in acidified water. *Nat. Clim. Chang.* **3**, 683–687 (2013).
128. Rasser, M. W. & Riegl, B. Holocene coral reef rubble and its binding agents. *Coral Reefs* **21**, 57–72 (2002).
129. Dalsgaard, T., Thamdrup, B. & Canfield, D. E. Anaerobic ammonium oxidation (anammox) in the marine environment. *Res. Microbiol.* **156**, 457–464 (2005).
130. Brunner, B. *et al.* Nitrogen isotope effects induced by anammox bacteria. *Proc. Natl. Acad. Sci.* **110**, 18994–18999 (2013).
131. Zhang, Y. *et al.* The functional gene composition and metabolic potential of coral-associated microbial communities. *Sci. Rep.* **5**, 1–11 (2015).
132. Richter, C., Wunsch, M., Rasheed, M., Kötter, I. & Badran, M. I. Endoscopic exploration of Red Sea coral reefs reveals dense populations of cavity-dwelling sponges. *Nature* **413**, 726–730 (2001).
133. Hill, J. & Wilkinson, C. Methods for ecological monitoring of coral reefs. *Aust. Inst. Mar. Sci. Townsv.* 117 (2004). doi:10.1017/CBO9781107415324.004
134. Kohler, K. E. & Gill, S. M. Coral Point Count with Excel extensions (CPCe): A Visual Basic program for the determination of coral and substrate coverage using random point count methodology. *Comput. Geosci.* **32**, 1259–1269 (2006).
135. Haas, A., el-Zibdah, M. & Wild, C. Seasonal monitoring of coral-algae interactions in fringing reefs of the Gulf of Aqaba, Northern Red Sea. *Coral Reefs* **29**, 93–103 (2010).
136. Bahartan, K. *et al.* Macroalgae in the coral reefs of Eilat (Gulf of Aqaba, Red Sea) as a possible indicator of reef degradation. *Mar. Pollut. Bull.* **60**, 759–764 (2010).
137. Woolstra, C. R. *et al.* Standardized short-term acute heat stress assays resolve historical differences in coral thermotolerance across microhabitat reef sites. *Glob. Chang. Biol.* **26**, 4328–4343 (2020).
138. Hynes, R. K. & Knowles, R. Inhibition by acetylene of ammonia oxidation in *Nitrosomonas europaea*. *FEMS Microbiol. Lett.* **4**, 319–321 (1978).
139. Oremland, R. S. & Capone, D. G. Use of ‘Specific’ Inhibitors in Biogeochemistry and Microbial Ecology. *Adv. Microbi. Ecol.* 285–383 (1988). doi:10.1007/978-1-4684-5409-3_8
140. Karcher, D. B. *et al.* Nitrogen eutrophication particularly promotes turf algae in coral reefs of the central Red Sea. *PeerJ* **8**, e8737 (2020).
141. Haines, J. R., Atlas, R. M., Griffiths, R. P. & Morita, R. Y. Denitrification and Nitrogen Fixation in Alaskan Continental Shelf Sediments. *Appl. Environ. Microbiol.* **41**, 412–421 (1981).
142. Joye, S. B. & Paerl, H. W. Contemporaneous nitrogen fixation and denitrification in intertidal microbial mats: rapid response to runoff events. *Mar. Ecol. Prog. Ser.* **94**, 267–274 (1993).
143. Miyajima, T., Suzumura, M., Umezawa, Y. & Koike, I. Microbiological nitrogen transformation in carbonate sediments of a coral-reef lagoon and associated seagrass beds. *Mar. Ecol. Prog. Ser.* **217**, 273–286 (2001).
144. Falkowski, P. G. *Enzymology of Nitrogen Assimilation. Nitrogen in the Marine Environment* (ACADEMIC PRESS, INC., 1983). doi:10.1016/b978-0-12-160280-2.50031-6

145. den Haan, J. *et al.* Nitrogen and phosphorus uptake rates of different species from a coral reef community after a nutrient pulse. *Sci. Rep.* **6**, 28821 (2016).
146. Grover, R., Maguer, J. F., Allemand, D. & Ferrier-Pagès, C. Nitrate uptake in the scleractinian coral *Stylophora pistillata*. *Limnol. Oceanogr.* **48**, 2266–2274 (2003).
147. Knapp, A. N. The sensitivity of marine N₂ fixation to dissolved inorganic nitrogen. *Front. Microbiol.* **3**, 374 (2012).
148. Dilworth, M. J. Acetylene reduction by nitrogen-fixing preparations from *Clostridium pasteurianum*. *Biochim. Biophys. Acta* **127**, 285–294 (1966).
149. Schöllhorn, R. & Burris, R. H. Acetylene as a competitive inhibitor of N₂ fixation. *Proc. Natl. Acad. Sci. U. S. A.* **58**, 213–216 (1967).
150. Balderston, W. L., Sherr, B. & Payne, W. J. Blockage By Acetylene of Nitrous-Oxide Reduction in *Pseudomonas-Perfectomarinus*. *Appl. Environ. Microbiol.* **31**, 504–508 (1976).
151. Yoshinari, T. & Knowles, R. Acetylene Inhibition of Nitrous Oxide Reduction by Denitrifying Bacteria. *Biochem. Biophys. Res. Commun.* **69**, 705–710 (1976).
152. Lavy, A. *et al.* A quick, easy and non-intrusive method for underwater volume and surface area evaluation of benthic organisms by 3D computer modelling. *Methods Ecol. Evol.* **6**, 521–531 (2015).
153. Gutierrez-Heredia, L., Benzoni, F., Murphy, E. & Reynaud, E. G. End to End Digitisation and Analysis of Three-Dimensional Coral Models, from Communities to Corallites. *PLoS One* **11**, e0149641 (2016).
154. Hughes, D. J. *et al.* Coral reef survival under accelerating ocean deoxygenation. *Nat. Clim. Chang.* **10**, 296–307 (2020).
155. Mulholland, M. R., Bronk, D. A. & Capone, D. G. Dinitrogen fixation and release of ammonium and dissolved organic nitrogen by *Trichodesmium* IMS101. *Aquat. Microb. Ecol.* **37**, 85–94 (2004).
156. Clarke, K. R. & Gorley, R. N. *PRIMER v6: Use manual/Tutorial. PRIMER-E:Plymouth* (2006).
157. Anderson, M., Gorley, R. & Clarke, K. PERMANOVA+ for PRIMER. Guide to software and statistical methods. (2008).
158. R Core Team. R: A language and environment for statistical computing. (2017).
159. RStudio Team. RStudio: Integrated Development for R. (2020).
160. Wilson, S. T., Böttjer, D., Church, M. J. & Karl, D. M. Comparative assessment of nitrogen fixation methodologies, conducted in the oligotrophic north pacific ocean. *Appl. Environ. Microbiol.* **78**, 6516–6523 (2012).
161. Yu, K., Seo, D. C. & Delaune, R. D. Incomplete acetylene inhibition of nitrous oxide reduction in potential denitrification assay as revealed by using ¹⁵N-Nitrate tracer. *Commun. Soil Sci. Plant Anal.* **41**, 2201–2210 (2010).
162. Groffman, P. M. *et al.* Methods for Measuring Denitrification: Diverse Approaches to a Difficult Problem. *Ecol. Appl.* **16**, 2091–2122 (2006).
163. Maldonado, M., Ribes, M. & van Duyl, F. C. *Nutrient Fluxes Through Sponges. Biology, Budgets, and Ecological Implications. Advances in Marine Biology* **62**, (Elsevier Ltd., 2012).

164. Roth, F. *et al.* *An in situ approach for measuring biogeochemical fluxes in structurally complex benthic communities.* *Methods in Ecology and Evolution* (2019). doi:10.1111/2041-210X.13151

Chapter 7

Chapter 7 | Nitrogen eutrophication particularly promotes turf algae in coral reefs of the central Red Sea

Denis B. Karcher^{1*}, Florian Roth^{2,3,4}, Susana Carvalho², **Yusuf C. El-Khaled**¹, Arjen Tilstra¹, Benjamin Kürten^{2,5}, Ulrich Struck^{6,7}, Burton H. Jones², Christian Wild¹

¹Marine Ecology Department, Faculty of Biology and Chemistry, University of Bremen, Bremen, Germany

²Red Sea Research Center, King Abdullah University of Science and Technology (KAUST), Thuwal, Saudi Arabia

³Baltic Sea Centre, Stockholm University, Stockholm, Sweden

⁴Tvärminne Zoological Station, Faculty of Biological and Environmental Sciences, University of Helsinki, Helsinki, Finland

⁵Project Management Jülich, Jülich Research Centre, Rostock, Germany

⁶Museum für Naturkunde, Leibniz Institute for Evolution and Biodiversity Science, Berlin, Germany

⁷Department of Earth Sciences, Freie Universität Berlin, Berlin, Germany

*Corresponding author: db.karcher@gmx.de

7.1 Abstract

While various sources increasingly release nutrients to the Red Sea, knowledge about their effects on benthic coral reef communities is scarce. Here, we provide the first comparative assessment of the response of all major benthic groups (hard and soft corals, turf algae and reef sands—together accounting for 80% of the benthic reef community) to in-situ eutrophication in a central Red Sea coral reef. For 8 weeks, dissolved inorganic nitrogen (DIN) concentrations were experimentally increased 3-fold above environmental background concentrations around natural benthic reef communities using a slow release fertilizer with 15% total nitrogen (N) content. We investigated which major functional groups took up the available N, and how this changed organic carbon (C_{org}) and N contents using elemental and stable isotope measurements. Findings revealed that hard corals (in their tissue), soft corals and turf algae incorporated fertilizer N as indicated by significant increases in $\delta^{15}N$ by 8%, 27% and 28%, respectively. Among the investigated groups, C_{org} content significantly increased in sediments (+24%) and in turf algae (+33%). Altogether, this suggests that among the benthic organisms only turf algae were limited by N availability and thus benefited most from N addition. Thereby, based on higher C_{org} content, turf algae potentially gained competitive advantage over, for example, hard corals. Local management should, thus, particularly address DIN eutrophication by coastal development and consider the role of turf algae as potential bioindicator for eutrophication.

Keywords: Coral reefs | Nutrients | Stable isotopes | Nitrogen cycling | Eutrophication | Turf algae | Zooxanthellae | Phase shifts

A modified version of this chapter has been published in *PeerJ* 8(6)

<https://doi.org/10.7717/peerj.8737>

7.2 Introduction

Coral reefs are among the most productive and biologically diverse ecosystems on the planet¹, even though they grow in oligotrophic waters of the tropics². The young and isolated Red Sea, with its thriving coral reefs, is highly oligotrophic, particularly in the subtropical central and northern areas³⁻⁶. However, nutrient inputs to the Red Sea from aquaculture⁷⁻¹⁰ and urban waste water^{5,11-13} affect marine life^{7,11,14,15}. At the same time, the expansion of aquaculture industries in view of the Saudi Arabian coastal development agenda (<https://vision2030.gov.sa/en/node>), and growing urban sources, for example, from the city of Jeddah with about 4.6 Mio. inhabitants, represent further stressors to coral reefs in the Red Sea. Significant parts of the city rely on septic tanks for wastewater which can be a source of nutrients and pollutants through leakages into the groundwater^{16,17}. Moreover, the discharge of insufficiently treated sewage from marine outfalls (i.e., pipe discharge) as a point-source^{12,18} was already shown to raise near-shore N availability¹⁹, affect planktonic²⁰ and coral²¹ microbial communities and reach nearby reefs^{13,18}. As nutrients, among several stressors, have the largest effect on Red Sea hard coral resilience to climate change²², a deeper understanding of the community response to eutrophication is fundamental.

Benthic coral reef communities are crucial for many ecosystem functions, including the cycling and retention of carbon (C) and nitrogen (N)²³⁻²⁵ but suffer from anthropogenic disturbances²⁶⁻²⁸. N availability is an important limiting factor for the biological productivity in oligotrophic reef environments²⁹. Local eutrophication may impact reef organisms that typically grow in nutrient-poor waters¹⁵, and the diverse array of metabolisms they are comprised of. One prominent example is the entirety of coral host, endosymbiotic algae (zooxanthellae), bacteria and other microorganisms³⁰, called the coral holobiont. The enrichment source^{31,32} and ratio of supplied nutrients is important to determine reef biota's reactions to eutrophication, particularly for corals^{33,34}. Metabolic differences, for example between autotrophic and heterotrophic lifestyles, as well as the feeding environment of heterotrophic organisms, can lead to imbalances of essential biochemicals, which may become limiting³⁵. Critical parameters to evaluate and trace nutrient fluxes as well as limitations in marine environments are the C and N elemental³⁶⁻³⁹ and isotopic^{5,40,41} composition. N uptake and circulation in the reef might be fast and while the input of N can be measured by the long-term increase in forms of N concentrations⁴², it is most directly traceable in the short-term by the isotopic signature of reef biota. As external sources and processes of N acquisition affect the isotopic composition, for example, of corals⁴³, anthropogenic N sources can be traced in the field^{41,44,45}). N enrichment has negative effects on coral growth^{22,46,47}, calcification^{48,49}, reproductive success^{7,47,50}, biodiversity⁵¹, bacterial communities²² and increases the susceptibility of corals to bleaching^{32,34,52,53}. In contrast, other benthic groups in coral reefs, such as turf- and macroalgae benefit from increased nutrient availability in many cases^{54,55}, particularly in combination with reduced herbivory. Hence, shifts from coral- to algal-dominated reefs, so-called phase shifts, can occur^{56,57}.

While extensive research investigated the causes of phase shifts^{58,59}, nutrient effects on the ecophysiology and elemental stoichiometry of reef functional groups are rarely assessed, overlooking connections between

uptake to utilization. Responding to the growing nutrient inputs to the central Red Sea, an assessment of their effects on coral reef communities is needed in this originally nutrient poor region, particularly which functional groups and ecophysiological parameters may indicate early-stage effects. Reefs in the oligotrophic Red Sea can serve as a “natural laboratory”^{60,61}, as anthropogenic nutrient inputs add on a comparably low baseline. However, most studies have been conducted in the laboratory rather than in-situ, with associated risks of experimental artifacts, oversimplification or overestimation⁶². Indeed, local boundary layers and contact zones are of major importance in terms of direct interaction, small scale flow regimes as well as accumulation and transfer of organic matter^{63,64}, which can hardly be simulated under controlled laboratory conditions. The few similar studies that exist were conducted in less oligotrophic seas^{47,65}, along the natural environmental gradient of the Red Sea⁵, focused on one individual benthic group only^{7,38,66}, or only investigated benthic cover or chlorophyll content, not considering other metabolic parameters^{15,33}.

Therefore, we assessed the responses of major benthic functional groups (hard corals (*Pocillopora* cf. *verrucosa*, that is, tissue and zooxanthellae), soft corals (Xeniidae), turf algae and sediments) to N enrichment through a manipulative in-situ experiment in the central Red Sea. Combining elemental and stable isotope analysis, this approach provides information starting from N in the water column, through N uptake, to its utilization. We address the following underlying research questions: (1) Which major functional groups take up available N and (2) how did this affect organic carbon (C_{org}) and N contents? Taken together, we aimed to draw conclusions about nutrient limitation for different functional groups.

7.3 Material and Methods

Study Site and Environmental Conditions

The experiments were conducted at Abu Shoosha reef (22°18'15"N, 39°02'56"E) on the west coast of Saudi Arabia in the central Red Sea from late January until late March 2018. The reef assessed in this study does not fall under any legislative protection or special designation as a protected area. Under the auspices of KAUST (King Abdullah University of Science and Technology, Thuwal, Saudi Arabia), sailing permits to the reef were granted that included the collection of corals and other reef benthos. This reef is characterized by generally high levels of herbivory and small fluctuations in ambient dissolved inorganic nitrogen (DIN) concentration during this period⁶. For example, in January to March of the previous year (i.e., 2017), sea water concentrations of ammonium (NH_4^+) ranged from 0.16 to 0.17 μM , nitrate (NO_3^-) from 0.25 to 0.40 μM , nitrite (NO_2^-) from 0.03 to 0.06 μM , phosphate (PO_4^{3-}) from 0.02 to 0.21 μM and the resulting $DIN(NO_3^- + NO_2^- + NH_4^+)/PO_4^{3-}$ ratio from 2.9:1 to 20:1 (Roth et al., 2018⁶; Table S7.1). Abu Shoosha reef features turf algae (37%) and hard corals (29%) as most abundant functional groups (Table 7.1).

Table 7.1 | Relative benthic cover of functional groups at the experimental reef. Data taken from Roth et al. (2018)

Major functional groups	Cover (%)
Filamentous turf algae	36.8
Hard coral	28.8
Rubble	10.2
Biogenic rock	8.7
Soft coral	8.5
Sediment	6.0
<i>Tridacna</i> sp.	0.7
Macroalgae	0.4

Key environmental variables were monitored every 2–3 weeks at the sampling site, as described in a related study by Roth et al. (2018)⁶. Briefly, water temperature was measured with continuous data loggers (Onset HOBO Water Temperature Pro v2 Data Logger—U22-001; accuracy: ± 0.21 °C) and are given in 3-day means (72 h). For background measurements of dissolved NO_3^- , NO_2^- and PO_4^{3-} , water samples were taken in triplicates at the study site at least 2 m away from any fertilizer source (see “Experimental Design and Sampling Strategy” for more details). Water samples were filtered on the boat (Isopore™ membrane filters, 0.2 μm GTTP) and stored dark and cool until they were frozen to -50 °C in the lab. Nutrient concentrations were determined with a continuous flow analyzer (AA3 HR, SEAL). The limits of quantification (LOQ) for NO_3^- , NO_2^- and PO_4^{3-} were 0.084 $\mu\text{mol L}^{-1}$, 0.011 $\mu\text{mol L}^{-1}$ and 0.043 $\mu\text{mol L}^{-1}$ respectively. Five mL subsamples for NH_4^+ were filtered into separate acid washed centrifuge tubes. A total of 1.2 mL ortho-phthalaldehyde solution (OPA) was added, and samples were incubated >4 h with OPA in the dark. NH_4^+ concentrations were determined fluorometrically within 8 h (Trilogy® Laboratory Fluorometer; Turner Designs Inc., San Jose, CA, USA). The LOQ for NH_4^+ was 0.094 $\mu\text{mol L}^{-1}$. The sum of NO_3^- , NO_2^- and NH_4^+ concentrations reflect DIN.

Experimental Design and Sampling Strategy

Eight distinct patches of reef communities, each surrounded by patches of reef sand, were chosen in the back reef of Abu Shoosha at a water depth of approximately 5 m. The chosen communities, which represented the surrounding reef in composition (Table 7.1), were exposed to simulated eutrophication for 8 weeks in total. More specifically, each of the replicate communities was surrounded by four pins with approximately 70 g of slow release fertilizer granulate (Osmocote® Plus (15-9-12)) (Fig. 7.1). Being one of the most commonly used fertilizers for eutrophication experiments^{39,67–69}, this approach provides a fast and high supply of macronutrients (15% total N (8% nitrate N, 7% ammoniacal N), 9% available phosphate, 12% soluble potash) from the 1st day of fertilization under local temperature regimes⁷⁰. Osmocote® Plus (15-9-12) provides a balanced fertilization of N and phosphorus (P), however, only the fate of N was considered in this experiment as particularly N effects were of interest. The fertilizer was renewed every 2–3 weeks to assure a continuous nutrient supply⁷⁰. To test whether the nutrient addition was effective locally,

water samples for nutrients were taken directly at the fertilizer pin, and 25 cm towards the manipulated communities according to the protocol outlined above.



Figure 7.1 | Example of a manipulated in-situ community surrounded by four pins with attached fertilizer (Osmocote®) bags, photo: Florian Roth.

The effect of eutrophication was then assessed at the major functional groups (in terms of benthic reef cover in the central Red Sea) that were present in the selected communities. Specifically, we chose autotrophic hard corals (*Pocillopora* cf. *verrucosa*), soft corals (Xeniidae), turf algae and reef sand (sediments). These groups covered ~80% of the sampled reef⁶. Turf algae were defined as dense and flat (less than 2 cm in height) assemblages of filamentous algae of different species, including small individuals of macroalgae and cyanobacteria.

Manipulated specimens (“treatment”) were sampled from within a close radius (~25 cm) of the fertilizer tubes. As the in-situ communities were also needed in other experiments investigating their C chemistry (F. Roth, 2018, unpublished data) and N fluxes (Y. El-Khaled, 2018, unpublished data), specimens for natural conditions at the beginning (“start”) of the experiment were collected in the surrounding reef. Additional samples in replicates of eight were collected in the surrounding non-fertilized reef at the end (“control”) of the experiment, to reflect non-fertilized control conditions. For start and control data, a distance of at least 10 m from any fertilizer pin was maintained and the same depth as well as light conditions were given.

Samples were acquired with hammer and chisel. Hard coral and turf fragments (their substrate) were of approx. 10 cm in length. Sediments were collected using a Petri dish, which was dragged into the sediment upside-down (max. depth 14 mm) and the sediment was fixed to the dish from underneath. The samples were stored at -80 °C until further preparation. Hard corals, soft corals and turf algae were rinsed with Milli-Q to remove excess salt. Epilithic turf algae were scraped off from their surface with a scalpel and tweezers.

Elemental and Stable Isotopic Compositions of C and N

Turf algae, soft corals and sediments were dried for 48 h (sediments: 72 h) at 40 °C. Following Jessen et al. (2013)³⁸, hard coral tissue was removed using an airbrush, and the resulting tissue slurry was weighed, homogenized (MicroDisTec 125) and centrifuged for 10 min (Eppendorf Centrifuge 5,430 R, 4 °C, 3,220 rcf) to separate algae (“zooxanthellae”) from animal “tissue”. The supernatant was filtered (Whatman, GF/F) and for each sample two filters were generated. Filters for N and inorganic C analysis were dried for 24 h at 40 °C. Filters for C_{org} measurements were exposed to HCl fumes (from 37% HCl) and dried for 24 h. The remaining zooxanthellae pellet was dried for 48 h at 40 °C.

Sub-samples of all groups were ground using an agate mortar and pestle. A mill grinder (Retsch, PM 200, 4 min) was used for the sediments. For preparation of C_{org} samples, 5–10 g of ground sediment were placed in an Erlenmeyer flask and covered with Milli-Q. Drops of HCl (37%) were added until the reaction ceased. The acidified liquid was transferred to 50 mL Falcon tubes which were filled up with Milli-Q, to stepwise wash the sample pellet and raise the pH up to neutrality, and subsequently centrifuged for 10 min (Eppendorf Centrifuge 5,430 R, 4 °C, 7,200 rcf). The liquid supernatant was discarded and tubes were then refilled with Milli-Q for 3–4 times to raise pH. The pellets were dried in the Falcon tubes for 48 h at 40 °C.

The dry, homogenous powder was analyzed for: (a) N and inorganic C quantities; and (b) C_{org} as in Roth et al. (2018)⁶. C_{org}/N ratios, fractions of organic and inorganic C and isotope ratios were measured as in Rix et al. (2018)⁷¹ using a Flash 1112 EA coupled to a Delta V IRMS via a ConFloIV-interface (Thermo Scientific, Waltham, MA, USA). Isotopic ratios are shown as $\delta^{13}C$ or $\delta^{15}N$ (‰) = $(R_{sample}/R_{ref} - 1) \times 1,000$. There, R is the ratio of heavier:lighter isotope ($^{13}C:^{12}C$ or $^{15}N:^{14}N$). As reference, Vienna Pee Dee Belemnite was used for C ($R_{ref} = 0.01118$) and atmospheric nitrogen for N ($R_{ref} = 0.00368$).

Zooxanthellae Cell Density and Mitotic Index

For hard corals, zooxanthellae cell density and the mitotic index were analyzed following the described sampling strategy (start, control and treatment), whereby “start” and “control” were from the surrounding reef. Aliquots of 20 μ L homogenized tissue sample and 80 μ L Milli-Q were vortexed (Gilson, GVLab) directly before taking 10 μ L on an improved Neubauer Levy hemocytometer (0.0100 mm deep). Pictures were taken with a ZEISS Primovert microscope via Labscope (Version 2.5) from the 5 \times 5 grid in 40-fold and randomly in 20-fold magnification. Manual counts of zooxanthellae and the mitotic index were related to the total amount of airbrushed slurry per individual. Here, clumps and inhomogeneous patches were not considered. For normalization to the coral surface area, 3D models for all coral skeletons were generated using the software AutodeskReCap Photo (v18.2.0.8).

Data Analysis

Nitrogen uptake by functional groups was assessed using stable isotope analysis. N utilization was assessed by elemental analysis, and C_{org}/N ratios served to identify nutrient limitations^{37,72,73}, along with zooxanthellae cell density and mitotic index (for hard corals). Statistical analysis was conducted with

RStudio⁷⁴. Xeniidae and *Pocillopora* cf. *verrucosa* were not abundant in all eight communities (only in 5 and 6, respectively). Due to logistical constraints, “start” data of soft corals was not available. A two-way ANOVA (factors: treatment, dominant functional group) showed no significant effect of community composition on our response parameters under N eutrophication, therefore data from more coral and more algae dominated communities were pooled. Significant differences between “start” and “control” as well as between “control” and “treatment” were checked with two-sample *t*-tests (test statistic: *t*) if test assumptions were fulfilled, otherwise Mann–Whitney–Wilcoxon Tests (test statistic: *W*) were applied. A similar approach was conducted for cell density of zooxanthellae and mitotic index per treatment. Tissue homogenization of the “start” samples was visually much worse than for “treatment” and “control” samples, but is shown for completeness and homogeneity.

7.4 Results

Environmental Parameters and N Availability

During the study period, water temperature increased from 25 °C to 28 °C (Table S7.1). The mean background concentration in sea water for DIN was $0.34 \pm 0.07 \mu\text{M N}$ and $0.10 \pm 0.02 \mu\text{M PO}_4^{3-}$ during the time of the experiment (measured after 2, 4 and 6.5 weeks). Accordingly, the environmental background DIN/ PO_4^{3-} ratio was 3.4 (± 0.08):1 on average. The manipulation of nutrients increased DIN concentrations (measured after 2, 4 and 6.5 weeks) on average 3-fold and to a maximum of 7-fold directly at the communities relative to background concentrations (Fig. 7.2). Namely, manipulated NO_3^- was $1.05 \pm 0.09 \mu\text{M}$ and manipulated NH_4^+ was $0.22 \pm 0.06 \mu\text{M}$. PO_4^{3-} remained at ambient condition, despite being present in the fertilizer (Table S7.1). As such, the mean DIN/ PO_4^{3-} ratio at the manipulated communities was 15.1 (± 3.46):1.

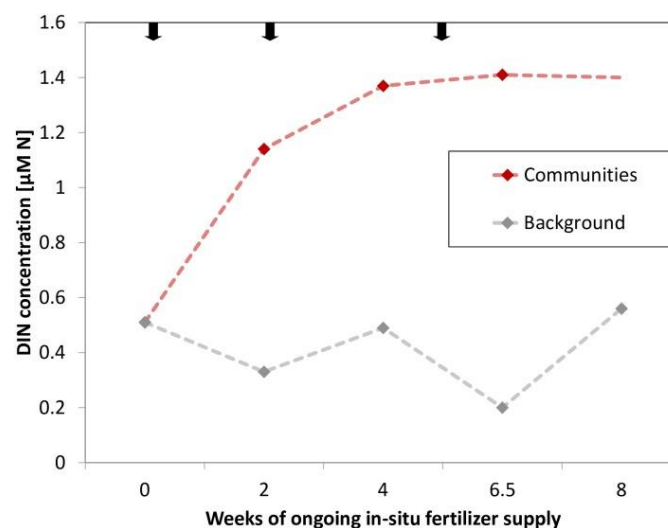


Figure 7.2 | Dissolved inorganic nitrogen (DIN) concentrations at experimental communities (red, last data point extrapolated) and of background sea water (grey) over time of in-situ manipulation. Black arrows symbolize introduction and renewal of fertilizer.

Uptake of Excess N by Benthic Functional Groups

Pure Osmocote® fertilizer was enriched in ^{15}N ($\delta^{15}\text{N} = 16.326 \pm 0.257$, Table S7.2). Hard corals (tissue), turf algae and soft corals took up excess N, as indicated by significantly ($t_{12} = 2.553, p = 0.025$; $t_{13} = 3.228, p = 0.007$; $t_9 = 6.705, p < 0.001$, respectively) increased $\delta^{15}\text{N}$ (Fig. 7.3A). The $\delta^{15}\text{N}$ values in manipulated functional groups were 8% (*Pocillopora* tissue), 27% (Xeniidae) and 28% (turf algae) higher compared to untreated controls after the same time.

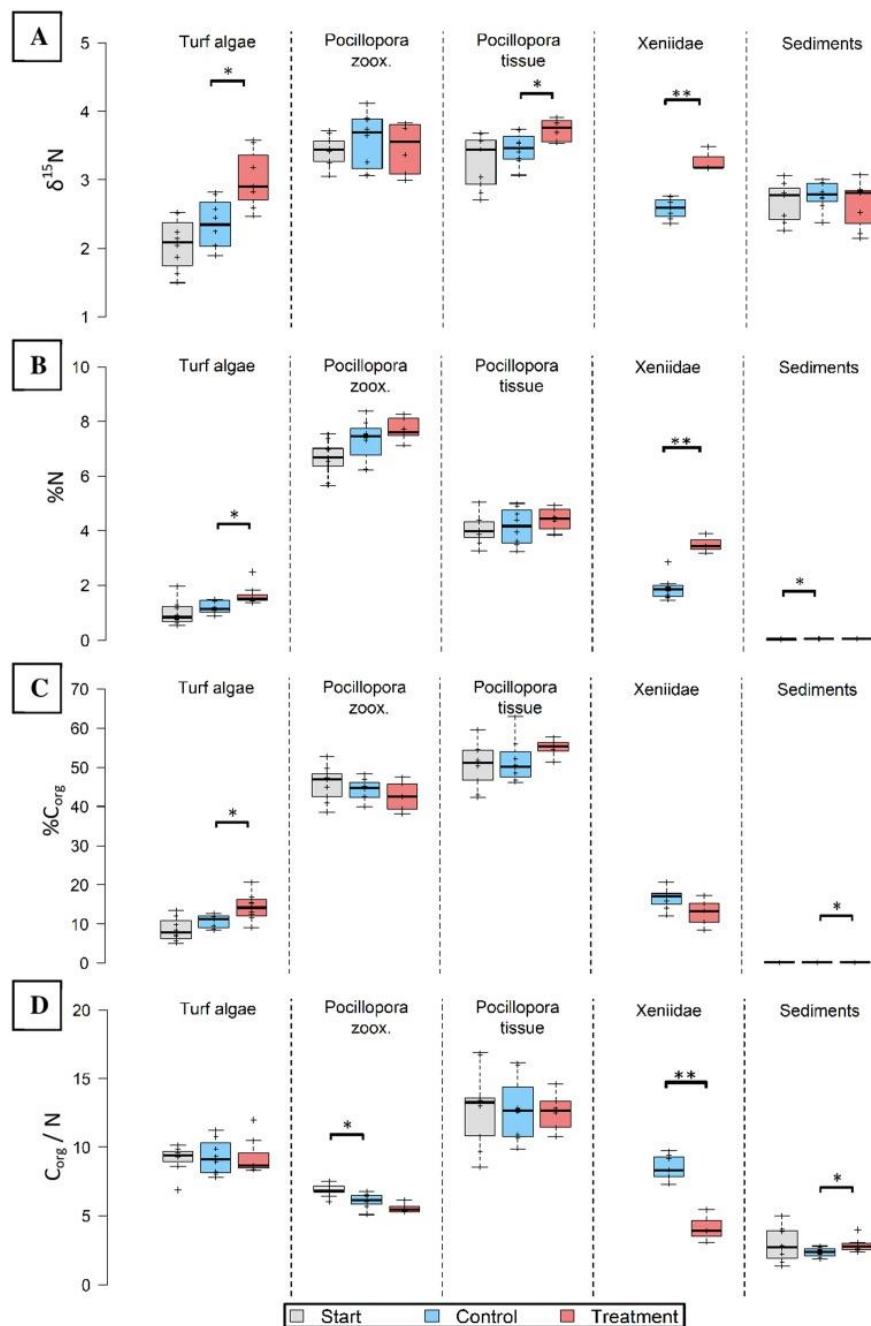


Figure 7.3 | Nitrogen (N) and carbon elemental and N isotopic composition of major functional groups before (grey), without (blue) and after 8 weeks in-situ eutrophication (red). Investigated groups are turf algae, *Pocillopora* cf. *verrucosa* zooxanthellae (“zoox.”) and -tissue, Xeniidae and sediments. Eight replicates per boxplot. **(A)** Nitrogen isotopes ($\delta^{15}\text{N}$), **(B)** nitrogen content (%N), **(C)** organic carbon content (%C_{org}), **(D)** organic carbon to nitrogen ratio (C_{org}/N). Asterisks indicate significant differences (* $p < 0.05$ and ** $p < 0.001$).

Utilisation of Excess N by Benthic Functional Groups

Nitrogen content was highest in hard coral zooxanthellae both before and after eutrophication (Fig. 7.3B). In the eutrophication treatment, N content was significantly higher in the tissues of Xeniidae ($t_9 = 5.667$, $p < 0.001$) and turf algae ($W = 49$, $p = 0.014$). Their tissues contained 85% (Xeniidae) and 39% (turf) more N compared to untreated controls. Increases in the other groups were not significant.

To investigate whether N was utilized to produce C_{org} under a metabolically stable ratio, the C_{org} content and C_{org}/N ratio are presented. The hard coral components showed the highest C_{org} content ranging from $50.39 \pm 1.83\%$ to $55.05 \pm 1.49\%$ in the tissue and between $42.64 \pm 1.39\%$ and $45.78 \pm 1.49\%$ in zooxanthellae (Fig. 7.3C). Minimum C_{org} content was observed in reef sediments, ranging between $0.09 \pm 0.01\%$ and $0.11 \pm 0.01\%$. Only turf algae and sediments showed a significant change in C_{org} content ($t_{14} = 2.568$, $p = 0.022$; $t_{14} = 2.537$, $p = 0.023$, respectively). This represents an increase in C_{org} content by 33% in turf algae and 24% in sediments in the treatment compared control specimen.

The C_{org}/N ratio for treated Xeniidae was significantly lower ($t_8 = -6.405$, $p < 0.001$) than for Xeniidae in the surrounding reef (8.520 ± 0.320 compared to 4.132 ± 0.566 , Fig. 7.3D). In sediments of the eutrophication “treatment” the C_{org}/N ratio was significantly higher than in controls ($W = 53$, $p = 0.028$), however it did not increase compared to start values. In hard coral zooxanthellae, C_{org}/N ratio declined over time but was not significantly different in treatment data compared to controls. C_{org}/N remained constant in hard coral tissue and turf algae.

Cell density of hard coral zooxanthellae (*Pocillopora cf. verrucosa*) doubled over the 8 weeks, while their mitotic index halved (Figs. 7.4A and 7.4B). However, zooxanthellae density and mitotic index in fertilized and control corals remained similar. After 8 weeks, cell densities ranged from 1.324 ± 0.147 Mio. cells cm^{-2} (treatment) to 1.373 ± 0.172 Mio. cells cm^{-2} (control), whereas the mitotic index ranged from $4.718 \pm 0.445\%$ to $4.901 \pm 0.244\%$ in organisms under control and N enrichment conditions, respectively.

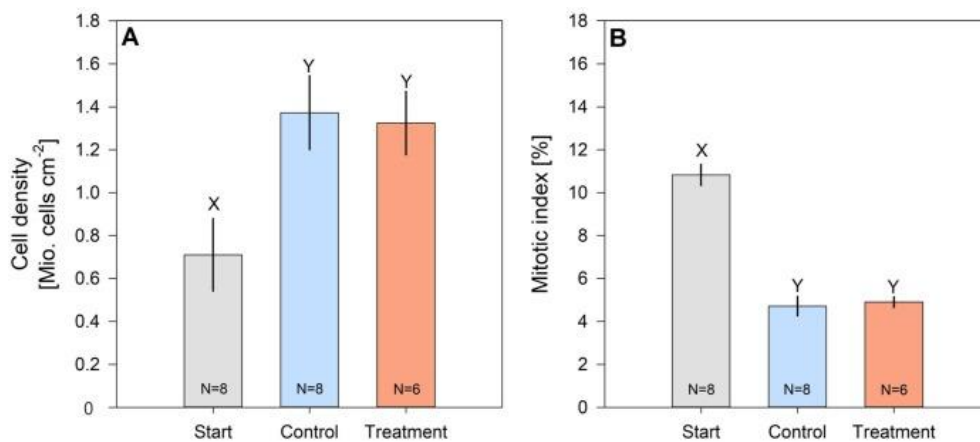


Figure 7.4 | Cell density (A) and mitotic index (B) of hard coral's (*Pocillopora cf. verrucosa*) zooxanthellae before (grey), without (blue) and with 8 weeks of N eutrophication (red). Error bars represent the standard error of the mean, letters X and Y indicate significant differences.

7.5 Discussion

Studies on the effects of eutrophication in the oligotrophic central Red Sea are scarce, and have, so far, focused on eutrophication effects on single functional groups only, used natural gradients or left out impacts on the elemental stoichiometry. In a comparative in-situ approach we therefore provide an assessment of eutrophication effects on several major functional groups' ecophysiology using elemental and stable isotope analysis, drawing conclusions on N uptake and utilization.

Uptake of Excess N by Major Benthic Functional Groups

In-situ N enrichment resulted in an uptake of N in the tissues of turf algae, soft corals and hard corals, but not in sediments and hard coral zooxanthellae. The fact that turf algae exhibited the lowest $\delta^{15}\text{N}$ at the start of our experiment suggests considerable assimilation of N from N_2 fixation⁷⁵⁻⁷⁷ (El-Khaled, 2018, unpublished data). Biological fixation of atmospheric N_2 leads to a depletion in ^{15}N in the N compounds of the fixer^{78,79}. After the experiment, turf algae showed one of the strongest uptakes of N from the fertilizer among the benthic reef functional groups, as indicated by significantly higher $\delta^{15}\text{N}$ values (Fig. 7.3A), which concurs with den Haan et al. (2016)⁶⁵. The low $\text{DIN}/\text{PO}_4^{3-}$ ratio in ambient waters at the reef further suggests a relatively low degree of P-limitation under ambient conditions, which may help to explain the strong uptake of N when available. Concordantly, Lapointe et al. (2019)⁴² showed that in the eutrophic waters of the Florida Keys, the N:P ratio of turf algae (293:1) increased to a much greater extent than that of macroalgae (71:1) as DIN concentrations increased over a 3-decade period. Also soft corals incorporated fertilizer N and reached higher $\delta^{15}\text{N}$ values than typical for soft corals that are exposed to industrial and urban run-off in the central Red Sea⁵.

In the present experiment, the uptake of excess N was not noticeable in the sediment $\delta^{15}\text{N}$, in contrast to a study by Miyajima et al. (2001)⁸⁰. There, sediment microflora took up NO_3^- and NH_4^+ in bottle incubations⁸⁰, and assimilation as well as adsorption of N compounds on carbonate reef sands were observed⁸¹. This would suggest fast nutrient uptake, especially in microalgae on the sediments, and high uptakes into pore water, as reported by Rasheed, Badran & Huettel (2003)⁸² and Erler, Santos & Eyre (2014)⁸¹. Pore water was not targeted in our study and a change of isotopic signature in the sediment could take longer than the current experimental period, as previously suggested by Cook et al. (2007)⁸³ who did not find clear $\delta^{15}\text{N}$ patterns in N manipulated sediments. This would account for the integration time of isotopic signatures through the food-web^{84,85}. In agreement to our study, Koop et al. (2001)⁴⁷ also did not find high $\delta^{15}\text{N}$ uptake in sediments. Potentially, organisms on and in the sediments are not N-limited, given that sediments are active sites of microbial N transformations⁸⁶ and remineralisation⁸⁷ allowing for N recycling.

Within the hard coral holobiont, the zooxanthellae did not incorporate excess N significantly. This generally agrees with Koop et al. (2001)⁴⁷ and den Haan et al. (2016)⁶⁵ showing that hard corals (i.e., *Madracis mirabilis* (now *Madracis myriaster*)) take up less excess nutrients than turf or macroalgae. Most studies, however, report

stronger $\delta^{15}\text{N}$ enrichment in the zooxanthellae fraction compared to host tissue^{88–90}. There are several possibilities why this was not observed in our study. Firstly, NO_3^- uptake in zooxanthellae can be highest under low NH_4^+ availability^{91,92}, however, NH_4^+ was elevated ~ 5 -fold compared to the environmental background in our experiment (Table S7.1). Secondly, P can be a limiting factor to zooxanthellae's N uptake⁹³. Unlike the highly increased N availability, the P provided by our fertilizer did not alter the PO_4^{3-} concentration 25 cm away from the source (Table S7.1). The resulting increased DIN/ PO_4^{3-} ratio at the communities underlines a stronger P-limitation under manipulation. Potentially, reef sediments⁹⁴ or organisms in the water column and the surrounding benthos took up PO_4^{3-} too quickly as P was stated crucial⁹⁵ and limiting^{5,72,96} for primary production in coral reefs. However, we acknowledge dissimilar findings on the limiting roles of N and P in the central Red Sea¹³. The understanding of P cycling and limitation in coral reef environments is still in its infancy⁹⁷, but PO_4^{3-} could have been limiting for significant N uptake in zooxanthellae⁹³. In contrast to other findings^{92,98}, coral tissue incorporated more available N than the symbionts. This suggests that the host tissue was less P-limited than the zooxanthellate fraction, and hence took up relatively more N. This is corroborated by the low DIN/ PO_4^{3-} ratio of 3.4 in ambient waters of the studied reef that indicates N-rather than P-limitation, confirming Al-Farawati, El Sayed & Rasul, (2019)⁹⁹.

Utilisation of Excess N by Benthic Functional Groups

Due to eutrophication, tissue N content significantly increased in turf algae and soft corals but not in hard corals and sediments. C_{org} content remained constant in hard and soft corals but increased in sediments and turf algae. Thus, turf algae and hard coral tissue remained at constant C_{org}/N ratio, while it decreased in soft corals and showed unclear trends in hard coral zooxanthellae and sediments.

For turf algae, N and C_{org} content were significantly higher under nutrient addition compared to controls, which contrasts findings by Stuhldreier et al. (2015)³⁹ reporting no such eutrophication effects on turf algae dominated settlement communities. In the present study, relatively similar increases in N content (+39%) and C_{org} content (+33%) occurred and the C_{org}/N ratio stayed constant (between 9.1 and 9.3). Hence we interpret N to be a limiting nutrient¹⁰⁰ for turf algae growth, which also corroborates other studies^{55,101,102}. Turf algae are strong opponents to corals^{6,103}, and their competitiveness under high-nutrient availability has been documented in Hawaii¹⁰⁴, the Caribbean¹⁰⁵, Brazil¹⁰⁶, Australia¹⁰⁷ and in the Red Sea¹⁵. As turf algae are also rapidly taking over bare substrates^{6,39} and are very resistant to disturbances¹⁰³, their monitoring should be on regional management agendas. Cover data was not documented in the present study but turf algae growth could be speculated upon based on increases in C_{org} content.

Nitrogen was taken up by soft corals while the C_{org} content did not increase, resulting in an altered elemental stoichiometry (C_{org}/N ratio). The strong decline in the soft corals' C_{org}/N ratio could be explained by an uptake of excess N as so-called “luxury consumption”, describing on-going uptake while a different nutrient (e.g., P) might limit growth and productivity. We interpret that in our eutrophication experiment P rather than N was the limiting nutrient for soft corals, which may limit chlorophyll *a* content and photosynthesis

in Xeniidae¹⁰⁸. Our data from elemental analysis and non-documented visual observations support the hypothesis of Fabricius et al. (2005)¹⁰⁹ that soft corals could react more timely and strongly to water quality gradients than hard corals.

Our results further correspond to other studies^{82,86,110} finding low C_{org} content in carbonate dominated reef sands (0.18–0.36%), which were even lower in our study (0.1%). We acknowledge that the utilized acid wash-out processing may underestimate C_{org} contents due to C_{org} losses to the liquid acid of 4–52%¹¹¹ and as such lower the C_{org}/N ratio. However, this is a commonly used method in comparative studies^{82,110}. The observed 21% increase in C_{org} could be attributed to P-supported algae growth on the sediments (Fig. S7.1) as fertilizer N was not taken up (constant $\delta^{15}N$) but gross primary production significantly increased (Y. El-Khaled, 2018, unpublished data). A different source for the increased C_{org} content in sediments could be the export of C_{org} from turf algae (F. Roth, 2018, unpublished data) for example, as dissolved organic carbon (DOC)¹¹² and subsequent uptake by reef sediments, as suggested by Cárdenas et al. (2015)¹¹³. This, along with the low C_{org}/N ratio, corroborates the previous assumption that life in and on the sediments, as well as its increase in C_{org} content was not N limited.

Regarding the hard coral holobiont, our results suggest that the incorporation of excess N only to the host tissue did not result in its utilization in terms of C_{org} production. As such, C_{org}/N ratios for *Pocillopora* cf. *verrucosa* contrast a study conducted in 10 km distance to our study site further offshore at the same time of the year in 2012¹¹⁴. There, the natural host total C:N ratio was around 5, which makes our presented host material appear more N depleted in comparison. Over time, we observed an increase in symbiont cell density, which contrasts with other studies finding higher zooxanthellae cell densities in *Pocillopora* species in cooler and more nutrient rich phases^{4,115,116}. However, particularly the similarity between treatment and non-fertilized controls should be considered where cell density and mitotic index did not differ. Similar findings have been reported by Ferrier-Pagès et al. (2001)¹¹⁷ and Rosset et al. (2017)¹¹⁸ during pure N fertilization but contrast with other studies^{119–121}. Increased zooxanthellae cell density in hard corals was found, for example, after only 18 days of eutrophication¹²² or following a natural nutrient gradient¹²³. Altogether, this suggests that N was not a limiting factor for zooxanthellae in our experiment. The production¹²⁴, health and density⁹¹ of zooxanthellae cells was found to be P limited. Accordingly, high P availability resulted in higher increases of zooxanthellae density (*Pocillopora damicornis* and *Euphyllia paradivisa* (now *Fimbriaphyllia paradivisa*)) than availability of only N^{118,120}. As a consequence, we hypothesize that hard corals also did not shift in primary productivity, even though a significant increase in $\delta^{13}C$ in hard coral zooxanthellae (Fig. S7.2) could be a sign of increased photosynthesis¹²⁵ for example, following a seasonal pattern (F. Roth, 2018, unpublished data). However, gross primary production did not increase in our manipulated hard corals (Y. El-Khaled, 2018, unpublished data). The increased $\delta^{13}C$ in the zooxanthellae (Fig. S7.2) could also be an indicator for a negative effect on hard coral health which was also found in relation to bleached *Favia favaus* (now *Dipsastraea favaus*) corals in the Northern Red Sea¹²⁶ but not *Montastraea faveolata* (now *Orbicella faveolata*) in Florida¹²⁷. Given our 8-week observation period and a comparatively cold water temperature, our study did not provide a setting to trace severe bleaching effects and for the Southern

Red Sea it was speculated that higher nutrient availability might even benefit *P. verrucosa* to resist higher water temperature⁴. This corroborates that effects of eutrophication on coral health are not always negative^{123,128,129} and do not necessarily harm or kill individual coral colonies but get outcompeted or overgrown over time (reviewed in Fabricius, 2005¹¹⁹). Longer (3 years)⁵³, and both longer and stronger (1 year, 36.2 $\mu\text{M NH}_4^+$)⁴⁷ N manipulation could, however, lead to increased coral mortality⁴⁷. In particular, reviewed findings¹³⁰, natural long-term observations⁴² and laboratory experiments^{34,118} with high N (>3 μM and 38 μM N, respectively) and low P supply (<0.07 μM and 0.18 μM P, respectively) increased susceptibility of corals to bleaching, which suggests negative effects. In agreement with Ezzat et al. (2016)¹²⁴ and Ferrier-Pagès et al. (2016)⁹⁷, we suggest increasing efforts investigating P cycling and limitation in current and future reef ecosystems. Besides this key role of nutrient ratios, Burkepille et al. (2019)³² highlight the importance to also account for varying effects of different forms of N. As N sources and pathways in corals and their reef environments are of major importance to better understand ecosystem functioning¹³¹, the uptake and utilization of N (this study) should be compared to eutrophication effects on the N cycle.

7.6 Conclusion

Anthropogenic pressures on the Red Sea are constantly increasing¹³² and 60% of Red Sea coral reefs are at stake¹³³. We were able to show cascaded, group-specific responses to N availability and link elemental and isotopic composition to group-specific nutrient limitations, N uptake and utilization, and highlight the importance of P limitations in hard and soft corals. Even over an 8-week N eutrophication and under high abundance of herbivores, significant uptake and utilization of fertilizer N was shown particularly for turf algae as strong competitors for space in struggling reef ecosystems. As such, our study corroborates that turf algae can be early indicators for changes and anthropogenic influence^{63,134}, reacting faster to eutrophication than hard coral zooxanthellae. As turf algae play a key role in phase shifts, are strong competitors to corals, rapidly take over bare substrates and are highly persistent, their substantial biochemical benefits from N supply should push coastal management to not only consider limiting future discharges but try to reduce both point-sources and non-point sources of nutrients already in place. Given the increasing coastal development in the central Red Sea, water quality management is challenged to improve future reef states^{135,136} and should be on regional agendas for coastal urban development and aquaculture. The context in which eutrophication effects should be seen comprises further local (e.g., fishing pressure and habitat destruction) and global (e.g., warming and ocean acidification) factors to which coastal development adds high nutrient loads on top. Low N concentrations were shown to be a crucial precondition for coral recovery¹³⁷ and particularly in the Red Sea the maintaining of oligotrophic conditions could be the key factor and challenge for coral health and resilience to climate change²².

7.7 Acknowledgements

We are thankful to Marianne Falk for helping in elemental-and isotopic analysis and Nils Rådecker for coral sample processing advice. We were happy to get further support by Pedro Ruiz-Compean (sediment samples), Aislinn Dunne (sediment samples), Sophia Tobler (image editing), Rodrigo Villalobos and João Cúrdia (both field work).

7.8 References

1. Roberts, C. M. *et al.* Marine Biodiversity Hotspots and Conservation Priorities for Tropical Reefs. *Science* **295**, 1280–1285 (2002).
2. Odum, H. T. & Odum, E. P. Trophic Structure and Productivity of a Windward Coral Reef Community on Eniwetok Atoll. *Ecol. Monogr.* **25**, 291–320 (1955).
3. Raitsos, D. E., Pradhan, Y., Brewin, R. J. W., Stenchikov, G. & Hoteit, I. Remote Sensing the Phytoplankton Seasonal Succession of the Red Sea. *PLoS One* **8**, (2013).
4. Sawall, Y., Al-Sofyani, A., Banguera-Hinestroza, E. & Voolstra, C. R. Spatio-temporal analyses of Symbiodinium physiology of the coral *Pocillopora verrucosa* along large-scale nutrient and temperature gradients in the Red Sea. *PLoS One* **9**, 1–12 (2014).
5. Kürten, B. *et al.* Influence of environmental gradients on C and N stable isotope ratios in coral reef biota of the Red Sea, Saudi Arabia. *J. Sea Res.* **85**, 379–394 (2014).
6. Roth, F. *et al.* Coral reef degradation affects the potential for reef recovery after disturbance. *Mar. Environ. Res.* **142**, 48–58 (2018).
7. Loya, Y., Lubinevsky, H., Rosenfeld, M. & Kramarsky-Winter, E. Nutrient enrichment caused by in situ fish farms at Eilat, Red Sea is detrimental to coral reproduction. *Mar. Pollut. Bull.* **49**, 344–353 (2004).
8. Kürten, B. *et al.* Ecohydrographic constraints on biodiversity and distribution of phytoplankton and zooplankton in coral reefs of the Red Sea, Saudi Arabia. *Mar. Ecol.* **36**, 1195–1214 (2015).
9. Dunne, A. F. Monitoring the effects of offshore aquaculture on water quality in the Red Sea. (King Abdullah University of Science and Technology, 2018).
10. Hozumi, A., Hong, P. Y., Kaartvedt, S., Røstad, A. & Jones, B. H. Water quality, seasonality, and trajectory of an aquaculture-wastewater plume in the Red Sea. *Aquac. Environ. Interact.* **10**, 61–77 (2018).
11. Basaham, A. S., Rifaat, A. E., El-Mamoney, M. H. & El Sayed, M. A. Re-evaluation of the impact of sewage disposal on coastal sediments of the southern Corniche, Jeddah, Saudi Arabia. *J. King Abdulaziz Univ. Mar. Sci.* **20**, 109–126 (2009).
12. Al-Farawati, R. Environmental conditions of the coastal waters of Southern corinche, Jeddah, eastern Red Sea: Physico-chemical approach. *Aust. J. Basic Appl. Sci.* **4**, 3324–3337 (2010).
13. Peña-García, D., Ladwig, N., Turki, A. J. & Mudarris, M. S. Input and dispersion of nutrients from the Jeddah Metropolitan Area, Red Sea. *Mar. Pollut. Bull.* **80**, 41–51 (2014).
14. Mohamed, Z. A. & Mesaad, I. First report on *Noctiluca scintillans* blooms in the Red Sea off the coasts of Saudi Arabia: Consequences of eutrophication. *Oceanologia* **49**, 337–351 (2007).
15. Naumann, M. S., Bednarz, V. N., Ferse, S. C. A. & Niggel, W. Monitoring of coastal coral reefs near Dahab (Gulf of Aqaba , Red Sea) indicates local eutrophication as potential cause for change in benthic communities. (2015). doi:10.1007/s10661-014-4257-9
16. Abu-Rizaiza, O. & Sarikaya, H. Z. Drainage Water Disposal, Jeddah, Saudi Arabia. *J. Water Resour. Plan. Manag.* **119**, 706–712 (1993).
17. Aljoufie, M. & Tiwari, A. Climate change adaptations for urban water infrastructure in Jeddah, Kingdom of Saudi Arabia. *J. Sustain. Dev.* **8**, 52–66 (2015).
18. Risk, M. J., Sherwood, O. A., Nairn, R. & Gibbons, C. Tracking the record of sewage discharge off Jeddah, Saudi Arabia, since 1950, using stable isotope records from antipatharians. *Mar. Ecol. Prog. Ser.* **397**, 219–226 (2009).
19. Sawall, Y. *et al.* Coral Communities, in Contrast to Fish Communities, Maintain a High Assembly Similarity along the Large Latitudinal Gradient along the Saudi Red Sea Coast. *J. Ecosyst. Ecography*

- 3, (2014).
20. Pearman, J. K., Afandi, F., Hong, P. & Carvalho, S. Plankton community assessment in anthropogenic-impacted oligotrophic coastal regions. *Environ. Sci. Pollut. Res.* **25**, 31017–31030 (2018).
 21. Ziegler, M. *et al.* Coral microbial community dynamics in response to anthropogenic impacts near a major city in the central Red Sea. *Mar. Pollut. Bull.* **105**, 629–640 (2016).
 22. Hall, E. R., Muller, E. M., Goulet, T., Bellworthy, J. & Ritchie, K. B. Eutrophication may compromise the resilience of the Red Sea coral *Stylophora pistillata* to global change. *Mar. Pollut. Bull.* **131**, 701–711 (2018).
 23. Johnson, C., Klumpp, D., Field, J. & Bradbury, R. Carbon flux on coral reefs: effects of large shifts in community structure. *Mar. Ecol. Prog. Ser.* **126**, 123–143 (1995).
 24. Wild, C. *et al.* Coral mucus functions as an energy carrier and particle trap in the reef ecosystem. *Nature* **428**, 66–70 (2004).
 25. O’Neil, J. M. & Capone, D. G. *Nitrogen Cycling in Coral Reef Environments. Nitrogen in the Marine Environment* (2008). doi:10.1016/B978-0-12-372522-6.00021-9
 26. Hoegh-Guldberg, O. *et al.* Coral Reefs Under Rapid Climate Change and Ocean Acidification. *Science (80-)*. **318**, 1737–1742 (2007).
 27. Carpenter, K. E. *et al.* One-Third of Reef-Building Corals Face Elevated Extinction Risk from Climate Change and Local Impacts. *Science (80-)*. **321**, 560–563 (2008).
 28. Hughes, T. P. *et al.* Spatial and temporal patterns of mass bleaching of corals in the Anthropocene. *Science (80-)*. **359**, 80–83 (2018).
 29. Lesser, M. P. *et al.* Nitrogen fixation by symbiotic cyanobacteria provides a source of nitrogen for the scleractinian coral *Montastraea cavernosa*. *Mar. Ecol. Prog. Ser.* **346**, 143–152 (2007).
 30. Wegley, L., Edwards, R., Rodriguez-Brito, B., Liu, H. & Rohwer, F. Metagenomic analysis of the microbial community associated with the coral *Porites astreoides*. *Environ. Microbiol.* **9**, 2707–2719 (2007).
 31. Shantz, A. A. & Burkpile, D. E. Context-dependent effects of nutrient loading on the coral-algal mutualism. *Ecology* **95**, 1995–2005 (2014).
 32. Burkpile, D. E. *et al.* Nitrogen Identity Drives Differential Impacts of Nutrients on Coral Bleaching and Mortality. *Ecosystems* (2019). doi:10.1007/s10021-019-00433-2
 33. Haas, A., Al-Zibdah, M. & Wild, C. Effect of inorganic and organic nutrient addition on coral-algae assemblages from the Northern Red Sea. *J. Exp. Mar. Bio. Ecol.* **380**, 99–105 (2009).
 34. Wiedenmann, J. *et al.* Nutrient enrichment can increase the susceptibility of reef corals to bleaching. *Nat. Clim. Chang.* **3**, 160–164 (2012).
 35. Müller-Navarra, D. C. Food web paradigms: The biochemical view on trophic interactions. *Int. Rev. Hydrobiol.* **93**, 489–505 (2008).
 36. Goldman, J. C. On phytoplankton growth rates and particulate C: N: P ratios at low light. *Limnol. Oceanogr.* **31**, 1358–1363 (1986).
 37. Hillebrand, H. & Sommer, U. The nutrient stoichiometry of benthic microalgal growth: Redfield proportions are optimal. *Limnol. Oceanogr.* **44**, 440–446 (1999).
 38. Jessen, C., Roder, C., Villa Lizcano, J. F., Woolstra, C. R. & Wild, C. In-Situ Effects of Simulated Overfishing and Eutrophication on Benthic Coral Reef Algae Growth, Succession, and Composition in the Central Red Sea. *PLoS One* **8**, e66992 (2013).
 39. Stuhldreier, I., Bastian, P., Schönig, E. & Wild, C. Effects of simulated eutrophication and

- overfishing on algae and invertebrate settlement in a coral reef of Koh Phangan, Gulf of Thailand. *Mar. Pollut. Bull.* **92**, 35–44 (2015).
40. Risk, M. J., Lapointe, B. E., Sherwood, O. A. & Bedford, B. J. The use of $\delta^{15}\text{N}$ in assessing sewage stress on coral reefs. *Mar. Pollut. Bull.* **58**, 793–802 (2009).
 41. Baker, D. M., Jordán-Dahlgren, E., Maldonado, M. A. & Harvell, C. D. Sea fan corals provide a stable isotope baseline for assessing sewage pollution in the Mexican Caribbean. *Limnol. Oceanogr.* **55**, 2139–2149 (2010).
 42. Lapointe, B. E., Brewton, R. A., Herren, L. W., Porter, J. W. & Hu, C. *Nitrogen enrichment, altered stoichiometry, and coral reef decline at Looe Key, Florida Keys, USA: a 3-decade study.* *Marine Biology* **166**, (Springer Berlin Heidelberg, 2019).
 43. Hoegh-Guldberg, O., Muscatine, L., Goiran, C., Siggaard, D. & Marion, G. Nutrient-induced perturbations to $\delta^{13}\text{C}$ and $\delta^{15}\text{N}$ in symbiotic dinoflagellates and their coral hosts. *Mar. Ecol. Prog. Ser.* **280**, 105–114 (2004).
 44. Costanzo, S. D., O'Donohue, M. J., Dennison, W. C., Loneragan, N. R. & Thomas, M. A New Approach for Detecting and Mapping Sewage Impacts. *Mar. Pollut. Bull.* **42**, 149–156 (2001).
 45. Kendall, C., Elliot & Wankel, S. D. Tracing anthropogenic inputs of nitrogen to ecosystems. in *Stable Isotopes in Ecology and Environmental Science* (eds. Michener, R. H. & Lajtha, K.) (Malden: Blackwell Publisher, 2007).
 46. Ferrier-Pagès, C., Gattuso, J. P., Dallot, S. & Jaubert, J. Effect of nutrient enrichment on growth and photosynthesis of the zooxanthellate coral *Stylophora pistillata*. *Coral Reefs* **19**, 103–113 (2000).
 47. Koop, K. *et al.* ENCORE: The effect of nutrient enrichment on coral reefs. Synthesis of results and conclusions. *Mar. Pollut. Bull.* **42**, 91–120 (2001).
 48. Kinsey, D. W. & Davies, P. J. Effects of elevated nitrogen and phosphorus on coral reef growth. *Limnol. Oceanogr.* **24**, 935–940 (1979).
 49. Silbiger, N. J. *et al.* Nutrient pollution disrupts key ecosystem functions on coral reefs. *Proc. R. Soc. B Biol. Sci.* **285**, 20172718 (2018).
 50. Harrison, L. & Ward, S. Elevated levels of nitrogen and phosphorus reduce fertilisation success of gametes from scleractinian reef corals. *Mar. Biol.* **139**, 1057–1068 (2001).
 51. Duprey, N. N., Yasuhara, M. & Baker, D. M. Reefs of tomorrow: eutrophication reduces coral biodiversity in an urbanized seascape. *Glob. Chang. Biol.* **22**, 3550–3565 (2016).
 52. Wooldridge, S. A. & Done, T. J. Improved water quality can ameliorate effects of climate change on corals. **19**, 1492–1499 (2009).
 53. Vega Thurber, R. L. *et al.* Chronic nutrient enrichment increases prevalence and severity of coral disease and bleaching. *Glob. Chang. Biol.* **20**, 544–554 (2014).
 54. Lapointe, B. E. Phosphorus- and nitrogen-limited photosynthesis and growth of *Gracilaria tikvahiae* (Rhodophyceae) in the Florida Keys: an experimental field study. *Mar. Biol.* **94**, 561–568 (1987).
 55. Williams, S. & Carpenter, R. Nitrogen-limited primary productivity of coral reef algal turfs: potential contribution of ammonium excreted by *Diadema antillarum*. *Mar. Ecol. Prog. Ser.* **47**, 145–152 (1988).
 56. Lapointe, B. E. Nutrient thresholds for bottom-up control of macroalgal blooms on coral reefs in Jamaica and southeast Florida. *Limnol. Oceanogr.* **42**, 1119–1131 (1997).
 57. Smith, J. E., Hunter, C. L. & Smith, C. M. The effects of top-down versus bottom-up control on benthic coral reef community structure. *Oecologia* **163**, 497–507 (2010).

58. McManus, J. W. & Polsenberg, J. F. Coral-algal phase shifts on coral reefs: Ecological and environmental aspects. *Prog. Oceanogr.* **60**, 263–279 (2004).
59. Norström, A. V., Nyström, M., Lokrantz, J. & Folke, C. Alternative states on coral reefs: Beyond coral-macroalgal phase shifts. *Mar. Ecol. Prog. Ser.* **376**, 293–306 (2009).
60. Pearman, J. K. *et al.* Microbial planktonic communities in the Red Sea: high levels of spatial and temporal variability shaped by nutrient availability and turbulence. *Sci. Rep.* **7**, 1–15 (2017).
61. Berumen, M. L. *et al.* The status of coral reef ecology research in the Red Sea. *Coral Reefs* **32**, 737–748 (2013).
62. Roth, F. *et al.* *An in situ approach for measuring biogeochemical fluxes in structurally complex benthic communities. Methods in Ecology and Evolution* (2019). doi:10.1111/2041-210X.13151
63. Barott, K. L. & Rohwer, F. L. Unseen players shape benthic competition on coral reefs. *Trends Microbiol.* **20**, 621–628 (2012).
64. Roach, T. N. F. *et al.* Microbial bioenergetics of coral-algal interactions. *PeerJ* **2017**, 1–19 (2017).
65. den Haan, J. *et al.* Nitrogen and phosphorus uptake rates of different species from a coral reef community after a nutrient pulse. *Sci. Rep.* **6**, 28821 (2016).
66. Jessen, C. & Wild, C. Herbivory effects on benthic algal composition and growth on a coral reef flat in the Egyptian Red Sea. *Mar. Ecol. Prog. Ser.* **476**, 9–21 (2013).
67. Wheeler, G. S. Minimal increase in larval and adult performance of the biological control agent *Oxyops vitiosa* when fed *Melaleuca quinquenervia* leaves of different nitrogen levels. *Biol. Control* **26**, 109–116 (2003).
68. Russell, B. D., Thompson, J. A. I., Falkenberg, L. J. & Connell, S. D. Synergistic effects of climate change and local stressors: CO₂ and nutrient-driven change in subtidal rocky habitats. *Glob. Chang. Biol.* **15**, 2153–2162 (2009).
69. Falkenberg, L. J., Russell, B. D. & Connell, S. D. Contrasting resource limitations of marine primary producers: Implications for competitive interactions under enriched CO₂ and nutrient regimes. *Oecologia* **172**, 575–583 (2013).
70. Adams, C., Frantz, J. & Bugbee, B. Macro- and micronutrient-release characteristics of three polymer-coated fertilizers: Theory and measurements. *J. Plant Nutr. Soil Sci.* **176**, 76–88 (2013).
71. Rix, L. *et al.* Reef sponges facilitate the transfer of coral-derived organic matter to their associated fauna via the sponge loop. **589**, 85–96 (2018).
72. Lapointe, B. E., Littler, M. M. & Littler, D. S. Nutrient availability to marine macroalgae in siliciclastic versus carbonate-rich coastal waters. *Estuaries* **15**, 75–82 (1992).
73. Lapointe, B. E. *et al.* Macroalgal blooms on southeast Florida coral reefs: I. Nutrient stoichiometry of the invasive green alga *Codium isthmocladum* in the wider Caribbean indicates nutrient enrichment. *Harmful Algae* **4**, 1092–1105 (2005).
74. R Core Team. R: A Language and Environment for Statistical Computing. (2017).
75. Yamamuro, M., Kayanne, H. & Minagawa, M. Carbon and nitrogen stable isotopes of primary producers in coral reef ecosystems. *Limnol. Oceanogr.* **40**, 617–621 (1995).
76. Rix, L. *et al.* Seasonality in dinitrogen fixation and primary productivity by coral reef framework substrates from the northern Red Sea. *Mar. Ecol. Prog. Ser.* **533**, 79–92 (2015).
77. Tilstra, A. *et al.* Seasonality affects dinitrogen fixation associated with two common macroalgae from a coral reef in the northern Red Sea. *Mar. Ecol. Prog. Ser.* **575**, 69–80 (2017).
78. Carpenter, E. J., Harvey, H. R., Fry, B. & Capone, D. G. Biogeochemical tracers of the marine cyanobacterium *Trichodesmium*. *Deep. Res. I* **44**, 27–38 (1997).

79. Karl, D. *et al.* Dinitrogen fixation in the world's oceans. *Biogeochemistry* **57–58**, 47–98 (2002).
80. Miyajima, T., Suzumura, M., Umezawa, Y. & Koike, I. Microbiological nitrogen transformation in carbonate sediments of a coral-reef lagoon and associated seagrass beds. *Mar. Ecol. Prog. Ser.* **217**, 273–286 (2001).
81. Erler, D. V., Santos, I. R. & Eyre, B. D. Inorganic nitrogen transformations within permeable carbonate sands. *Cont. Shelf Res.* **77**, 69–80 (2014).
82. Rasheed, M., Badran, M. I. & Huettel, M. Particulate matter filtration and seasonal nutrient dynamics in permeable carbonate and silicate sands of the Gulf of Aqaba, Red Sea. *Coral Reefs* **22**, 167–177 (2003).
83. Cook, P. L. M., Veuger, B., Böer, S. & Middelburg, J. J. Effect of nutrient availability on carbon and nitrogen incorporation and flows through benthic algae and bacteria in near-shore sandy sediment. *Aquat. Microb. Ecol.* **49**, 165–180 (2007).
84. Rolff, C. Seasonal variation in $\delta^{13}\text{C}$ and $\delta^{15}\text{N}$ of size-fractionated plankton at a coastal station in the northern Baltic proper. *Mar. Ecol. Prog. Ser.* **203**, 47–65 (2000).
85. O'Reilly, C. M., Hecky, R. E., Cohen, A. S. & Plisnier, P. D. Interpreting stable isotopes in food webs: Recognizing the role of time averaging at different trophic levels. *Limnol. Oceanogr.* **47**, 306–309 (2002).
86. Capone, D. G., Dunham, S. E., Horrigan, S. G. & Duguay, L. E. Microbial nitrogen transformations in unconsolidated coral reef sediments. *Mar. Ecol. Prog. Ser.* **80**, 75–88 (1992).
87. Tribble, G. W., Sansone, F. J. & Smith, S. V. Stoichiometric modeling of carbon diagenesis within a coral reef framework. *Geochim. Cosmochim. Acta* **54**, 2439–2449 (1990).
88. Grover, R., Maguer, J. F., Reynaud-Vaganay, S. & Ferrier-Pagès, C. Uptake of ammonium by the scleractinian coral *Stylophora pistillata*: Effect of feeding, light, and ammonium concentrations. *Limnol. Oceanogr.* **47**, 782–790 (2002).
89. Pernice, M. *et al.* A single-cell view of ammonium assimilation in coral-dinoflagellate symbiosis. *ISME J.* **6**, 1314–1324 (2012).
90. Kopp, C. *et al.* Highly Dynamic Cellular-Level Response of Symbiotic Coral to a Sudden Increase in Environmental Nitrogen. *MBio* **4**, e00052-13 (2013).
91. Tanaka, Y., Grottoli, A. G., Matsui, Y., Suzuki, A. & Sakai, K. Effects of nitrate and phosphate availability on the tissues and carbonate skeleton of scleractinian corals. *Mar. Ecol. Prog. Ser.* **570**, 101–112 (2017).
92. Grover, R., Maguer, J. F., Allemand, D. & Ferrier-Pagès, C. Nitrate uptake in the scleractinian coral *Stylophora pistillata*. *Limnol. Oceanogr.* **48**, 2266–2274 (2003).
93. Godinot, C., Grover, R., Allemand, D. & Ferrier-Pagès, C. High phosphate uptake requirements of the scleractinian coral *Stylophora pistillata*. *J. Exp. Biol.* **214**, 2749–2754 (2011).
94. Millero, F., Huang, F., Zhu, X., Liu, X. & Zhang, J. Z. Adsorption and desorption of phosphate on calcite and aragonite in seawater. *Aquat. Geochemistry* **7**, 33–56 (2001).
95. Cuet, P. *et al.* CNP budgets of a coral-dominated fringing reef at La Réunion, France: Coupling of oceanic phosphate and groundwater nitrate. *Coral Reefs* **30**, 45–55 (2011).
96. Eyre, B. D., Glud, R. N. & Patten, N. Mass coral spawning: A natural large-scale nutrient addition experiment. *Limnol. Oceanogr.* **53**, 997–1013 (2008).
97. Ferrier-Pagès, C., Godinot, C., D'Angelo, C., Wiedenmann, J. & Grover, R. Phosphorus metabolism of reef organisms with algal symbionts. *Ecol. Monogr.* **86**, 262–277 (2016).
98. Tanaka, Y., Miyajima, T., Koike, I., Hayashibara, T. & Ogawa, H. Translocation and conservation

- of organic nitrogen within the coral-zooxanthella symbiotic system of *Acropora pulchra*, as demonstrated by dual isotope-labeling techniques. *J. Exp. Mar. Bio. Ecol.* **336**, 110–119 (2006).
99. Al-Farawati, R., El-Sayed & Rasul. Nitrogen, phosphorus and organic carbon in the Saudi Arabian Red Sea Coastal Waters: behaviour and human impact. in *Oceanographic and Biological Aspects of the Red Sea* (eds. Rasul, N. & Stewart, I.) 89–104 (Springer International Publishing, 2019).
 100. Hecky, R. E., Campbell, P. & Hendzel, L. L. The stoichiometry of carbon, nitrogen, and phosphorus in particulate matter of lakes and oceans. *Limnol. Oceanogr.* **38**, 709–724 (1993).
 101. Hatcher, B. G. & Larkum, A. W. D. An experimental analysis of factors controlling the standing crop of the epilithic algal community on a coral reef. *J. Exp. Mar. Bio. Ecol.* **69**, 61–84 (1983).
 102. McCook, L. J. Macroalgae, nutrients and phase shifts on coral reefs: Scientific issues and management consequences for the Great Barrier Reef. *Coral Reefs* **18**, 357–367 (1999).
 103. Airoidi, L. Roles of disturbance, sediment stress, and substratum retention on spatial dominance in algal turf. *Ecology* **79**, 2759–2770 (1998).
 104. Smith, J. E., Smith, C. M. & Hunter, C. L. An experimental analysis of the effects of herbivory and nutrient enrichment on benthic community dynamics on a Hawaiian reef. *Coral Reefs* **19**, 332–342 (2001).
 105. Vermeij, M. J. A. *et al.* The effects of nutrient enrichment and herbivore abundance on the ability of turf algae to overgrow coral in the Caribbean. *PLoS One* **5**, 1–8 (2010).
 106. Costa, O. S., Leão, Z. M. A. N., Nimmo, M. & Attrill, M. J. Nutrifcation impacts on coral reefs from northern Bahia, Brazil. *Hydrobiologia* **440**, 307–315 (2000).
 107. Gorgula, S. K. & Connell, S. D. Expansive covers of turf-forming algae on human-dominated coast: The relative effects of increasing nutrient and sediment loads. *Mar. Biol.* **145**, 613–619 (2004).
 108. Bednarz, V. N., Naumann, M. S., Niggel, W. & Wild, C. Inorganic nutrient availability affects organic matter fluxes and metabolic activity in the soft coral genus *Xenia*. *J. Exp. Biol.* **215**, 3672–3679 (2012).
 109. Fabricius, K., De'ath, G., McCook, L., Turak, E. & Williams, D. M. B. Changes in algal, coral and fish assemblages along water quality gradients on the inshore Great Barrier Reef. *Mar. Pollut. Bull.* **51**, 384–398 (2005).
 110. Wild, C. *et al.* Degradation and mineralization of coral mucus in reef environments. *Mar. Ecol. Prog. Ser.* **267**, 159–171 (2004).
 111. Yamamoto, M., Kayanne, H. & Yamamuro, M. Characteristics of organic matter in lagoonal sediments from the great barrier reef. *Geochem. J.* **35**, 385–401 (2001).
 112. Haas, A. F. *et al.* Effects of Coral Reef Benthic Primary Producers on Dissolved Organic Carbon and Microbial Activity. *PLoS One* **6**, e27973 (2011).
 113. Cárdenas, A., Meyer, F., Schwieder, H., Wild, C. & Gärdes, A. The formation of aggregates in coral reef waters under elevated concentrations of dissolved inorganic and organic carbon : A mesocosm approach. *Mar. Chem.* **175**, 47–55 (2015).
 114. Ziegler, M., Roder, C. M., Büchel, C. & Voolstra, C. R. Limits to physiological plasticity of the coral *Pocillopora verrucosa* from the central Red Sea. *Coral Reefs* **33**, 1115–1129 (2014).
 115. Stimson, J. The annual cycle of density of zooxanthellae in the tissues of field and laboratory-held *Pocillopora damicornis* (Linnaeus). *J. Exp. Mar. Bio. Ecol.* **214**, 35–48 (1997).
 116. Al-Sofyani, A. A. & Floos, Y. A. M. Effect of temperature on two reef-building corals *Pocillopora damicornis* and *P. verrucosa* in the Red Sea. *Oceanologia* **55**, 917–935 (2013).

117. Ferrier-Pagès, C., Schoelzke, V., Jaubert, J., Muscatine, L. & Hoegh-Guldberg, O. Response of a scleractinian coral, *J. Exp. Mar. Bio. Ecol.* **259**, 249–261 (2001).
118. Rosset, S., Wiedenmann, J., Reed, A. J. & D'Angelo, C. Phosphate deficiency promotes coral bleaching and is reflected by the ultrastructure of symbiotic dinoflagellates. *Mar. Pollut. Bull.* **118**, 180–187 (2017).
119. Fabricius, K. E. Effects of terrestrial runoff on the ecology of corals and coral reefs: Review and synthesis. *Mar. Pollut. Bull.* **50**, 125–146 (2005).
120. Stambler, N., Popper, N., Dubinsky, Z. & Stimson, J. Effects of nutrient enrichment and water motion on the coral *Pocillopora damicornis*. *Pacific Sci.* **45**, 299–307 (1991).
121. Muller-Parker, G., Cook, C. & D'Elia, C. Elemental Composition of the Coral *Pocillopora damicornis* Exposed to Elevated Seawater Ammonium. *Pacific Sci.* **48**, 234–246 (1994).
122. Falkowski, P. P. G., Dubinsky, Z., Muscatine, L. & McCloskey, L. Population Control in Symbiotic Corals. *Bioscience* **43**, 606–611 (1993).
123. Sawall, Y. *et al.* Nutritional status and metabolism of the coral *Stylophora subseriata* along a eutrophication gradient in Spermonde Archipelago (Indonesia). *Coral Reefs* **30**, 841–853 (2011).
124. Ezzat, L., Maguer, J., Grover, R. & Ferrier-pagès, C. Limited phosphorus availability is the Achilles heel of tropical reef corals in a warming ocean. *Nat. Publ. Gr.* 1–11 (2016). doi:10.1038/srep31768
125. Swart, P. K., Saied, A. & Lamb, K. Temporal and spatial variation in the $\delta^{15}\text{N}$ and $\delta^{13}\text{C}$ of coral tissue and zooxanthellae in *Montastraea faveolata* collected from the Florida reef tract. *Limnol. Oceanogr.* **50**, 1049–1058 (2005).
126. Grottoli, A. G., Tchernov, D. & Winters, G. Physiological and biogeochemical responses of super-corals to thermal stress from the northern gulf of Aqaba, Red Sea. *Front. Mar. Sci.* **4**, 1–12 (2017).
127. Wall, C. B., Ritson-Williams, R., Popp, B. N. & Gates, R. D. Spatial variation in the biochemical and isotopic composition of corals during bleaching and recovery. *Limnol. Oceanogr.* **64**, 2011–2028 (2019).
128. Bongiorno, L., Shafir, S., Angel, D. & Rinkevich, B. Survival, growth and gonad development of two hermatypic corals subjected to in situ fish-farm nutrient enrichment. *Mar. Ecol. Prog. Ser.* **253**, 137–144 (2003).
129. Rice, M. M., Ezzat, L. & Burkepile, D. E. Corallivory in the Anthropocene: Interactive Effects of Anthropogenic Stressors and Corallivory on Coral Reefs. *Front. Mar. Sci.* **5**, 1–14 (2019).
130. Morris, L. A., Voolstra, C. R., Quigley, K. M., Bourne, D. G. & Bay, L. K. Nutrient Availability and Metabolism Affect the Stability of Coral–Symbiodiniaceae Symbioses. *Trends Microbiol.* 1–12 (2019). doi:10.1016/j.tim.2019.03.004
131. Rådecker, N., Pogoreutz, C., Voolstra, C. R., Wiedenmann, J. & Wild, C. Nitrogen cycling in corals: The key to understanding holobiont functioning? *Trends Microbiol.* **23**, 490–497 (2015).
132. Carvalho, S., Kürten, B., Krokos, G., Hoteit, I. & Ellis, J. The Red Sea. in *World Seas: An Environmental Evaluation Volume II: The Indian Ocean to the Pacific* (ed. Sheppard, C.) 49–74 (Academic Press, 2019). doi:10.1016/B978-0-08-100853-9.00004-X
133. Burke, L., Reytar, K., Spaulding, M. & Perry, A. *Reefs at Risk*. (World Resources Institute, 2011).
134. Roth, F., Stuhldreier, I., Sánchez-Noguera, C., Morales-Ramírez, T. & Wild, C. Effects of simulated overfishing on the succession of benthic algae and invertebrates in an upwelling-influenced coral reef of Pacific Costa Rica. *J. Exp. Mar. Bio. Ecol.* **468**, 55–66 (2015).
135. Gurney, G. G., Melbourne-Thomas, J., Geronimo, R. C., Aliño, P. M. & Johnson, C. R. Modelling coral reef futures to inform management: Can reducing local-scale stressors conserve reefs under climate change? *PLoS One* **8**, 1–17 (2013).

136. D'Angelo, C. & Wiedenmann, J. Impacts of nutrient enrichment on coral reefs: New perspectives and implications for coastal management and reef survival. *Curr. Opin. Environ. Sustain.* **7**, 82–93 (2014).
137. Robinson, J. P. W., Wilson, S. K. & Graham, N. A. J. Abiotic and biotic controls on coral recovery 16 years after mass bleaching. *Coral Reefs* **38**, 1255–1265 (2019).

Chapter 8

Chapter 8 | In situ eutrophication stimulates dinitrogen fixation, denitrification, and productivity in Red Sea coral reefs

Yusuf C. El-Khaled^{1*}, Florian Roth^{2,3,4}, Arjen Tilstra¹, Nils Rådecker^{2,5}, Denis B. Karcher¹, Benjamin Kürten^{2,6}, Burton H. Jones², Christian R. Woolstra^{2,5}, Christian Wild¹

¹ Marine Ecology Department, Faculty of Biology and Chemistry, University of Bremen, 28359 Bremen, Germany

² Red Sea Research Center, King Abdullah University of Science and Technology (KAUST), 23995 Thuwal, Saudi-Arabia

³ Baltic Sea Centre, Stockholm University, 10691 Stockholm, Sweden

⁴ Faculty of Biological and Environmental Sciences, Tvärminne Zoological Station, University of Helsinki, 00014 Helsinki, Finland

⁵ Department of Biology, University of Konstanz, 78464 Konstanz, Germany

⁶ Jülich Research Centre GmbH, Project Management Jülich, 18069 Rostock, Germany

*corresponding author: yek2012@uni-bremen.de

8.1 | Abstract

Eutrophication (i.e. the increase of (in-) organic nutrients) may affect functioning of coral reefs, but knowledge about the effects on nitrogen (N) cycling and its relationship to productivity within benthic reef communities is scarce. We thus investigated how in situ manipulated eutrophication impacted productivity along with two counteracting N-cycling pathways (dinitrogen (N₂) fixation, denitrification), using a combined acetylene assay. We hypothesised that N₂ fixation would decrease, and denitrification increase in response to eutrophication. N fluxes and productivity (measured as dark and light oxygen fluxes assessed in incubations experiments) were determined for three dominant coral reef functional groups (reef sediments, turf algae, and the scleractinian coral *Pocillopora verrucosa*) after eight weeks of in situ nutrient enrichment in the central Red Sea. Using slow-release fertiliser, we increased the dissolved inorganic N concentration by up to 7-fold compared to ambient concentrations. Experimental nutrient enrichment stimulated both N₂ fixation and denitrification across all functional groups compared by 2- to 7-fold, and 2- to 4-fold, respectively. Productivity doubled in reef sediments and remained stable for turf algae and *P. verrucosa*. Our data therefore suggest that i) turf algae are major N₂-fixers in coral reefs, while denitrification is widespread among all investigated groups; ii) surprisingly and against hypothesis both N₂ fixation and denitrification are involved in processing moderate N eutrophication, and iii) stimulated N₂ fixation and denitrification are not directly influenced by productivity. Our findings underline the importance and ubiquity of microbial N cycling in (Red Sea) coral reefs along with its sensitivity to eutrophication.

Keywords: Nitrogen cycle | Climate change | Pollution | Red Sea | Acetylene reduction assay | Acetylene inhibition assay

A modified version of this chapter has been published in *Marine Ecology Progress Series 645*

<https://doi.org/10.3354/meps13352>

Permission to publish in thesis granted by Ian Steward (Rights and Permission, Inter-Research) on March 16th 2021

8.2 | Introduction

Coastal zones have always attracted humans for various reasons (e.g., resources, transportation and logistics, recreational activities), and migration to coastal cities and areas is increasing¹. Eutrophication is one of many stressors that intensifies congruently to growing coastal populations². Coastal nutrient point-sources, i.e., excessive nutrient loads from (un-) controlled sewage dumping or agricultural fertiliser runoff, play a major role in reshaping nearshore ecosystems such as coral reefs^{3,4}. Coral reefs, however, are usually adapted to low nutrient (i.e., oligotrophic) environments, but paradoxically belong to the most diverse and productive ecosystems on earth⁵ with nitrogen (N) acting as an important factor limiting productivity (reviewed in Lesser et al. (2007))⁶.

Determining the effects of excessive nutrient availability on tropical coral reefs has been part of numerous studies in the last decades displaying beneficial as well as negative effects. It has been demonstrated that an increase in inorganic matter can shift roles of heterotrophy and autotrophy in coral energetics⁷, and that high loads of particulate organic matter do not always negatively impact on the physiology of corals⁸. Furthermore, enhanced heterotrophic feeding on zooplankton can facilitate coral tissue growth and calcification rates⁹, whereas coral starvation can lead to lower photosynthetic activity, congruently with lower lipid and protein concentrations¹⁰. Investigations of long-term nutrient enrichment effects revealed threats on coral reefs on multiple levels, ranging from a higher susceptibility of corals to bleaching and mortality^{11,12}, to negative effects on coral growth and calcification rates^{13,14} or reproductive success^{15,16}. When nutrient availability increases over extended periods, phase shifts from coral-dominated reefs to (macro-) algae-dominated states of a reef are likely to occur (e.g., Graham et al. (2015))¹⁷. Moreover, nutrient enrichment together with other anthropogenic stressors that haven proven to alter N-cycling processes, such as ocean warming¹⁸ or ocean acidification^{19,20}, may result in synergistic effects that ultimately decrease reef resilience and eventually lead to reef degradation or reef losses (e.g., Graham et al. (2015))¹⁷.

For a better understanding of ecosystem functioning in general, and the effects of elevated nutrients on ecosystem functioning in particular, studying N-cycling in coral reefs is of paramount interest. The import of de novo bioavailable N to the system is partly performed by diazotrophs, i.e. microbes capable of fixing atmospheric dinitrogen (N_2) into bioavailable ammonium (NH_4^+). This dinitrogen fixation (hereafter N_2 fixation) is crucial for coral reef ecosystems to maintain the N supply and satisfy N demands^{6,21}. N_2 fixation rates in coral reefs can fluctuate seasonally and with response to variation in environmental conditions²². At the same time, microbial denitrification removes bioavailable N from the ecosystem as it facilitates the reduction of nitrate (NO_3^-) to N_2 and can, thus, be described as a counteracting pathway to N_2 fixation^{23,24}. However, knowledge about denitrification in coral reef environments is scarce. Hypothetically, denitrification is vital to coral reef ecosystem functioning, especially under eutrophic conditions as this process removes excess N from the reef system^{14,25}.

N cycling activity in coral reefs depends on the environmental nutrient availability^{14,22} that can naturally be shaped by upwelling²⁶, terrestrial runoff after rainfalls²⁷ or by anthropogenic sources^{16,28}. As such, N cycling in coral reef environments has the potential to exacerbate or attenuate eutrophication events. However, little

is known about N-cycling in coral reefs under elevated nutrient availability. We hypothesised significant responses of N₂ fixation and denitrification rates to eutrophication²⁹. In case of N₂ fixation, we expect decreasing activity in eutrophic environments as hypothesised before³⁰. Koop et al. (2001)¹⁴ were able to demonstrate this in coral reef-associated sediments of the Great Barrier Reef (GBR). This phenomenon was attributed to the idea that bioavailable N, e.g. in the form of NH₄⁺ or NO₃⁻, offers a more cost-efficient, alternative source of N to an organism^{31,32}. Furthermore, the presence of fixed N potentially inhibits the enzyme (nitrogenase) activity responsible for N₂ fixation^{32,33}. For denitrification, we expected an increase with increasing nutrient availability in accordance to other studies^{25,29} to subsequently sustain favourable N limitation¹¹. Overall, we anticipate a dynamic interplay of N₂ fixation and denitrification which counterbalances changes in environmental dissolved inorganic nitrogen (hereafter DIN) availability.

We here aimed to assess the effects of elevated nutrient availability on N cycling in a coral reef. We used an eight-week in situ nutrient manipulation experiment in natural reef communities in the oligotrophic central Red Sea to investigate the effects of eutrophication on several metabolic processes (N₂ fixation, denitrification, respiration, and photosynthesis) in a comparative framework with three major functional groups (scleractinian coral, filamentous turf algae, and carbonate reef sediments).

8.3 | Methods

Experimental Design

The in situ manipulation experiment was conducted from late January until late March 2018 in a semi-exposed area of the Abu Shosha reef in the Jeddah Region (22° 18' 15" N, 39° 02' 56" E) on the west coast of Saudi Arabia in the central Red Sea. Eight distinct (i.e., > 5 m apart from each other) natural reef communities at a water depth of 5 – 6 m were chosen. Four slow-release fertiliser tubes (Osmocote Plus (15-9-12)) were attached with pins around each reef community (Fig. 8.1). Osmocote Plus fertiliser supplied various macronutrients non-stop (15 % total N, 9 % available phosphate (P), 12 % soluble potash, a detailed list of released micronutrients can be found in Table S8.1) from the 1st day of fertilisation under local temperature regimes³⁴, and has been successfully utilised in previous eutrophication studies^{35,36}. As nutrients tend to leach out during the first weeks³⁴ and to reduce resulting bias, fertiliser pins were renewed every two weeks to ensure continuous nutrient inputs. To account for dilution effects with surrounding waters, water samples from different distances to the fertiliser were taken every second week to quantify nutrient concentrations. Specimens of target organisms and substrates were taken from close radius (max. 25 cm) from the fertiliser. The eutrophication phase lasted for eight weeks and specimens of the fertilised communities (hereafter “eutrophied communities”) were taken at the end of the manipulation phase. Specimens from the surrounding, non-fertilised reef communities (hereafter “control communities”) were taken for comparative analysis at the same time.



Figure 8.1 | Manipulated in situ community. Four pins with attached fertiliser bags. Photo: Florian Roth.

Collection and Maintenance

We tested three of the most dominant biotic and abiotic functional groups of benthic reef communities of the Central Red Sea (carbonaceous reef sediments, filamentous turf algae, and the scleractinian coral – *Pocillopora verrucosa*). These three groups contribute to more than 70 % of the benthic community composition of the sampled reef³⁷. Sediments were collected using a Petri dish (material: polystyrene; diameter: 5.5 cm, height: 1.4 cm) that was pushed carefully into the sediment. Sediments were then fixed to the dish from underneath so that upper sediment “cores” with a max. sediment depth of 14 mm were sampled. Turf algae were defined as dead coral fragments of approx. 10 cm length, overgrown with dense and flat (< 2 cm in height) assemblages of filamentous algae of different species, including small individuals of macroalgae and cyanobacteria. Examples from Northern Red Sea studies show that turf algae account for the highest fraction (up to 90 %) of benthic algal cover³⁸. Fragments were collected with hammer and chisel. *P. verrucosa* fragments were approx. 10 cm long and were collected with the same tools from different coral colonies to ensure genetic variability. Coral colonies had a minimum of 8 – 10 m distance between each other. All fragments and Petri dishes containing reef sediment samples were immediately transferred to recirculation aquaria on the boat after sampling (n = 4 from eutrophied communities into aquaria each filled with 10 L of 5 μ M NO₃ enriched seawater; n = 5 from control communities into ambient seawater; NO₃ enrichment consisted of previously prepared NaNO₃ stock solution, prepared with MilliQ water and NaNO₃, \geq 99.0 %, Sigma-Aldrich) and kept at ambient water temperature and light conditions until the experimental incubations started within 3 h after sampling.

Environmental Parameters

Key environmental parameters were assessed every second week throughout the total manipulation period of eight weeks. Details for analytical approaches are described in Roth et al. (2018)³⁷. Briefly, seawater temperature was measured continuously with data loggers (Onset HOBO Water Temperature Pro v2 Data Logger – U22-001; accuracy: ± 0.021 °C). Seawater samples for assessing concentrations of NO_3^- , nitrite (NO_2^-), and phosphorus (PO_4^{3-}) were taken from various distances from fertiliser pins (i.e., directly at the fertiliser pins, 25 cm from inside the communities, > 200 cm outside the communities serving as controls). Water samples were filtered immediately on the boat (Isopore™ membrane filters, 0.2 μm GTTP) and the filtrate was stored at 4 °C in the dark until frozen at -50 °C in the lab within 3 h after collection. Nutrient concentrations were determined using a continuous flow analyser (AA3, HR, SEAL), following colourimetric standard methods³⁹. Limits of quantification (LOQ) for NO_3^- , NO_2^- and PO_4^{3-} were 0.084 $\mu\text{mol L}^{-1}$, 0.011 $\mu\text{mol L}^{-1}$, and 0.043 $\mu\text{mol L}^{-1}$ respectively. From these seawater samples, 5 mL subsamples were taken for NH_4^+ determination using the ortho-phthaldialdehyde (OPA) method^{40,41}. Samples were filtered into separate acid-washed centrifuge tubes, and 1.2 mL OPA solution was added. Samples were then stored for > 4 h in the dark. NH_4^+ was determined fluorometrically within 8 h (Trilogy® Laboratory Fluorometer, Turner Designs Inc.). The LOQ for NH_4^+ was 0.094 $\mu\text{mol L}^{-1}$. NO_3^- , NO_2^- and NH_4^+ were measured in combination, termed DIN, and presented in [mean \pm standard error of mean $\mu\text{M N}$] hereafter.

Primary Production, Dinitrogen Fixation and Denitrification Measurements

Incubations were conducted ex situ and < 3 h after sample collection. For O_2 flux measurements, incubation chambers (1 L volume) were filled exclusively with ambient seawater collected the same day ($n = 5$, with specimens from control communities), and four incubation chambers were filled with seawater and amended with 5 μM NO_3^- to provide and keep eutrophic conditions ($n = 4$, with specimens from eutrophic communities). Additionally, two chambers without specimens (one filled with seawater, one filled with 5 μM NO_3^- enriched seawater) served as controls to correct for planktonic background metabolism. All chambers were sealed gastight and without any air enclosure. During the incubations, the incubation chambers were placed in a tempered water bath and constantly stirred (500 rpm) to ensure stable measurement conditions (27 °C). A 2 h light (photon flux of ~ 200 μM quanta $\text{m}^{-2} \text{s}^{-1}$) incubation was followed by a 2 h dark incubation with fresh ambient and nutrient-enriched seawater respectively. O_2 levels were measured immediately before starting the respective incubations and after 2 h using a WTW Multi 3430 which was equipped with a WTW DFO 925 oxygen sensor. Measured values from dark and light incubations were used to calculate dark respiration (hereafter R_{dark}) and net primary production (hereafter P_{net}): O_2 start concentrations were subtracted from end concentrations and results were then normalised to incubation time. In the next step, O_2 fluxes were corrected for the seawater control signal, related to incubation volume and normalised to the surface area of the organisms/substrates. Surface areas for turf algae fragments and *P. verrucosa* were calculated using cloud-based 3D models of samples (Autodesk Remake v19.1.1.2)⁴². Surface areas of sediments were mathematically calculated (Surface area = $\pi * \text{radius}^2$) as Petri

dishes were used for sampling sediment cores. Subsequently, gross primary production (hereafter P_{gross}) rates were calculated according to $P_{\text{gross}} = P_{\text{net}} - |R_{\text{dark}}|$.

N_2 fixation and denitrification incubations were performed using a COmbined Blockage/Reduction acetylene Assay (COBRA) with the same specimens 3 to 4 h after the O_2 flux measurements. The incubations were performed as described previously in El-Khaled et al. (2019)⁴³. Briefly, all COBRA incubations were conducted in gas-tight 1 L glass chambers, each filled with 800 mL of nutrient-enriched seawater (5 μM NO_3^-) and 200 mL headspace. Nutrient-enriched seawater was used in all treatments, as acetylene inhibits the production of NO_3^- in the nitrification pathway⁴⁴. As NO_3^- serves as a substrate for denitrification, the inhibition of nitrification potentially results in an underestimation of denitrification rates. To compensate for that, and to provide an incubation environment that is similar to eutrophic reef communities, NO_3^- was added to the incubation water to preclude substrate limitation^{29,45}. Both incubation water and headspace were 10 % acetylene enriched. Acetylene a) leads to a preferential reduction of acetylene to ethylene (hereafter C_2H_4) instead of N_2 to NH_4^+ by the nitrogenase enzyme⁴⁶, and b) inhibits denitrification at the nitrous oxide (N_2O) stage leading to an evolution of nitrous oxide⁴⁷. Each chamber contained a single sample (scleractinian coral fragment, turf algae, or reef sediment core). Four or five respectively, replicate samples were incubated, additional two chambers without specimens served as controls to correct for planktonic background metabolism. During the 24 h incubations, chambers were submersed in a tempered water bath and stirred continuously (500 rpm) to ensure stable physical conditions and homogenous environment (27 °C, 12:12 h dark/light cycle, photon flux of $\sim 200 \mu\text{M}$ quanta $\text{m}^{-2} \text{s}^{-1}$). Samples were taken at the beginning (t_0) and after 24 h (t_{24}). Both N_2O (for denitrification quantification) and C_2H_4 (for N_2 fixation quantification) concentrations were quantified by gas chromatography and helium pulsed discharge detector (Agilent 7890B GC system with HP-Plot/Q column, lower detection limits for both target gases were 0.3 ppm). Gas fluxes were corrected for the seawater control signal and normalised to the surface area of the organisms/substrates. C_2H_4 fluxes were converted into corresponding N_2 fluxes assuming a theoretical molar ratio of $\text{C}_2\text{H}_4:\text{N}_2 = 4$, which has been used in previous studies in similar environments^{22,48}.

Statistical Analysis

The dataset was analysed using non-parametric permutational multivariate analysis of variance (PERMANOVA) using PRIMER-E version 6 software⁴⁹ with the PERMANOVA+ add on⁵⁰. To test for differences in N_2 fixation, denitrification and O_2 fluxes between functional groups and eutrophied and control communities, 2-factorial PERMANOVAs were performed (factors were “functional group” and “control/eutrophied reef community”), based on Bray-Curtis similarities of square-root transformed data. Therefore, Type III (partial) sum of squares was used with unrestricted permutation of raw data (999 permutations), and PERMANOVA pairwise tests with parallel Monte Carlo tests were carried out when significant differences occurred. To identify correlations between N_2 fix, denitrification, P_{gross} , P_{net} and R_{dark} , a Spearman-Rank-Order correlation was performed using SigmaPlot (SigmaPlot for Windows version 12.0).

8.4 | Results

Environmental Parameters

Water temperature increased from 24.8 to 28.1 °C during the in situ manipulation period of eight weeks. Background DIN concentrations remained stable throughout the experiment at 0.40 ± 0.03 . When nutrient manipulation was initiated, DIN concentrations increased up to seven-fold (measured directly at the communities) compared to background values (Fig. 8.2). At the same time, PO_4^{3-} remained stable. For a detailed summary of nutrient concentrations at the centre of eutrophied communities, directly at the fertiliser pins and in surrounding waters, we refer to Table S7.1.

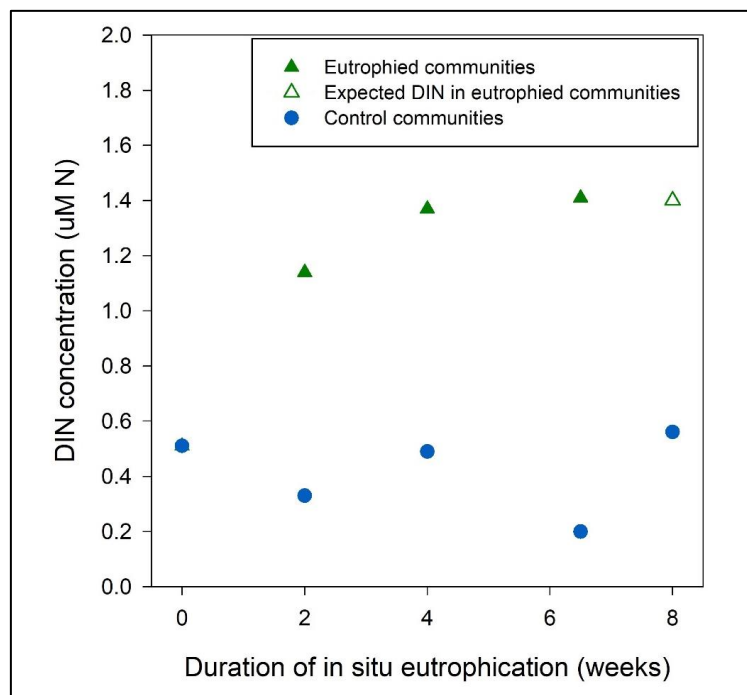


Figure 8.2 | Dissolved inorganic nitrogen (DIN) concentrations in control (blue) and eutrophied communities (green). Due to technical issues, no DIN concentrations were determined in eutrophied communities after eight weeks. Expected DIN concentrations, based on previous measurements are displayed here.

Oxygen Fluxes

In both eutrophied and control communities (Fig. 8.3), reef sediments showed lowest P_{gross} being three to four times lower than in turf algae and five to six times lower than in *Pocillopora verrucosa*. A significant increase in P_{gross} between control and eutrophied reef communities was only detected for reef sediments (Table S8.2).

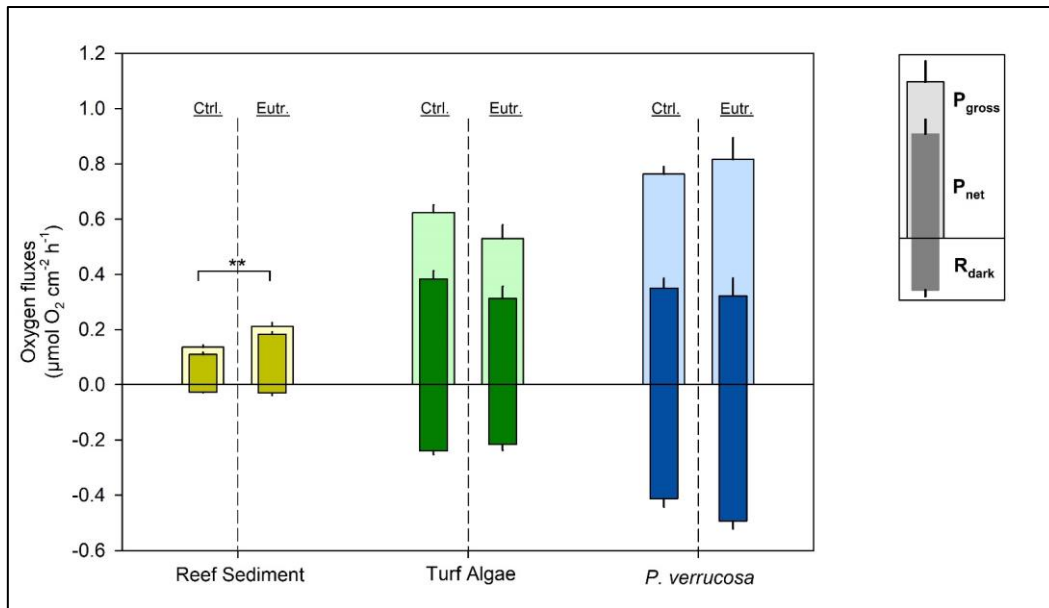


Figure 8.3 | Respiration (R_{dark}), net photosynthesis (P_{net}) and gross photosynthesis (P_{gross}) of three functional groups from control (Ctrl.; $n = 5$) and eutrophied (Eutr.; $n = 4$) communities. Asterisks indicate significant differences in P_{gross} (** = $p < 0.01$). Data are presented in mean of replicates \pm standard error of mean.

Dinitrogen Fixation and Denitrification

Concentrations for both C_2H_4 and N_2O control incubations over the incubation time of 24 h were stable (Fig. S8.1). In control communities, turf algae showed the highest N_2 fixation activity ($13.68 \pm 1.42 \text{ nmol N}_2 \text{ cm}^{-2} \text{ d}^{-1}$) among the investigated functional groups, with N_2 fixation rates being 13 times higher than of sediments (Table S8.3) and 274 times higher than the investigated scleractinian coral (Fig. 8.4; Table S8.3). Denitrification rates did not differ significantly between investigated groups due to high variation, with *P. verrucosa* showing denitrification rates 2 times lower than turf algae and 2 to 3 times lower than reef sediments.

In eutrophied communities, N_2 fixation rates of turf algae ($27.12 \pm 1.57 \text{ nmol N}_2 \text{ cm}^{-2} \text{ d}^{-1}$) were 3 times higher than those of sediments (Table S8.3) and 2 orders of magnitude higher than those of *P. verrucosa* (Table S8.3). For sediments in manipulated reef communities, significantly higher N_2 fixation rates were observed compared to control communities (Table S8.3), being 8-fold higher than without nutrient manipulation. Similar patterns of increasing N_2 fixation activity were observed for turf algae and the scleractinian coral of eutrophic communities, though not statistically significant. In eutrophied communities, no statistical difference in denitrification rates between functional groups was observed. However, compared to untreated specimens, denitrification rates in functional groups from eutrophied reef communities increased significantly for turf algae (0.39 ± 0.03 ; Table S8.2). Denitrification rates increased, though not significantly (Table S8.2), 3-fold in sediments (0.49 ± 0.08) and 5-fold for *P. verrucosa* (0.20 ± 0.06) compared to control communities.

We observed positive correlations between N_2 fixation and denitrification (Table 8.1; correlation coefficient $R_s = 0.480$, $p = 0.012$), and between N_2 fixation and R_{dark} (Table 8.1; $R_s = 0.454$, $p = 0.018$), and P_{net} and P_{gross} (Table 8.1; $R_s = 0.843$, $p < 0.001$). Negative correlations were identified for R_{dark} and P_{net} (Table 8.1; $R_s = -0.621$, $p < 0.001$), along with R_{dark} and P_{gross} (Table 8.1; $R_s = -0.891$, $p < 0.001$).

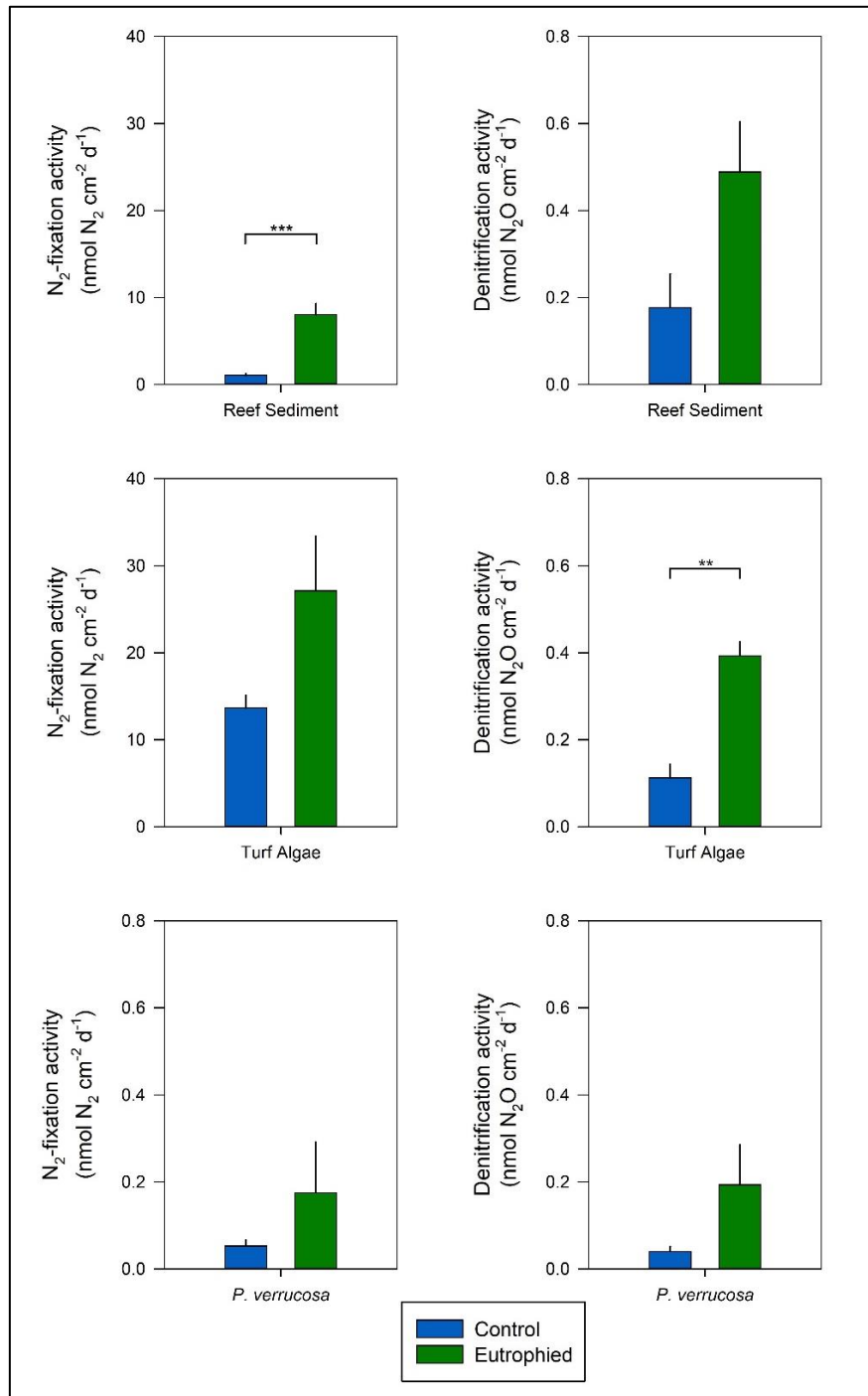


Figure 8.4 | N_2 fixation (left figures) and denitrification (right figures) activity of investigated functional groups from control (blue bars; $n = 5$) and eutrophied (green; $n = 4$) communities. Asterisks indicate significant differences (** = $p < 0.01$, *** = $p < 0.001$). Data are presented in mean of replicates \pm standard error of mean. Note different scale for denitrification and N_2 fixation and for N_2 fixation in scleractinian coral.

Table 8.1 | Spearman-Rank-Order correlation coefficients between N₂ fixation, denitrification, respiration (R_{dark}), net primary production (P_{net}) and gross primary production (P_{gross}). Pairs of variables with positive correlation coefficients and significant p values < 0.05 tend to increase together, for pairs with negative correlation coefficient and p values < 0.05, one variable tends to decrease while the other increases. * p < 0.05. *** p < 0.001.

	Denitrification	R _{dark}	P _{net}	P _{gross}
N ₂ fixation	0.480*	0.454*	0.116	-0.311
Denitrification		0.332	-0.221	-0.256
R _{dark}			-0.621***	-0.891***
P _{net}				0.843***

8.5 | Discussion

Anthropogenically induced nutrient inputs to coral reefs have multi-level impacts^{12,51}. This study extends previous work of Koop et al. (2001)¹⁴ and Capone et al. (1992)⁵² by showing that increasing DIN concentrations alter essential biochemical processes such as primary productivity, N₂ fixation and denitrification in coral reef communities.

Environmental Parameters

As background DIN concentrations remained stable throughout the experiment (Fig. 8.2), we are confident that further pulses of nutrient inputs, e.g., through terrestrial runoffs, were not present. DIN concentrations in experimentally nutrient-enriched communities constantly exceeded concentrations of control communities and were up to 7-fold higher. Compared to other studies, in which manipulative eutrophication was performed^{14,53}, DIN concentrations in eutrophied communities of the current experiments were about 4 to 39 times lower and reflect a more realistic ecological scenario in the context of the oligotrophic Red Sea^{54,55}. We here simulated eutrophication in a season in which DIN concentrations are usually low³⁷. The manipulation can, thus, be considered as an unnaturally appearing moderate eutrophication event simulating nutrient inputs in the Red Sea from point-sources such as aquaculture¹⁶ or urban wastewater²⁸. Still, eutrophied communities of the present study experienced DIN concentrations that were higher than the “eutrophication thresholds” of ~1.0 μM suggested by Lapointe (1997)³, which was also referred to in a previous study in the Red Sea⁵⁶, confirming a successful enrichment over the eight week manipulation period.

Dinitrogen Fixation and Denitrification under Elevated Nutrients

Results of the study showed increasing N₂ fixation and denitrification in all functional groups in response to higher nutrient availability compared to control communities. High variability caused a lack of statistical significances which could be explained by low replication (n = 4 or n = 5, resp.). Descriptive trends for increasing N₂ fixation and denitrification were homogenous for all functional groups of eutrophied communities, and are referred to hereafter when discussed. Potentially, high variability could be counteracted by higher replication. For N₂ fixation, these findings contradict our expectations and

observations from previous studies that found reduced N_2 fixation activities under high DIN availability in coral reef-associated sediments^{14,32}. For denitrification, this is in line with other studies that have demonstrated increased denitrification activities in coral reef-associated sediments under elevated nutrient availability^{14,52}.

Theoretically, an energetically more cost-efficient alternative to N_2 fixation is the assimilation of N (in the form of NO_3^- and/or NH_4^+), which was provided by performed in situ manipulation^{31,32}. As a result, we expected a lower N_2 fixation activity. However, a stimulating effect on N_2 fixation in response to increased DIN in surrounding waters was observed. Generally, the activity of diazotrophs is inhibited by elevated N availability, as shown in mesotrophic or eutrophic lakes⁵⁷, sediments in bays²⁹, seagrass roots in an estuary⁵⁸ and in agricultural crops⁵⁹. However, the role of nutrients on N_2 fixation remains arguable, as there is also continued N_2 fixation activity in response to elevated DIN concentrations of up to $30 \mu M NO_3^-$ ³². Even stimulating effects by providing N have been observed⁶⁰, likely explained by the added form of combined N (Chloramphenicol) and the time of day when respective incubations were initiated (afternoon).

The converse response of N_2 fixation to elevated N concentrations reported by many studies highlights that N-cycling processes are impacted by multiple environmental factors. For example, in general, both N cycling processes are performed in anaerobic milieus: elevated O_2 concentrations can result in a depression of nitrogenase activity and subsequently in lower N_2 fixation activity⁶¹; likewise, denitrification is mediated by anaerobic bacteria⁶² and thus also depends (besides other factors) on low O_2 availability⁶³. Therefore, we tested whether O_2 concentrations explained the changes in both N cycling pathways⁶⁴. However, the lack of a correlation between N cycling pathways and P_{net} and/or P_{gross} excluded O_2 as a potential driver for both N_2 fixation and denitrification activity. We, thus, hypothesise that both processes may be spatially or temporally separated from O_2 evolution in reef sediments, turf algae and *Pocillopora verrucosa*⁶⁵. A temporal separation in hard corals can occur due to heavily varying O_2 concentrations within boundary layers, ranging from super-saturation during daylight to anoxia at night, caused by metabolic processes of the coral host and Symbiodiniaceae⁶⁶. Especially these alternating changes from anaerobic to aerobic conditions can even fuel denitrification, as nitrification, i.e. the oxidation from NH_4^+ to NO_2^- and NO_3^- , is stimulated by the presence of O_2 ⁶⁷, subsequently resulting in the formation of NO_3^- which serves as a substrate for denitrification⁴⁵. Alternatively, increased N_2 fixation and denitrification in all groups indicate that the involved N-cycling prokaryotes are capable of performing N_2 fixation and denitrification in the presence of O_2 ²⁴. From this, we conclude that N_2 fixation and denitrification activities were not directly altered by the presence of O_2 .

Besides an oxic-anoxic environment, the availability of organic C (hereafter C_{org}) can be decisive for diazotrophs and denitrifiers, as it poses as an important energy source^{68,69}. C_{org} can be acquired via the uptake from the water column⁷⁰, or, in coral holobionts, it is translocated by C-rich photosynthates from symbionts²⁵.

We here report elevated P_{gross} activity in reef sediments of eutrophied communities compared to the control, suggesting increased C_{org} in reef sediments, which was potentially caused by higher photosynthetic rates of

epilithic algae on the sediment as described by Cook et al. (2007)⁷¹. Additionally, the export of C_{org} from neighbouring turf algal assemblages in the form of dissolved organic carbon (hereafter DOC)⁷², with a subsequent DOC uptake by reef sediments⁷³, potentially provides sufficient C_{org} as an energy source leading to increasing N_2 fixation activities. We thus conclude, that even though N of the fertiliser pins was not taken up by reef sediments directly⁷⁴, an indirect effect via the interplay with other functional groups lead to a stimulation of N_2 fixation. This, along with findings of a related study⁷⁴ indicates that reef sediments and their associated microbial community were not N-limited.

For turf algae, denitrification rates measured in eutrophied communities were significantly higher than those from control communities. Similarly, N_2 fixation was increased in turf algae from eutrophied communities. Our data reveal no changes in P_{gross} , P_{net} and R_{dark} in turf algae from eutrophied communities compared to controls; thus, no further (direct) source of energy was provided for N cycling processes. Turf algae can, however, be highly flexible in acquiring N from different sources. For example, N_2 fixation in turf algae was highest among all measured functional groups, thus, this process contributed considerably to satisfy N demands in control communities^{48,75}. Shifts to a preferable uptake of allochthonous N in eutrophied communities⁷⁴ were detected, emphasising the turf algae's flexibility, and underlining their role as opportunists efficiently taking up environmentally offered N²⁷. We support the idea of turf algae assemblages being N-limited and benefiting from increased DIN concentrations. In this context, the ability to take up N fast²⁷, as well as assimilate and process N compounds can subsequently result in rapid takeover of bare substrates^{35,37}, which underlines the competitiveness of turf algae under elevated nutrient concentrations⁷⁶. Thus, an assumed incorporation and processing of N can ultimately enhance microbial growth as assimilates can be stored or used for metabolic processes⁷⁷. We suggest a continuously increasing abundance of diazotrophs⁷⁸ and likely denitrifiers, which could explain the increased N_2 fixation and denitrification activities, although microbial communities may vary and respond strongly to environmental changes.

In *P. verrucosa*, we observed increasing N_2 fixation and denitrification rates in eutrophied communities compared to controls. Stimulated N_2 fixation by elevated DIN concentrations contradicts expected patterns. Potentially, longer experiments (36 months)¹² and/or longer experiments mimicking a more severe eutrophication event (12 months, $36.2 \mu\text{M NH}_4^+$)¹⁴ could lead to suppressed N_2 fixation rates in coral holobionts. This underlines that elevated nutrient concentrations not necessarily negatively impact coral holobionts under certain conditions. Indeed, Atkinson et al. (1995)⁷⁹ demonstrated that hard corals can flourish across a wide range of nutrients without showing signs of stress. Moreover, Bongiorni et al. (2003)⁸⁰ showed that increased nutrient availability can promote coral growth. Thus, we speculate that nutrient enrichment (i.e., eutrophication) may not always negatively impact scleractinian corals^{81,82}. Additionally, it has been demonstrated that *P. verrucosa* harbours a stable, rather inflexible microbial composition⁸³. This ultimately questions whether the N_2 fixation pathway is continually facultative as previously assumed²⁵ or if it can be considered obligate to some extent under certain conditions, a N_2 fixation strategy that has been observed in terrestrial ecosystems⁸⁴. Moreover, stimulated denitrification and N_2 -fixation activity through

increased DIN concentrations suggest that both denitrification and N₂ fixation may potentially be carried out – at least to a certain degree – by the same microbes, as previously postulated for seagrass associated bacteria^{85,86}. Furthermore, we assume a shift from originally N^{87–89} towards P limitation¹¹ and/or other micronutrients^{20,51} in *P. verrucosa* from treated communities. This is likely occurring when excess inorganic N is available¹¹. We here utilised fertiliser bags for manipulation that also contained P. Although, P concentrations were increased at the fertiliser pins directly (Table S7.1), the role of P in our study remains speculative, as no increase inside the eutrophied communities was observed. This can be explained either by a) an immediate uptake by benthic and pelagic organisms^{90,91} as P is considered crucial⁹² and limiting^{89,93} for primary productivity; or b) a discontinuous P supply from the fertiliser due solubility and quick leaching. By all means, N₂ fixation is often limited by micronutrients²⁰, so that even minor changes in their availability may result in N₂-fix stimulation, as reported for many marine and limnetic systems⁹⁴. The assessment of P enrichment effects on corals reefs by D'Angelo & Wiedenmann (2014)⁵¹ supports this hypothesis, as they describe the complex dimension of a rapid P utilisation by N-fixing *Trichodesmium* transforming high P levels into P-depleted conditions.

Ecological Implications

This the first study showing that microbial N cycling in tropical coral reef communities may not provide an effective relief and may even exacerbate anthropogenic eutrophication due to stimulated N₂ fixation. We further posit that N₂-fixers are rather inflexible to respond to anthropogenic N inputs (i.e., increasing N inputs to coastal ecosystems³ under certain conditions. Extrapolating these findings in the light of climate change, we suggest that microbial N cycling may contribute to N oversupply and thereby increases the likelihood of phase shifts from a coral-dominated to an algae-dominated reef⁴.

Released nutrients from the fertiliser pins added on a low baseline, even though final DIN concentrations did not exceed natural occurring DIN fluctuations³⁷. Thus, the observed N₂ fixation and denitrification stimulation in the present study conceivably occur due to the inflexibility to respond to anthropogenically induced DIN changes, even though the capacity to react to natural DIN inconstancies has been demonstrated before^{22,48}. Additionally, we suspect that specific DIN thresholds, which regulate the activity of N₂ fixation and subsequently also of denitrification, have not been exceeded in the present study.

Moreover, denitrification is only one mechanism within the N cycle that can relieve coral reef ecosystems from excessive N. Further processes, such as anaerobic ammonium oxidation (ANAMMOX) transform fixed ammonium into elemental N₂, thereby removing bioavailable N from the system. ANAMMOX occurs in many marine environments^{95,96} and has been detected in coral reef-associated sponges⁹⁷. Likely, it also appears in coral holobionts²⁵, for which the role of ANAMMOX in coral reefs needs to be targeted in future studies.

Synoptically, future research should, thus, aim to a) address the effects of severe eutrophication on N₂ fixation and denitrification in coral reef communities and by that identifying DIN thresholds by which N₂-

fix is suppressed; b) detect and quantify the interaction between N_2 fixation and denitrification with other N cycling pathways (i.e., nitrification and ANAMMOX) and c) identify a coral reef community-wide N_2 fixation and denitrification budget under ambient and stressed scenarios, precisely because the role of symbiotic and planktonic diazotrophs providing fixed N in bleached corals is still under debate^{93,98}.

8.6 | Acknowledgements

This work was funded by the German Research Association (DFG Project: Wi 2677/9-1) to CW and KAUST baseline funding to BHJ and CRV. We are thankful to Rüdiger Willhaus for his expertise in graph visualisation, and to Najeh Kharbatia for technical support.

8.7 | References

1. Neumann, B., Vafeidis, A. T., Zimmermann, J. & Nicholls, R. J. Future Coastal Population Growth and Exposure to Sea-Level Rise and Coastal Flooding - A Global Assessment. *PLoS One* e0118571 (2015). doi:10.1371/journal.pone.0118571
2. Burke, L., Reytar, K., Spaulding, M. & Perry, A. *Reefs at Risk*. (World Resources Institute, 2011).
3. Lapointe, B. E. Nutrient thresholds for bottom-up control of macroalgal blooms on coral reefs in Jamaica and southeast Florida. *Limnol. Oceanogr.* **42**, 1119–1131 (1997).
4. McManus, J. W. & Polsenberg, J. F. Coral-algal phase shifts on coral reefs: Ecological and environmental aspects. *Prog. Oceanogr.* **60**, 263–279 (2004).
5. Odum, H. T. & Odum, E. P. Trophic Structure and Productivity of a Windward Coral Reef Community on Eniwetok Atoll. *Ecol. Monogr.* **25**, 291–320 (1955).
6. Lesser, M. P. *et al.* Nitrogen fixation by symbiotic cyanobacteria provides a source of nitrogen for the scleractinian coral *Montastraea cavernosa*. *Mar. Ecol. Prog. Ser.* **346**, 143–152 (2007).
7. Anthony, K. R. N. & Fabricius, K. E. Shifting roles of heterotrophy and autotrophy in coral energetics under varying turbidity. *J. Exp. Mar. Bio. Ecol.* **252**, 221–253 (2000).
8. Anthony, K. R. N. Enhanced energy status of corals on coastal, high-turbidity reefs. *Mar. Ecol. Prog. Ser.* **319**, 111–116 (2006).
9. Ferrier-Pagès, C., Witting, J., Tambutté, E. & Sebens, K. P. Effect of natural zooplankton feeding on the tissue and skeletal growth of the scleractinian coral *Stylophora pistillata*. *Coral Reefs* **22**, 229–240 (2003).
10. Borell, E. M., Yuliantri, A. R., Bischof, K. & Richter, C. The effect of heterotrophy on photosynthesis and tissue composition of two scleractinian corals under elevated temperature. *J. Exp. Mar. Bio. Ecol.* **364**, 116–123 (2008).
11. Wiedenmann, J. *et al.* Nutrient enrichment can increase the susceptibility of reef corals to bleaching. *Nat. Clim. Chang.* **3**, 160–164 (2013).
12. Vega Thurber, R. L. *et al.* Chronic nutrient enrichment increases prevalence and severity of coral disease and bleaching. *Glob. Chang. Biol.* **20**, 544–554 (2014).
13. Ferrier-Pagès, C., Gattuso, J. P., Dallot, S. & Jaubert, J. Effect of nutrient enrichment on growth and photosynthesis of the zooxanthellate coral *Stylophora pistillata*. *Coral Reefs* **19**, 103–113 (2000).
14. Koop, K. *et al.* ENCORE: The effect of nutrient enrichment on coral reefs. Synthesis of results and conclusions. *Mar. Pollut. Bull.* **42**, 91–120 (2001).
15. Harrison, L. & Ward, S. Elevated levels of nitrogen and phosphorus reduce fertilisation success of gametes from scleractinian reef corals. *Mar. Biol.* **139**, 1057–1068 (2001).
16. Loya, Y., Lubinevsky, H., Rosenfeld, M. & Kramarsky-Winter, E. Nutrient enrichment caused by in situ fish farms at Eilat, Red Sea is detrimental to coral reproduction. *Mar. Pollut. Bull.* **49**, 344–353 (2004).
17. Graham, N. A. J., Jennings, S., MacNeil, M. A., Mouillot, D. & Wilson, S. K. Predicting climate-driven regime shifts versus rebound potential in coral reefs. *Nature* **518**, 94–97 (2015).
18. Hughes, T. P. *et al.* Spatial and temporal patterns of mass bleaching of corals in the Anthropocene. *Science (80-)*. **359**, 80–83 (2018).
19. Rådecker, N., Meyer, F. W., Bednarz, V. N., Cardini, U. & Wild, C. Ocean acidification rapidly reduces dinitrogen fixation associated with the hermatypic coral *Seriatopora hystrix*. *Mar. Ecol. Prog. Ser.* **511**, 297–302 (2014).
20. Luo, Y. W. *et al.* Reduced nitrogenase efficiency dominates response of the globally important

- nitrogen fixer *Trichodesmium* to ocean acidification. *Nat. Commun.* **10**, 1521 (2019).
21. Benavides, M. *et al.* Diazotrophs: a non-negligible source of nitrogen for the tropical coral *Sylophora pistillata*. *J. Exp. Biol.* **219**, 2608–2612 (2016).
 22. Cardini, U. *et al.* Budget of Primary Production and Dinitrogen Fixation in a Highly Seasonal Red Sea Coral Reef. *Ecosystems* **19**, 771–785 (2016).
 23. Vitousek, P. M. *et al.* Human alteration of the global nitrogen cycle: sources and consequences. *Ecol. Appl.* **7**, 737–750 (1997).
 24. Silvennoinen, H., Liikanen, A., Torssonen, J., Stange, C. F. & Martikainen, P. J. Denitrification and N₂O effluxes in the Bothnian Bay (northern Baltic Sea) river sediments as affected by temperature under different oxygen concentrations. *Biogeochemistry* **88**, 63–72 (2008).
 25. Rådecker, N., Pogoreutz, C., Voolstra, C. R., Wiedenmann, J. & Wild, C. Nitrogen cycling in corals: The key to understanding holobiont functioning? *Trends Microbiol.* **23**, 490–497 (2015).
 26. Radice, V. Z., Hoegh-Guldberg, O., Fry, B., Fox, M. D. & Dove, S. G. Upwelling as the major source of nitrogen for shallow and deep reef-building corals across an oceanic atoll system. *Funct. Ecol.* **33**, 1120–1134 (2019).
 27. den Haan, J. *et al.* Nitrogen and phosphorus uptake rates of different species from a coral reef community after a nutrient pulse. *Sci. Rep.* **6**, 28821 (2016).
 28. Peña-García, D., Ladwig, N., Turki, A. J. & Mudarris, M. S. Input and dispersion of nutrients from the Jeddah Metropolitan Area, Red Sea. *Mar. Pollut. Bull.* **80**, 41–51 (2014).
 29. Joye, S. B. & Paerl, H. W. Contemporaneous nitrogen fixation and denitrification in intertidal microbial mats: rapid response to runoff events. *Mar. Ecol. Prog. Ser.* **94**, 267–274 (1993).
 30. Cardini, U., Bednarz, V. N., Foster, R. A. & Wild, C. Benthic N₂ fixation in coral reefs and the potential effects of human-induced environmental change. *Ecol. Evol.* **4**, 1706–1727 (2014).
 31. Holl, C. M. & Montoya, J. P. Interactions between nitrate uptake and nitrogen fixation in continuous cultures of the marine diazotroph *Trichodesmium* (Cyanobacteria). *J. Phycol.* **41**, 1178–1183 (2005).
 32. Knapp, A. N. The sensitivity of marine N₂ fixation to dissolved inorganic nitrogen. *Front. Microbiol.* **3**, 374 (2012).
 33. Fay, P. Oxygen relations of nitrogen fixation in cyanobacteria. *Microbiol. Rev.* **56**, 340–73 (1992).
 34. Adams, C., Frantz, J. & Bugbee, B. Macro- and micronutrient-release characteristics of three polymer-coated fertilizers: Theory and measurements. *J. Plant Nutr. Soil Sci.* **176**, 76–88 (2013).
 35. Stuhldreier, I., Bastian, P., Schönig, E. & Wild, C. Effects of simulated eutrophication and overfishing on algae and invertebrate settlement in a coral reef of Koh Phangan, Gulf of Thailand. *Mar. Pollut. Bull.* **92**, 35–44 (2015).
 36. Falkenberg, L. J., Russell, B. D. & Connell, S. D. Contrasting resource limitations of marine primary producers: Implications for competitive interactions under enriched CO₂ and nutrient regimes. *Oecologia* **172**, 575–583 (2013).
 37. Roth, F. *et al.* Coral reef degradation affects the potential for reef recovery after disturbance. *Mar. Environ. Res.* **142**, 48–58 (2018).
 38. Haas, A., el-Zibdah, M. & Wild, C. Seasonal monitoring of coral-algae interactions in fringing reefs of the Gulf of Aqaba, Northern Red Sea. *Coral Reefs* **29**, 93–103 (2010).
 39. Grasshoff, K., Kremling, K. & Ehrhardt, M. *Methods of seawater analysis*. (Wiley-VCH, 1999).
 40. Taylor, B. W. *et al.* Improving the fluorometric ammonium method: matrix effects, background fluorescence, and standard additions. *J. North Am. Benthol. Soc.* **26**, 167–177 (2007).

41. Holmes, R. M., Aminot, A., K erouel, R., Hooker, B. A. & Peterson, B. J. A simple and precise method for measuring ammonium in marine and freshwater ecosystems. *Can. J. Fish. Aquat. Sci.* **56**, 1801–1808 (1999).
42. Gutierrez-Heredia, L., Benzoni, F., Murphy, E. & Reynaud, E. G. End to End Digitisation and Analysis of Three-Dimensional Coral Models, from Communities to Corallites. *PLoS One* **11**, e0149641 (2016).
43. El-Khaled, Y. C. *et al.* Combined Acetylene Blockage and Reduction Assay (COBRA) for Dinitrogen Fixation and Denitrification Estimation. 1–7 (2019). doi:10.17504/protocols.io.9ith4en
44. Oremland, R. S. & Capone, D. G. Use of ‘Specific’ Inhibitors in Biogeochemistry and Microbial Ecology. *Adv. Microbi. Ecol.* 285–383 (1988). doi:10.1007/978-1-4684-5409-3_8
45. Devol, A. H. *Denitrification Including Anammox. Nitrogen in the Marine Environment* (2008). doi:10.1016/B978-0-12-372522-6.00006-2
46. Balderston, W. L., Sherr, B. & Payne, W. J. Blockage By Acetylene of Nitrous-Oxide Reduction in Pseudomonas-Perfectomarinus. *Appl. Environ. Microbiol.* **31**, 504–508 (1976).
47. Yoshinari, T. & Knowles, R. Acetylene Inhibition of Nitrous Oxide Reduction by Denitrifying Bacteria. *Biochem. Biophys. Res. Commun.* **69**, 705–710 (1976).
48. Rix, L. *et al.* Seasonality in dinitrogen fixation and primary productivity by coral reef framework substrates from the northern Red Sea. *Mar. Ecol. Prog. Ser.* **533**, 79–92 (2015).
49. Clarke, K. R. & Gorley, R. N. *PRIMER v6: Use manual/Tutorial. PRIMER-E:Plymouth* (2006).
50. Anderson, M. J. A new method for non-parametric multivariate analysis of variance. *Austral Ecol.* **26**, 32–46 (2001).
51. D’Angelo, C. & Wiedenmann, J. Impacts of nutrient enrichment on coral reefs: New perspectives and implications for coastal management and reef survival. *Curr. Opin. Environ. Sustain.* **7**, 82–93 (2014).
52. Capone, D. G., Dunham, S. E., Horrigan, S. G. & Duguay, L. E. Microbial nitrogen transformations in unconsolidated coral reef sediments. *Mar. Ecol. Prog. Ser.* **80**, 75–88 (1992).
53. Wiedenmann, J. *et al.* Nutrient enrichment can increase the susceptibility of reef corals to bleaching. *Nat. Clim. Chang.* **3**, 160–164 (2013).
54. Churchill, J. H., Bower, A. S., McCorkle, D. C. & Abualnaja, Y. The transport of nutrient-rich Indian Ocean water through the Red Sea and into coastal reef systems. *J. Mar. Res.* **72**, 165–181 (2014).
55. Wafar, M. *et al.* Patterns of distribution of inorganic nutrients in Red Sea and their implications to primary production. *J. Mar. Syst.* **156**, 86–98 (2016).
56. Jessen, C., Roder, C., Villa Lizcano, J. F., Voolstra, C. R. & Wild, C. In-Situ Effects of Simulated Overfishing and Eutrophication on Benthic Coral Reef Algae Growth, Succession, and Composition in the Central Red Sea. *PLoS One* **8**, e66992 (2013).
57. Flett, R. J., Schindler, D. W., Hamilton, R. D. & Campbell, N. E. R. Nitrogen Fixation in Canadian Precambrian Shield Lakes. *Can. J. Fish. Aquat. Sci.* **37**, 494–505 (1980).
58. Welsh, D. T., Bourgu es, S., De Wit, R. & Herbert, R. A. Seasonal variations in nitrogen-fixation (acetylene reduction) and sulphate-reduction rates in the rhizosphere of *Zostera noltii*: Nitrogen fixation by sulphate-reducing bacteria. *Mar. Biol.* **125**, 619–628 (1996).
59. Vadez, V., Sinclair, T. R. & Serraj, R. Asparagine and ureide accumulation in nodules and shoots as feedback inhibitors of N₂ fixation in soybean. *Physiol. Plant.* **110**, 215–223 (2000).
60. Capone, D. G., O’Neil, J. M., Zehr, J. & Carpenter, E. J. Basis for diel variation in nitrogenase

- activity in the marine planktonic cyanobacterium *Trichodesmium thiebautii*. *Appl. Environ. Microbiol.* **56**, 3532–3536 (1990).
61. Bebout, B. M., Paerl, H. W., Crocker, K. M. & Prufert, L. E. Diel Interactions of Oxygenic Photosynthesis and N₂ Fixation (Acetylene Reduction) in a Marine Microbial Mat Community. *Appl. Environ. Microbiol.* **53**, 2353–2362 (1987).
 62. Cornwell, J. C., Kemp, W. M. & Kana, T. M. Denitrification in coastal ecosystems: methods, environmental controls, and ecosystem level controls, a review. *Aquat. Ecol.* **33**, 41–54 (1999).
 63. Piña-Ochoa, E. & Álvarez-Cobelas, M. Denitrification in aquatic environments: A cross-system analysis. *Biogeochemistry* **81**, 111–130 (2006).
 64. Brandes, J. A., Devol, A. H. & Deutsch, C. New developments in the marine nitrogen cycle. *Chem. Rev.* **107**, 577–589 (2007).
 65. Tilstra, A. *et al.* Denitrification Aligns with N₂ Fixation in Red Sea Corals. *Sci. Rep.* **9**, 19460 (2019).
 66. Shashar, N., Cohen, Y. & Loya, Y. Extreme Diel Fluctuations of Oxygen in Diffusive Boundary Layers Surrounding Stony Corals. *Biol. Bull.* **185**, 455–461 (1993).
 67. Rysgaard, S. *et al.* Oxygen regulation of nitrification and denitrification in sediments. *Limnol. Oceanogr.* **39**, 1643–1652 (1994).
 68. Lema, K. A., Willis, B. L. & Bourne, D. G. Corals form characteristic associations with symbiotic nitrogen-fixing bacteria. *Appl. Environ. Microbiol.* **78**, 3136–3144 (2012).
 69. Beauchamp, E. G., Trevors, J. T. & Paul, J. W. Carbon Sources for Bacterial Denitrification. in *Advances in Soil Science* (ed. Stewart, B. A.) **10**, 113–142 (Springer, 1989).
 70. Sorokin, Y. I. on the Feeding of Some Scleractinian Corals With Bacteria and Dissolved Organic Matter. *Limnol. Oceanogr.* **18**, 380–386 (1973).
 71. Cook, P. L. M., Veuger, B., Böer, S. & Middelburg, J. J. Effect of nutrient availability on carbon and nitrogen incorporation and flows through benthic algae and bacteria in near-shore sandy sediment. *Aquat. Microb. Ecol.* **49**, 165–180 (2007).
 72. Haas, A. F. *et al.* Effects of Coral Reef Benthic Primary Producers on Dissolved Organic Carbon and Microbial Activity. *PLoS One* **6**, e27973 (2011).
 73. Cárdenas, A., Meyer, F., Schwieder, H., Wild, C. & Gärdes, A. The formation of aggregates in coral reef waters under elevated concentrations of dissolved inorganic and organic carbon : A mesocosm approach. *Mar. Chem.* **175**, 47–55 (2015).
 74. Nitrogen eutrophication particularly promotes turf algae in coral reefs of the central Red Sea.
 75. Yamamuro, M., Kayanne, H. & Minagawa, M. Carbon and nitrogen stable isotopes of primary producers in coral reef ecosystems. *Limnol. Oceanogr.* **40**, 617–621 (1995).
 76. Gorgula, S. K. & Connell, S. D. Expansive covers of turf-forming algae on human-dominated coast: The relative effects of increasing nutrient and sediment loads. *Mar. Biol.* **145**, 613–619 (2004).
 77. Kopp, C. *et al.* Highly Dynamic Cellular-Level Response of Symbiotic Coral to a Sudden Increase in Environmental Nitrogen. *MBio* **4**, e00052-13 (2013).
 78. Muscatine, L., Falkowski, P. G., Dubinsky, Z., Cook, P. A. & McCloskey, L. R. The Effect of External Nutrient Resources on the Population Dynamics of Zooxanthellae in a Reef Coral. *Proc. R. Soc. B Biol. Sci.* **236**, 311–324 (1989).
 79. Atkinson, M. J., Carlson, B. & Crow, G. L. Coral growth in high-nutrient, low-pH seawater: a case study of corals cultured at the Waikiki Aquarium, Honolulu, Hawaii. *Coral Reefs* **14**, 215–223 (1995).
 80. Bongiorno, L., Shafir, S., Angel, D. & Rinkevich, B. Survival, growth and gonad development of

- two hermatypic corals subjected to in situ fish-farm nutrient enrichment. *Mar. Ecol. Prog. Ser.* **253**, 137–144 (2003).
81. Sawall, Y. *et al.* Nutritional status and metabolism of the coral *Stylophora subseriata* along a eutrophication gradient in Spermonde Archipelago (Indonesia). *Coral Reefs* **30**, 841–853 (2011).
 82. Lirman, D. & Fong, P. Is proximity to land-based sources of coral stressors an appropriate measure of risk to coral reefs? An example from the Florida Reef Tract. *Mar. Pollut. Bull.* **54**, 779–791 (2007).
 83. Pogoreutz, C. *et al.* Sugar enrichment provides evidence for a role of nitrogen fixation in coral bleaching. *Glob. Chang. Biol.* **23**, 3838–3848 (2017).
 84. Menge, D. N. L., Levin, S. A. & Hedin, L. O. Facultative versus obligate nitrogen fixation strategies and their ecosystem consequences. *Am. Nat.* **174**, 465–477 (2009).
 85. Bothe, H., Klein, B., Stephan, M. P. & Döbereiner, J. Transformations of inorganic nitrogen by *Azospirillum* spp. *Arch. Microbiol.* **130**, 96–100 (1981).
 86. Patriquin, D. G. Nitrogen fixation (acetylene reduction) associated with cord grass, *Spartina alterniflora* Loisel. *Ecol. Bull.* **26**, 20–27 (1978).
 87. Lapointe, B. E. Nutrient thresholds for bottom-up control of macroalgal blooms on coral reefs in Jamaica and southeast Florida. *Limnol. Oceanogr.* **42**, 1119–1131 (1997).
 88. Lesser, M. P. *et al.* Nitrogen fixation by symbiotic cyanobacteria provides a source of nitrogen for the scleractinian coral *Montastraea cavernosa*. *Mar. Ecol. Prog. Ser.* **346**, 143–152 (2007).
 89. Eyre, B. D., Glud, R. N. & Patten, N. Mass coral spawning: A natural large-scale nutrient addition experiment. *Limnol. Oceanogr.* **53**, 997–1013 (2008).
 90. Fabricius, K. E. Effects of terrestrial runoff on the ecology of corals and coral reefs: Review and synthesis. *Mar. Pollut. Bull.* **50**, 125–146 (2005).
 91. Ferrier-Pagès, C., Godinot, C., D’Angelo, C., Wiedenmann, J. & Grover, R. Phosphorus metabolism of reef organisms with algal symbionts. *Ecol. Monogr.* **86**, 262–277 (2016).
 92. Cuet, P. *et al.* CNP budgets of a coral-dominated fringing reef at La Réunion, France: Coupling of oceanic phosphate and groundwater nitrate. *Coral Reefs* **30**, 45–55 (2011).
 93. Bednarz, V. N., Grover, R., Maguer, J. F., Fine, M. & Ferrier-Pagès, C. The assimilation of diazotroph-derived nitrogen by scleractinian corals depends on their Metabolic Status. *MBio* **8**, 1–14 (2017).
 94. Howarth, R. W., Marino, R., Lane, J. & Cole, J. J. Nitrogen fixation in freshwater, estuarine, and marine ecosystems. 1. Rates and importance. *Limnol. Oceanogr.* **33**, 669–687 (1988).
 95. Brunner, B. *et al.* Nitrogen isotope effects induced by anammox bacteria. *Proc. Natl. Acad. Sci.* **110**, 18994–18999 (2013).
 96. Dalsgaard, T., Thamdrup, B. & Canfield, D. E. Anaerobic ammonium oxidation (anammox) in the marine environment. *Res. Microbiol.* **156**, 457–464 (2005).
 97. Hoffmann, F. *et al.* Complex nitrogen cycling in the sponge *Geodia barretti*. *Environ. Microbiol.* **11**, 2228–2243 (2009).
 98. Meunier, V. *et al.* Bleaching forces coral’s heterotrophy on diazotrophs and *Synechococcus*. *ISME J.* **13**, 2882–2886 (2019).

Chapter 9

Chapter 9 | Nutrient pollution enhances productivity and framework dissolution in algae- but not in coral-dominated reef communities

Florian Roth^{1,2,3*}, Yusuf C. El-Khaled⁴, Denis B. Karcher^{4,5}, Nils Rådecker^{1,6,7}, Susana Carvalho¹, Carlos M. Duarte^{1,8}, Luis Silva¹, Maria Ll. Calleja^{1,9}, Xosé Anxelu G. Morán¹, Burton H. Jones¹, Christian R. Woolstra^{1,7}, Christian Wild⁴

¹Red Sea Research Center, King Abdullah University of Science and Technology (KAUST), Thuwal, Saudi Arabia

²Baltic Sea Centre, Stockholm University, Stockholm, Sweden

³Tvärminne Zoological Station, University of Helsinki, Helsinki, Finland

⁴Marine Ecology, Faculty of Biology and Chemistry, University of Bremen, Bremen, Germany

⁵Australian National Centre for the Public Awareness of Science, Australian National University, Canberra, Australia

⁶Laboratory for Biological Geochemistry, School of Architecture, Civil and Environmental Engineering, École Polytechnique Fédérale de Lausanne, Lausanne, Switzerland

⁷Department of Biology, University of Konstanz, Konstanz, Germany

⁸Computational Biology Research Center, King Abdullah University of Science and Technology (KAUST), Thuwal, Saudi Arabia

⁹Department of Climate Geochemistry, Max Planck Institute for Chemistry (MPIC), Mainz, Germany

*Corresponding author: florian.roth@su.se

9.1 Abstract

Ecosystem services provided by coral reefs may be susceptible to the combined effects of benthic species shifts and anthropogenic nutrient pollution, but related knowledge does not exist. We thus investigated *in situ* how dissolved inorganic nutrient enrichment, maintained for two months, affected community-wide biogeochemical functions of intact coral- and degraded algae-dominated reef patches in the central Red Sea. Results from benthic chamber incubations revealed 74% increased gross productivity and a shift from net calcification to dissolution in algae- compared to neighboring coral-dominated communities at the end of the experiments. Both community types changed from net dissolved organic nitrogen sinks to sources, but the increase in net release was 56% higher in algae-dominated communities. Nutrient pollution may thus amplify effects of community shifts on key ecosystem services of coral reefs, possibly leading to a loss of structurally complex habitats with carbonate dissolution and altered nutrient recycling.

Keywords: Eutrophication | ecosystem functioning | carbon and nitrogen cycles | erosion | phase-shifts | nutrient enrichment

A modified version of this chapter has been submitted to *Marine Pollution Bulletin* and is currently in review

9.2 | Introduction

Coral reefs are among the most productive and biologically diverse ecosystems on Earth, despite generally growing in oligotrophic tropical waters¹. Under these conditions, the photo-symbiotic association of corals with dinoflagellate algae^{2,3} and the efficient retention and recycling of carbon (C) and nitrogen (N) are critical to maintaining ecosystem functioning and support growth⁴⁻⁶. As reef organisms are adapted to low exogenous nutrient inputs⁷, nutrient pollution (particularly excessive N inputs) has been recognized as one of the main local stressors leading to coral reef degradation⁸⁻¹⁰. At the same time, global stressors have led to extensive coral mortality events in recent decades^{11,12}. The resulting changes in the benthic community composition are often expressed by shifts from formerly coral-dominated to turf and fleshy macroalgae-dominated reefs¹³⁻¹⁵. As a consequence, many extant coral reefs are characterized by a mosaic of co-occurring species¹⁶⁻¹⁸, a state with a lower coral cover that may evolve into a stable state supported by coral degradation events worldwide^{19,20}.

Intrinsically, important biogeochemical processes, such as the cycling of C and N or the accumulation of calcium carbonate (CaCO₃) within the reef ecosystem, are linked to the community composition of the benthos²¹. For example, coral-dominated communities ensure constant reef accretion through calcification that changes the physical, chemical, and biological environment and provides habitats for associated reef organisms²². In these communities, low net community production despite high gross productivity warrants that biomass accumulates slowly^{23,24}, while the release of large amounts of C-rich dissolved and particulate organic materials by corals functions as energy carriers and particle traps that enhance the retention of essential elements within the wider ecosystem traps^{5,25,26}. In addition, benthic N inputs by microbial dinitrogen (N₂) fixation (diazotrophy) of the coral holobiont during nutrient-depleted conditions suggest a strong biogeochemical coupling between diazotrophy and the reef C cycle²⁷. Algae-dominated communities, on the other hand, display significantly higher net primary productivity^{27,28} with a greater potential for autotrophic biomass production^{29,30} and a more direct transfer of organic C to higher trophic levels through grazing²⁹. Organic material exuded by algae tends to be more labile³¹ and can increase the microbial abundance on algae-dominated reefs³².

The differences in biogeochemical processes mediated by these reef organisms and their associated communities may be compounded by distinct responses to environmental change, which, in turn, may promote alterations in the species composition of the impacted reef¹⁵. At a local scale, nutrient pollution is a prevailing anthropogenic stressor³³ that can affect the functioning of (co-occurring) reef communities differently³⁴. Although still debated, nutrient pollution in corals often has adverse effects on growth^{35,36}, calcification³⁷, reproductive success³⁸, and increases the susceptibility of corals to bleaching^{10,39,40}. Moderate N enrichment can also stimulate both N₂ fixation and denitrification⁴¹, highlighting the sensitivity of important N pathways of corals to altered nutrient conditions. In contrast, other benthic groups present in coral reefs, such as turf and macroalgae benefit from increased nutrient availability in many cases (reviewed in McCook (1999)⁴²), potentially gaining a competitive advantage over corals³⁴.

Despite this in-depth knowledge of the species-specific effects of excess nutrients on the organism's physiology, there is a limited understanding of how biogeochemical processes mediated by entire reef communities are impacted by nutrient pollution in the natural environment. On the one hand, the cycling of C and N within the reef is not only facilitated by dominant functional groups of the visible reef surface (e.g., corals or algae). Instead, community-wide biogeochemical processes result from the interplay of complex species communities⁴³, including the surrounding benthic and pelagic microbiome^{44,45} and organisms living in cryptic habitats. For example, cracks and crevices within the reef matrix can encompass about 60% – 75% of the total surface area of a reef^{46,47}, with the organisms inhabiting these spaces (e.g., sponges, bryozoans, and tunicates) metabolizing and recycling considerable amounts of C and N^{6,48}. On the other hand, while experimental exposure to elevated nutrient concentrations in laboratory studies often induce negative responses (see above paragraph and citations therein), several *in situ* observations failed to reveal direct adverse effects of increased nutrient levels on the physiology of reef organisms or found them only at unnaturally high concentrations (reviewed in D'Angelo and Wiedenmann (2014)⁴⁹, Szmant (2002)⁵⁰). Thus, the results of experimental exposure to elevated nutrient concentrations, particularly from laboratory studies, need to be interpreted carefully. Consequently, measurements under *in situ* conditions with intact reef communities and under realistic nutrient exposure concentrations are required to better understand how C and N cycles mediated by tropical reef communities will respond to elevated nutrient availability in the natural environment.

To overcome these constraints and to account for ongoing coral-algal phase shifts worldwide, we used an eight-week *in situ* nutrient addition experiment and benthic incubation chambers to directly compare community-wide biogeochemical processes of naturally co-occurring coral- and algae-dominated communities in response to nutrient enrichment in a reef of the central Red Sea. Nutrient enrichment (3-fold on average compared to environmental background values) reflected nutrient inputs in the Red Sea from sources such as aquaculture³⁸ or urban wastewater⁵¹. Using benthic incubations chambers, we quantified *in situ* community-wide biogeochemical processes such as net and gross productivity, respiration, calcification, and fluxes of dissolved organic carbon (DOC), dissolved inorganic nitrogen (DIN), and dissolved organic nitrogen (DON), all of which are central to the balanced C and N dynamics enabling coral reefs to thrive in the oligotrophic waters of the tropics. Thereby, we a) directly compared the magnitudes and directions of key biogeochemical processes of co-occurring coral- and algae-dominated reef communities under ambient nutrient conditions, and b) assessed the responses of the above processes to environmental change induced by enhanced nutrient availability.

9.3 Material and methods

Experimental Design

The experiments were conducted at Abu Shosha reef located in the central Red Sea on the west coast of Saudi Arabia (22°18'16.3"N; 39°02'57.7"E) from late January until late March 2018. Both coral- and algae-

dominated communities are present at Abu Shosha reef. Thus, this site allows quantifying biogeochemical processes mediated by both communities under identical environmental conditions. Eight distinct natural communities were chosen for *in situ* investigations at 5 m water depth within an area of 50 x 50 m. The same communities were selected previously for a seasonal study (January 2017 until January 2018) to assess carbon and nitrogen fluxes⁵². The communities were randomly selected among communities that had the following characteristics: 1) The four coral-dominated communities had at least >40% coral but <10% algae cover; 2) The four algae-dominated communities had >40% algae but <10% coral cover; 3) All communities had to fit into the incubation chambers (max. diameter 50 cm, max. height 39 cm. The detailed compositions of the benthic communities used for this study are presented in Fig. S9.1.

For the nutrient enrichment experiments, each community was surrounded by four pins with mesh bags containing 70g of slow-release fertilizer granulate (Osmocote® Plus 15-9-12) (Fig. S9.2). Osmocote® Plus fertilizer supplies various macronutrients continuously (15% total N, 9% available phosphorus (P) in the form of phosphate (PO_4^{3-}), 12% soluble potash; see detailed list of released micronutrients in Table S8.1), and has been used successfully in many previous nutrient enrichment studies on coral reefs^{30,53} and other ecosystems⁵⁴. The fertilizer was renewed every two weeks to assure a continuous nutrient supply. Every two weeks, water samples for nutrients were taken directly at the fertilizer pins, 25 cm towards the center of the four pins (roughly corresponding to the center of the communities), and 25 cm and 200 cm away from the investigated communities to test whether the nutrient addition was effective locally. The nutrient enrichment phase lasted for eight weeks. *In situ* incubations of all communities were performed before the fertilizer pins were deployed (hereafter "before nutrient enrichment"), and after eight weeks of manipulated nutrient conditions (hereafter "after nutrient enrichment"), thus, followed a quasi-experimental one-group pre-/post-test research design⁵⁵. While the lack of an experimental control group is often unavoidable in complex field studies^{56,57}, particularly productivity and the release of DOC may have been enhanced by slightly rising temperature during the study period⁵⁸. Thus, we further compared metabolic rates from community incubations (present study) to incubations of individual functional groups of the same communities, where control groups were tested as well (refer to El-Khaled et al. (2020)⁵⁹ for details). While El-Khaled et al. (2020)⁵⁹ showed similar productivity patterns with nutrient enrichment, the control group did not respond to changes in water temperature during the study period. The alignment of the observed patterns in both studies improves the validity of associating any changes described here with the experimental intervention rather than seasonal variability.

Environmental Monitoring and Conditions during the Experiments

Key environmental variables were monitored at the sampling site. Water temperature was measured continuously (logging interval = 30 min) for the whole study period with Onset HOBO data loggers (accuracy: $\pm 0.2^\circ\text{C}$) deployed at the seafloor. Light availability was measured continuously (logging interval = 1 minute) on three full days per month with an Onset HOBO Pendant data logger. Light readings were

converted from lux to photosynthetically active radiation ($\mu\text{mol quanta m}^{-2} \text{ s}^{-1}$; 400 to 700 nm wavelengths) by intercalibration and conversion as outlined in Roth et al. (2018)⁶⁰, and values are presented as daytime means. Seawater samples for the determination of dissolved nitrate (NO_3^-), nitrite (NO_2^-), ammonium (NH_4^+), phosphate (PO_4^{3-}), and monomeric silicate ($\text{Si}(\text{OH})_4$) were taken in triplicates every second week from at least 10 m away from the fertilizer pins as an environmental background control. Details for sampling and analysis can be found in Appendix S1 of the supporting information. The sum of NO_3^- , NO_2^- and NH_4^+ is termed 'dissolved inorganic nitrogen' (DIN) henceforth.

Water temperature increased from 24.8 to 28.1°C during the *in situ* manipulation period of 8 weeks. Environmental background DIN concentrations remained stable throughout the experiments at $0.40 \pm 0.03 \mu\text{mol N L}^{-1}$. When nutrient manipulation was initiated, DIN concentrations increased on average 3-fold compared to background values to $1.31 \pm 0.14 \mu\text{mol N L}^{-1}$ (measured directly at the communities). PO_4^{3-} around the communities remained stable, despite being present in the fertilizer (Table S7.1).

In Situ Incubations and Quantification of Community Functions

In situ incubations with benthic chambers (Fig. S9.2) were performed to measure fluxes of dissolved oxygen (O_2), total alkalinity (TA), dissolved inorganic carbon (DIC), dissolved organic carbon (DOC), total dissolved nitrogen (TDN), dissolved organic nitrogen (DON), and dissolved inorganic nitrogen (DIN). Incubations were performed according to an adapted protocol described in Roth et al. (2019)⁴³, and according to the same procedures outlined in Roth et al. (2020)⁵². Briefly, polymethyl methacrylate cylinders ($n = 8$) with removable gas-tight lids of the same material were used for the experiments. All chambers were equipped with individual water circulation pumps with adjustable flow control, autonomous recording dissolved O_2 sensors (HOBO U26), and two sampling ports for discrete water samples. Incubations were carried out on three consecutive days in January (before nutrient enrichment), and March (after nutrient enrichment) 2018, respectively. On day one, divers deployed four chambers on coral-dominated, and four chambers on algae-dominated reef communities. The chambers were left in place without lids until the next morning, reducing the stress response of organisms and allowing for sufficient water exchange. On day two, incubations started at around 9:00 a.m. by tightly securing the lids and closing all sampling ports during natural daylight conditions. The exact incubation start- and end-time were recorded for each chamber. Incubations duration was approximately 2 h. The chambers were then left in place without lids for a second set of incubation on the following day. On day three, benthic communities were incubated at "simulated" darkness (i.e., chambers were covered with thick black PVC covers), starting at around 9:00 a.m. for around 2 h. Between deployments, all materials were rinsed with freshwater, washed with 4% hydrochloric acid (HCl), and subsequently rinsed with deionized water for reliable water chemistry measurements that included sensitive DOC samples.

Discrete water samples for TA, DOC, TDN, and DIN were withdrawn from the sampling ports with acid-washed syringes at the beginning and the end of each incubation (Supplementary Material SM9.1). Changes

in seawater chemistry between start and end of incubations were used to calculate rates of net community production (NCP), community respiration (CR), gross primary production (GPP), net community calcification (NCC), and fluxes of DOC, TDN, DON, and DIN. All rates/fluxes were extrapolated to incubation water volume (in L) and normalized to incubation duration (in h) and the planar reef area (in m²) of the enclosed benthic community adapted after Roth et al. (2019)⁴³. NCP and CR were calculated based on O₂ fluxes from continuous measurements with dissolved O₂ sensors. Values from light and dark incubations were used to calculate NCP and CR, respectively. GPP was calculated as $GPP = NCP + |CR|$. Rates were expressed as mmol O₂ m⁻² h⁻¹. NCC (in mmol CaCO₃ m⁻² h⁻¹) was calculated by concentration differences in TA, which are primarily caused by calcification and dissolution of CaCO₃, whereby TA is reduced (increased) by two molar equivalents for every mole of CaCO₃ produced (dissolved)⁶¹. Nutrient fluxes (i.e., NO₃⁻, NH₄⁺, PO₄³⁻, and Si(OH)₄) that cause a change in TA unrelated to calcification and dissolution were accounted for calculations according to Zeebe and Wolf (2001)⁶¹ and Wolf-Gladrow et al. (2007)⁶². DOC (in μmol C m⁻² h⁻¹), TDN (in μmol N m⁻² h⁻¹), DON (in μmol N m⁻² h⁻¹) and, DIN (in μmol N m⁻² h⁻¹) fluxes were calculated from concentration differences between start and endpoints. In addition to the community-wide functions measured with benthic incubation chambers in the present study, individual functional groups and organisms of the communities were also used for additional measurements presented in Karcher et al. (2020)⁶³ and El-Khaled et al. (2020)⁵⁹. Specifically, organic carbon (C_{org}) and N contents using elemental and stable isotope analysis, along with organism-specific productivity, N₂ fixation and denitrification measurements were performed. While detailed findings can be found in the above studies, we will refer to some of the results in relevant sections of the discussion to complement our findings.

Data Treatment and Statistical Analysis

Hourly rates from light and dark incubations (presented in Table S9.1) were used to calculate daily net fluxes based on the light/dark regime of the exact day of incubations. To minimize the error associated with extrapolating hourly rates, we chose a time window for daylight incubations (from around 9 a.m. to 11 a.m.) that is closest to average daytime irradiation and excludes the "ramping up" phase in the early morning hours and extreme values that can occur during midday. The ratio of GPP to CR (i.e., GPP:CR) was calculated based on daily net fluxes. The C:N molar ratio of dissolved organic matter (DOM; comprised of DOC and DON) was calculated based on the elemental composition of organic matter released by the respective communities. All values are reported as means ± standard error. The dataset was analyzed using non-parametric permutational multivariate analysis of variance (PERMANOVA) using PRIMER-E version 6 software⁶⁴ with the PERMANOVA+ add on⁶⁵. To test for differences in various C, CaCO₃, and N fluxes, and before and after nutrient enrichment, 2-factorial PERMANOVAs were performed (factors were respective fluxes and coral- or algae-dominated communities) based on Bray-Curtis similarities of square-root transformed data. Therefore, Type III (partial) sum of squares was used with unrestricted permutation of raw data (999 permutations), and PERMANOVA pairwise tests with parallel Monte Carlo tests were carried out when significant differences occurred. Significant relationships between community types (coral-

vs algae-dominated) and treatment (before vs after nutrient enrichment) are represented with letters in Fig. 9.1-9.3, and statistical details can be found in Table S9.2.

9.4 Results

Community-Wide Biogeochemical Processes at the Onset of the Experiments

Before the nutrient enrichment experiments started, coral- and algae-dominated reef communities exhibited no significant difference in rates of GPP (518 ± 19 and 531 ± 25 mmol O₂ m⁻² d⁻¹, respectively; Fig. 9.1A), CR (-223 ± 28 and -258 ± 14 mmol O₂ m⁻² d⁻¹, respectively), and NCP (295 ± 9 and 273 ± 12 mmol O₂ m⁻² d⁻¹, respectively) (Fig. S9.3; Table S9.2). As a result, both community types showed similar GPP:CR ratios (2.4 ± 0.3 in coral- and 2.1 ± 0.2 in algae-dominated communities, respectively; Fig. 9.3A). NCC was one order of magnitude higher in coral- (150.7 ± 13.2 mmol CaCO₃ m⁻² d⁻¹), compared to algae-dominated (9.8 ± 7.6 mmol CaCO₃ m⁻² d⁻¹) communities (Fig. 9.1B). Net DOC fluxes (Fig. 9.1C) ranged from -1.1 to 11.3 mmol C m⁻² d⁻¹ in coral-, and from 0.2 to 4.5 mmol C m⁻² d⁻¹ in algae-dominated communities. Due to the high variability of DOC fluxes between replicates, no significant differences were detected between the two community-types. TDN fluxes were close to zero in both coral- and algae-dominated communities (Fig. 9.2A), balanced by the consumption of DON (-0.7 ± 1.2 and -1.4 ± 0.6 mmol N m⁻² d⁻¹, respectively; Fig. 9.2B) and a concomitant release of DIN (1.8 ± 0.4 and 2.4 ± 0.8 mmol N m⁻² d⁻¹, respectively; Fig. 9.2C).

Community-Wide Biogeochemical Processes after Nutrient Enrichment

GPP was 74% higher in algae- compared to coral-dominated communities after nutrient enrichment (968 ± 57 and 556 ± 42 mmol O₂ m⁻² d⁻¹, respectively; Fig. 9.1A). Thereof, CR consumed two-times more O₂ in algae- (-502 ± 25 mmol O₂ m⁻² d⁻¹) than in coral-dominated (-258 ± 39 mmol O₂ m⁻² d⁻¹) communities, while NCP was 55% higher (465 ± 22 compared to 300 ± 14 mmol O₂ m⁻² d⁻¹, respectively) (Fig. S9.3). The resulting GPP:CR ratio was 26% lower in algae- (1.7 ± 0.1) compared to coral-dominated communities (2.3 ± 0.2) (Fig. 9.3A). *In situ* nutrient enrichment led to a non-significant increase in NCC in coral-dominated communities, while it caused a shift from net calcification to carbonate dissolution in algae-dominated communities (i.e., negative NCC rates; -6.8 ± 1.6 mmol CaCO₃ m⁻² d⁻¹; Fig. 9.1B). In both community-types, nutrient enrichment did not affect the magnitude nor the direction of net DOC fluxes (Fig. 9.1C). In contrast, TDN fluxes were significantly altered by nutrient addition (Fig. 9.2A), mainly driven by changes in net DON fluxes (Fig. 9.2B). Nutrient enrichment caused both communities to shift from being DON sinks to sources (after nutrient enrichment: 3.6 ± 0.3 and 2.5 ± 0.1 mmol N m⁻² d⁻¹ in coral- and algae-dominated communities, respectively); however, the average increase in DON released from before to after nutrient enrichment was 56% higher in algae- ($+ 5.0 \pm 0.8$ mmol N m⁻² d⁻¹) compared to coral-dominated ($+ 3.2 \pm 0.7$ mmol N m⁻² d⁻¹) communities. Due to the high variability in DIN fluxes across replicates, neither significant changes from before to after nutrient enrichment nor between the community-types were detected (Fig. 9.2C). The imbalanced changes in the released amount of DOC and DON caused a small

(~10%) but significant reduction of the C:N molar ratio of DOM released by coral- and algae-dominated communities (Fig. 9.3B).

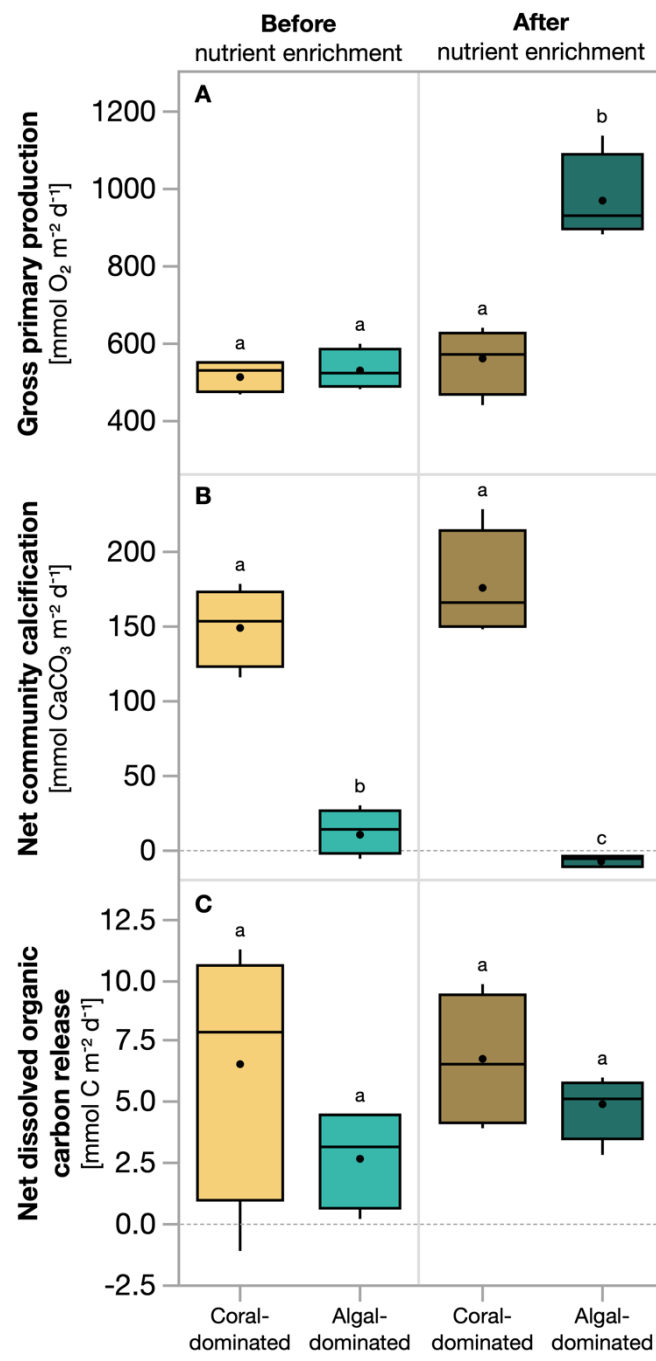


Figure 9.1 | Gross primary production (**A**), net community calcification (**B**), and net release of dissolved organic carbon (**C**) in coral- and algal dominated reef communities, before and after nutrient enrichment. Boxplots show the median (line across a box), mean (dot in the box), first and third quartiles (upper and lower bounds of each box), and the minimum and maximum value (i.e., upper and lower whisker, respectively). Significant differences between community types (coral- vs algae-dominated) and treatment (before vs after nutrient enrichment) are represented with letters. Statistical details are presented in Table S9.2.

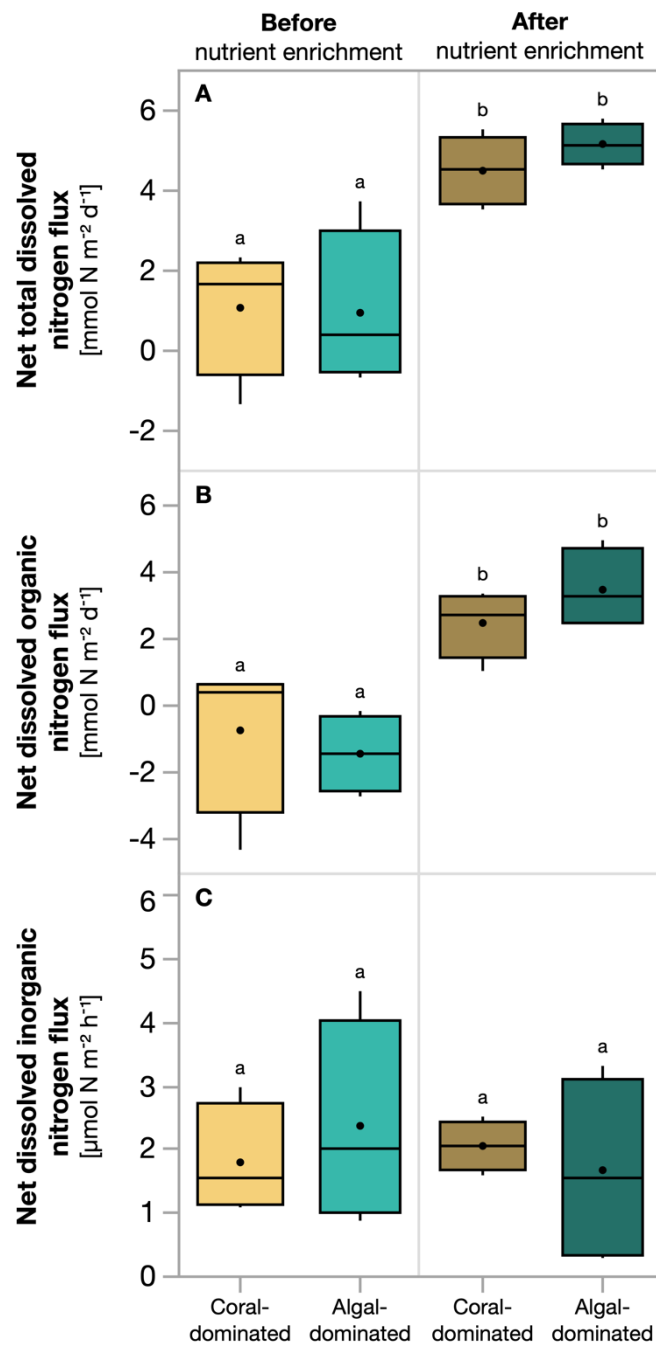


Figure 9.2 | Total dissolved nitrogen (**A**), dissolved organic nitrogen (**B**), and dissolved inorganic nitrogen (**C**) net fluxes in coral- and algal dominated reef communities, before and after nutrient enrichment. Boxplots show the median (line across a box), mean (dot in the box), first and third quartiles (upper and lower bounds of each box), and the minimum and maximum value (i.e., upper and lower whisker, respectively). Significant differences between community types (coral- vs algae-dominated) and treatment (before vs after nutrient enrichment) are represented with letters. Negative nutrient fluxes (<0) indicate a net uptake of nutrients by the communities. Statistical details are presented in Table S9.2.

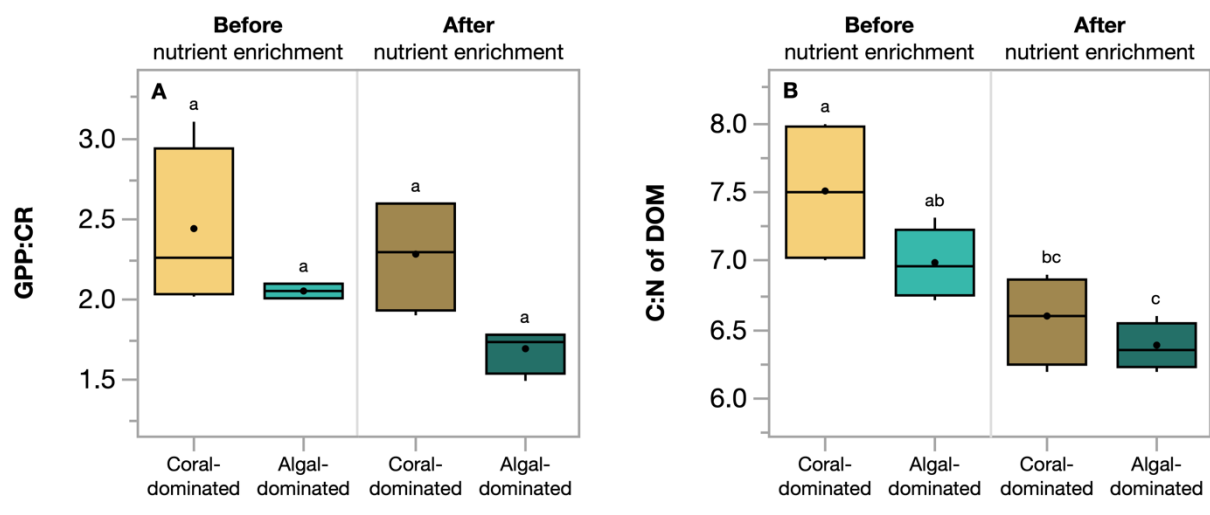


Figure 9.3 | Ratio of gross primary production to community respiration **(A)**, and the molar carbon to nitrogen (C:N) ratio of dissolved organic matter (DOM) **(B)** from coral- and algae-dominated communities, before and after nutrient enrichment. Boxplots show the median (line across a box), mean (dot in the box), first and third quartiles (upper and lower bounds of each box), and the minimum and maximum value (i.e., upper and lower whisker, respectively). Significant differences between community types (coral- vs algae-dominated) and treatment (before vs after nutrient enrichment) are represented with letters. Statistical details are in Table S9.2. Abbreviations: GPP = gross primary production; CR = community respiration; DOM = dissolved organic matter.

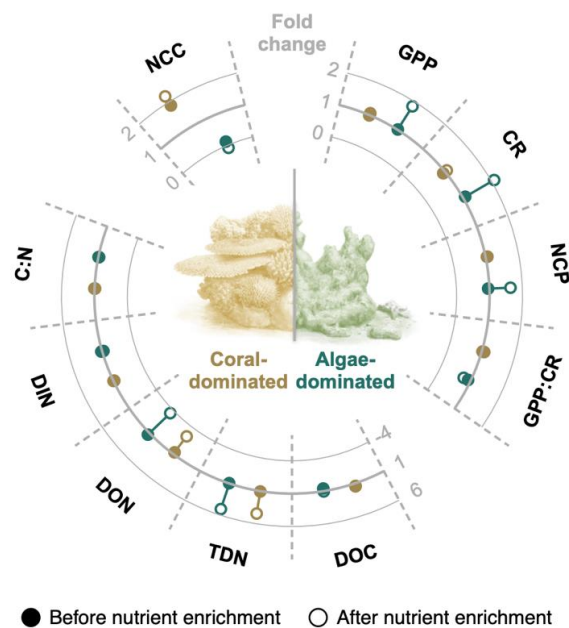


Figure 9.4 | Summary of changes of major biogeochemical response parameters in coral- (brown) and algae-dominated (green) reef communities before (full circle) and after (empty circle) nutrient enrichment. All changes are expressed as “fold change” relative to the combined mean of both communities before nutrient enrichment. Abbreviations: GPP = gross primary production; CR = community respiration; NCP = net community production; DOC = net dissolved organic carbon fluxes; TDN = net total dissolved nitrogen flux; DON = net dissolved organic nitrogen flux; DIN = net dissolved inorganic nitrogen flux; C:N = molar ratio of carbon to nitrogen of dissolved organic matter released by the communities; NCC = net community calcification. Empty circles (after nutrient enrichment) can be masked behind closed circles (before nutrient enrichment). Reefscape by Xavier Pita, scientific illustrator at KAUST, adapted from Roth et al. (2020)⁵² under the CC-BY 4.0 License.

9.5 Discussion

Similar Biogeochemical Processes in Coral- and Algae-Dominated Reef Communities under Ambient Nutrient Conditions

The present study suggests similar directions and magnitudes of major biogeochemical processes of coral- and algae-dominated communities at Abu Shosha reef in January 2018 (i.e., before nutrient enrichment was initiated). Specifically, both community-types showed similar rates of GPP, CR, and NCP. Although the rates are in line with the literature^{52,66,67}, they are in contrast with some studies reporting significantly higher organic C turnover with a greater potential for autotrophic biomass accumulation per planar square meter of the reef for algae- compared to coral-dominated communities^{29,30}. However, Roth et al. (2020)⁵² showed comparable productivity of coral- and algae-dominated communities in the central Red Sea, particularly during winter and spring (present study period). Further, we observed that both community-types were net sources of DOC, suggesting the production of extracellular photosynthates to outpace its consumption^{31,68}. However, while coral-dominated communities were net sources of DOC both during light and dark incubations, algae-dominated communities were strong sources of DOC during the light, and sinks of DOC during the dark (Table S9.1). The consumption of algal-derived C can be promoted by heterotrophic bacterioplankton^{69–71} or sponges and other filter feeders that are commonly associated with degraded reef habitats and feed on DOC or algal debris^{48,72,73}. In coral-dominated communities, we measured high net community calcification rates, consistent with the accretion of carbonate structures typical for tropical coral reefs^{23,24,74}. On the other hand, algae-dominated communities exhibited residual net calcification, which indicates the shift in the relative proportion of calcifying to non-calcifying organisms^{67,75}.

Quantifying N pathways in coral reefs is crucial to understand how productivity is supported despite low ambient nutrient concentrations⁷⁶. Both coral- and algae-dominated communities were net sources of DIN. The present study's flux rates generally fell within the range of *in situ* measurements elsewhere⁷⁴. Thereby, the effects of assimilation are likely masked by concurrent community-wide processes that produce DIN *in situ*. Cavities within coral reefs can be considerable DIN sources as sponges and other filter feeders utilize and remineralize DOM⁴⁷. Also, microbial communities can consume and transform organic N compounds^{77–79}, potentially increasing the community-wide DIN release into the environment. Other pathways, such as N₂ fixation²⁷ or heterotrophic feeding on particulate materials^{80,81} may also produce dissolved N that potentially mask the DIN uptake. The net production of DIN may also be ascribed to the mineralization of dissolved or particulate N. In support of this, we here report that both coral- and algae-dominated communities were, in fact, net sinks of DON. Corals, for example, use multiple ways to supply their N needs: they can efficiently take up and retain DIN^{82,83}, but also use DON in the form of amino acids and urea^{84,85}. In addition, a substantial fraction of DOC and DON produced by both corals and algae can be assimilated by sponges which subsequently convert it into and release it as particulate detritus⁷². Overall, balance between DIN production and DON consumption within both community-types highlights a balanced N cycle and the efficient reuse of resources in the studied reef under ambient nutrient conditions.

Varying Responses of Biogeochemical Processes to Nutrient Enrichment in Coral- and Algae-Dominated Communities

In situ nutrient enrichment had distinctive effects on benthic C, CaCO₃, and N dynamics in coral- and algae-dominated communities (Fig. 9.4). Thereby, the responses of the major biogeochemical processes to excess nutrients (N, specifically) were likely both a direct physiological reaction by N-limited key primary producers and an indirect response to shifts in the availability and quality of dissolved organic compounds for remineralization by bacteria and cryptic species within the communities.

Specifically, we observed significantly enhanced productivity by nutrient enrichment in algae-dominated communities, while no such changes were apparent in co-occurring communities dominated by corals. The increased productivity of algae-dominated communities with nutrient enrichment aligns with many previous findings⁸⁶⁻⁸⁸. Complementing these results, Karcher et al. (2020)⁶³ highlighted concomitant increases of N (+39%) and C_{org} (+33%) content in turf algae (the dominant key functional group within the "algae-dominated" communities) after eight weeks of the same *in situ* nutrient enrichment, suggesting that N was indeed a limiting nutrient for algal growth in the current experiments^{86,89} (potential phosphorus (P) limitation discussed at the end of this section). In otherwise oligotrophic reef environments, benthic algae can have high uptake rates of nutrients per unit biomass, benefiting from episodic inputs of N to coral reefs⁹⁰. However, while NCP increased by >50%, an even stronger response in CR (100% increase) was apparent. As a result, algae-dominated communities had a greater potential for autotrophic biomass accumulation both in absolute numbers and relative to the "before nutrient enrichment" measurements; however, the proportionally greater increase in CR resulted in a lowered GPP:CR ratio, indicative of an overall faster turnover of organic C through respiratory processes. Algae-dominated reef structures provide habitat for numerous heterotrophs that rely on algal biomass, fueling community-wide respiration. Particularly heterotrophic bacteria within these communities remineralize labile DOC released by algae⁶⁹⁻⁷¹ and sponges and other filter feeders within the reef matrix feed on algal debris and DOC^{48,72}. Although we did not observe any change in the net DOC flux integrated over 24 h, we measured both an increase in DOC production during light incubations, and a concomitant increase in DOC consumption during dark incubations, such as the release in the light was effectively balanced by consumption in the dark. In coral-dominated communities, neither GPP, CR, nor NCP responded to excess N. Although this is in contrast to previous reports (e.g., Koop et al (2001)⁹¹), El-Khaled et al. (2020)⁵⁹ showed that individual corals of the same experiment indeed did not increase primary production during single organism incubations. Likewise, Karcher et al. (2020)⁶³ showed that these corals incorporated excess N into the host tissue, however, that corals did not utilize N for the production of C_{org}. These results support that N was not a limiting factor for corals in the present experiments. We find two plausible explanations for this observation. Firstly, additional nutrient sources may have contributed to supporting photosynthesis even under low ambient nutrient concentrations (<0.5 μmol DIN L⁻¹). Corals and other benthic organisms contribute to benthic N inputs by N₂ fixation during nutrient-depleted conditions, suggesting a strong biogeochemical coupling between diazotrophy and the reef C cycle²⁷. In addition, heterotrophic feeding may complement N demands by

corals⁹². Secondly, the previously observed P limitation in coastal Red Sea waters^{71,93,94} may cause coral-dominated communities to be limited by P rather than N⁹³, restraining the zooxanthellae's N uptake and subsequent coral growth^{34,95}. In contrast to the evident increase in N availability in our experiments, P provided by the fertilizer did not alter the PO_3^{-4} concentration in the seawater surrounding the communities. While we cannot reconstruct the fate of P from the fertilizer pins with the current experimental design, the communities themselves, reef sediments⁹⁶ or organisms in the water column and the surrounding benthos could have contributed to the rapid depletion of P⁹⁷.

We observed neither a change in the direction nor magnitude of DOC fluxes from coral-dominated communities after nutrient enrichment. This aligns with the common assumption that the release of DOC is closely coupled to productivity⁹⁸ (although, in corals, DOC release can also be stimulated by stress or as a protective mechanism⁹⁹). Moreover, and unlike previously suggested³⁷, we did not observe any change in calcification of coral-dominated communities with moderate nutrient enrichment, neither during light nor dark incubations. The increased competition for dissolved inorganic carbon (DIC) between the coral host and its endosymbionts under elevated nutrient concentrations can directly drive the reported lower calcification rates in other studies¹⁰⁰. Drawing from the same DIC pool will result in one process being enhanced (likely productivity), while the other is suppressed (i.e., calcification). However, here, we did not see a positive effect of nutrients on productivity, and, likewise, there was no associated change in calcification. In stark contrast to that, we not only observed a decrease in calcification rates in algae-dominated communities but a shift from net calcification to net dissolution in algae-dominated communities with nutrient enrichment. The decline in calcification in response to nutrient addition could be induced by a combination of decreasing calcification rates from encrusting algae and invertebrates and increasing bioerosion or dissolution. Under field conditions, high bioerosion rates correlated with high nutrient conditions, likely because many bioeroders are filter-feeding invertebrates or photosynthetic endoliths^{101,102}. Dissolution of CaCO_3 could also occur due to local CO_2 -induced acidification caused by natural respiration of benthic fauna and flora at night, as observed in other coastal habitats^{103,104}. The doubling of respiration rates within algae-dominated communities may support the latter, especially.

To the best of our knowledge, we here present the first results of the impacts of short-term nutrient enrichment on major N fluxes (specifically TDN, DIN, and DON) of intact reef communities in the natural environment. Our findings indicate that increases in environmental N can alter the critical balance of nitrogenous compounds being taken up and released by both types of reef communities. Specifically, nutrient enrichment caused a reversal of DON fluxes, that is, coral- and algae-dominated communities shifted from being net DON sinks (before nutrient enrichment) to net DON sources (after nutrient enrichment). The absolute increase was, however, significantly higher in algae-dominated communities. We find several possible explanations for how DON was produced in excess, or how its consumption was hampered. First, the export of organic N by reef biota can be enhanced by primary production and the availability of N relative to P. This is supported by results from a study measuring the distribution and partitioning of DON on a Pacific reef showing that DON in the water column increases when productivity

and the DIN:DIP ratio are high¹⁰⁵. Secondly, DIN from anthropogenic sources (in our case, the fertilizer) can increase internal N availability (shown by the complementary study by Karcher et al. (2020)⁶³) and induce DON release¹⁰⁶. Likewise, as a secondary effect, increased environmental N availability can enhance N₂ fixation⁵⁹, which in turn increases the internal N availability and induces DON release¹⁰⁶. Lastly, degradation experiments of reef organic matter showed that DON degradation could be slower than that of DOC, and, therefore, the C:N ratio of organic matter decreases¹⁰⁷. Indeed, we detected significant reductions of the C:N ratio of DOM retrieved from the communities after nutrient enrichment, indicating that DOC relative to DON was consumed faster or released less. In conclusion, after nutrient enrichment, the reversal of DON fluxes led to benthic reef communities being TDN sources rather than having balanced DIN and DON fluxes that leaves the overall TDN flux close to zero. The observed imbalance of the uptake of inorganic and release of organic nitrogenous compounds grants further investigation, especially with regards to cascading microbial-mediated, bottom-up effects on the reefs trophodynamics^{72,108}.

Ecological Implications and Outlook

We showed that *in situ* nutrient enrichment did not directly affect organic C budgets and calcification of coral-dominated communities in their natural environment. In contrast, excess nutrients significantly enhanced productivity, respiration, and caused a dissolution of the carbonate framework in co-occurring algae-dominated communities of the same reef. These results may have important implications for the competitive relationship of coral- and algae-dominated communities and the ecosystem services these communities can provide. Specifically, on reefs where the two community-types co-occur, algae-dominated communities may have a higher potential for biomass accumulation that can enhance space occupation and rapid succession on bare reef substrates^{109,110}. The loss of the structurally complex CaCO₃ reef framework and an increased space occupation by algae may hamper the replenishment of adult coral populations due to recruitment inhibition through limited habitat complexity and grazing pressure. Together, this may restrain reef recovery⁶⁰ and the high biodiversity characteristic of tropical coral reef ecosystems¹¹¹. However, some of the results also open questions for future research directions, particularly highlighting the complexity of and the limited knowledge about reef processes at a community level. For example, the underlying mechanisms of the net dissolution of the reef framework in algae-dominated communities after nutrient enrichment remain highly speculative (e.g., local CO₂-induced acidification due to higher microbial respiration rates)^{103,104} and should be addressed in the future. Moreover, the increased DOC turnover (increased release during light and concomitant increased consumption in the dark) in algae-dominated communities may indicate a higher activity of opportunistic microbes and other heterotrophs feeding on DOC. Future studies should thus assess if nutrient enrichment in coral reefs dominated by algae can shift the microbial community towards opportunistic pathogens, which can further adversely influence the coral-algal competition³². Also, intriguingly, both coral- and algae-dominated communities were sources of DIN at all times, even before experimental nutrient addition. Whether DIN producing processes masked N uptake by autotroph organisms of the communities, or if other elements (e.g., P) limited their growth

remains unresolved from the current experiment. However, it highlights a general knowledge gap on organic and inorganic N and P fluxes from whole reef communities in the natural environment; particularly so under the influence of anthropogenic nutrient addition. Overall, the results highlight that complex interactions of community shifts and nutrient pollution occur in the natural environment, which can likely not be resolved by laboratory or mesocosm studies. Nutrient pollution may amplify effects of community shifts on key ecosystem services of coral reefs, possibly leading to a loss of structurally complex habitats with carbonate dissolution and altered nutrient recycling.

9.6 References

1. Hatcher, B. G. Coral-Reef Primary Productivity - a Hierarchy of Pattern and Process. *Trends Ecol. Evol.* **5**, 149–155 (1990).
2. LaJeunesse, T. C. *et al.* Systematic Revision of Symbiodiniaceae Highlights the Antiquity and Diversity of Coral Endosymbionts. *Curr. Biol.* **28**, 2570–2580.e6 (2018).
3. Muscatine, L. & Porter, J. W. Reef Corals: Mutualistic Symbioses Adapted to Nutrient-Poor Environments. *Bioscience* **27**, 454–460 (1977).
4. Odum, H. T. & Odum, E. P. Trophic Structure and Productivity of a Windward Coral Reef Community on Eniwetok Atoll. *Ecol. Monogr.* **25**, 291–320 (1955).
5. Wild, C. *et al.* Coral mucus functions as an energy carrier and particle trap in the reef ecosystem. *Nature* **428**, 66–70 (2004).
6. De Goeij, J. M. *et al.* Surviving in a marine desert: The sponge loop retains resources within coral reefs. *Science (80-.)*. **342**, 108–110 (2013).
7. Yellowlees, D., Rees, T. A. V. & Leggat, W. Metabolic interactions between algal symbionts and invertebrate hosts. *Plant, Cell Environ.* **31**, 679–694 (2008).
8. Naumann, M. S., Bednarz, V. N., Ferse, S. C. A., Niggel, W. & Wild, C. Monitoring of coastal coral reefs near Dahab (Gulf of Aqaba, Red Sea) indicates local eutrophication as potential cause for change in benthic communities. *Environ. Monit. Assess.* **187**, 44 (2015).
9. D'Angelo, C. & Wiedenmann, J. Impacts of nutrient enrichment on coral reefs: New perspectives and implications for coastal management and reef survival. *Curr. Opin. Environ. Sustain.* **7**, 82–93 (2014).
10. Wiedenmann, J. *et al.* Nutrient enrichment can increase the susceptibility of reef corals to bleaching. *Nat. Clim. Chang.* **3**, 160–164 (2013).
11. Hughes, T. P. *et al.* Spatial and temporal patterns of mass bleaching of corals in the Anthropocene. *Science (80-.)*. **359**, 80–83 (2018).
12. Pandolfi, J. M. *et al.* Global trajectories of the long-term decline of coral reef ecosystems. *Science (80-.)*. **301**, 955–958 (2003).
13. Hughes, T. P. *et al.* Global warming transforms coral reef assemblages. *Nature* **556**, 492–496 (2018).
14. McCook, L. J., Jompa, J. & Diaz-Pulido, G. A. Competition between corals and algae on coral reefs: a review of evidence and mechanisms. *Coral Reefs* **19**, 400–417 (2001).
15. Anton, A. *et al.* Differential thermal tolerance between algae and corals may trigger the proliferation of algae in coral reefs. *Glob. Chang. Biol.* 0–2 (2020). doi:10.1111/gcb.15141
16. Ninio, R. & Meekan, M. G. Spatial patterns in benthic communities and the dynamics of a mosaic ecosystem on the Great Barrier Reef, Australia. *Coral Reefs* **21**, 95–104 (2002).
17. Tkachenko, K. S., Wu, B. J., Fang, L. S. & Fan, T. Y. Dynamics of a coral reef community after mass mortality of branching *Acropora* corals and an outbreak of anemones. *Mar. Biol.* **151**, 185–194 (2007).
18. Lin, Y. V. & Denis, V. Acknowledging differences: Number, characteristics, and distribution of marine benthic communities along Taiwan coast. *Ecosphere* **10**, (2019).
19. Bellwood, D. R. *et al.* Coral reef conservation in the Anthropocene: Confronting spatial mismatches and prioritizing functions. *Biol. Conserv.* **236**, 604–615 (2019).

20. Hughes, T. P. *et al.* Coral reefs in the Anthropocene. *Nature* **546**, 82–90 (2017).
21. Wild, C. *et al.* Climate change impedes reef ecosystem engineers. *Mar. Freshw. Res.* **62**, 205–215 (2011).
22. Graham, N. A. J. Habitat complexity: Coral structural loss leads to fisheries declines. *Curr. Biol.* **24**, R359–R361 (2014).
23. Gattuso, J. P., Frankignoulle, M. & Smith, S. V. Measurement of community metabolism and significance in the coral reef CO₂ source-sink debate. *Proc. Natl. Acad. Sci. U. S. A.* **96**, 13017–13022 (1999).
24. Gattuso, J.-P., Frankignoulle, M. & Wollast, R. Carbon and Carbonate Metabolism in Coastal Aquatic Ecosystems. *Annu. Rev. Ecol. Syst.* **29**, 405–434 (1998).
25. Rusch, A., Huettel, M., Wild, C. & Reimers, C. E. Benthic oxygen consumption and organic matter turnover in organic-poor, permeable shelf sands. *Aquat. Geochemistry* **12**, 1–19 (2006).
26. Naumann, M. S. *et al.* Budget of coral-derived organic carbon in a fringing coral reef of the Gulf of Aqaba, Red Sea. *J. Mar. Syst.* **105–108**, 20–29 (2012).
27. Cardini, U. *et al.* Budget of Primary Production and Dinitrogen Fixation in a Highly Seasonal Red Sea Coral Reef. *Ecosystems* **19**, 771–785 (2016).
28. Rix, L. *et al.* Seasonality in dinitrogen fixation and primary productivity by coral reef framework substrates from the northern Red Sea. *Mar. Ecol. Prog. Ser.* **533**, 79–92 (2015).
29. Fong, P. & Paul, V. J. Coral Reef Algae. in *Coral Reefs: An Ecosystem in Transition* (eds. Dubinsky, Z. & Stambler, N.) 241–272 (Springer, Dordrecht, 2011). doi:10.1007/978-94-007-0114-4_17
30. Kelly, E. L. A. *et al.* A budget of algal production and consumption by herbivorous fish in an herbivore fisheries management area, Maui, Hawaii. *Ecosphere* **8**, ecs2.1899 (2017).
31. Nelson, C. E. *et al.* Coral and macroalgal exudates vary in neutral sugar composition and differentially enrich reef bacterioplankton lineages. *ISME J.* **7**, 962–79 (2013).
32. Haas, A. F. *et al.* Global microbialization of coral reefs. *Nat. Microbiol.* 16042 (2016). doi:10.1038/nmicrobiol.2016.42
33. Fabricius, K. E. Effects of terrestrial runoff on the ecology of corals and coral reefs: Review and synthesis. *Mar. Pollut. Bull.* **50**, 125–146 (2005).
34. Nitrogen eutrophication particularly promotes turf algae in coral reefs of the central Red Sea.
35. Ferrier-Pagès, C., Gattuso, J. P., Dallot, S. & Jaubert, J. Effect of nutrient enrichment on growth and photosynthesis of the zooxanthellate coral *Stylophora pistillata*. *Coral Reefs* **19**, 103–113 (2000).
36. Hall, E. R., Muller, E. M., Goulet, T., Bellworthy, J. & Ritchie, K. B. Eutrophication may compromise the resilience of the Red Sea coral *Stylophora pistillata* to global change. *Mar. Pollut. Bull.* **131**, 701–711 (2018).
37. Silbiger, N. J. *et al.* Nutrient pollution disrupts key ecosystem functions on coral reefs. *Proc. R. Soc. B Biol. Sci.* **285**, 20172718 (2018).
38. Loya, Y., Lubinevsky, H., Rosenfeld, M. & Kramarsky-Winter, E. Nutrient enrichment caused by in situ fish farms at Eilat, Red Sea is detrimental to coral reproduction. *Mar. Pollut. Bull.* **49**, 344–353 (2004).
39. Burkepille, D. E. *et al.* Nitrogen Identity Drives Differential Impacts of Nutrients on Coral Bleaching and Mortality. *Ecosystems* (2019). doi:10.1007/s10021-019-00433-2

40. DeCarlo, T. M. *et al.* Nutrient-supplying ocean currents modulate coral bleaching susceptibility. *Sci. Adv.* **6**, eabc5493 (2020).
41. El-Khaled, Y. C. *et al.* Simultaneous Measurements of Dinitrogen Fixation and Denitrification Associated With Coral Reef Substrates : Advantages and Limitations of a Combined Acetylene Assay. *Front. Mar. Sci.* **7**, 411 (2020).
42. McCook, L. J. Macroalgae, nutrients and phase shifts on coral reefs: Scientific issues and management consequences for the Great Barrier Reef. *Coral Reefs* **18**, 357–367 (1999).
43. Roth, F. *et al.* *An in situ approach for measuring biogeochemical fluxes in structurally complex benthic communities. Methods in Ecology and Evolution* (2019). doi:10.1111/2041-210X.13151
44. Walsh, K. *et al.* Aura-biomes are present in the water layer above coral reef benthic macro-organisms. *PeerJ* **5**, e3666 (2017).
45. Tout, J. *et al.* Variability in microbial community composition and function between different niches within a coral reef. *Microb. Ecol.* **67**, 540–552 (2014).
46. Richter, C. & Wunsch, M. Cavity-dwelling suspension feeders in coral reefs - A new link in reef trophodynamics. *Mar. Ecol. Prog. Ser.* **188**, 105–116 (1999).
47. Richter, C., Wunsch, M., Rasheed, M., Kötter, I. & Badran, M. I. Endoscopic exploration of Red Sea coral reefs reveals dense populations of cavity-dwelling sponges. *Nature* **413**, 726–730 (2001).
48. Rix, L. *et al.* Reef sponges facilitate the transfer of coral-derived organic matter to their associated fauna via the sponge loop. **589**, 85–96 (2018).
49. D'Angelo, C. & Wiedenmann, J. Impacts of nutrient enrichment on coral reefs: New perspectives and implications for coastal management and reef survival. *Curr. Opin. Environ. Sustain.* **7**, 82–93 (2014).
50. Szmant, A. M. Nutrient Enrichment on Coral Reefs: Is It a Major Cause of Coral Reef Decline? *Estuaries* **25**, 743–766 (2002).
51. Peña-García, D., Ladwig, N., Turki, A. J. & Mudarris, M. S. Input and dispersion of nutrients from the Jeddah Metropolitan Area, Red Sea. *Mar. Pollut. Bull.* **80**, 41–51 (2014).
52. Roth, F. *et al.* *High summer temperatures amplify functional differences between coral- and algae-dominated reef communities. Ecology* (2020). doi:10.1002/ecy.3226
53. Falkenberg, L. J., Russell, B. D. & Connell, S. D. Contrasting resource limitations of marine primary producers: Implications for competitive interactions under enriched CO₂ and nutrient regimes. *Oecologia* **172**, 575–583 (2013).
54. Wheeler, G. S. Minimal increase in larval and adult performance of the biological control agent *Oxyops vitiosa* when fed *Melaleuca quinquenervia* leaves of different nitrogen levels. *Biol. Control* **26**, 109–116 (2003).
55. Marsden, E. & Torgerson, C. J. Single group, pre- and post-test research designs: Some methodological concerns. *Oxford Rev. Educ.* **38**, 583–616 (2012).
56. Albright, R. *et al.* Carbon dioxide addition to coral reef waters suppresses net community calcification. *Nature* **555**, 516–519 (2018).
57. Albright, R. *et al.* Reversal of ocean acidification enhances net coral reef calcification. *Nature* **531**, 362–365 (2016).
58. Roth, F. Consequences of Coral-Algal Phase Shifts for Tropical Reef Ecosystem Functioning. (King Abdullah University of Science and Technology, 2019). doi:10.25781/KAUST-K6KP2

59. El-Khaled, Y. *et al.* In situ eutrophication stimulates dinitrogen fixation, denitrification, and productivity in Red Sea coral reefs. *Mar. Ecol. Prog. Ser.* **645**, 55–66 (2020).
60. Roth, F. *et al.* Coral reef degradation affects the potential for reef recovery after disturbance. *Mar. Environ. Res.* **142**, 48–58 (2018).
61. Zeebe, R. E. & Wolf-Gladrow, D. A. *CO₂ in Seawater: Equilibrium, Kinetics, Isotopes*. (Elsevier Science, 2001).
62. Wolf-Gladrow, D. A., Zeebe, R. E., Klaas, C., Körtzinger, A. & Dickson, A. G. Total alkalinity: The explicit conservative expression and its application to biogeochemical processes. *Mar. Chem.* **106**, 287–300 (2007).
63. Karcher, D. B. *et al.* Nitrogen eutrophication particularly promotes turf algae in coral reefs of the central Red Sea. *PeerJ* **8**, e8737 (2020).
64. Clarke, K. & Gorley, R. PRIMER V6: user manual-tutorial. (2006).
65. Anderson, M. J. & Walsh, D. C. I. PERMANOVA, ANOSIM, and the Mantel test in the face of heterogeneous dispersions: What null hypothesis are you testing? *Ecol. Monogr.* **83**, 557–574 (2013).
66. Albright, R., Benthuisen, J., Cantin, N., Caldeira, K. & Anthony, K. Coral reef metabolism and carbon chemistry dynamics of a coral reef flat. *Geophys. Res. Lett.* **42**, 3980–3988 (2015).
67. Albright, R., Langdon, C. & Anthony, K. R. N. Dynamics of seawater carbonate chemistry, production, and calcification of a coral reef flat, Central Great Barrier Reef. *Biogeosciences Discuss.* **10**, 7641–7676 (2013).
68. Quinlan, Z. A. *et al.* Fluorescent organic exudates of corals and algae in tropical reefs are compositionally distinct and increase with nutrient enrichment. *Limnol. Oceanogr. Lett.* **3**, 331–340 (2018).
69. Haas, A. F. *et al.* Influence of coral and algal exudates on microbially mediated reef metabolism. *PeerJ* **1**, e108 (2013).
70. Nelson, C. E., Alldredge, A. L., McCliment, E. A., Amaral-Zettler, L. A. & Carlson, C. A. Depleted dissolved organic carbon and distinct bacterial communities in the water column of a rapid-flushing coral reef ecosystem. *ISME J.* **5**, 1374–1387 (2011).
71. Silva, L. *et al.* Heterotrophic bacterioplankton responses in coral- and algae-dominated Red Sea reefs show they might benefit from future regime shift. *Sci. Total Environ.* **751**, 141628 (2021).
72. Rix, L. *et al.* Differential recycling of coral and algal dissolved organic matter via the sponge loop. *Funct. Ecol.* **31**, 778–789 (2017).
73. Wooster, M. K., McMurray, S. E., Pawlik, J. R., Morán, X. A. G. & Berumen, M. L. Feeding and respiration by giant barrel sponges across a gradient of food abundance in the Red Sea. *Limnol. Oceanogr.* **64**, 1790–1801 (2019).
74. Atkinson, M. J. & Falter, J. L. *Coral reefs. 40 - 64. In Book: Biogeochemistry of Marine Systems* (Blackwell Publishing, 2003).
75. Takeshita, Y. *et al.* Assessment of net community production and calcification of a coral reef using a boundary layer approach. *J. Geophys. Res. Ocean.* **121**, 5655–5671 (2016).
76. D’Elia, C. F. & Wiebe, W. J. Biogeochemical nutrient cycles in coral reef ecosystems. in *Ecosystems of the World 25: Coral Reefs* (ed. Dubinsky, Z.) 49–74 (Elsevier, 1990).
77. Moulton, O. M. *et al.* Microbial associations with macrobiota in coastal ecosystems: Patterns and implications for nitrogen cycling. *Front. Ecol. Environ.* **14**, 200–208 (2016).

78. Yahel, G., Sharp, J. H., Marie, D., Häse, C. & Genin, A. In situ feeding and element removal in the symbiont-bearing sponge *Theonella swinhoei*: Bulk DOC is the major source for carbon. *Limnol. Oceanogr.* **48**, 141–149 (2003).
79. Pfister, C. A. & Altabet, M. A. Enhanced microbial nitrogen transformations in association with macrobiota from the rocky intertidal. *Biogeosciences* **16**, 193–206 (2019).
80. Ribes, M., Coma, R., Atkinson, M. & Kinzie, R. Particle removal by coral reef communities: picoplankton is a major source of nitrogen. *Mar. Ecol. Prog. Ser.* **257**, 13–23 (2003).
81. Houlbrèque, F. & Ferrier-Pagès, C. Heterotrophy in tropical scleractinian corals. *Biol. Rev.* **84**, 1–17 (2009).
82. Grover, R., Maguer, J.-F., Allemand, D. & Ferrier-Pagès, C. Nitrate uptake in the scleractinian coral *Stylophora pistillata*. *Limnol. Oceanogr.* **48**, 2266–2274 (2003).
83. Grover, R., Maguer, J. F., Reynaud-Vaganay, S. & Ferrier-Pagès, C. Uptake of ammonium by the scleractinian coral *Stylophora pistillata*: Effect of feeding, light, and ammonium concentrations. *Limnol. Oceanogr.* **47**, 782–790 (2002).
84. Ferrier, M. D. Net uptake of dissolved free amino acids by four scleractinian corals. *Coral Reefs* **10**, 183–187 (1991).
85. Hoegh-Guldberg, O. & Williamson, J. Availability of two forms of dissolved nitrogen to the coral *Pocillopora damicornis* and its symbiotic zooxanthellae. *Mar. Biol.* **133**, 561–570 (1999).
86. McCook, L. J. Macroalgae, nutrients and phase shifts on coral reefs: scientific issues and management consequences for the Great Barrier Reef. *Coral Reefs* **18**, 357–367 (1999).
87. Littler, M. M., Littler, D. S., Brooks, B. L. & Lapointe, B. E. Nutrient manipulation methods for coral reef studies : A critical review and experimental field data. *J. Exp. Mar. Bio. Ecol.* **336**, 242–253 (2006).
88. Burkepille, D. E. & Hay, M. E. Nutrient versus herbivore control of macroalgal community development and coral growth on a Caribbean reef. *Mar. Ecol. Prog. Ser.* **389**, 71–84 (2009).
89. Hatcher, B. G. & Larkum, A. W. D. An experimental analysis of factors controlling the standing crop of the epilithic algal community on a coral reef. *J. Exp. Mar. Bio. Ecol.* **69**, 61–84 (1983).
90. den Haan, J. *et al.* Nitrogen and phosphorus uptake rates of different species from a coral reef community after a nutrient pulse. *Sci. Rep.* **6**, 1–13 (2016).
91. Koop, K. *et al.* ENCORE: The effect of nutrient enrichment on coral reefs. Synthesis of results and conclusions. *Mar. Pollut. Bull.* **42**, 91–120 (2001).
92. Gustafsson, M. S. M., Baird, M. E. & Ralph, P. J. The interchangeability of autotrophic and heterotrophic nitrogen sources in Scleractinian coral symbiotic relationships: A numerical study. *Ecol. Modell.* **250**, 183–194 (2013).
93. Ezzat, L., Maguer, J.-F., Grover, R. & Ferrier-Pagès, C. Limited phosphorus availability is the Achilles heel of tropical reef corals in a warming ocean. *Sci. Rep.* **6**, 31768 (2016).
94. Silva, L. *et al.* Low Abundances but High Growth Rates of Coastal Heterotrophic Bacteria in the Red Sea. *Front. Microbiol.* **9**, (2019).
95. Godinot, C., Grover, R., Allemand, D. & Ferrier-Pages, C. High phosphate uptake requirements of the scleractinian coral *Stylophora pistillata*. *J. Exp. Biol.* **214**, 2749–2754 (2011).
96. Millero, F., Huang, F., Zhu, X., Liu, X. & Zhang, J.-Z. Adsorption and Desorption of Phosphate on Calcite and Aragonite in Seawater. *Aquat. Geochemistry* **7**, 33–56 (2001).

97. Cuet, P. *et al.* CNP budgets of a coral-dominated fringing reef at La Réunion, France: Coupling of oceanic phosphate and groundwater nitrate. *Coral Reefs* **30**, 45–55 (2011).
98. Haas, A. F. *et al.* Effects of Coral Reef Benthic Primary Producers on Dissolved Organic Carbon and Microbial Activity. *PLoS One* **6**, e27973 (2011).
99. Niggli, W., Glas, M. & Laforsch, C. First evidence of coral bleaching stimulating organic matter release by reef corals. in *Proceedings of the 11th International Coral Reef Symposium* (ed. Riegl, B.) 905–910 (2009).
100. Marubini, F. & Davies, P. S. Nitrate increases zooxanthellae population density and reduces skeletogenesis in corals. *Mar. Biol.* **127**, 319–328 (1996).
101. DeCarlo, T. M. *et al.* Coral macrobioerosion is accelerated by ocean acidification and nutrients. *Geology* **43**, 7–10 (2015).
102. Lubarsky, K. A., Silbiger, N. J. & Donahue, M. J. Effects of submarine groundwater discharge on coral accretion and bioerosion on two shallow reef flats. *Limnol. Oceanogr.* **63**, 1660–1676 (2018).
103. Kwiatkowski, L. *et al.* Nighttime dissolution in a temperate coastal ocean ecosystem increases under acidification. *Sci. Rep.* **6**, 22984 (2016).
104. Saderne, V. *et al.* Total alkalinity production in a mangrove ecosystem reveals an overlooked Blue Carbon component. *Limnol. Oceanogr. Lett.* (2020). doi:10.1002/lol2.10170
105. Miyajima, T., Hata, H., Umezawa, Y., Kayanne, H. & Koike, I. Distribution and partitioning of nitrogen and phosphorus in a fringing reef lagoon of Ishigaki Island, northwestern Pacific. *Mar. Ecol. Prog. Ser.* **341**, 45–57 (2007).
106. Thibodeau, B. *et al.* Heterogeneous dissolved organic nitrogen supply over a coral reef: First evidence from nitrogen stable isotope ratios. *Coral Reefs* **32**, 1103–1110 (2013).
107. Suzuki, Y. & Casareto, B. E. *The role of dissolved organic nitrogen (DON) in coral biology and reef ecology. Coral Reefs: An Ecosystem in Transition* (2011). doi:10.1007/978-94-007-0114-4_14
108. Silveira, C. B. *et al.* Microbial and sponge loops modify fish production in phase-shifting coral reefs. *Environ. Microbiol.* **17**, 3832–3846 (2015).
109. Stuhldreier, I., Bastian, P., Schöning, E. & Wild, C. Effects of simulated eutrophication and overfishing on algae and invertebrate settlement in a coral reef of Koh Phangan, Gulf of Thailand. *Mar. Pollut. Bull.* **92**, 35–44 (2015).
110. Roth, F., Stuhldreier, I., Sánchez-Noguera, C., Morales-Ramírez, T. & Wild, C. Effects of simulated overfishing on the succession of benthic algae and invertebrates in an upwelling-influenced coral reef of Pacific Costa Rica. *J. Exp. Mar. Bio. Ecol.* **468**, 55–66 (2015).
111. Bellwood, D. R. Regional-Scale Assembly Rules and Biodiversity of Coral Reefs. *Science (80-.).* **292**, 1532–1535 (2001).

Chapter 10

Chapter 10 | High plasticity of nitrogen fixation and denitrification of common coral reef substrates in response to nitrate availability

Yusuf C. El-Khaled^{1*}, Rassil Nafeh¹, Florian Roth^{2,3,4}, Nils Rådecker^{2,5,6}, Denis B. Karcher^{1,7}, Burton H. Jones², Christian R. Woolstra^{2,5}, Christian Wild¹

¹Marine Ecology Department, Faculty of Biology and Chemistry, University of Bremen, 28359 Bremen, Germany

²Red Sea Research Center, King Abdullah University of Science and Technology (KAUST), 23995 Thuwal, Saudi-Arabia

³Baltic Sea Centre, Stockholm University, 10691 Stockholm, Sweden

⁴Faculty of Biological and Environmental Sciences, Tvärminne Zoological Station, University of Helsinki, 00014 Helsinki, Finland

⁵Department of Biology, University of Konstanz, 78457 Konstanz, Germany

⁶Laboratory for Biological Geochemistry, School of Architecture, Civil and Environmental Engineering, École Polytechnique Fédérale de Lausanne (EPFL), CH-1015 Lausanne, Switzerland

⁷Australian National Centre for the Public Awareness of Science, Australian National University, ACT 2601 Canberra, Australia

*corresponding author: yek2012@uni-bremen.de

10.1 | Abstract

Nitrogen cycling in coral reefs may be affected by nutrient availability, but knowledge about concentration-dependent thresholds that modulate dinitrogen fixation and denitrification is missing. We determined the effects of different nitrate concentrations (ambient, 1, 5, 10 μM) on both processes under two light scenarios (i.e., day and night) using a combined acetylene assay for two common benthic reef substrates, i.e., turf algae and coral rubble. For both substrates, dinitrogen fixation rates peaked at 5 μM nitrate addition in light, whereas denitrification activity was highest at 10 μM nitrate addition in the dark. A near-complete collapse of dinitrogen fixation concurrent with a 76-fold increase in denitrification activity was observed for coral rubble at 10 μM nitrate in the dark, suggesting potential threshold responses linked to the nutritional state of the community. We conclude that dynamic nitrogen cycling activity may help stabilise nitrogen availability in microbial communities associated with coral reef substrates.

Keywords: Coral reefs | Nutrient pollution | Eutrophication | Nitrogen Cycling | Turf Algae | Coral Rubble

A modified version of this chapter has been submitted to *Marine Pollution Bulletin* and currently in review

10.2 | Introduction

In the Anthropocene, almost all marine ecosystems worldwide have experienced a range of threats that are relatable to human activities¹, and those anthropogenic impacts are increasing². Consequences of anthropogenic stressors are well-documented, ranging from ecosystem to individual and cellular levels. Eutrophication, as an evolving consequence of increasing coastal population³, is among the most impactful local stressors. This is particularly true for ecosystems adapted to oligotrophic, i.e., nutrient-poor environmental conditions, such as tropical coral reefs, where nitrogen (N) is a key factor limiting primary production⁴⁻⁶.

The acquisition, retention and disposal of N are of particular importance in coral reefs, which is partly moderated by microbial N cycling⁷. More specifically, the interplay between two counteracting N cycling pathways, i.e., dinitrogen (N₂) fixation and denitrification contribute to maintaining a stable N availability, and ultimately, ecosystem functioning. N₂ fixation is the conversion of atmospheric N₂ into bioavailable ammonium by prokaryotic microbes (diazotrophs) serving as a potential alternative nutrient source in times of N scarcity that fluctuates seasonally and in response to varying environmental conditions⁸. In contrast, the microbially performed conversion of nitrate to atmospheric N₂ referred to as denitrification, effectively removes excess N from the reef system. The relief of N could be vital to coral reef functioning during excess N availability, particularly under eutrophic conditions⁷.

Eutrophication divergently affects N fluxes in coral reef environments on the community (Koop et al. (2001)⁹, Roth et al. in review) and organism level^{10,11}. For example, Koop et al. (2001)⁹ reported consistently lower N₂ fixation activities and concurrent higher denitrification rates in reef patches under elevated nutrient availability (up to 20 μM N), Roth et al. (in review) reported a shift in small, distinct coral reef communities from a sink to a source of N due to nutrient pollution. A recent study, however, demonstrated that moderately (1-2 μM N) elevated nutrient concentrations may stimulate both N₂ fixation and denitrification in turf algae, reef sediments and hard corals¹¹, suggesting ambivalent responses of N fluxes to nutrient pollution. Consequentially, certain nutrient concentration thresholds that regulate the suppression or stimulation of both N cycling pathways might exist but have not been determined in coral reef environments yet. Additionally, all aforementioned studies have performed their experimental eutrophication experiments on a relatively large time-scale ranging from months (El-Khaled et al (2020)¹¹, Roth et al. in review) to years¹². Due to these timescales, these studies do not allow for disentangle the indirect consequences of potential community shifts from the direct consequences of altered N availability on the N cycling pathways themselves. Studies investigating responses on a shorter time scale in coral reefs, however, are non-existent. Rapid responses of both N cycling pathways to runoff events (and a subsequent increase in inorganic N) were previously observed in intertidal mudflats covered by microbial mats¹³. Hence, we hypothesise decreasing N₂ fixation and increasing denitrification rates with increasing nitrate availability.

For this purpose, we investigated the plasticity of coral reef-associated N₂ fixation and denitrification in response to inorganic N availability of two coral reef substrates (i.e., heterogeneous algal assemblages and coral rubble), that commonly increase in their abundance when coral-algae phase shifts occur¹⁴⁻¹⁶ and, thus,

may have an impact on ‘post phase shift’ reef-wide N budgets (El-Khaled et al. in review). The selection and investigation of both substrates will, thus, contribute to the understanding of rapid responses of contemporaneous N₂ fixation and denitrification to eutrophication of post-phase shift coral reefs. We aimed i) to investigate the relative activity of N₂ fixation and denitrification in the two coral reef substrates, ii) to assess the direct responses of both N fluxes to nutrient enrichment, and iii) to identify potential thresholds that mediate both N cycling pathways. For this purpose, we carried out acetylene-based short-term incubations, which allowed us to quantify the effect of four different nitrate concentrations on N₂ fixation and denitrification simultaneously.

10.3 | Material and Methods

Study Site, Sampling and Experimental Design

The experiment was conducted at the laboratory facilities of the King Abdullah University of Science and Technology (KAUST), Saudi Arabia, in May 2018. Sampling of substrates took place at a semi-exposed area of the Abu Shosha reef in the Jeddah Region (22° 18' 15" N, 39° 02' 56" E) on the west coast of Saudi Arabia in the central Red Sea. Turf algae and coral rubble as predominant coral reef substrates were chosen a) for their dominant spatial benthic distribution (26.2 to 47.5% and 3.3 to 12.1%, resp., benthic cover)¹⁷, particularly when phase shifts occur¹⁷, and b) their evidently active role as important N fixers and denitrifiers^{18–20}. ‘Turf algae’ were defined as dead coral substrates of approx. 10 cm length that were overgrown (1 – 2 cm in height) with heterogeneous assemblages of different filamentous algae and cyanobacteria (see Fig. S10.1). ‘Coral rubble’ was defined as dislodged parts of dead coral skeletons of approx. 5 – 10 cm length that were partly covered with crustose coralline algae and microbial biofilms (see Fig. S10.2)²¹. Both substrates were sampled for the present study to allow for comparisons between fragile filamentous algal assemblages and cyanobacterial structures and with coral rubble fragments without turf algal cover. A total of 40 turf algae fragments and 32 coral rubble fragments were sampled from 5 m water depth using hammer and chisel. All samples were stored in recirculation aquaria equipped with ambient reef water on the research vessel. Aquaria were kept at ambient temperature and light levels. Experimental incubations (see below) started < 3 h after sampling.

Nitrogen Fluxes

Four different N concentrations were used for the present study: ambient concentration typical for the central Red Sea (0.1 – 0.3 μM nitrate) as measured previously¹⁷, 1 and 5 μM nitrate addition covering ranges of natural⁸ as well as anthropogenic²² nutrient inputs to local waters and as previously utilised in nutrient-enrichment studies^{11,23}, and 10 μM nitrate addition being well above observed scenarios in the Red Sea. Nitrate enrichment consisted of previously prepared nitrate stock solution, prepared with MilliQ water and sodium nitrate (≥ 99.0 %, Sigma-Aldrich). Nitrate was added immediately prior incubations (< 5 min). To determine N₂ fixation and denitrification activity, a combined blockage/reduction acetylene assay (COBRA) was performed as previously described¹⁹. Briefly, all COBRA incubations were conducted in 1 L gastight

glass chambers, each filled with 800 mL of either ambient or nutrient-amended seawater. Acetylene gas was then added to both incubation water and remaining headspace at a concentration of 10 %. Acetylene in the gastight chambers leads to the preferential reduction of acetylene to ethylene (C_2H_4), instead of N_2 to ammonia by the key enzyme nitrogenase²⁴. Further, acetylene blocks the nitrous oxide (N_2O) activity in the denitrification pathway leading to an accumulation of N_2O ²⁵. Replicate samples were incubated and two additional chambers per respective nutrient concentration and light condition without specimens served as controls to correct for planktonic background activity (Fig. 10.1). All incubations lasted 12 h, with dark and light incubations being performed separately with differing specimens (Fig. 10.1). Light was set at a photon flux of $\sim 200 \mu M \text{ quanta m}^{-2} \text{ s}^{-1}$, representing the daytime average photon flux of the studied reef and water depth at this time of the year. All incubation chambers were submerged in a temperature-controlled water bath at 27 °C, resembling the ambient water temperature measured at the reef in 5 m water depth during sampling. Incubation chambers were constantly stirred (500 rpm) to ensure sufficient exchange between the water body and headspace. Gas samples were taken at the start (t_0), after 4h (t_4), and after 12 h (t_{12} , i.e., at the end of the incubation), to consider potential initial lag phases¹⁹ and to account for incomplete inhibition of the denitrification pathway^{19,26}. Both target gases (i.e., C_2H_4 and N_2O) were quantified using gas chromatography (Agilent 7890B GC system, Agilent Technologies) and helium pulsed discharge detection with an HP-Plot/Q 19091P-QO4 column (30 m length, I. D. 0.320 mm, film 20.0 μM ; Agilent J&W GC Columns, Agilent Technologies). The lower detection limit for both target gases was 0.3 ppm. Gas concentrations were normalised to incubation time and surface area. The latter was calculated using cloud-based 3D models^{27,28} for all specimens (Autodesk Remake v19.1.1.2). We refrained from converting C_2H_4 into actual N_2 fixation rates as we acknowledge the ongoing discussion regarding an appropriate conversion factor^{29,30}. We used sampling point t_4 and t_{12} as a basis for N_2 fixation rate calculation, therefore omitting an initial lag phase; and t_0 and t_4 for denitrification to avoid an underestimation due to a potential incomplete inhibition of the denitrification pathway (see El-Khaled et al. (2020)¹⁹ and references therein).

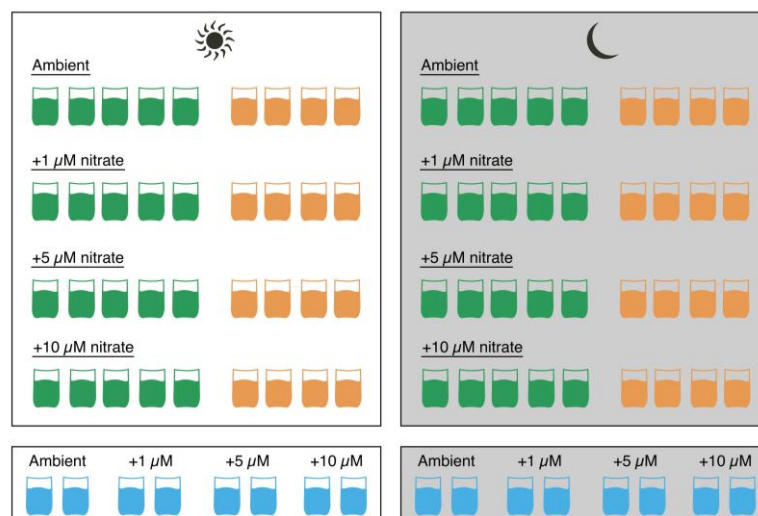


Figure 10.3 | Replication of turf algae (green), coral rubble (orange) and control (blue) incubations in various nitrate treatments and light and dark (grey) conditions for N_2 fixation and denitrification quantification.

Statistical Analysis

Data were analysed using PRIMER-E version 6 software³¹ with the PERMANOVA+ add-on³². Since the assumptions for the parametric analyses were not met, data were analysed using a non-parametric permutational analysis of variance (PERMANOVA). Analyses were based on Bray-Curtis similarities of measured physiological parameters (square-root transformed data). To test for differences between N fluxes and light conditions between the substrates under various nutrient treatments, 3-factorial PERMANOVAs (factor: N flux, light condition, nutrient treatment) with type III (partial) sums of squares and unrestricted permutation of raw data (999 permutations) with Monte Carlo tests were used. Subsequent pairwise tests were performed when significant differences occurred ($p \leq 0.05$).

10.4 | Results

N₂ fixation

Both substrates showed detectable rates of N₂ fixation under all scenarios (Fig. 10.2). The detected N₂ fixation throughout all treatments ranged from 0.04 ± 0.00 nmol C₂H₄ cm⁻² h⁻¹ (coral rubble dark 10 μM) to 5.08 ± 0.88 nmol C₂H₄ cm⁻² h⁻¹ (turf light 5 μM). The highest N₂ fixation rates were generally observed in light conditions with both substrates showing an optimum curve response peaking at 5 μM nitrate addition (Fig. 10.2A). For turf algae under light conditions, this resulted in a distinct pattern, where N₂ fixation rates at both 1 μM and 10 μM nitrate were significantly lower than at 5 μM. During dark incubations, turf algae N₂ fixation rates were highest in 5 and 10 μM and did not decrease under the highest nitrate treatment. In contrast to this, for coral rubble in the dark, a significant decrease of N₂ fixation rates at 10 μM compared to all other nutrient treatments was observed.

Denitrification

Both substrates also performed denitrification in all scenarios, except for coral rubble in dark incubations under ambient conditions, where denitrification remained below the detection limit (Fig. 10.2B). Overall, an increasing trend of denitrification with increasing nitrate addition was apparent. Under light conditions, this trend was less pronounced, and coral rubble and turf algae performed comparable denitrification rates. For both substrates, the peaks of denitrification activity were observed at 10 μM under dark conditions. The highest rate was observed for coral rubble at 10 μM in the dark, which represents a significantly higher denitrification activity for coral rubble in the dark at 10 μM compared to all other nutrient treatments. This significant increase in denitrification corresponds with the sharp decrease in N₂ fixation for coral rubble in the dark (described above; Fig. 10.2, Table 10.1). A similar increase in denitrification activities at 10 μM compared to other nutrient treatments was observed for turf algae (Fig. 10.2B). The aforementioned peaks of denitrification for both turf algae and coral rubble in the dark were about four- to 800-fold higher, respectively, compared to all other quantified denitrification rates (Fig. 10.2, Table 10.1).

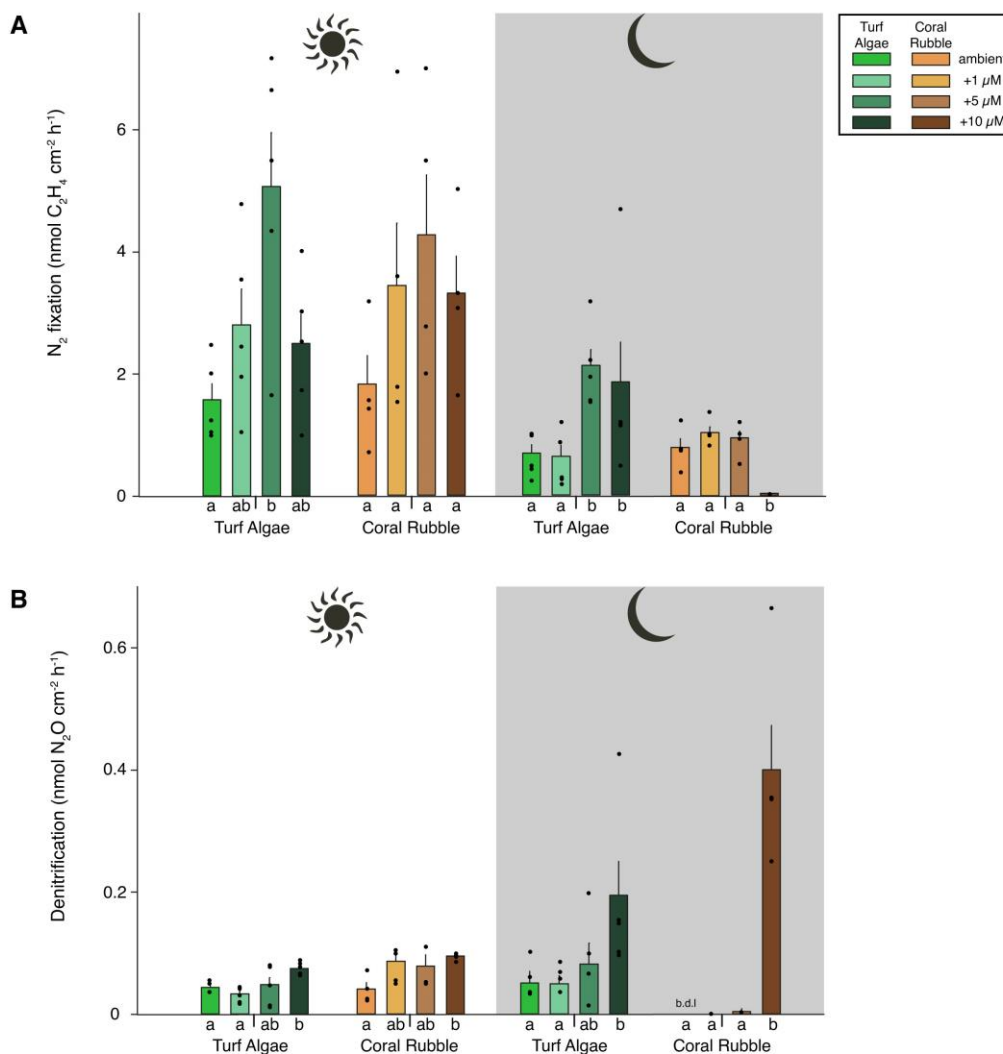


Figure 10.4 | N_2 fixation (A) and denitrification (B) activities for turf algae (green) and coral rubble (earth coloured) measured under four different nutrient treatments (ambient, 1, 5, and 10 μM nitrate addition) in light and dark (grey) incubations. Means are shown \pm SE. Different letters on x-axis indicate significant differences between groups from the same substrate and light/dark condition. Black dots represent quantified N_2 fixation/denitrification activity. Note different scales for N_2 fixation and denitrification. b.d.l. = below detection limit.

Table 10.2 | Results of pairwise permutational analysis of variance (PERMANOVA) for N_2 fixation (A, B) and denitrification (C, D) measured under four nutrient treatments (ambient, 1, 5, and 10 μM nitrate addition) under light and dark (grey) incubations. Significant values in bold. Top: t-values; bottom: p-values.

A - N_2 Fixation		Turf Algae			
		Ambient	+1 μM	+5 μM	+10 μM
Turf Algae	Ambient		0.0495 0.639	4.437 0.001	2.011 0.061
	+1 μM	1.636 0.144		3.944 0.006	2.126 0.053
	+5 μM	3.380 0.011	1.600 0.139		1.065 0.324
	+10 μM	1.336 0.204	0.277 0.826	1.874 0.102	

B - N ₂ Fixation		Coral Rubble			
	Ambient	+1 μ M	+5 μ M	+10 μ M	
Coral Rubble	Ambient		1.349 0.233	0.8377 0.411	6.155 0.001
	1 μ M	1.285 0.253		0.567 0.583	7.603 0.001
	5 μ M	1.993 0.075	0.605 0.556		7.098 0.002
	10 μ M	1.691 0.109	0.209 0.902	0.568 0.592	

C - Denitrification		Turf Algae			
	Ambient	+1 μ M	+5 μ M	+10 μ M	
Turf Algae	Ambient		0.004 0.971	0.685 0.519	2.345 0.032
	+1 μ M	0.826 0.406		0.757 0.468	2.451 0.043
	+5 μ M	0.236 0.801	1.059 0.321		1.612 0.154
	+10 μ M	2.448 0.049	6.89 0.001	1.948 0.098	

D - Denitrification		Coral Rubble			
	Ambient	+1 μ M	+5 μ M	+10 μ M	
Coral Rubble	Ambient		1.000 0.358	1.000 0.356	5.7759 0.002
	+1 μ M	2.302 0.069		0.885 0.432	5.767 0.001
	+5 μ M	1.571 0.164	0.298 0.783		5.672 0.002
	+10 μ M	4.160 0.006	0.570 0.604	0.794 0.471	

10.5 | Discussion

The interplay of N₂ fixation and denitrification is key for moderating N availability to either supply N or relieve excess N depending on environmental conditions. We here demonstrate that the (in-)activity of N cycling pathways appears to be nutrient dependant with substrate-specific thresholds stimulating or suppressing N₂ fixation and denitrification in coral reef environments.

Nitrogen Fluxes of Turf Algae and Coral Rubble

Both substrates showed detectable levels of N₂ fixation and denitrification simultaneously under all given scenarios except for the absence of detectable denitrification in coral rubble substrates in the dark with no additional nitrate (i.e., under ambient conditions). Potentially, rates for coral rubble that were below the detection limit can be explained as follows: Nitrification, the oxidation of ammonium to nitrite and nitrate, functions as a recycling mechanism within the N cycle⁵. The final product of the nitrification pathway (i.e.,

nitrate) serves as a substrate for denitrification. Nitrification, particularly, is an aerobic pathway³³ that potentially redeems substrate (i.e., nitrate) limitation for the denitrification pathway during light incubations and closely linked oxygen formation due to photosynthesis (El-Khaled et al. in review). This hypothesis is supported through the quantification of denitrification activity for coral rubble during light incubations (Fig. 10.2B) and for incubations where nitrate was provided, whereas denitrification remained below the detection limit under ambient conditions and during dark incubations where nitrate is limited and not additionally provided via nitrification. Similarly, denitrification rates quantified for coral rubble in dark were consistently lower than under light conditions (except for 10 μ M nitrate addition, see below). The denitrification activity of turf algae in all scenarios (Fig. 10.2B) indicates that these algal assemblages differ in their N cycling properties compared to coral rubble and may be able to maintain higher levels of nitrate concentrations even at night.

The N₂ fixation and denitrification rates in the present study are in line with rates reported for the Red Sea using acetylene-based measuring techniques^{8,11,20}. N₂ fixation rates for turf algae and coral rubble quantified in the present study are higher than those of other coral reef organisms and substrates such as scleractinian corals^{34,35}, soft corals³⁶, or top-layers of coral reef-associated reef sediments¹¹. Comparatively high N₂ fixation rates associated with both substrates confirm their role as important N₂-fixers on coral reefs⁸. Particularly, turf algae have been described as opportunists^{37,38} implementing a high N demand to build up biomass and to fuel their metabolism. Previous findings show that this high N demand can be satisfied with N₂ fixation^{20,39,40}, which in return could explain the findings of the present study.

Both substrates performed more N₂ fixation during light than during dark incubations (Fig. 10.2A). For turf algae, these findings are in line with previous studies^{41,42}, but contradict those of Rix et al. (2015)²⁰ who showed substantially higher night-time N₂ fixation. Varying diel N₂ fixation activity for turf algae with high rates depending on the presence of light indicates the presence of heterocystous turf community. Potentially, heterocystous cyanobacteria dominated in turf algae fragments that were used for the present study can prevalently perform N₂ fixation despite the presence of oxygen generated via photosynthesis^{43,44}, even though being capable of fixing N in the dark under oxygen-depleted conditions^{44,45}. For coral rubble, we hypothesise the abundance of a diazotroph community consisting of heterotrophic bacteria equally adapted to both dark and light conditions⁴⁴, as N₂ fixation was observed during light and dark (Fig. 10.2A).

Rapid N₂ fixation and Denitrification Responses to Nutrient Enrichment

Both substrates followed the pattern of increasing N₂ fixation activities with increasing nutrient concentrations up to a treatment of 5 μ M nitrate, despite lacking statistical significance. Interestingly, N₂ fixation rates for both substrates tend to diminish with higher nitrate treatments (i.e., 10 μ M), except for turf algae during dark incubations, where rates quantified in 5 and 10 μ M nitrate treatments remained higher than those at ambient and 1 μ M nitrate treatments. Congruent to decreasing N₂ fixation rates under 10 μ M nitrate treatments, we observed significant increases in the denitrification activity for both substrates in both dark and light incubations compared to ambient, and to a certain extent to 1 or 5 μ M nitrate amended

incubations (Fig. 10.2B). The observed patterns generally confirm the above-formulated hypotheses of decreased N₂ fixation and increased denitrification under high nitrate availability.

Interestingly, turf algae continued to fix N despite the presence of nitrate well above ambient concentrations, even though acquiring N via N₂ fixation is an energetically costly pathway^{46,47}. Turf algae are capable of rapidly taking up environmentally available N as well^{10,48}, which we assume to be the case in the present study as well. Further, turf algal growth form with a relatively high surface area to volume ratio due to its filamentous morphology have been identified as key parameters for a significant capacity to take up environmentally offered nutrients^{38,49}. We, thus, conclude that the immense N demand of turf algae may effectively limit N availability within the substrate even under high levels of seawater nitrate concentrations. Hence, efficient N uptake (via assimilation) and N₂ fixation contribute to their capacity to proliferate rapidly, particularly in continuously eutrophied environments^{50,51}. Following this pattern, N-stimulated growth in the algae is likely closely linked to an enhanced growth of the overall microbial community⁵². Thereby, the abundance of diazotrophs⁵³ and potentially denitrifiers increases, which in return could explain the increased N₂ fixation and denitrification activity under 5 and 10 μM nitrate concentrations during incubations.

Coral rubble-associated microbes continued to fix N in all scenarios except for dark incubations at 10 μM nitrate enriched conditions. Coral rubble can be colonised by epilithic and endolithic microbial communities⁵⁴ enabling the substrate 'holobiont' to fix N⁵⁵. We conclude that microbial communities associated with coral rubble utilise the available N to stimulate N₂ fixation and promote growth. Potentially, an increase of N via the uptake of added nitrate or N₂ fixation could have altered N to phosphate (P) ratios⁵⁶. A shift from initially N-limited to P-limited conditions has been suggested previously for hard coral holobionts^{35,57}, for which a resulting imbalance in the N:P ratios leads to P-starvation. Hypothetically, similar patterns could appear in further coral reef substrates⁵⁰. We assume ambient P concentrations during the incubations (0.01-0.09 μM)^{10,11}, as no P enrichment was performed and ambient reef water was used. We conclude that detected patterns in microbial N cycling reflects N availability within the respective system.

Threshold Identification

Interestingly, the short time scale, which was intentionally set for the present experimental design suggests a rapid, definite switch from active N₂ fixation to stimulation of denitrification to relieve N depending on nitrate addition. In the present study, we were able to observe the stimulation or suppression of N₂ fixation and denitrification (Fig. 10.2). This ambiguity has been recognised in coral reef environments in previous studies. For example, reef patch-wide denitrification increased with a congruent decrease of N₂ fixation under high (i.e., 10 – 30 μM) N addition¹², Roth et al. (2020)⁴⁰ modelled decreasing N₂ fixation with increasing nitrate availability for benthic pioneer communities, whereas a nitrate-dependent stimulation (10 – 500 μM) of denitrification was observed for coral reef sediments⁵⁸. Opposite effects on N₂ fixation and denitrification, however, were reported for turf algae, reef sediments and a hard coral under moderate eutrophication¹¹. We conclude that divergent effects of nutrient enrichment on both N₂ fixation and denitrification observed here and in previous studies^{11–13,58} could be, thus, related to the amount of nutrients

added, either stimulating or suppressing N fluxes depending on nutrient availability. In how far divergent effects can be observed in further substrates, with potentially different microbial communities or life histories, e.g., through the exposure to other environmental conditions, remains to be targeted in future studies. Furthermore, the role of P and further micronutrients^{56,59} and potential shift from N to P-limitation²³ needs to be considered, and should be targeted in future studies. Based on the data of the present study, we hypothesise an identification of a threshold for a common benthic coral reef substrate (i.e., coral rubble), at which N₂ fixation is largely inactive and denitrification is initiated. Our data suggest that thresholds are substrate-specific and that thresholds for N₂ fixation and denitrification may (i.e., as identified for coral rubble) but do not have to be (i.e., as identified for turf algae) linked.

Ecological Implications

Under increasing global anthropogenic disturbances, especially those of nutrient enrichment due to sewage outfalls¹⁵, terrestrial run-offs⁴⁸, or aquaculture²², it is of paramount importance to understand their effects on nutrient cycles maintaining the functioning of coral reef ecosystems.

We identified turf algae and coral rubble as important importers of de novo N under ambient and elevated nutrient concentrations (Fig. 10.2A). Algae are likely to increase in dominance in future coral reefs^{60,61}, due to their aforementioned opportunistic behaviour and their competitive advantage compared to classical reef framework builders (i.e., hard corals) under stressed environmental parameters. Shifts from coral to algae dominance have been recognised worldwide (see Norström et al. (2009)¹⁴ and references therein), potentially resulting in an increase of bioavailable N as i) a direct consequence of increases in turf algae abundance (El-Khaled et al. in review) or ii) due to the stimulation of N₂ fixation under moderate eutrophied conditions¹¹. In this context, a rapid response to short-term nutrient pollution by increasing N₂ fixation for turf algae might have several implications on a shorter time scale. The fast on-set and increase of N₂ fixation within minutes to hours after nitrate addition, for example in turf algae, might add to explaining their competitive advantages. Given turf algae's opportunistic use of N for growth, this might provide an additional 'head start' under eutrophication, however more functional groups would need to be analysed to hypothesise on the first hours of competition under pulse N availability. Besides that, a rapid accumulation of biomass based on the availability of N may eventually result in an energy transfer to higher trophic levels⁴⁰ by either herbivorous grazing⁶² or a decay of biomass⁶³.

Whereas turf algae and coral rubble have been identified as major N fixers before, their role as denitrifiers under ambient conditions is comparatively small (El-Khaled et al. in review). However, particularly under eutrophied scenarios, a key role in rapidly relieving substrates from N can be aligned for coral rubble, for which we were able to identify a threshold that suppresses N₂ fixation and stimulates denitrification (Fig. 10.2). Hence, the fast response to short-term eutrophication might be key under nutrient pulses⁴⁸ by alleviating excess N via denitrification. In how far previously identified key denitrifiers such as hard and soft corals (El-Khaled et al. in review) or reef sediments⁵⁸ respond to short-term eutrophication remains to be determined. Hypothetically, their role in eutrophied and degraded coral reefs has been overlooked yet.

Given the observed threshold under high nitrate addition, it needs to be considered that such high N availability (i.e. 10 μM nitrate) is far above the environmental conditions, even under anthropogenic impact. Under lower, more realistic N availability, N_2 fixation appeared to increase more strongly and steadily with increasing nitrate additions than denitrification. In return, this means that the ‘threshold’ for a drastic N relief via denitrification (vs. N_2 fixation) is likely not ‘hit’ soon enough to counter eutrophication. Therefore, the role of microbial nutrient cycling in enhancing the effects of moderate, even short-term, eutrophication should be realised and considered in coastal development and planning (e.g., runoff events, drainage, sewage outfalls, etc.).

Our study, therefore, concludes that short-term eutrophication has strong implications on the reef N-cycling, that substrate specific thresholds (N_2 fixation vs. denitrification) seem to exist, that those substrate- and context-specific thresholds may help explaining varying outcomes of eutrophication studies, and that the effects of moderate eutrophication may physiologically alter the overall N budget in the reef.

10.6 | Acknowledgements

We are grateful to Najeh Kharbatia from CORE Labs of the King Abdullah University of Science and Technology (KAUST) for his technical support with the GC.

10.7 | References

1. Halpern, B. S., Selkoe, K. A., Micheli, F. & Kappel, C. V. Evaluating and ranking the vulnerability of global marine ecosystems to anthropogenic threats. *Conserv. Biol.* **21**, 1301–1315 (2007).
2. Halpern, B. S. *et al.* Spatial and temporal changes in cumulative human impacts on the world's ocean. *Nat. Commun.* **6**, 1–7 (2015).
3. Burke, L., Reytar, K., Spaulding, M. & Perry, A. *Reefs at Risk*. (World Resources Institute, 2011).
4. Vitousek, P. M. & Howarth, R. W. Nitrogen limitation on land and in the sea: How can it occur? *Biogeochemistry* **13**, 87–115 (1991).
5. Webb, K. L., DuPaul, W. D., Wiebe, W., Sottile, W. & Johannes, R. E. Enewetak (Eniwetok) Atoll: Aspects of the nitrogen cycle on a coral reef. *Limnol. Oceanogr.* **20**, 198–210 (1975).
6. Lesser, M. P. *et al.* Nitrogen fixation by symbiotic cyanobacteria provides a source of nitrogen for the scleractinian coral *Montastraea cavernosa*. *Mar. Ecol. Prog. Ser.* **346**, 143–152 (2007).
7. Rädecker, N., Pogoreutz, C., Voolstra, C. R., Wiedenmann, J. & Wild, C. Nitrogen cycling in corals: The key to understanding holobiont functioning? *Trends Microbiol.* **23**, 490–497 (2015).
8. Cardini, U. *et al.* Budget of Primary Production and Dinitrogen Fixation in a Highly Seasonal Red Sea Coral Reef. *Ecosystems* **19**, 771–785 (2016).
9. Koop, K. *et al.* ENCORE: The effect of nutrient enrichment on coral reefs. Synthesis of results and conclusions. *Mar. Pollut. Bull.* **42**, 91–120 (2001).
10. Karcher, D. B. *et al.* Nitrogen eutrophication particularly promotes turf algae in coral reefs of the central Red Sea. *PeerJ* **8**, e8737 (2020).
11. El-Khaled, Y. *et al.* In situ eutrophication stimulates dinitrogen fixation, denitrification, and productivity in Red Sea coral reefs. *Mar. Ecol. Prog. Ser.* **645**, 55–66 (2020).
12. Koop, K. *et al.* ENCORE: The effect of nutrient enrichment on coral reefs. Synthesis of results and conclusions. *Mar. Pollut. Bull.* **42**, 91–120 (2001).
13. Joye, S. B. & Paerl, H. W. Contemporaneous nitrogen fixation and denitrification in intertidal microbial mats: rapid response to runoff events. *Mar. Ecol. Prog. Ser.* **94**, 267–274 (1993).
14. Norström, A. V., Nyström, M., Lokrantz, J. & Folke, C. Alternative states on coral reefs: Beyond coral-macroalgal phase shifts. *Mar. Ecol. Prog. Ser.* **376**, 293–306 (2009).
15. McManus, J. W. & Polsenberg, J. F. Coral-algal phase shifts on coral reefs: Ecological and environmental aspects. *Prog. Oceanogr.* **60**, 263–279 (2004).
16. Holmes, K. E., Edinger, E. N., Hariyadi, Limmon, G. V. & Risk, M. J. Bioerosion of live massive corals and branching coral rubble on Indonesian coral reefs. *Mar. Pollut. Bull.* **40**, 606–617 (2000).
17. Roth, F. *et al.* Coral reef degradation affects the potential for reef recovery after disturbance. *Mar. Environ. Res.* **142**, 48–58 (2018).
18. Davey, M., Holmes, G. & Johnstone, R. High rates of nitrogen fixation (acetylene reduction) on coral skeletons following bleaching mortality. *Coral Reefs* **27**, 227–236 (2008).
19. El-Khaled, Y. C. *et al.* Simultaneous Measurements of Dinitrogen Fixation and Denitrification Associated With Coral Reef Substrates : Advantages and Limitations of a Combined Acetylene Assay. *Front. Mar. Sci.* **7**, 411 (2020).
20. Rix, L. *et al.* Seasonality in dinitrogen fixation and primary productivity by coral reef framework substrates from the northern Red Sea. *Mar. Ecol. Prog. Ser.* **533**, 79–92 (2015).
21. Rasser, M. W. & Riegl, B. Holocene coral reef rubble and its binding agents. *Coral Reefs* **21**, 57–72 (2002).

22. Loya, Y., Lubinevsky, H., Rosenfeld, M. & Kramarsky-Winter, E. Nutrient enrichment caused by in situ fish farms at Eilat, Red Sea is detrimental to coral reproduction. *Mar. Pollut. Bull.* **49**, 344–353 (2004).
23. Wiedenmann, J. *et al.* Nutrient enrichment can increase the susceptibility of reef corals to bleaching. *Nat. Clim. Chang.* **3**, 160–164 (2013).
24. Balderston, W. L., Sherr, B. & Payne, W. J. Blockage By Acetylene of Nitrous-Oxide Reduction in *Pseudomonas-Perfectomarinus*. *Appl. Environ. Microbiol.* **31**, 504–508 (1976).
25. Yoshinari, T. & Knowles, R. Acetylene Inhibition of Nitrous Oxide Reduction by Denitrifying Bacteria. *Biochem. Biophys. Res. Commun.* **69**, 705–710 (1976).
26. Yu, K., Seo, D. C. & Delaune, R. D. Incomplete acetylene inhibition of nitrous oxide reduction in potential denitrification assay as revealed by using ¹⁵N-Nitrate tracer. *Commun. Soil Sci. Plant Anal.* **41**, 2201–2210 (2010).
27. Gutierrez-Heredia, L., Benzoni, F., Murphy, E. & Reynaud, E. G. End to End Digitisation and Analysis of Three-Dimensional Coral Models, from Communities to Corallites. *PLoS One* **11**, e0149641 (2016).
28. Lavy, A. *et al.* A quick, easy and non-intrusive method for underwater volume and surface area evaluation of benthic organisms by 3D computer modelling. *Methods Ecol. Evol.* **6**, 521–531 (2015).
29. Hardy, R. W. F., Holsten, R. D., Jackson, E. K. & Burns, R. C. The acetylene - ethylene assay for N₂ fixation: laboratory and field evaluation. *Plant Physiol.* **43**, 1185–1207 (1968).
30. Wilson, S. T., Böttjer, D., Church, M. J. & Karl, D. M. Comparative assessment of nitrogen fixation methodologies, conducted in the oligotrophic north pacific ocean. *Appl. Environ. Microbiol.* **78**, 6516–6523 (2012).
31. Clarke, K. R. & Gorley, R. N. *PRIMER v6: Use manual/Tutorial. PRIMER-E: Plymouth* (2006).
32. Anderson, M. J. A new method for non-parametric multivariate analysis of variance. *Austral Ecol.* **26**, 32–46 (2001).
33. O'Neil, J. M. & Capone, D. G. Nitrogen Cycling in Coral Reef Environments. in *Nitrogen in the Marine Environment* 949–989 (2008). doi:10.1016/B978-0-12-372522-6.00021-9
34. Cardini, U. *et al.* Microbial dinitrogen fixation in coral holobionts exposed to thermal stress and bleaching. *Environ. Microbiol.* **18**, 2620–2633 (2016).
35. Tilstra, A. *et al.* Denitrification Aligns with N₂ Fixation in Red Sea Corals. *Sci. Rep.* **9**, 19460 (2019).
36. Bednarz, V. N., Cardini, U., Van Hoytema, N., Al-Rshaidat, M. M. D. & Wild, C. Seasonal variation in dinitrogen fixation and oxygen fluxes associated with two dominant zooxanthellate soft corals from the northern Red Sea. *Mar. Ecol. Prog. Ser.* **519**, 141–152 (2015).
37. Littler, M. & Littler, D. The Nature of Turf and Boring Algae and Their Interactions on Reefs. *Smithson. Contrib. to Mar. Sci.* 213–217 (2013).
38. Rosenberg, G. & Ramus, J. Uptake of inorganic nitrogen and seaweed surface area: Volume ratios. *Aquat. Bot.* **19**, 65–72 (1984).
39. Yamamuro, M., Kayanne, H. & Minagawa, M. Carbon and nitrogen stable isotopes of primary producers in coral reef ecosystems. *Limnol. Oceanogr.* **40**, 617–621 (1995).
40. Roth, F. *et al.* High rates of carbon and dinitrogen fixation suggest a critical role of benthic pioneer communities in the energy and nutrient dynamics of coral reefs. *Funct. Ecol.* (2020). doi:10.1111/1365-2435.13625
41. den Haan, J. *et al.* Nitrogen fixation rates in algal turf communities of a degraded versus less degraded coral reef. *Coral Reefs* **33**, 1003–1015 (2014).

42. Williams, S. L. & Carpenter, R. C. Grazing effects on nitrogen fixation in coral reef algal turfs. *Mar. Biol.* **130**, 223–231 (1997).
43. Bergman, B., Gallon, J. R., Rai, A. N. & Stal, L. J. N₂ Fixation by non-heterocystus cyanobacteria. *FEMS Microbiol. Rev.* **19**, 139–185 (1997).
44. Staal, M., Te Lintel Hekkert, S., Herman, P. & Stal, L. J. Comparison of models describing light dependence of N₂ fixation in heterocystous cyanobacteria. *Appl. Environ. Microbiol.* **68**, 4679–4683 (2002).
45. Millineaux, P. M., Gallon, J. R. & Chaplin, A. E. Acetylene reduction (nitrogen fixation) by cyanobacteria grown under alternating light-dark cycles. *FEMS Microbiol. Lett.* **10**, 245–247 (1981).
46. Holl, C. M. & Montoya, J. P. Interactions between nitrate uptake and nitrogen fixation in continuous cultures of the marine diazotroph *Trichodesmium* (Cyanobacteria). *J. Phycol.* **41**, 1178–1183 (2005).
47. Knapp, A. N. The sensitivity of marine N₂ fixation to dissolved inorganic nitrogen. *Front. Microbiol.* **3**, 374 (2012).
48. den Haan, J. *et al.* Nitrogen and phosphorus uptake rates of different species from a coral reef community after a nutrient pulse. *Sci. Rep.* **6**, 28821 (2016).
49. Littler, M. M. & Littler, D. S. The Evolution of Thallus Form and Survival Strategies in Benthic Marine Macroalgae. *Am. Nat.* **116**, 25–44 (1980).
50. Kuffner, I. B. & Paul, V. J. Effects of nitrate, phosphate and iron on the growth of macroalgae and benthic cyanobacteria from Cocos Lagoon, Guam. *Mar. Ecol. Prog. Ser.* **222**, 63–72 (2001).
51. Smith, J. E., Runcie, J. W. & Smith, C. M. Characterization of a large-scale ephemeral bloom of the green alga *Cladophora sericea* on the coral reefs of West Maui, Hawaii. *Mar. Ecol. Prog. Ser.* **302**, 77–91 (2005).
52. Kopp, C. *et al.* Highly Dynamic Cellular-Level Response of Symbiotic Coral to a Sudden Increase in Environmental Nitrogen. *MBio* **4**, e00052-13 (2013).
53. Muscatine, L., Falkowski, P. G., Dubinsky, Z., Cook, P. A. & McCloskey, L. R. The Effect of External Nutrient Resources on the Population Dynamics of Zooxanthellae in a Reef Coral. *Proc. R. Soc. B Biol. Sci.* **236**, 311–324 (1989).
54. Tribollet, A., Langdon, C., Golubic, S. & Atkinson, M. Endolithic microflora are major primary producers in dead carbonate substrates of Hawaiian coral reefs. *J. Phycol.* **42**, 292–303 (2006).
55. Charpy, L., Palinska, K. A., Suzuki, Y., Abed, R. M. M. & Golubic, S. Dinitrogen-Fixing Cyanobacteria in Microbial Mats of Two Shallow Coral Reef Ecosystems. *Microb. Ecol.* **59**, 174–186 (2010).
56. Ferrier-Pagès, C., Godinot, C., D'Angelo, C., Wiedenmann, J. & Grover, R. Phosphorus metabolism of reef organisms with algal symbionts. *Ecol. Monogr.* **86**, 262–277 (2016).
57. Wiedenmann, J. *et al.* Nutrient enrichment can increase the susceptibility of reef corals to bleaching. *Nat. Clim. Chang.* **3**, 160–164 (2012).
58. Capone, D. G., Dunham, S. E., Horrigan, S. G. & Duguay, L. E. Microbial nitrogen transformations in unconsolidated coral reef sediments. *Mar. Ecol. Prog. Ser.* **80**, 75–88 (1992).
59. Luo, Y. W. *et al.* Reduced nitrogenase efficiency dominates response of the globally important nitrogen fixer *Trichodesmium* to ocean acidification. *Nat. Commun.* **10**, 1521 (2019).
60. Pandolfi, J. M., Connolly, S. R., Marshall, D. J. & Cohen, A. L. Projecting coral reef futures under global warming and ocean acidification. *Science (80-.)*. **333**, 418–422 (2011).
61. Hughes, T. P. *et al.* Coral reefs in the Anthropocene. *Nature* **546**, 82–90 (2017).

62. Fong, P. & Paul, V. J. Coral Reef Algae. in *Coral Reefs: An Ecosystem in Transition* (eds. Dubinsky, Z. & Stambler, N.) 241–272 (Springer, Dordrecht, 2011). doi:10.1007/978-94-007-0114-4_17
63. Duarte, C. M. & Cebrián, J. The fate of marine autotrophic production. *Limnol. Oceanogr.* **41**, 1758–1766 (1996).

Chapter 11

Chapter 11 | General discussion

Yusuf C. El-Khaled^{1*}

¹Marine Ecology Department, Faculty of Biology and Chemistry, University of Bremen, Germany

*Corresponding author: yek2012@uni-bremen.de

11.1 | Key Findings

- Both N₂ fixation and denitrification are simultaneously quantified in coral reef substrates for the first time (Chapter 2)¹
- Benthic *in situ* chambers are used to account for the structural complexity of reef communities with surprising differences between community-wide and extrapolated, *ex situ* generated oxygen fluxes (Chapter 3)²
- Denitrification is actively performed by coral holobionts and aligns with N₂ fixation (Chapter 4)³
- The ratio of hard coral associated denitrification and N₂ fixation may dynamically shift in response to environmental dissolved inorganic N (Chapter 5)
- Functional groups associated with high N₂ fixation show low denitrification activity, and *vice versa*, with coral holobionts being major denitrifiers (Chapter 6)
- In situ eutrophication increases $\delta^{15}\text{N}$ in hard coral tissues and soft corals, but not in Symbiodiniaceae cells, and particularly promoted turf algae (Chapter 7)⁴
- Moderate in situ eutrophication surprisingly stimulates both N₂ fixation and denitrification in major functional groups of a coral reef (Chapter 8)⁵
- Nutrient enrichment affects coral- and algae-dominated reef communities differently, evoking various responses concerning productivity, calcification and dissolved organic nitrogen fluxes (Chapter 9)
- Nitrate availability moderates N₂ fixation and denitrification in turf algae and coral rubble with substrate-specific and nitrate concentration-depending thresholds that suppress or stimulate both N cycle pathways (Chapter 10)

11.2 | Overview

Coral reefs all over the world have experienced a suite of anthropogenically induced environmental threats^{6–9}, with threats increasing in their frequency and severity^{10–12}. It is of paramount interest to not only address direct consequences of global change and enhanced local human activities that contribute to coral reef collapse (e.g. coral-algal phase shifts), but to go beyond in order to understand how future, differently

composed reefs will function, and how their functioning directly affects coral reef resilience and prospects for recovery¹³. Our understanding, however, of coral reef functional ecology and its climate change evoked alterations yet remains rudimentary¹⁴. This dissertation contributes to a more comprehensive understanding of baseline coral reef functioning, but also provides valuable insights to understand how stressors such as eutrophication affects biogeochemical cycling on an organism-level, and models how coral-algal phase shifts influence ecosystem-wide processes.

The central Red Sea was chosen as a study area, serving as an ideal location for the present research. The Red Sea close-to-pristine coral-dominated and degraded, phase-shifted algae-dominated reef communities on a small spatial scale, as well as naturally occurring fluctuations of environmental conditions due to seasonality. Experiments of the present dissertation took place investigating a wide range of functional groups and their associated microbial communities that were located in the Abo Shosha reef (N22°18'15", E39°02'26") of the central Red Sea. Investigations not only focussed on classical framework builders, i.e., hard corals, but also included the major functional groups of this particular reef to provide a more comprehensive, realistic and reef-wide understanding of N₂ fixation and denitrification, and to understand the interplay between both pathways under ambient as well as stressed conditions. The knowledge gained in the framework of this thesis, provides valuable insights on a) a new methodology to simultaneously address N₂ fixation and denitrification in coral reef environments, b) hard coral denitrification rates that were quantified for the first time, c) a reef-wide N₂ fixation denitrification budget extrapolated for intact and degraded reef states, and d) the effects of short- and long-term eutrophication on key functional groups of a coral reef, e) for two of which substrate-specific thresholds that regulate N cycling were identified. Generally, we show that denitrification (as well as N₂ fixation) is an actively performed N cycling pathway within coral reef environments that might be shaped by the naturally or anthropogenically introduced nitrogenous compounds such as nitrite, ultimately contributing to the overall functioning of coral reefs.

11.3 | Nitrogen Cycling in Coral Reef Environments

Coral reefs are commonly adapted to flourish in nutrient-poor, i.e., oligotrophic, environments^{15,16}, with all organisms competing for a limited amount of (bio-)available nutrients. The strategy of exchanging nutrients in a mutualistic relationship is well-known for corals and their symbiotic partners of the family 'Symbiodiniaceae', providing the coral holobiont an ecological advantage over its competitors.

Whereas N₂ fixation in coral reef environments has been targeted in numerous previous studies, denitrification rates have not been quantified yet. Both N cycling pathways can be quantified using acetylene based techniques, because a) the key enzyme involved in the N₂ fixation process 'nitrogenase' reduces acetylene to ethylene if present, and b) acetylene blocks the denitrification pathway at its nitrous oxide state. Subsequently, occurring target gases (ethylene, nitrous oxide) can be determined via gas chromatography. Methods to quantify one of the two pathways have been used previously, however, comprehensive approaches to combine both to quantify N₂ fixation and denitrification in coral reef environments have

been missing. For this purpose, and as a basis for the majority of chapters included in this dissertation (i.e., Chapters 4, 6, 8, 10), an acetylene-based approach to determine N fluxes simultaneously in coral reef environments termed COBRA (= combined blockage/reduction assay) was developed and described in Chapter 2. COBRA offers an opportunity to simultaneously quantify N₂ fixation and denitrification, with a high sample throughput that enables the generation of profound datasets in a minimum of time.

COBRA was used in Chapter 4 and 6 to assess baseline N₂ fixation and denitrification rates in the hard corals *Acropora hemprichii*, *Stylophora pistillata*, *Pocillopora verrucosa*, *Pleuractis granulosa* and the Hydrozoan *Millepora dichotoma*. Interestingly, marker genes for denitrification were identified for *A. hemprichii*, *P. granulosa* and *M. dichotoma* in parallel experiments (Chapter 4), and previously in *Montastraea faveolata*^{17,18}, *Fungia* sp.¹⁹, *Favia* sp.¹⁹, *Acanthastrea* sp.¹⁹, and *Tubastraea coccinea*²⁰. Based on this dual approach (i.e., physiological and molecular) and previous findings, denitrification is very likely present in most coral holobionts. As such, denitrification rates and marker genes for *nirS* gene copy abundances for three common Red Sea corals were aligned, revealing that *nirS* gene can act as a proxy for the denitrification potential of investigated coral holobionts (Chapter 4). Furthermore, denitrification rates correlate with N₂ fixation, potentially due to a shared availability of organic C from associated algal symbionts.

Generally, N₂ fixation rates for hard corals (Chapter 4 and 6) were lower than those of other functional groups of the same reef, but in the same range^{21–23} or significantly lower than rates²⁴ measured in previous studies, potentially due to phosphate limitation occurred in the present study (Chapter 4 and 6)^{25–27} or discrepancies determining surface areas^{24,28}. Turf algae and coral rubble were identified as the largest N₂ fixers, thus, functioning as key importers of bioavailable *de novo* N, also as denitrification rates were comparatively low. These findings are well in line with emphasising the role of turf algae as pioneers²⁹ and opportunists^{30,31} that form extensive mats under oligotrophic conditions^{32,33}. Thus, their high N demand for metabolism and to build up biomass can, to a large extent, be satisfied by high N₂ fixation^{29,34–36}. Ultimately, fixed N of turf algal biomass can be exported to the wider reef. Interestingly, turf algae solely play a minor role in relieving N (Chapter 6). Here, soft and hard corals, which both display lowest N₂ fixation activities, showed highest denitrification activities. The interplay of multiple stressors^{6–9} is happening while writing this thesis, and resulting degraded algae-dominated reefs are visible worldwide^{37–39}. Results of the present thesis demonstrate – for the first time – that reef-wide N fluxes in intact coral-dominated reef differ significantly from those of degraded algae-dominated reefs, with total N₂ fixation being twice as high in algae-dominated compared to coral-dominated areas, whereas denitrification remained stable (Chapter 6). These results suggest that algae-dominated reefs promote net N accumulation, which aligns with findings of Chapter 9. Ultimately, N accumulation could support higher net productivity, resulting in a positive feedback loop, hence, increasing competitive advantages of algae compared to corals in changing reefs (Chapter 6).

Strong seasonal fluctuations in nitrate concentrations were identified to moderate N cycling in coral holobionts (Chapter 5), by adjusting N₂ fixation and denitrification to environmental nitrate availability. Ultimately, coral holobionts may actively regulate internal N availability to maintain the coral –

Symbiodiniaceae symbiosis. However, it remains speculative if anthropogenically induced eutrophication could lead to similar response patterns. To address this question, eutrophication events were simulated.

11.4 | Effects of Eutrophication on Nitrogen Cycling in Coral Reef Environments

A large *in situ* eutrophication experiment was the core of the present thesis (Chapter 7-9). The aim of the experiment was to i) provide a comparative assessment of the response of major benthic groups to *in situ* eutrophication by determining the uptake of organic C and nitrogenous compounds using stable isotope measurements (Chapter 7); to ii) assess the effects of elevated nutrient availability on N fluxes of various functional groups (Chapter 8) using the COBRA approach (Chapter 2); and to investigate *in situ* how nutrient enrichment affected community-wide biogeochemical functions of intact coral- and degraded algae-dominated reef patches (Chapter 9) using benthic chamber incubations (Chapter 3). For the experiment, distinct natural communities were chosen and surrounded by fertiliser pins (see respective Chapters for details). Nutrient enrichment (up to 7-fold compared to environmental background values) reflected nutrient inputs in the Red Sea from point-sources such as aquaculture⁴⁰ or urban wastewater inputs⁴¹, and were believed to simulate a realistic ecological scenario in the context of the oligotrophic Red Sea^{42,43}. Results presented in Chapters 8-10 are of particular interest as anthropogenic pressures on the Red Sea are constantly increasing⁴⁴, and 60 % of Red Sea coral reefs are already jeopardised⁴⁵. Results of Chapter 8 indicate cascaded, group-specific responses to long-term N availability, and link elemental and isotopic composition to group-specific nutrient limitations, N uptake and utilisation, and highlight the importance of P limitations in hard and soft corals. Results of the present dissertation emphasise the role of turf algae as strong competitors for space and nutrients in reefs under stress, particularly considering their fast response to eutrophication (Chapter 10), their ability to incorporate N faster than hard coral symbionts (Chapter 7), their increasing N fixation and denitrification activity under moderate eutrophication (Chapter 8), implicating that algae-dominated reefs may have a higher potential for biomass accumulation that can enhance space occupation and rapid succession on bare reef substrates^{46,47}. The loss of the structurally complex calcium carbonate reef framework and an increased space occupation by algae (Chapter 9) may hamper the replenishment of adult coral populations due to recruitment inhibition through limited habitat complexity and grazing pressure⁴⁸. Together, this may restrain reef recovery⁴⁸ and the high biodiversity characteristic of tropical coral reef ecosystems⁴⁹.

The *in situ* eutrophication experiment resulted in a moderate N increase, and lasted for eight weeks. Findings of Chapter 8 revealed increased N₂ fixation and denitrification rates for coral reef substrates and organisms under moderately elevated nutrient concentrations (1-2 µM N), which contradicts previous studies that reported consistently lower N₂ fixation activities and concurrent higher denitrification rates for reef patches and reef sediments under elevated nutrient availability (up to 20 µM N)^{25,50}. To investigate potential nutrient- and substrate-specific response patterns, four different nutrient concentrations were chosen to reflect ambient, realistic and above-realistic nutrient scenarios (Chapter 10) using the COBRA approach (Chapter 2). Indeed, nutrient-specific, ambiguous responses of stimulated and suppressed N₂ fixation and

denitrification were observed for turf algae and coral rubble (Chapter 10), with a specific thresholds identified for coral rubble at which N_2 fixation is turned off and denitrification was initiated. Whereas turf algae and coral rubble have been identified as major N fixers before, their role as denitrifiers is comparatively small. However, particularly under eutrophied scenarios, a key role in rapidly relieving substrates from N can be aligned for coral rubble, for which we were able to identify a threshold that suppresses N_2 fixation and stimulates denitrification (Chapter 6 and 10). Hence, the fast response to short-term eutrophication might be key under nutrient pulses⁵¹ by alleviating excess N via denitrification. In how far previously identified key denitrifiers such as hard and soft corals (Chapter 6) respond to short-term eutrophication remains to be determined. Hypothetically, their role in eutrophied and degraded coral reefs has been overlooked yet.

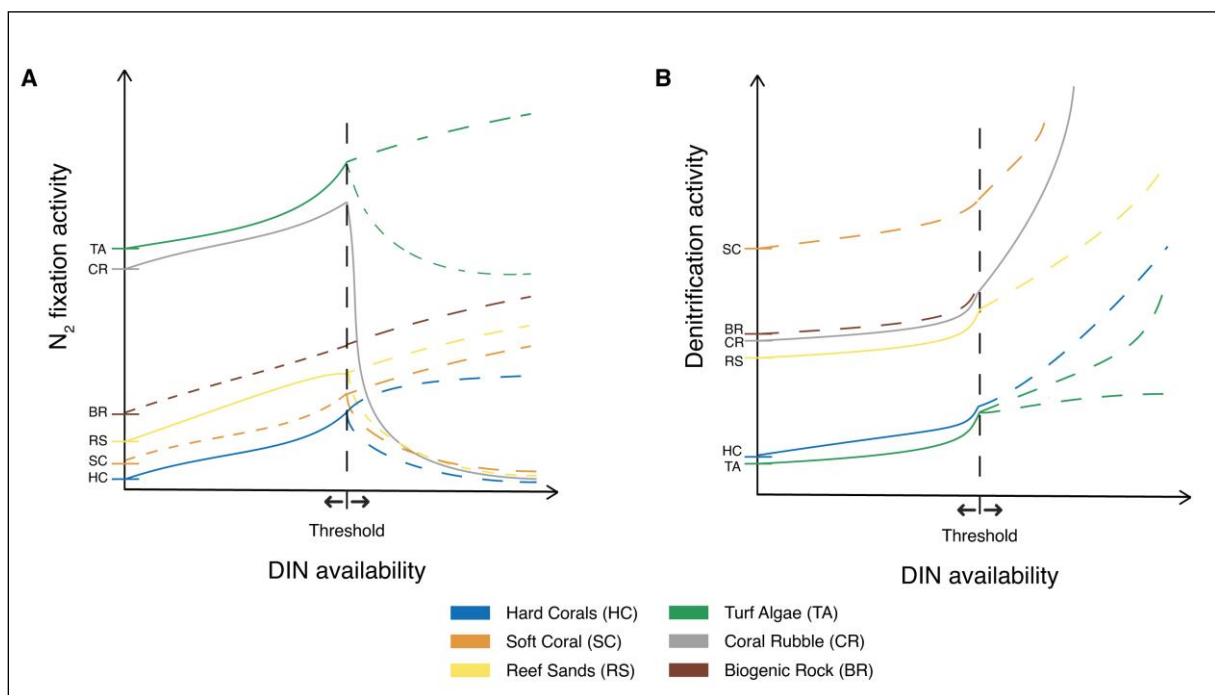


Figure 11.5 | Quantified (solid lines, based on Chapters 2, 4, 6, 8, and 10) and hypothesised (dashed lines) N_2 fixation and denitrification activities of investigated functional groups in dependence of DIN availability with hypothesised or detected (Chapter 8 and 10) concentration- and substrate-specific thresholds that stimulate or suppress N_2 fixation and denitrification, respectively.

11.5 | Synoptic Answers to the Specific Research Questions

Research Question 1: How can nitrogen fluxes be determined simultaneously in coral reef environments?

What are suitable techniques to address nitrogen and oxygen fluxes *in* and *ex situ*?

An acetylene-based approach was established to quantify N_2 fixation and denitrification in coral reef environments (Chapter 2) by combining already existing methods (i.e., acetylene reduction assay⁵² and acetylene blockage technique^{53–55}) that are commonly used to determine one of the two target N pathways. Even though acetylene-based techniques have faced criticism in the last decades^{56–58}, the approach presented and utilised in this dissertation facilitates cost-efficient sample processing, and opens the door to directly

adjust incubation parameters such as nutrient addition (Chapter 8 and 10), temperature, or light intensity according to the experimental design. Chapter 3 and 9 describe the development and successful usage of benthic *in situ* chambers that were used to investigate community-wide biogeochemical fluxes such as N or oxygen *in situ*.

Research Question 2: What are the baseline rates of N₂ fixation and denitrification in the major functional groups, and what is their relative importance regarding intact coral- and degraded algae-dominated reef communities?

Major functional groups that together account for >98 % of the benthic cover of the investigated coral reef⁴⁸ were used to determine respective N₂ fixation and denitrification activities. Results presented in Chapter 4 and 6 are the first to provide a comparative overview of denitrification activities of major coral reef related functional groups. The results suggest a clear distinction between key functional groups, in which the most active N₂ fixers showed lowest denitrification potentials and vice versa, with turf algae and coral rubble functioning as major N₂ fixers, whereas soft corals displaying highest denitrification activities. Extrapolated to coral- and algae-dominated reef areas, respectively, overall N₂ fixation increased by 100 % in algae-dominated areas compared to coral-dominated areas, whereas denitrification remained stable. Turf algae and coral rubble are key N₂ fixers, and together account for 91 % of overall N₂ fixation in coral-dominated and 99 % in algae-dominated reef areas, whereas hard and soft corals contribute equally to the 78 % of overall denitrification in coral dominated areas, and still account for > 50 % of overall denitrification despite covering only approx. 22 % of the seafloor in algae-dominated reef areas.

Research Question 3: What are the effects of both short- and long-term eutrophication on coral reef associated functional groups? How does eutrophication alter functioning of coral reef communities?

Long-term *in situ* eutrophication (added on low background nutrient availability) has multi-fold effects on coral reef organisms, substrates and communities: i) it particularly promotes the incorporation of excess N into turf algae biomass (Chapter 7), ii) moderate long-term eutrophication stimulates both N₂ fixation and denitrification in turf algae, hard corals and reef sediments (Chapter 8), and iii) ultimately increases gross productivity and shifts from net calcification to dissolution in algae- compared to coral-dominated reef communities, concurrent to change from net dissolved organic N sink to sources of both community types (Chapter 9). Short-term eutrophication was found to lead to substrate-specific and concentration-depending alterations of N₂ fixation and denitrification, with specific thresholds for turf algae and coral rubble that either stimulate or suppress both N cycling pathways (Chapter 10).

11.6 | Perspective and Future Research Directions

The work presented and included in this dissertation provides new insight to the functional aspects concerning biogeochemical cycling in coral- and algae-dominated reef communities and the organisms and substrates that shape coral reefs. This thesis provided the first evidence that denitrification is an active pathway occurring not only in coral reef framework builders, but is present across a wide range of coral reef associated organisms and substrates. Further, results of the thesis show that local stressors, such as eutrophication, directly alter functioning and biogeochemical cycling of coral reefs, with evoking varying responses in coral- compared to algae-dominated reef areas. However, knowledge about coral reef functioning and N cycling is still limited and in its infancies^{14,59}, and by answering the research questions included in this thesis, many more aspects remain elusive and future research question arose.

1) Coral reefs are adapted to flourish in nutrient-poor waters of the tropics, thus, understanding the cycling of key nutrients such as C and N is paramount^{16,59,60}. The importance of nitrogen cycling in coral reefs has been highlighted in recent studies^{16,59,61}, however, a holistic understanding and proof of all N cycling pathways that have been suggested to occur in coral reef environments, such as nitrification or ANAMMOX, is missing yet. Furthermore, most studies have provided evidence for N₂ fixation and denitrification to appear in coral reef organisms and substrates, with studies being carried out *ex situ*^{21,36,62,63} (Chapter 2, 4, 6, 8, and 10). While laboratory studies provide excellent insights, *in situ* approaches capture factors such as the inorganic nitrogen retention and recycling between different compartments of the benthos^{64,65} or the occurrence of interstitial waters of the reef structure^{16,66} that could potentially alter N cycling processes. For these reasons, future studies should target the *in situ* assessment of N cycling pathways, such as N₂ fixation, denitrification, nitrification, ANAMMOX, and fluxes of dissolved organic N by using isotope tracer approaches. By doing so, the quantification of N flux rates and the localisation of fixed or released nitrogenous compounds could be targeted.

2) Aforementioned recommendations would furthermore address the inclusion of rather overseen functional groups in coral reef environments, such as sponges or crustose coralline algae (CCA)⁶⁷. Both sponges and CCA are dominant functional groups in coral reef cavities⁶⁷⁻⁶⁹, and the biomass in such cryptic cavities might exceed that of the reef surface^{70,71} with encrusting biota covering more than 93 % of the available hard substrate^{72,73}. Generally, heterotrophic organisms are dominant in cavities, mainly due to low light conditions⁶⁷. As there are links between the autotrophic and heterotrophic capacity, respectively (Chapter 4)⁶³ regarding N cycling in corals and their resilience against local⁷⁴ and global stressors⁷⁵⁻⁷⁷, this might ultimately hold true for further coral reef organisms and substrates.

3) Current and future reef face unprecedented environmental changes^{78,79}, with research focussing on understanding and predicting the effects of climate change on marine ecosystems and their organisms^{6,80,81}. Understanding the effects of environmental change on marine microbial communities as major drivers of elemental transformations of marine biogeochemical cycles^{82,83} will be of key importance. As such, eutrophication, as well as ocean warming and acidification belong to the mainly discussed and

assessed threats. Chapters 7-10 of the present dissertation illustrate the divergent effect of solely one stressor on N cycling pathways, but in how far multiple stressors interact and effect these pathways remains unknown. By far, most of the present studies target the effects of single stressors. Studies investigating a combination of multiple stressors to determine synergetic or attenuating effects (not only but also) on biogeochemical cycling, and should be, thus, prioritised in future experimental designs.

4) Results of Chapter 10 discuss substrate-specific and concentration-depending thresholds that either stimulate or suppress N₂ fixation and denitrification. Whereas both investigated functional groups (i.e., turf algae and coral rubble) were identified as major N fixers, their role as denitrifiers is comparatively small (Chapter 6). In how far previously identified key denitrifiers such as hard and soft corals (Chapter 6) respond to short-term eutrophication remains to be determined. Hypothetically, their role in eutrophied and degraded coral reefs has been yet overlooked, but could potentially fulfil a key role in relieving the ecosystem from excess N under nutrient enriched scenarios.

11.7 | References

1. El-Khaled, Y. C. *et al.* Simultaneous Measurements of Dinitrogen Fixation and Denitrification Associated With Coral Reef Substrates : Advantages and Limitations of a Combined Acetylene Assay. *Front. Mar. Sci.* **7**, 411 (2020).
2. Roth, F. *et al.* *An in situ approach for measuring biogeochemical fluxes in structurally complex benthic communities.* *Methods in Ecology and Evolution* (2019). doi:10.1111/2041-210X.13151
3. Tilstra, A. *et al.* Denitrification Aligns with N₂ Fixation in Red Sea Corals. *Sci. Rep.* **9**, 19460 (2019).
4. Karcher, D. B. *et al.* Nitrogen eutrophication particularly promotes turf algae in coral reefs of the central Red Sea. *PeerJ* **8**, e8737 (2020).
5. El-Khaled, Y. *et al.* In situ eutrophication stimulates dinitrogen fixation, denitrification, and productivity in Red Sea coral reefs. *Mar. Ecol. Prog. Ser.* **645**, 55–66 (2020).
6. Pandolfi, J. M., Connolly, S. R., Marshall, D. J. & Cohen, A. L. Projecting coral reef futures under global warming and ocean acidification. *Science (80-.)*. **333**, 418–422 (2011).
7. Hughes, T. P. *et al.* Coral reefs in the Anthropocene. *Nature* **546**, 82–90 (2017).
8. Fabricius, K. E. Factors Determining the Resilience of Coral Reefs to Eutrophication: A Review and Conceptual Model. in *Coral Reefs: An Ecosystem in Transition* (eds. Dubinsky, Z. & Stambler, N.) 493–505 (2011). doi:10.1007/978-94-007-0114-4_28
9. Bellwood, D. R., Hughes, T. P., Folke, C. & Nyström, M. Confronting the coral reef crisis. *Nature* **429**, 827–833 (2004).
10. Hoegh-Guldberg, O. *et al.* Coral Reefs Under Rapid Climate Change and Ocean Acidification. *Science (80-.)*. **318**, 1737–1742 (2007).
11. Van Hooidonk, R. *et al.* Local-scale projections of coral reef futures and implications of the Paris Agreement. *Sci. Rep.* **6**, 1–8 (2016).
12. Osborne, K. *et al.* Delayed coral recovery in a warming ocean. *Glob. Chang. Biol.* **23**, 3869–3881 (2017).
13. Hughes, T. P., Graham, N. A. J., Jackson, J. B. C., Mumby, P. J. & Steneck, R. S. Rising to the challenge of sustaining coral reef resilience. *Trends Ecol. Evol.* **25**, 633–642 (2010).
14. Williams, G. J. & Graham, N. A. J. Rethinking coral reef functional futures. *Funct. Ecol.* **33**, 942–947 (2019).
15. Muscatine, L. & Porter, J. W. Reef Corals: Mutualistic Symbioses Adapted to Nutrient-Poor Environments. *Bioscience* **27**, 454–460 (1977).
16. O’Neil, J. M. & Capone, D. G. *Nitrogen Cycling in Coral Reef Environments.* *Nitrogen in the Marine Environment* (2008). doi:10.1016/B978-0-12-372522-6.00021-9
17. Kimes, N. E., Van Nostrand, J. D., Weil, E., Zhou, J. & Morris, P. J. Microbial functional structure of *Montastraea faveolata*, an important Caribbean reef-building coral, differs between healthy and yellow-band diseased colonies. *Environ. Microbiol.* **12**, 541–556 (2010).
18. Budd, A. F., Fukami, H., Smith, N. D. & Knowlton, N. Taxonomic classification of the reef coral family Mussidae (Cnidaria: Anthozoa: Scleractinia). *Zool. J. Linn. Soc.* **166**, 465–529 (2012).
19. Siboni, N., Ben-Dov, E., Sivan, A. & Kushmaro, A. Global distribution and diversity of coral-

- associated Archaea and their possible role in the coral holobiont nitrogen cycle. *Environ. Microbiol.* **10**, 2979–2990 (2008).
20. Yang, S., Sun, W., Zhang, F. & Li, Z. Phylogenetically Diverse Denitrifying and Ammonia-Oxidizing Bacteria in Corals *Alcyonium gracillimum* and *Tubastraea coccinea*. *Mar. Biotechnol.* **15**, 540–551 (2013).
 21. Cardini, U. *et al.* Budget of Primary Production and Dinitrogen Fixation in a Highly Seasonal Red Sea Coral Reef. *Ecosystems* **19**, 771–785 (2016).
 22. Bednarz, V. N., Cardini, U., Van Hoytema, N., Al-Rshaidat, M. M. D. & Wild, C. Seasonal variation in dinitrogen fixation and oxygen fluxes associated with two dominant zooxanthellate soft corals from the northern Red Sea. *Mar. Ecol. Prog. Ser.* **519**, 141–152 (2015).
 23. Pogoreutz, C. *et al.* Nitrogen fixation aligns with nifH abundance and expression in two coral trophic functional groups. *Front. Microbiol.* **8**, 1–7 (2017).
 24. Shashar, N., Feldstein, T., Cohen, Y. & Loya, Y. Nitrogen fixation (acetylene reduction) on a coral reef. *Coral Reefs* **13**, 171–174 (1994).
 25. Koop, K. *et al.* ENCORE: The effect of nutrient enrichment on coral reefs. Synthesis of results and conclusions. *Mar. Pollut. Bull.* **42**, 91–120 (2001).
 26. Mills, M. M., Ridame, C., Davey, M., La Roche, J. & Geider, R. J. Iron and phosphorus co-limit nitrogen fixation in the eastern tropical North Atlantic. *Nature* **429**, 292–294 (2004).
 27. Arrigo, K. K. Marine microorganisms and global nutrient cycles. *Nature* **437**, 349–355 (2004).
 28. Veal, C. J., Holmes, G., Nunez, M., Hoegh-Guldberg, O. & Osborn, J. A comparative study of methods for surface area and three dimensional shape measurement of coral skeletons. *Limnol. Oceanogr. Methods* **8**, 241–253 (2010).
 29. Roth, F. *et al.* High rates of carbon and dinitrogen fixation suggest a critical role of benthic pioneer communities in the energy and nutrient dynamics of coral reefs. *Funct. Ecol.* (2020). doi:10.1111/1365-2435.13625
 30. Littler, M. & Littler, D. The Nature of Turf and Boring Algae and Their Interactions on Reefs. *Smithson. Contrib. to Mar. Sci.* 213–217 (2013).
 31. Rosenberg, G. & Ramus, J. Uptake of inorganic nitrogen and seaweed surface area: Volume ratios. *Aquat. Bot.* **19**, 65–72 (1984).
 32. Fong, P., Rudnicki, R. & Zedler, J. B. *Algal community response to nitrogen and phosphorus loading in experimental mesocosms: Management recommendations for southern California lagoons.* (1987).
 33. Fong, C. R., Gaynus, C. J. & Carpenter, R. C. Complex interactions among stressors evolve over time to drive shifts from short turfs to macroalgae on tropical reefs. *Ecosphere* **11**, (2020).
 34. Yamamuro, M., Kayanne, H. & Minagawa, M. Carbon and nitrogen stable isotopes of primary producers in coral reef ecosystems. *Limnol. Oceanogr.* **40**, 617–621 (1995).
 35. Tilstra, A. *et al.* Seasonality affects dinitrogen fixation associated with two common macroalgae from a coral reef in the northern Red Sea. *Mar. Ecol. Prog. Ser.* **575**, 69–80 (2017).
 36. Rix, L. *et al.* Seasonality in dinitrogen fixation and primary productivity by coral reef framework substrates from the northern Red Sea. *Mar. Ecol. Prog. Ser.* **533**, 79–92 (2015).

37. Done, T. J. Phase shifts in coral reef communities and their ecological significance. *Hydrobiologia* **247**, 121–132 (1992).
38. Hughes, T. P. Catastrophes, phase shifts, and large-scale degradation of a Caribbean coral reef. *Science (80-.)*. **265**, 1547–1551 (1994).
39. McManus, J. W. & Polsenberg, J. F. Coral-algal phase shifts on coral reefs: Ecological and environmental aspects. *Prog. Oceanogr.* **60**, 263–279 (2004).
40. Loya, Y., Lubinevsky, H., Rosenfeld, M. & Kramarsky-Winter, E. Nutrient enrichment caused by in situ fish farms at Eilat, Red Sea is detrimental to coral reproduction. *Mar. Pollut. Bull.* **49**, 344–353 (2004).
41. Peña-García, D., Ladwig, N., Turki, A. J. & Mudarris, M. S. Input and dispersion of nutrients from the Jeddah Metropolitan Area, Red Sea. *Mar. Pollut. Bull.* **80**, 41–51 (2014).
42. Wafar, M. *et al.* Patterns of distribution of inorganic nutrients in Red Sea and their implications to primary production. *J. Mar. Syst.* **156**, 86–98 (2016).
43. Churchill, J. H., Bower, A. S., McCorkle, D. C. & Abualnaja, Y. The transport of nutrient-rich Indian Ocean water through the Red Sea and into coastal reef systems. *J. Mar. Res.* **72**, 165–181 (2014).
44. Carvalho, S., Kürten, B., Krokos, G., Hoteit, I. & Ellis, J. The Red Sea. in *World Seas: An Environmental Evaluation Volume II: The Indian Ocean to the Pacific* (ed. Sheppard, C.) 49–74 (Academic Press, 2019). doi:10.1016/B978-0-08-100853-9.00004-X
45. Burke, L., Reytar, K., Spaulding, M. & Perry, A. *Reefs at Risk*. (World Resources Institute, 2011).
46. Roth, F., Stuhldreier, I., Sánchez-Noguera, C., Morales-Ramírez, T. & Wild, C. Effects of simulated overfishing on the succession of benthic algae and invertebrates in an upwelling-influenced coral reef of Pacific Costa Rica. *J. Exp. Mar. Bio. Ecol.* **468**, 55–66 (2015).
47. Stuhldreier, I. *et al.* Upwelling increases net primary production of corals and reef-wide gross primary production along the pacific coast of costa rica. *Front. Mar. Sci.* **2**, (2015).
48. Roth, F. *et al.* Coral reef degradation affects the potential for reef recovery after disturbance. *Mar. Environ. Res.* **142**, 48–58 (2018).
49. Bellwood, D. R. Regional-Scale Assembly Rules and Biodiversity of Coral Reefs. *Science (80-.)*. **292**, 1532–1535 (2001).
50. Capone, D. G., Dunham, S. E., Horrigan, S. G. & Duguay, L. E. Microbial nitrogen transformations in unconsolidated coral reef sediments. *Mar. Ecol. Prog. Ser.* **80**, 75–88 (1992).
51. den Haan, J. *et al.* Nitrogen and phosphorus uptake rates of different species from a coral reef community after a nutrient pulse. *Sci. Rep.* **6**, 28821 (2016).
52. Hardy, R. W. F., Holsten, R. D., Jackson, E. K. & Burns, R. C. The acetylene - ethylene assay for N₂ fixation: laboratory and field evaluation. *Plant Physiol.* **43**, 1185–1207 (1968).
53. Fedorova, R. I., Milekhina, E. I. & Il'Yukhina, N. I. Evaluation of the method of 'gas metabolism' for detecting extraterrestrial life. Identification of nitrogen-fixation microorganisms. *Izv. Akad. Nauk SSSR Ser. Biol.* **6**, 797–806 (1973).
54. Balderston, W. L., Sherr, B. & Payne, W. J. Blockage By Acetylene of Nitrous-Oxide Reduction in *Pseudomonas-Perfectomarinus*. *Appl. Environ. Microbiol.* **31**, 504–508 (1976).

55. Yoshinari, T. & Knowles, R. Acetylene Inhibition of Nitrous Oxide Reduction by Denitrifying Bacteria. *Biochem. Biophys. Res. Commun.* **69**, 705–710 (1976).
56. Giller, K. E. Use and abuse of the acetylene reduction assay for measurement of ‘associative’ nitrogen fixation. *Soil Biol. Biochem.* **19**, 783–784 (1987).
57. Groffman, P. M. *et al.* Methods for Measuring Denitrification: Diverse Approaches to a Difficult Problem. *Ecol. Appl.* **16**, 2091–2122 (2006).
58. Wilson, S. T., Böttjer, D., Church, M. J. & Karl, D. M. Comparative assessment of nitrogen fixation methodologies, conducted in the oligotrophic north pacific ocean. *Appl. Environ. Microbiol.* **78**, 6516–6523 (2012).
59. Rädercker, N., Pogoreutz, C., Voolstra, C. R., Wiedenmann, J. & Wild, C. Nitrogen cycling in corals: The key to understanding holobiont functioning? *Trends Microbiol.* **23**, 490–497 (2015).
60. Szmant, A. M. Nutrient Enrichment on Coral Reefs: Is It a Major Cause of Coral Reef Decline? *Estuaries* **25**, 743–766 (2002).
61. Morris, L. A., Voolstra, C. R., Quigley, K. M., Bourne, D. G. & Bay, L. K. Nutrient Availability and Metabolism Affect the Stability of Coral–Symbiodiniaceae Symbioses. *Trends Microbiol.* **xx**, 1–12 (2019).
62. Bednarz, V. N. *et al.* Contrasting seasonal responses in dinitrogen fixation between shallow and deep-water colonies of the model coral *Stylophora pistillata* in the northern Red Sea. *PLoS One* **13**, e0199022 (2018).
63. Pogoreutz, C. *et al.* Nitrogen fixation aligns with *nifH* abundance and expression in two coral trophic functional groups. *Front. Microbiol.* **8**, 1–7 (2017).
64. Wild, C. *et al.* Coral mucus functions as an energy carrier and particle trap in the reef ecosystem. *Nature* **428**, 66–70 (2004).
65. De Goeij, J. M. *et al.* Surviving in a marine desert: The sponge loop retains resources within coral reefs. *Science (80-.)*. **342**, 108–110 (2013).
66. Hatcher, B. G. Coral-Reef Primary Productivity - a Hierarchy of Pattern and Process. *Trends Ecol. Evol.* **5**, 149–155 (1990).
67. De Goeij, J. M. & Van Duyl, F. C. Coral cavities are sinks of dissolved organic carbon (DOC). *Limnol. Oceanogr.* **52**, 2608–2617 (2007).
68. Gili, J. M. & Coma, R. Benthic suspension feeders: Their paramount role in littoral marine food webs. *Trends Ecol. Evol.* **13**, 316–321 (1998).
69. Wunsch, M., Al-Moghrabi, S. M. & Kötter, I. Communities of coral reef cavities in Jordan, Gulf of Aqaba (Red Sea). *Proc. 9th Int. Coral Reef Symp.* **2**, 595–600 (2002).
70. Brock, R. E. & Brock, J. H. A method for quantitatively assessing the infaunal community in coral rock. *Limnol. Oceanogr.* **22**, 948–951 (1977).
71. Meesters, E. *et al.* Sub-rubble communities of Curaçao and Bonaire coral reefs. *Coral Reefs* **10**, 189–197 (1991).
72. Richter, C., Wunsch, M., Rasheed, M., Kötter, I. & Badran, M. I. Endoscopic exploration of Red Sea coral reefs reveals dense populations of cavity-dwelling sponges. *Nature* **413**, 726–730 (2001).

73. Richter, C. & Wunsch, M. Cavity-dwelling suspension feeders in coral reefs - A new link in reef trophodynamics. *Mar. Ecol. Prog. Ser.* **188**, 105–116 (1999).
74. Seemann, J. *et al.* Importance of heterotrophic adaptations of corals to maintain energy reserves. *Proc. 12th Int. Coral Reef Symp.* 9–13 (2012).
75. Rädecker, N., Pogoreutz, C., Gegner, H. M., Cárdenas, A. & Roth, F. Heat stress destabilizes symbiotic nutrient cycling in corals. *Proceeding Natl. Acad. Sci. United States Am.* **118**, e2022653118 (2021).
76. Grottoli, A. G., Rodrigues, L. J. & Palardy, J. E. Heterotrophic plasticity and resilience in bleached corals. *Nature* **440**, 1186–1189 (2006).
77. Tremblay, P., Gori, A., Maguer, J. F., Hoogenboom, M. & Ferrier-Pagès, C. Heterotrophy promotes the re-establishment of photosynthate translocation in a symbiotic coral after heat stress. *Sci. Rep.* **6**, (2016).
78. Harnik, P. G. *et al.* Extinctions in ancient and modern seas. *Trends Ecol. Evol.* **27**, 608–617 (2012).
79. Halpern, B. S., Selkoe, K. A., Micheli, F. & Kappel, C. V. Evaluating and ranking the vulnerability of global marine ecosystems to anthropogenic threats. *Conserv. Biol.* **21**, 1301–1315 (2007).
80. Runge, J. A. *et al.* End of the century CO₂ concentrations do not have a negative effect on vital rates of *Calanus finmarchicus*, an ecologically critical planktonic species in North Atlantic ecosystems. *ICES J. Mar. Sci.* **73**, 937–950 (2016).
81. Bijma, J., Pörtner, H. O., Yesson, C. & Rogers, A. D. Climate change and the oceans - What does the future hold? *Mar. Pollut. Bull.* **74**, 495–505 (2013).
82. Gruber, N. & Galloway, J. N. An Earth-system perspective of the global nitrogen cycle. *Nature* **451**, 293–296 (2008).
83. Gruber, N. Warming up, turning sour, losing breath: Ocean biogeochemistry under global change. *Philos. Trans. R. Soc. A Math. Phys. Eng. Sci.* **369**, 1980–1996 (2011).

APPENDIX

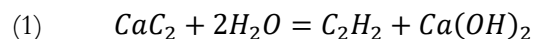
Appendix | Supplementary material

Supplementary Material to Chapter 2:

Supplementary Material 2.1: Incubation Preparation, Processing and Gas Concentration Calculations

Incubations and Headspace Sampling

Both acetylene (hereafter C₂H₂)-enriched seawater and C₂H₂ gas were prepared within 24 h prior to sample collection and incubations. For one gas bag (Tedlar 7"x7", 1 L volume) and 1 L of filtered seawater, 12.5 g of calcium carbide (CaC₂, Sigma-Aldrich, pieces, thickness < 10 mm) was added to 100 mL MilliQ filtered water in an Erlenmeyer flask. C₂H₂ gas was formed according to:



The gas was led through two consecutive 1 L Duran gas washing bottles; the first one filled with MilliQ water for filtration¹ and the second one with filtered seawater. The second bottle with filtered seawater was used in the incubation processes as it has been enriched with C₂H₂. Finally, the C₂H₂ was collected in a gas bag attached to the second Duran bottle (Fig. S2A). After producing C₂H₂ gas and C₂H₂-enriched seawater, specimens were prepared for the incubations. All preparations considered potential acclimatization phases in aquaria facilities after the sampling from the field or from fragmentation/cutting of the collected specimen to fit into the incubation chambers.

For the COBRA (=combined blockage/reduction assay), substrates/organisms were transferred to 1 L glass chambers with gastight seals and lids. The lids were equipped with a hole closed by a rubber septum (thickness: 10 mm) that was penetrated using a Luer Lock needle with a push-pull valve. This enabled sampling with a syringe whilst the chambers stayed airtight. Incubation chambers were filled with 720 mL of seawater that was collected in the field on the same day, and 80 mL C₂H₂-enriched seawater was added. Each incubation chamber contained a pedestal for the specimen, giving room to a magnetic stirrer. Seals and lids were placed on the incubation chambers and closed gastight. Using a syringe (50 mL PTFE Tipped Plunger and Dispenser Syringe, equipped with push-pull valve with Luer Lock, SGE Analytical Science), 20 mL of the headspace was substituted with 20 mL C₂H₂ gas. Thus both incubation water and headspace contained 10 % C₂H₂ (Fig. S2B). The incubation chambers were immersed in a tempered water bath that was placed on inductive drive stirrers (Variomag Telesystem, Thermo Scientific, Germany, 500 rpm) to ensure stable measurement conditions and constant water circulation within the chambers to promote an equilibrium between both liquid and gaseous stage². Gas samples (2.5 mL) were collected using a gastight syringe (2.5 mL PTFE Tipped Plunger and Dispenser Syringe, equipped with push-pull valve with Luer Lock, SGE Analytical Science) immediately after starting the incubation (t₀) to correct for background C₂H₄ concentrations and the sample was transferred into a gastight vacuum tube (Monoject Blood Collection Tube 10.25 mm x 64 mm, 3 mL, Covidien).

Instrumentation and Measurement of Samples

The static headspace analysis was performed using either manual injection via a gastight syringe (1 mL Hamilton, equipped with push-pull valve with Luer Lock) or a headspace autosampler (Agilent G1888 Network Headspace Sampler). The headspace heated transfer line was connected to a capillary split-splitless inlet (inlet, in which the injected sample vaporizes and mixes with the carrier gas before a subset of the injected sample is transferred to the column) of an Agilent 7890B Gas Chromatograph (GC). The chromatographic separation was performed using the HP-Plot/Q column (19091P-QO4 with ID 0.32 mm, 30 m length, 20 µm film, Agilent technologies, Santa Clara, CA, USA) connected to the GC inlet and a helium pulsed discharge detector (VICI, Houston, TX, USA).

In case of the manual injection, a sample size of 1 mL was sampled and directly injected to the inlet of the GC using a gastight syringe (1 mL Hamilton, equipped with push-pull valve with Luer Lock). For the autosampler, a custom-built adapter was used to accommodate the Monoject blood collection vials. An

auxiliary EPC (electron pressure control) module mounted on the GC was used for the vial pressurization. The GC raw data files were acquired and processed using Agilent Chemstation software. Peak identification was performed using a mass spectrometer that was attached to the GC (GC/MS system Agilent 7890A/5975, USA).

The headspace parameters were set as follows: the oven temperature was set at 50 °C with an oven stabilization time of 0.20 min; vial equilibration time was set at 1 min; vial pressurization time was set at 0.05 min; loop temperature was set at 100 °C; loop equilibrium and fill time were set at 0.01 min and 0.05 min, respectively; vial pressure was set at 13.50 psi; GC cycle time was set at 15 min; temperature of the transfer line was set at 150 °C.

A HP-Plot/Q capillary column was used for the chromatographic separation of nitrous oxide (hereafter N₂O) and ethylene (hereafter C₂H₄). The flow of helium as a carrier gas was set at a constant flow rate of 3.0 mL/min. The split-splitless inlet was held at 140 °C with a split ratio of 10:1. The initial column oven temperature was set at 36 °C and was held for 1 min, subsequently ramped to 76 °C for 4 min with a rate of 10 °C/min. The post-run temperature was set at 250 °C and was held for 3 min. In the GC/MS experimental phase for peak identification, the same GC parameters and column were used. The MS instrument parameters were set as follows: the temperature of the MS source and MS quad analyzer were set to 230 °C and 150 °C respectively, the scan range was from 20 to 50 Da and the electron energy was set at 70 eV. With these settings, peaks and retention times were identified. Prior to starting the measurements, a calibration of the GC system is required. For this purpose, the calibration curve should cover the expected ranges of C₂H₄ and N₂O rates for reliable measurements.

Calculation of N₂ Fixation and Denitrification Rates

The measured headspace concentrations of C₂H₄ and N₂O, respectively, were used to calculate the total dissolved amount of C₂H₄ and N₂O in the incubation chamber. The total amount of C₂H₄ and N₂O in the incubation chamber can be calculated via the addition of headspace and incubation water. These values can be used to approximate N₂ fixation and denitrification rates^{3,4}. The calculation process can be described as presented here for the measurement of C₂H₄ via manual injection (the calculation for N₂O and injections via autosampler differ marginally, see end of this section).

The calculation of the absolute amount of C₂H₄ in the incubation chamber headspace (C₂H_{4_HS}; [nM]) can be described according to the following equation:

$$(2) \quad C_{2H_4_{HS}} = R^{-1} * C_{2H_4_{ms}} * Vol_{HS} * 10^3$$

With:

R	ideal gas constant; defined as 24,465 cm ³ mol ⁻¹ at 25 °C in our case as both gases act identical to ideal gases;
C ₂ H _{4_ms}	measured headspace concentration [ppm]; possible equilibrium transformations (Boyle-Mariotte law, according to Job and Rüffler (2016) ⁵) have to be considered depending on the volume of the syringes used for sampling and transferring the gaseous sample from collection tube to the GC and the volume of the collection tube itself;
Vol _{HS}	headspace volume [cm ³].
10 ³	result of cancelations from unit-transformations for ppm to mol conversion

Accordingly, the total C₂H₄ amount in the incubation water (C₂H_{4_IW}; [nM]) was calculated according to:

$$(3) \quad C_{2H_4_{IW}} = R^{-1} * C_{2H_4_{ms}} * \beta * Vol_{IW} * 10^3$$

With:

β Bunsen-solubility coefficient for C₂H₄ according to Breitbarth et al. (2004)⁶;
Vol_{IW} incubation water volume [mL].

The total C₂H₄ amount of the incubation chamber (C₂H_{4_{tot}}; [nM]) can be calculated with a simple addition as:

$$(4) \quad C_2H_{4_{tot}} = C_2H_{4_{HS}} + C_2H_{4_{IW}}$$

To ensure comparability between different specimens, rates should be normalized to either surface area (SA; e.g., by creating 3D models of the specimens with computer software) or dry weight (DW)^{3,7,8}. To calculate for metabolic background activities, rates of control incubations/seawater blanks have to be considered at this point too. In addition, rates should also be normalized to incubation time (e.g., rates per hour, rates per day, etc.). These two reference parameters (SA or DW, time) can be included according to the following equation, resulting in comparable rates between replicates (C₂H_{4_{rate}}; [nM time⁻¹ SA⁻¹ or nM time⁻¹ g⁻¹ DW]):

$$(5) \quad C_2H_{4_{rate}} = \frac{(C_2H_{4_{tot_smp1_tx}} - C_2H_{4_{tot_smp1_t0}}) - (C_2H_{4_{tot_ctrl_tx}} - C_2H_{4_{tot_ctrl_t0}})}{(t_x - t_0) * RP}$$

With:

C ₂ H _{4_{tot_smp1_tx}}	C ₂ H _{4_{tot}} at t _x ;
C ₂ H _{4_{tot_smp1_t0}}	C ₂ H _{4_{tot}} at t ₀ ;
C ₂ H _{4_{tot_ctrl_tx}}	C ₂ H _{4_{tot}} of control incubation/seawater blank at t _x ;
C ₂ H _{4_{tot_ctrl_t0}}	C ₂ H _{4_{tot}} of control incubation/seawater blank at t ₀ ;
RP	reference parameter (i.e., SA or DW).

A transformation from C₂H₄ evolution to N₂ fixation rates could be considered by using accurate conversion factors according to Mulholland et al. (2004)⁹ or Charpy-Roubaud et al. (2001)¹⁰.

The calculations for the total N₂O concentration can be performed similarly to the approach presented before with the annotation of considering a different solubility factor β ¹¹ and neglecting a conversion factor for N₂O for the quantification of total denitrification.

The calculation of both N₂ fixation and denitrification via autosampler can be carried out as described above with the short annotation that the correction factors differ as the transfer from the vacuum tube immediately to the GC inlet happens (i.e., without the use of a syringe) and, therefore, no dilution effect appears.

Supplementary Material 1.2: Example of Equilibrium Transformations for Syringes

Possible equilibrium transformations have to be considered, depending on a) the volume of the syringes used for sampling and transferring the gaseous sample from the collection tube to the gas chromatograph (GC), and b) on the volume of the collection tube itself. In our setup, we used a 2.5 mL PTFE Tipped Plunger and Dispenser Syringe (SGE Analytical Science) equipped with a push-pull valve with a Luer Lock for sampling and transferring from the incubation chambers to the collection tube (3 mL), and a 1 mL gastight syringe (Hamilton) equipped with a push-pull valve with a Luer Lock for injecting samples to the GC. According to Boyle-Mariotte law, the following example demonstrates the transformations with the used syringe/collection tube volumes:

$$C_2H_{4_{ms_ctd}} = C_2H_{4_{ms}} * CF_a * CF_b$$

With:

$C_2H_4_{ms\ ctd}$	corrected C_2H_4 concentration [ppm]
$C_2H_4_{ms}$	measured C_2H_4 concentration [ppm]
CF_a	correction factor for the equilibrium in sample size and collection tube (here: 2.5 mL * (3 mL) ⁻¹)
CF_b	correction factor for the equilibrium in transferring the sample the GC (here: 4 mL * (3 mL) ⁻¹)

Identical calculations are used for the correction of measured N_2O concentrations.

Table S1.3 | Detailed list of equipment which is required to perform the presented method. If not indicated elsewhere, amount of products depends on the respective experimental design.

Product	Amount
Agilent 7890A Gas Chromatograph System, Agilent Technologies	1
Agilent 5977A MSD, Agilent Technologies	1
HP-Plot/Q 19091P-QO4, Agilent J&W GC columns, length: 30m, I.D. 0,320mm, Film 20.00 um, Temp from -60°C to 270°C (290°C)	1
Helium pulsed discharge detector, VICI	1
Agilent G1888 Network Headspace Sampler, Agilent Technologies	1
Monoject Blood Collection Tube 10.25mm x 64mm, Covidien	1 per sample
2.5 mL PTFE Tipped Plunger and Dispenser Syringe, SGE Analytical Science, with push-pull valve with Luer Lock	1
50 mL PTFE Tipped Plunger and Dispenser Syringe, SGE Analytical Science, with push-pull valve with Luer Lock	1
1 mL Gastight syringe, Hamilton, with push-pull valve with Luer Lock	1
Tedlar Sampling Bag, 1 L, 7" x 7"	1
Calcium Carbide, pieces, thickness <10 mm, typically, technical grade, ~80%	
Woulff's bottle (incl. Duran bottles)	2
Erlenmeyer flask, 250 mL with a sidearm, lid	1
Connecting tubes	
1 L incubation chambers with gastight seals including rubber septum (>10 mm thickness)	
Radion XR 15w Pro light system	
Water bath, e.g. made of PVC	
Variomag Telesystem, Thermo Scientific	

Table S1.4 | Measured values of nitrous oxide (N₂O) concentrations before surface area correction (nmol N₂O mL⁻¹) at respective time point (t₀, t₂, t₄, t₈, t₁₂), and N₂O concentrations corrected with seawater blank and related to surface area of respective specimens (nmol N₂O cm⁻²). Asterisks indicate that initial (t₀) N₂O concentrations were lower than seawater blank concentrations (indicated with asterisks), value “zero” was used for rate calculation.

	Substrate	Surface Area	nmol N ₂ O mL ⁻¹					nmol N ₂ O cm ⁻²				
			t ₀	t ₂	t ₄	t ₈	t ₁₂	t ₀	t ₂	t ₄	t ₈	t ₁₂
Dark	Turf Algae I	68	0.0133	0.0329	0.0440	0.0291	0.0449	0.0075	0.3439	0.4846	0.2479	0.4656
	Turf Algae II	42	0.0111	0.0493	0.0384	0.0269	0.0274	0*	0.9473	0.6530	0.3490	0.3376
	Turf Algae III	39	0.0102	0.0399	0.0350	0.0241	0.0331	0*	0.7804	0.6156	0.3030	0.5089
	Turf Algae IV	68	0.0124	0.0323	0.0377	0.0268	0.0488	0*	0.3352	0.3925	0.2133	0.5225
	Turf Algae V	34	0.0138	0.0614	0.0706	0.0579	0.0588	0.0297	1.5263	1.7519	1.3436	1.3403
Light	Turf Algae I	50	0.0132	0.0252	0.0310	0.0333	0.0291	0*	0.2765	0.3271	0.3757	0.2885
	Turf Algae II	52	0.0113	0.0256	0.0289	0.0292	0.0354	0*	0.2739	0.2735	0.2834	0.3974
	Turf Algae III	33	0.0142	0.0142	0.0260	0.0364	0.0263	0.0000	0.0844	0.3446	0.6628	0.3525
	Turf Algae IV	50	0.0122	0.0154	0.0282	0.0295	0.0274	0*	0.0808	0.2701	0.2991	0.2537
	Turf Algae V	64	0.0142	0.0258	0.0344	0.0214	0.0255	0.0000	0.2247	0.3091	0.1081	0.1683
Dark	Coral Rubble I	70	0.0142	0.0098	0.0148	0.0131	0.0199	0.0209	0.0036	0.0547	0.0124	0.0957
	Coral Rubble II	48	0.0109	0.0148	0.0147	0.0199	0.0249	0*	0.1102	0.0781	0.1585	0.2437
	Coral Rubble III	67	0.0120	0.0141	0.0111	0.0177	0.0159	0*	0.0692	0.0019	0.0815	0.0393
	Coral Rubble IV	79	0.0136	0.0182	0.0120	0.0176	0.0251	0.0112	0.1104	0.0127	0.0679	0.1506
Light	Coral Rubble I	62	0.0153	0.0133	0.0276	0.0148	0.0171	0.0176	0.0305	0.2086	0.0049	0.0385
	Coral Rubble II	39	0.0126	0.0140	0.0370	0.0174	0.0208	0*	0.0664	0.5716	0.0744	0.1556
	Coral Rubble III	43	0.0179	0.0134	0.0257	0.0194	0.0243	0.0866	0.0470	0.2555	0.1135	0.2240
	Coral Rubble IV	68	0.0151	0.0142	0.0305	0.0227	0.0220	0.0137	0.0406	0.2328	0.1204	0.1071
Dark	Seawater Blank		0.0127	0.0095	0.0110	0.0123	0.0132					
Light	Seawater Blank		0.0142	0.0114	0.0147	0.0145	0.0147					

Table S1.5 | Measured values of ethylene (C₂H₄) concentrations before surface area correction (nmol C₂H₄ mL⁻¹) at respective time point (t₀, t₂, t₄, t₈, t₁₂), and C₂H₄ concentrations corrected with seawater blank and related to surface area of respective specimens (nmol C₂H₄ cm⁻²).

	Substrate	Surface Area	nmol C ₂ H ₄ mL ⁻¹					nmol C ₂ H ₄ cm ⁻²				
			t ₀	t ₂	t ₄	t ₈	t ₁₂	t ₀	t ₂	t ₄	t ₈	t ₁₂
Dark	Turf Algae I	68	0.0271	0.0566	0.0802	0.1553	0.2778	0.3978	0.4468	0.8093	1.9739	3.7496
	Turf Algae II	42	0.0227	0.0600	0.0713	0.1047	0.1906	0.5404	0.8042	1.0996	1.9893	3.9957
	Turf Algae III	39	0.0278	0.0730	0.0894	0.1805	0.5130	0.7127	1.2003	1.6492	4.0876	12.5683
	Turf Algae IV	68	0.0212	0.0554	0.0712	0.0850	0.2109	0.3112	0.4297	0.6777	0.9398	2.7662
	Turf Algae V	34	0.0208	0.0532	0.0788	0.1584	0.3033	0.6128	0.7941	1.5799	4.0380	8.2489
Light	Turf Algae I	50	0.0242	0.1186	0.4623	1.7398	3.1162	0.4844	1.9050	8.8386	34.3805	61.9032
	Turf Algae II	52	0.0239	0.1219	0.4942	1.5807	2.8176	0.4603	1.8957	9.1115	29.9983	53.7790
	Turf Algae III	33	0.0263	0.1230	0.4255	1.4745	2.3223	0.7966	3.0191	12.2765	44.0509	69.7348
	Turf Algae IV	50	0.0217	0.0666	0.1385	0.5139	0.8055	0.4338	0.8656	2.3628	9.8622	15.6891
	Turf Algae V	64	0.0222	0.1193	0.4528	1.5736	2.6606	0.3470	1.4998	6.7567	24.2616	41.2432
Dark	Coral Rubble I	70	0.0203	0.0407	0.1078	0.3370	0.7991	0.2900	0.2069	1.1806	4.5123	11.0900
	Coral Rubble II	48	0.0232	0.0424	0.0832	0.2124	0.4289	0.4839	0.3381	1.2104	3.9840	8.4607
	Coral Rubble III	67	0.0226	0.0370	0.0651	0.1716	0.3953	0.3378	0.1615	0.5971	2.2457	5.5596
	Coral Rubble IV	79	0.0202	0.0431	0.0906	0.3509	0.7526	0.2551	0.2141	0.8287	4.1745	9.2379
Light	Coral Rubble I	62	0.0253	0.0955	0.4161	1.4480	3.1108	0.4076	1.1642	6.3833	23.0190	49.8350
	Coral Rubble II	39	0.0212	0.0253	0.0931	0.3120	0.7245	0.5447	0.0512	1.8655	7.4674	18.0377
	Coral Rubble III	43	0.0221	0.0629	0.2618	1.1644	2.6165	0.5131	0.9213	5.6151	26.5958	60.3590
	Coral Rubble IV	68	0.0257	0.0558	0.2197	0.9207	1.7352	0.3773	0.4768	2.9319	13.2341	25.2072
Dark	Seawater Blank		0.0221	0.0262	0.0251	0.0211	0.0228					
Light	Seawater Blank		0.0219	0.0233	0.0204	0.0208	0.0211					

Table S1.4 | Results from performed two-way analysis of variance (ANOVA) with factors “Time” and “Substrate” for both N₂ fixation and denitrification in respective incubation environments (dark or light, respectively). Significant p-values in bold.

		Factor	
		Time	Substrate
Process & Incubation Environm	Dark – N ₂ Fixation	F = 28.670; p < 0.001	F = 0.0795; p = 0.379
	Light – N ₂ Fixation	F = 26.849; p < 0.001	F = 2.750; p = 0.106
	Dark – denitrification	F = 2.836; p = 0.039	F = 21.137; p < 0.001
	Light – denitrification	F = 18.238; p < 0.001	F = 7.313; p < 0.010

Table S1.5 | P-values for comparisons within the factor “substrate” (i.e., coral rubble vs. turf algae) at samplings t₀, t₂, t₄, t₈ and t₁₂ for both N₂-fixation and denitrification in respective incubation environment (dark and light, respectively). Significant p-values in bold.

	t ₀	t ₂	t ₄	t ₈	t ₁₂
Dark – N ₂ -Fixation	0.664	0.652	0.852	0.318	0.441
Light – N ₂ -Fixation	0.946	0.869	0.604	0.133	0.164
Dark – denitrification	0.633	0.003	0.002	0.033	0.027
Light – denitrification	0.334	0.041	0.881	0.048	< 0.001

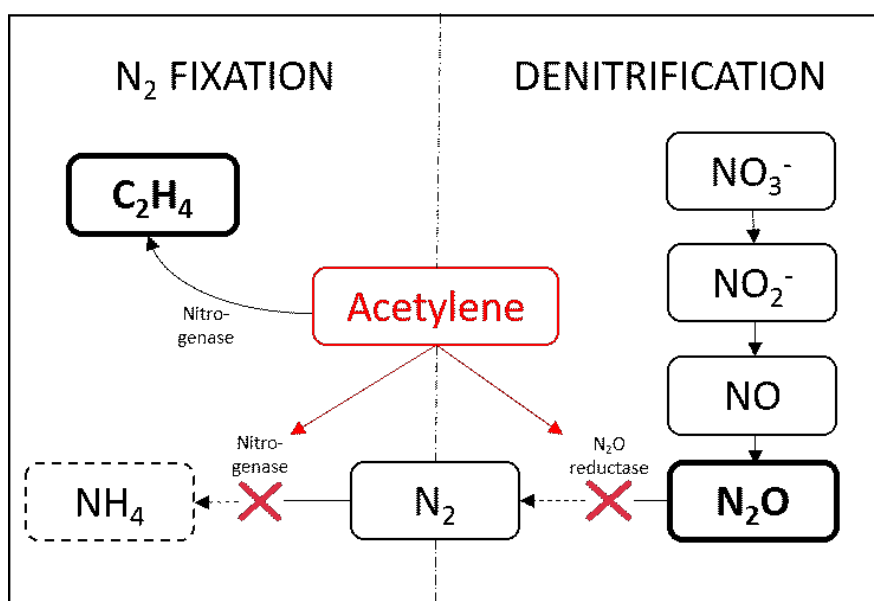


Figure S1.1 | Effect of acetylene on N₂ fixation and denitrification; red X on the left symbolizes a disruption of N₂-fixation in the presence of acetylene, resulting in an accumulation of ethylene (C₂H₄) via the enzyme nitrogenase. Acetylene inhibits (red X on the right) the last step of denitrification (i.e., nitrous oxide reductase of denitrifying bacteria), resulting in an accumulation of nitrous oxide; dashed arrows symbolize the theoretical pathways/formation in an acetylene-free environment. NO₃⁻ = nitrate, NO₂⁻ = nitrite, NO = nitric oxide, N₂O = nitrous oxide, N₂ = atmospheric dinitrogen, NH₄ = ammonium.

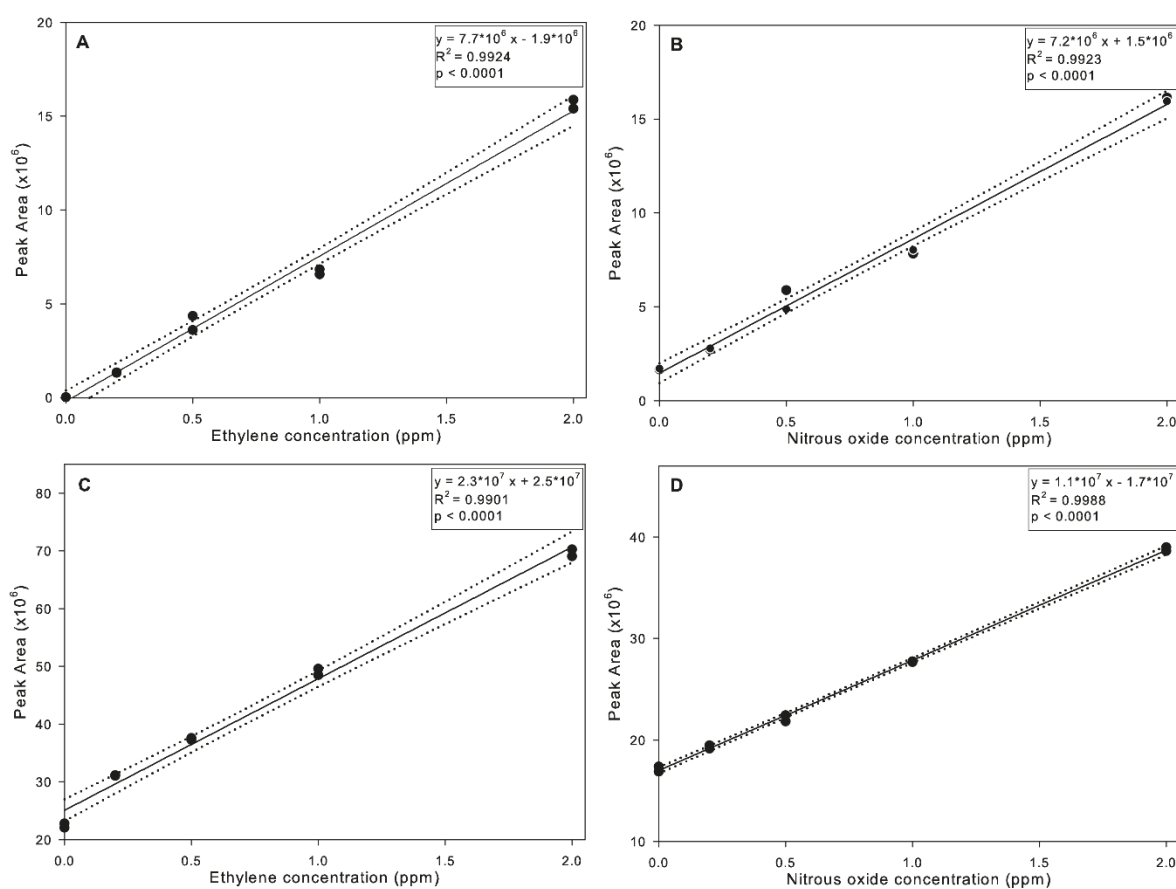


Figure S1.2 | Calibration curves measured via manual injection for ethylene **(A)** and nitrous oxide **(B)** and via autosampler for ethylene **(C)** and nitrous oxide **(D)**; black dots = measured values; black line = regression line; dotted line = 95 %-confidence interval.

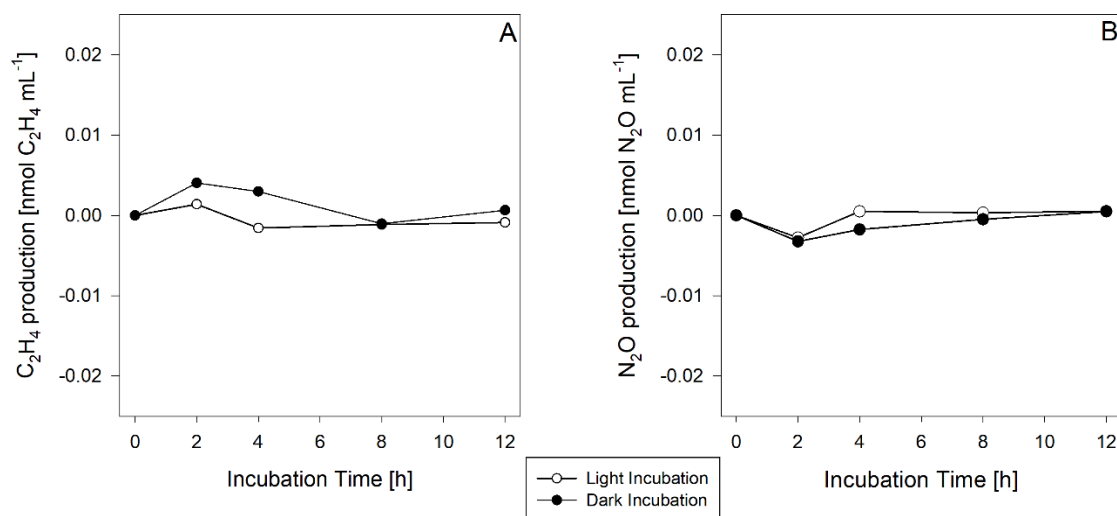


Figure S1.3 | Ethylene (C_2H_4 ; **A**) and nitrous oxide (N_2O ; **B**) production in both dark and light seawater blank incubation chambers ($n = 1$) over the whole incubation time of 12 h with samplings at t_0 , t_2 , t_4 , t_8 and t_{12} .

Supplementary Material to Chapter 3:

Table S3.1 | Material list of main system components for the construction of benthic incubation chambers and adjustable flow control pumps.

Part #	Description	Vendor (website)	Price per unit (in EUR)	Price per chamber (in EUR)
1	Polymethyl methacrylate (PMMA) cylinders, 500 mm diameter 390 mm length with drop-on cover, Manufacturer: LIQUILUX, Gladbeck, Germany	www.liquilux.de	177.50	177.50
2	PVC skirts, cut from 1 mm thick, black PVC fabric, 680g/m ²	www.planen-markt.de	17.85	7.14
3	M5 x 0.8 mm wing-head PVC bolts, 6 pieces per chamber	www.kunststoffschraube.de	0.32	1.92
4	O-ring, 450 x 35 mm	www.hug-technik.com	8.31	8.31
5	One-way stopcock female to male luer-lock	www.sigmaaldrich.com	4.45	4.45
6	Stopcock 3/4 inch with barbed hose adapter	www.pool-profi24.de	9.90	9.90
7	6V DC motors (300 mA, 2W) with magnetic impeller	www.lightobject.com	10.97	10.97
8	Low voltage pulse-width modulation speed controller: WINOMO LM2596 1.23-30V DC DC	www.amazon.de	2.52	2.52
9	Rechargeable mignon cells: ANSMANN 1.2 V AA NimH (2400 mAh)	www.amazon.de	2.50	9.99
10	PVC tube (housing) for circulation pump, 2" x 100mm	www.pvc-welt.de	3.84	3.84
11	PVC screw-cap with o-ring for circulation pump, 2"	www.pvc-welt.de	1.29	1.29
12	Additional parts include: glue, cables, cable connectors, epoxy resin etc.; price is an approximation per chamber	Different		15
Total Price per chamber:				252.83

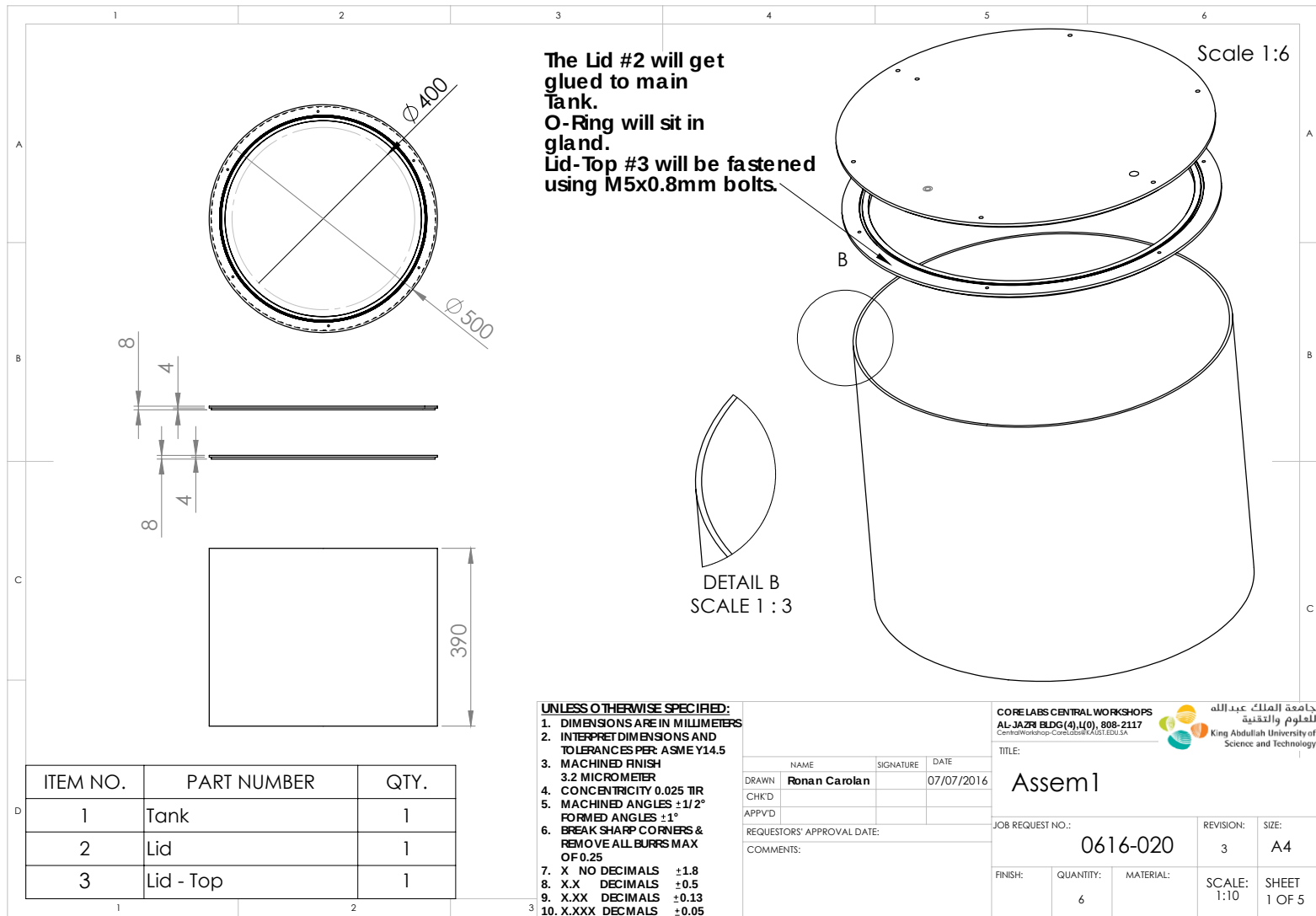


Figure S3.1 | Overview of the design and assembly schematics of benthic incubation chambers.

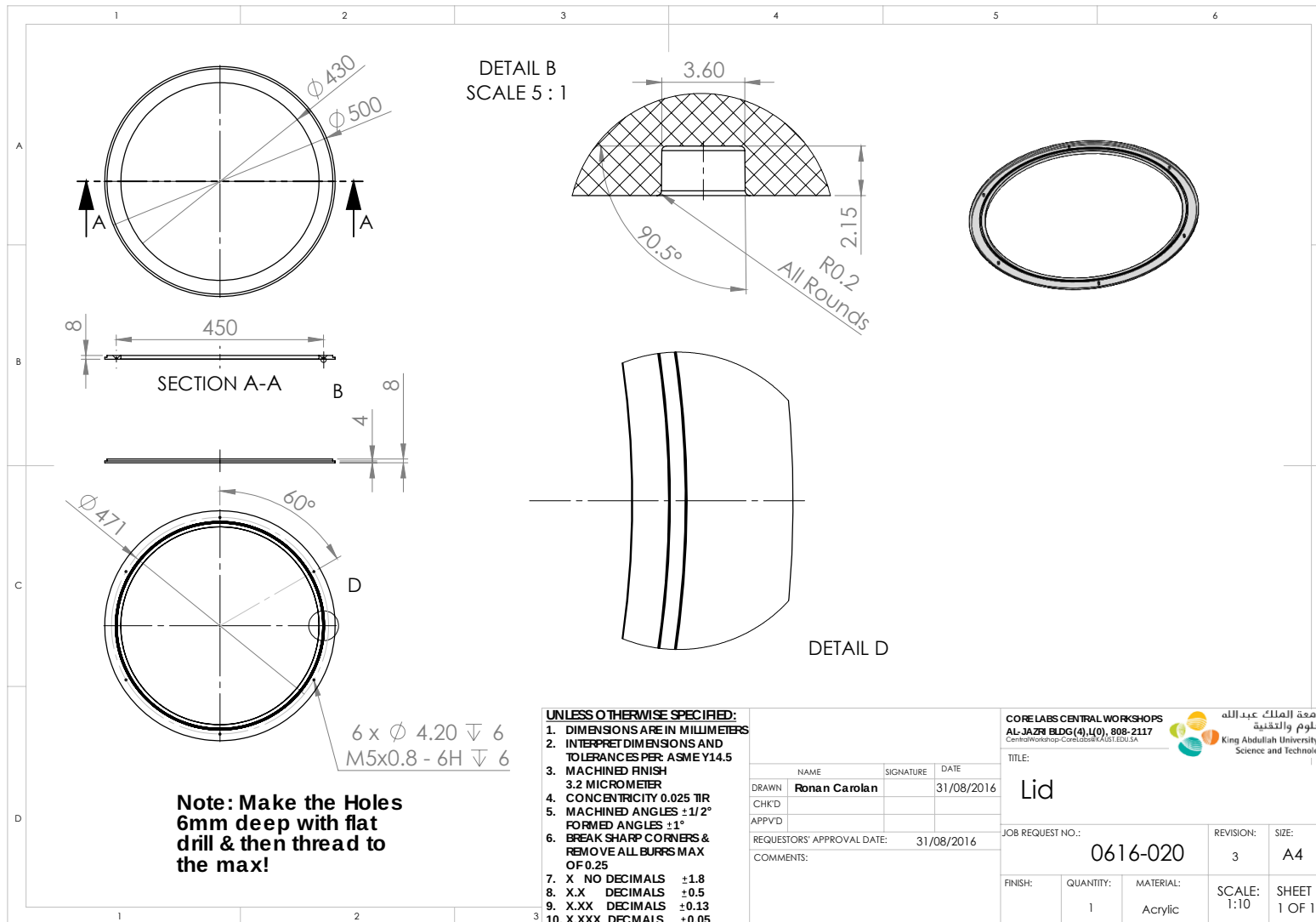


Figure S3.2 | Detailed design and assembly schematics of the lid with the gland for the O-ring of benthic incubation chambers.

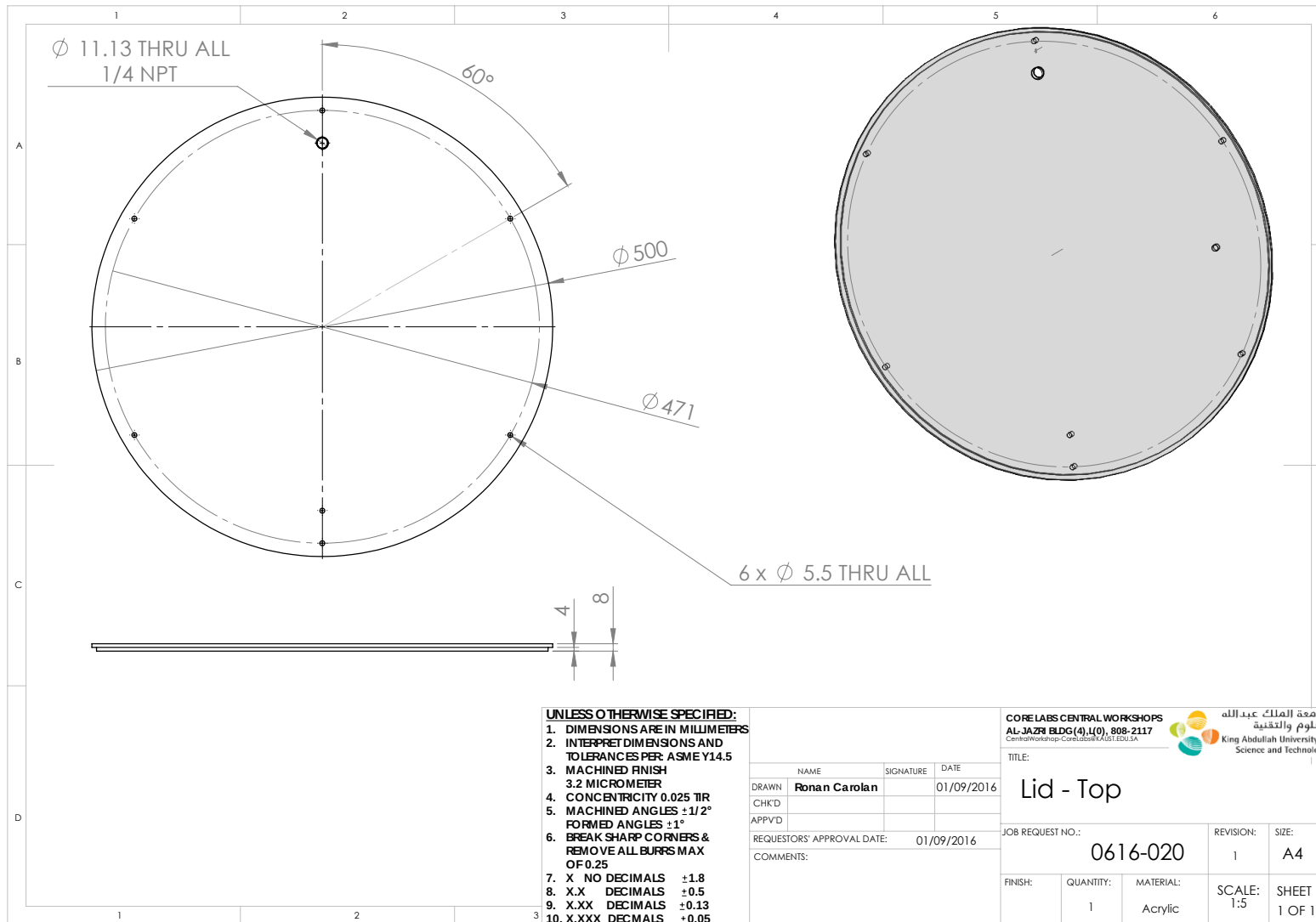


Figure S3.3 | Detailed design and assembly schematics of the lid-top of benthic incubation chambers.

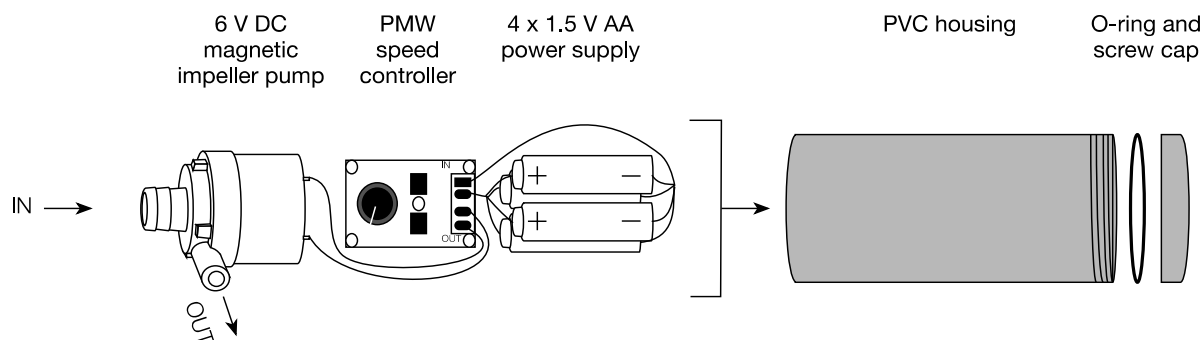


Figure S3.4 | Semi-schematic drawing of an autonomous adjustable flow control pump. From left to right: The 6V DC magnetic impeller pump can be controlled by a low voltage pulse-width modulation (PMW) speed controller. The pump is powered by 4 x 1.5 AA rechargeable batteries. All electronic parts are encapsulated in a polyvinyl chloride (PVC) housing with screw cap end.

Table S3.2 | Results of community-wide dissolved oxygen fluxes during field incubations in coral- and algae-dominated reef habitats and sediments. Surface area (SA) was calculated from 3D models; Water volume (V) in incubations chambers was calculated subtracting the measured community volume (V_C) from the geometric volume (V_G) of the chamber, with an adjustment for the volume occupied by the sensors (V_S) and the pump (V_P) as: $V = V_G - V_C - V_S - V_P$; The duration of incubations was measured from the start (closing the lids) until the end (opening the lids) of the incubations; Dissolved oxygen (O_2) readings were derived from HOBO U26 loggers with a precision 0.02 mg L^{-1} , accuracy $\pm 2\%$, automatic temperature and pressure compensated and salinity corrected; Community fluxes were calculated by converting sensor readings from mg L^{-1} to mol L^{-1} according to the molecular weight of oxygen, fluxes were then determined as hourly rates ($\text{mmol } O_2 \text{ m}^{-2} \text{ h}^{-1}$) by local linear regressions of the time series data. Coral1 – Coral4 = replicates of coral-dominated communities; Algae1 – Algae4 = replicates of algae-dominated communities; Sediment1 – Sediment4 = replicates of carbonate sediment habitats.

Light Incubations

Community	Surface area (SA) [m^2]	Water volume (V) in chamber [L]	Duration incubation (IT) [min]	O_2 Start [mg L^{-1}]	O_2 End [mg L^{-1}]	% Data points in local linear	Slope (m) of local linear regression	Calculated flux [$\text{mmol } O_2 \text{ m}^{-2} \text{ h}^{-1}$]
Coral1	0.731	41	130	5.16	8.61	89	0.0309833	3.26
Coral2	0.687	48	123	5.16	8.61	88	0.0296099	3.88
Coral3	0.698	48	122	5.10	7.80	73	0.0250962	3.24
Coral4	0.813	37	123	5.12	9.35	56	0.0324310	2.77
Algae1	0.287	62	124	5.13	8.51	68	0.0288341	11.68
Algae2	0.365	60	127	4.78	8.80	90	0.0319182	9.84
Algae3	0.299	61	123	5.21	7.85	62	0.0219231	8.39
Algae4	0.391	58	129	5.23	8.00	84	0.0218120	6.07
Sediment1	0.200	66	101	5.77	6.02	91	0.0031713	1.96
Sediment2	0.200	66	105	5.78	5.91	93	0.0011129	0.69
Sediment3	0.200	65	108	5.89	6.08	88	0.0020712	1.26
Sediment4	0.200	66	113	5.81	5.81	87	0.0000298	0.02

Dark Incubations

Community	Surface area (SA) [m ²]	Water volume in chamber (V) (L)	Duration incubation (IT) [min]	O ₂ Start [mg L ⁻¹]	O ₂ End [mg L ⁻¹]			Calculated flux [mmol O ₂ m ⁻² h ⁻¹]
Coral1	0.731	41	123	5.40	2.07	69	-0.0309912	-3.26
Coral2	0.687	48	116	5.40	2.07	81	-0.0291238	-3.82
Coral3	0.698	48	114	5.30	2.13	87	-0.0289419	-3.73
Coral4	0.813	37	113	5.38	1.36	68	-0.0312390	-2.67
Algae1	0.287	62	121	5.43	3.46	58	-0.0179891	-7.29
Algae2	0.365	60	121	5.64	3.57	41	-0.0188341	-5.81
Algae3	0.299	61	115	5.30	3.58	73	-0.0159912	-6.12
Algae4	0.391	58	115	5.40	2.99	59	-0.0237273	-6.60
Sediment1	0.200	66	136	6.03	5.48	89	-0.0041231	-2.55
Sediment2	0.200	66	138	6.08	5.31	91	-0.0057310	-3.55
Sediment3	0.200	65	137	4.99	5.20	90	-0.0056877	-3.47
Sediment4	0.200	66	135	6.11	5.22	86	-0.0065240	-4.04

Table S3.3 | Results of the fully factorial two-way analysis of variance (ANOVA) comparing net primary production (NPP), respiration (R) and gross primary production (GPP) between different benthic habitats (i.e., *coral-dominated*, *algae-dominated*, and *sediments*) and among the different methods (i.e., *in situ* vs. *ex situ* incubations). Response variables are shown in the first row, the two factors “habitat” (*coral-dominated* vs. *algae-dominated* vs. *sediments*) and “method” (*in situ* vs. *ex situ* incubations) in the first column. The lower part of the table shows the results of the all pairs Tukey’s HSD post hoc test. Significant differences are indicated by the asterisks. Algae = algae-dominated communities; Coral = coral-dominated communities; Sediment = carbonate reef sediments; DF = degrees of freedom; Prob = Probability.

Net primary production (NPP)

	DF	Sum of squares	F Ratio	Prob > F
Source				
Habitat	2	132.96318	60.1130	<.0001*
Method	1	4.43042	3.9970	0.0609
Habitat*Method	2	29.16566	13.1859	0.0003*

Tukey HSD All Pairwise Comparisons

Habitat	Method	Habitat	Method	t Ratio	Prob> t
Algae	<i>Ex situ</i>	Algae	<i>In situ</i>	-5.34	0.0005*
Algae	<i>Ex situ</i>	Coral	<i>Ex situ</i>	1.21	0.8247

Algae	<i>Ex situ</i>	Coral	<i>In situ</i>	2.33	0.2316
Algae	<i>Ex situ</i>	Sand	<i>Ex situ</i>	4.67	0.0022*
Algae	<i>Ex situ</i>	Sand	<i>In situ</i>	5.43	0.0005*
Algae	<i>In situ</i>	Coral	<i>Ex situ</i>	6.56	<.0001*
Algae	<i>In situ</i>	Coral	<i>In situ</i>	7.68	<.0001*
Algae	<i>In situ</i>	Sand	<i>Ex situ</i>	10.02	<.0001*
Algae	<i>In situ</i>	Sand	<i>In situ</i>	10.77	<.0001*
Coral	<i>Ex situ</i>	Coral	<i>In situ</i>	1.12	0.867
Coral	<i>Ex situ</i>	Sand	<i>Ex situ</i>	3.46	0.0284*
Coral	<i>Ex situ</i>	Sand	<i>In situ</i>	4.22	0.0058*
Coral	<i>In situ</i>	Sand	<i>Ex situ</i>	2.34	0.2291
Coral	<i>In situ</i>	Sand	<i>In situ</i>	3.1	0.0583
Sand	<i>Ex situ</i>	Sand	<i>In situ</i>	0.76	0.9709

Respiration (R)

	DF	Sum of squares	F Ratio	Prob > F
Source				
Habitat	2	24.513808	64.2255	<.0001*
Method	1	45.760817	239.7842	<.0001*
Habitat* Method	2	12.035758	31.5334	<.0001*

Tukey HSD All Pairwise Comparisons

Habitat	Method	Habitat	Method	t Ratio	Prob> t
Algae	<i>Ex situ</i>	Algae	<i>In situ</i>	13.88	<.0001*
Algae	<i>Ex situ</i>	Coral	<i>Ex situ</i>	1.06	0.8906
Algae	<i>Ex situ</i>	Coral	<i>In situ</i>	3.89	0.0116*
Algae	<i>Ex situ</i>	Sand	<i>Ex situ</i>	-6.11	0.0001*
Algae	<i>Ex situ</i>	Sand	<i>In situ</i>	4	0.0093*
Algae	<i>In situ</i>	Coral	<i>Ex situ</i>	-12.82	<.0001*
Algae	<i>In situ</i>	Coral	<i>In situ</i>	-9.99	<.0001*
Algae	<i>In situ</i>	Sand	<i>Ex situ</i>	-19.99	<.0001*
Algae	<i>In situ</i>	Sand	<i>In situ</i>	-9.88	<.0001*
Coral	<i>Ex situ</i>	Coral	<i>In situ</i>	2.83	0.0971
Coral	<i>Ex situ</i>	Sand	<i>Ex situ</i>	-7.17	<.0001*
Coral	<i>Ex situ</i>	Sand	<i>In situ</i>	2.94	0.0797
Coral	<i>In situ</i>	Sand	<i>Ex situ</i>	-10.00	<.0001*

Coral	<i>In situ</i>	Sand	<i>In situ</i>	0.11	0.9999
Sand	<i>Ex situ</i>	Sand	<i>In situ</i>	10.11	<.0001*

Gross primary production (GPP)

	DF	Sum of squares	F Ratio	Prob > F
Source				
Habitat	2	271.72360	97.4047	<.0001*
Method	1	78.66260	56.3936	<.0001*
Habitat* Method	2	70.84643	25.3963	<.0001*

Tukey HSD All Pairwise Comparisons

Habitat	Method	Habitat	Method	t Ratio	Prob> t
Algae	<i>Ex situ</i>	Algae	<i>In situ</i>	-9.89	<.0001*
Algae	<i>Ex situ</i>	Coral	<i>Ex situ</i>	0.69	0.9806
Algae	<i>Ex situ</i>	Coral	<i>In situ</i>	0.64	0.9862
Algae	<i>Ex situ</i>	Sand	<i>Ex situ</i>	6.43	<.0001*
Algae	<i>Ex situ</i>	Sand	<i>In situ</i>	3.36	0.0348*
Algae	<i>In situ</i>	Coral	<i>Ex situ</i>	10.58	<.0001*
Algae	<i>In situ</i>	Coral	<i>In situ</i>	10.53	<.0001*
Algae	<i>In situ</i>	Sand	<i>Ex situ</i>	16.32	<.0001*
Algae	<i>In situ</i>	Sand	<i>In situ</i>	13.25	<.0001*
Coral	<i>Ex situ</i>	Coral	<i>In situ</i>	-0.05	1
Coral	<i>Ex situ</i>	Sand	<i>Ex situ</i>	5.74	0.0002*
Coral	<i>Ex situ</i>	Sand	<i>In situ</i>	2.67	0.1313
Coral	<i>In situ</i>	Sand	<i>Ex situ</i>	5.79	0.0002*
Coral	<i>In situ</i>	Sand	<i>In situ</i>	2.72	0.1198
Sand	<i>Ex situ</i>	Sand	<i>In situ</i>	-3.07	0.062

Case study | Protocol for *In Situ* Incubations of Coral- and Algae-Dominated Reef Communities, and Carbonate Sediments

For the incubations, four coral-dominated communities (> 40% coral cover, but less than 10% algal cover), four rocky communities overgrown by heterogeneous assemblages of algae (hereafter ‘algae-dominated’; > 40% algae, but less than 10% coral cover), and carbonate sediments (hereafter ‘sediments’) were selected haphazardly with a minimum distance of 3 m. Twelve identical benthic incubation chambers were assembled, comprising three treatment levels with four replicates each. Experiments were carried out on three consecutive days for coral- and algae-dominated communities, and on three separate consecutive days for the sediments. On day one, two divers deployed four chambers on coral-dominated, and four chambers

on algae-dominated reef communities. The chambers were positioned carefully and left in place with open tops (no lids) until the next morning. This assured that swirled-up sediments would settle down and organisms inside the chambers were not stressed by the deployment of the chambers. The open top enabled constant water exchange and natural flow conditions during the “waiting” period. On the second day, communities were incubated for net primary production (NPP) during natural daylight conditions. The lids were prepared on the boat by attaching and switching on the pumps and sensors. Temperature, light availability and DO concentrations were logged every 1 min. Light intensities (lx) were converted to photosynthetically active radiation (PAR, $\mu\text{mol quanta m}^{-2} \text{s}^{-1}$, 400 to 700 nm) using the following approximation: $1 \mu\text{mol quanta m}^{-2} \text{s}^{-1} = 51.8 \text{ lux}$. This conversion factor was obtained by inter-calibrating the lux readings with data obtained from a parallel deployment of a PAR sensor (LI-COR LI-1500 quantum sensor) and the HOBO Pendant loggers during four hours of daylight. Readings correlated (Pearson correlation: $r^2 = 0.91$, $p = 0.0002$) and the obtained conversion factor of 51.8 was similar to 52.0, as reported previously (e.g., Valiela 1984). During the days of *in situ* incubations, light intensities at the study site (and water depth) averaged $231 \pm 31 \mu\text{mol quanta m}^{-2} \text{s}^{-1}$ within PAR.

Two divers started the incubations at around 8:30 a.m. by tightly securing the lids and closing all sampling ports. The exact incubation start time was recorded for each chamber. Incubations ran for approximately two hours. Incubations were terminated by opening the lids. The exact end-time of incubations was noted for each individual chamber. The chambers were left in place with open top (allowing for flushing and natural water flow) for a second set of incubation on the following day. On day three, benthic communities were incubated for dark respiration (R) during “simulated” darkness during the same time window as incubations on the previous day. The procedure followed the same as on day two (NPP incubation), however, all incubation chambers were covered with thick black PVC covers, prohibiting any light penetration into the chambers. The same three-day procedure was applied for sediments on separate days.

Case study | Protocol for *Ex Situ* Community Budgets Estimated from Single-Organism Incubations

Community budgets from single-organism incubations were estimated by an adapted protocol from Cardini et al. (2016)¹². Four fragments of the hard coral *Pocillopora* sp. ($89.75 \pm 6.50 \text{ cm}^2$, 3D surface area), four fragments of dead corals overgrown with turf algae ($73.75 \pm 10.31 \text{ cm}^2$, 3D surface area), and four sediment cores (23.76 cm^2 , 2D planar surface area; 1.5 cm depth), were collected at Abu Shosha reef during summer. These three groups represented the dominant functional components from benthic chambers during *in situ* incubations. After collection, functional groups were immediately transferred to three recirculation aquaria on the boat (each filled with 10 L of ambient seawater) and acclimated until experiments at ambient water temperature and light conditions. In the laboratory, NPP and R rates were assessed from O_2 evolution/depletion measurements in 2 h light and dark incubations in 1 L gas-tight glass chambers, respectively. To correct O_2 fluxes for planktonic background metabolism, two incubations with seawater only were included. Glass chambers were placed on inductive drive stirrers (500 rpm) in laboratory incubators set to *in situ* temperature (29°C) and light ($200 \mu\text{mol quanta m}^{-2} \text{s}^{-1}$). O_2 fluxes were assessed based on differences in O_2 concentrations before and after the incubation using an optical oxygen multiprobe (FDO®, 925, WTW, temperature and salinity corrected; accuracy: $\pm 0.5\%$ of value). O_2 production (NPP) and consumption (R) rates were corrected for seawater controls and normalized to surface area (3D surface area for coral- and turf fragments, derived via photogrammetry via Autodesk Recap®; planar 2D surface area of sediments derived from petri dish diameter) and incubation time. GPP rates were calculated by adding positive R rates to their corresponding NPP rates: ($\text{GPP} = \text{NPP} + |\text{R}|$). Lastly, individual *ex situ* incubations were used to estimate overall community oxygen fluxes based on the composition of communities incubated during *in situ* measurements. For this, *ex situ* NPP, R and GPP rates of single-organism incubations were extrapolated to the metabolism in *in situ* chambers, considering the specific 3D area covered by the respective functional groups from the chambers’ communities and the volume of seawater included in the chambers.

Supplementary Material to Chapter 4:

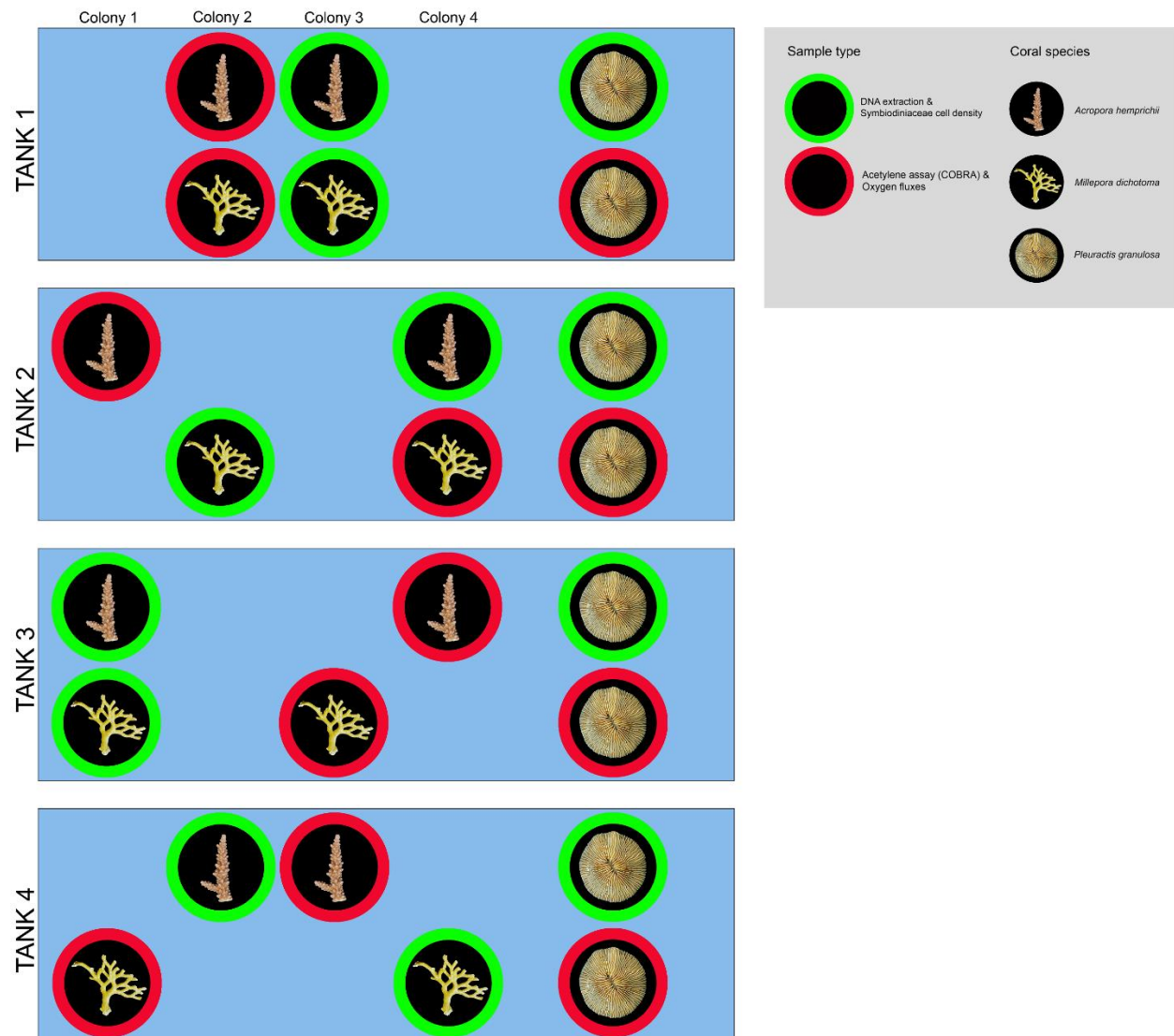


Figure S4.1 | Overview of sampling scheme of fragmented coral colonies, i.e. four colonies of *A. hemprichii*, four colonies of *M. dichotoma* and eight individual polyps of *P. granulosa*, which were divided over four independent replicate tanks. The outline colour denotes the type of analysis that the sampled fragments were used for.

Supplementary Methods to Chapter 4:

Primer Assessment

Approach

For the purpose of finding suitable primer pairs for the relative quantification of denitrifying prokaryotes, the selected primers were first tested with total DNA from corals previously collected for a comparative assessment of *nifH* gene copy numbers¹³ in a temperature gradient PCR (range 51 to 62 °C). If one or more primers gave a single or dominant amplicon of the correct size at a given annealing temperature, the primer(s) and the annealing temperature were selected for testing quantification using quantitative PCR (qPCR). When amplification products of the same samples were similar between conventional PCR and qPCR, the primer(s) and corresponding annealing temperature were further tested on five additional common species of central Red Sea corals. Finally, all additional coral species that revealed a single and/or dominant band of the correct size were tested with qPCR.

Sample Collection

This study was conducted at the King Abdullah University of Science and Technology (KAUST) in Saudi Arabia. Two species of Fungiidae (*Pleuractis granulosa* and *Ctenactis echinata*) and two species of Pocilloporidae (*Pocillopora verrucosa* and *Stylophora pistillata*) were collected ($n = 3$ colonies each) at the inshore reef Inner Fsar (22°13'97.4"N; 39°01'76.0"E) located in the Saudi Arabian central Red Sea in February 2016¹³. Five additional coral species ($n = 3$ colonies each) were collected at the inshore reef Abu Shosha (22°18'16.3"N; 39°02'57.7"E) located in the Saudi Arabian central Red Sea in September 2017; specifically, two species of Acroporidae (*Acropora hemprichii* and *Acropora pharaonis*), one species of Poritidae (*Porites lutea*), one species of Merulinidae (*Echinopora fruticulosa*) and one hydrozoan (*Millepora dichotoma*). Sailing permits were issued by the Saudi Arabian Coastguard Authority to the sites that included coral collection. Immediately after collection, the coral samples were flash-frozen in liquid nitrogen on board the boat and stored at -80 °C until further processing.

DNA Extraction

For DNA extraction, coral tissues were removed from the skeleton by airblasting with RNase free water using a sterile airbrush (Agora-Tec GmbH, Schmalkalden, Germany). The resulting tissue slurry was collected into sterile 2.0 ml Eppendorf cups, subsequently homogenized and stored at -20 °C until further processing. DNA was extracted from 100 µL of tissue slurry using the Qiagen DNeasy Plant Mini Kit (Qiagen, Germany) according to manufacturer's instructions. DNA extraction yields were quantified and qualified using a NanoDrop 2000C spectrophotometer (Thermo Fisher Scientific, Waltham, MA, USA) and stored at -20 °C until further processing.

Primer Selection and Quantitative PCR (qPCR)

A total of 18 primers were selected for this study (Table S4.1), that resulted in 10 primer pairs selected for further testing (Table S4.2 and Table S4.3). Primer selection was done by examining the scientific literature for primers that have been used to assess denitrifying microbes preferably performed associated with coral reef organisms or substrates. If unavailable, denitrification primers that have been used on samples from other marine ecosystems were selected. A minimum of two primer pairs targeting functional genes encoding for each enzyme present in the denitrification pathway were selected, i.e. the *narG* gene encoding for nitrate reductase, the *nirK* and *nirS* genes encoding for nitrite reductase, the *norB* gene for nitric oxide reduction and the *nosZ* gene encoding for nitrous oxide reduction (Table S4.1).

Table S4.1 | Selected primers used for amplification of denitrification genes.

Enzyme	Target gene	Primer ^a	Nucleotide sequence (5' → 3') ^b	Reference
Nitrate reductase	<i>narG</i>	narGW9F	MGNNGGNTGYCCNMGNGGN	Gregory et al. ¹⁴
		narGT38R	GC	
		narG–F	ACRTCNGTYTGYTCNCCCCA	Bru et al. ¹⁵
		narG–R	TCGCCSATYCCGGCSATGTC	
Nitrite reductase	<i>nirK</i>	nirK1F	GAGTTGTACCAGTCRGCSGA	Braker et al. ¹⁶
		nirK5R	YTCSG	
		nirK127R	GGMATGGTKCCSTGGCA	Zhang et al. ¹⁷
			GCCTCGATCAGRTRTRIGG	
Nitrite reductase	<i>nirS</i>	nirS1F	CCTGCTCACCGACATAATAG	Braker et al. ¹⁶
		nirS6R	A	
		cd3aF	CCTAYTGGCCGCCRCART	Michotey et al. ¹⁸
		R3cd	CGTTGAACTTRCCGGT	
Nitric oxide reductase	<i>norB</i>	qnorB2F	GTSAACGTSAAAGGARACSGG	Braker and Tiedje ¹⁹
		qnorB5R	GASTTCGGRTGSGTCTTGA	
		cnorB2F	GGNCAYCARGGNTAYGA	Kloos et al. ²⁰
		cnorB6R	ACCCANAGRTGNACNACCCA	
Nitrous oxide reductase	<i>nosZ</i>	nosZ–F	CCA	Throbäck et al. ²¹
		nosZ–R	GACAAGNNNTACTGGTGGT	
		nosZ1622R	GAANCCCCANACNCCNGC	

^a Forward and reverse primers are indicated by the letters F and R, respectively.

^b K = G or T; M = A or C; N = A, C, G or T; R = A or G; S = G or C; Y = C or T

A temperature gradient PCR was applied (from 51 °C to 62 °C) to assess the optimal annealing temperature of every primer pair. All PCRs were run in duplicates containing 10 µL of Qiagen Multiplex mix (from the Qiagen Multiplex PCR Kit), 0.5 µM of each primer (10 µM), 1 µL of DNA template and PCR water to adjust the total reaction volume to 20 µL. The thermal cycler protocol was 94 °C for 15 min, followed by 50 cycles of 94 °C for 30 s, 51 to 62 °C for 1 min followed by 72 °C for 1 min, with a final extension at 72 °C for 10 min. The amplification products were visually analysed using 1 % agarose gel electrophoresis in 1x TAE buffer.

Quantitative PCR (qPCR) was used to test primers that gave a single or dominant amplicon of the correct size with conventional PCR. qPCR assays were performed in triplicates for each coral replicate. Each assay contained 9 µL reaction mixture and 1 µL DNA template. Reaction mixture contained Platinum SYBR Green qPCR Master Mix (Invitrogen, Carlsbad, CA, United States), 0.2 µL of each primer (10 µM), 0.2 µL of ROX dye and 3.4 µL of RNase–free water. The thermal cycling protocol was 50 °C for 2 min, 95 °C for 2 min, 50 cycles of 95 °C for 30 s, “optimal annealing temperature” for 1 min, 72 °C for 1 min and a 72 °C extension cycle for 2 min. Amplification specificity was determined by adding a dissociation step. All assays were performed on the ABI 7900HT Fast Real–Time PCR System (Applied Biosystems, CA, USA). The amplification products were visually analysed using 1 % agarose gel electrophoresis in 1x TAE buffer.

Table S4.2 | Amplification results^a of PCR using a range of primers for the denitrification pathway on four Red Sea corals^b at different annealing temperatures.

Primer pair	Coral species	51.0 °C	51.9 °C	54.1 °C	57.0 °C	59.8 °C	62.0 °C
narGW9F/narGT38R	Pg	–	–	–	–	–	–
	Ce	–	–	–	–	–	–
	Pv	–	–	–	–	–	–
	Sp	–	–	–	–	–	–

narG-F/narG-R	Pg	-	-	-	-	-	-
	Ce	nsa	nsa	-	-	-	-
	Pv	-	-	-	-	-	-
	Sp	nsa	nsa	-	-	-	-
nirK1F/nirK5R	Pg	nsa	nsa	nsa	nsa	-	-
	Ce	nsa	nsa	nsa	nsa	nsa	nsa
	Pv	nsa	nsa	nsa	-	-	nsa
	Sp	nsa	nsa	nsa	nsa	nsa	nsa
nirK1F/nirK127R	Pg	nsa	nsa	-	-	-	-
	Ce	nsa	nsa	nsa	nsa	nsa	nsa
	Pv	nsa	nsa	nsa	nsa	-	nsa
	Sp	nsa	nsa	nsa	nsa	nsa	nsa
nirS1F/nirS6R	Pg	-	-	-	-	-	-
	Ce	nsa	nsa	nsa	nsa	nsa	-
	Pv	nsa	nsa	nsa	nsa	nsa	-
	Sp	nsa	nsa	nsa	nsa	nsa	-
cd3aF/R3cd	Pg	+	+	+	+	+	-
	Ce	nsa	nsa	-	-	-	-
	Pv	nsa	nsa	-	-	-	-
	Sp	+	+	+	+	+	-
qnorB2F/qnorB5R	Pg	-	-	-	-	-	-
	Ce	-	-	-	-	-	-
	Pv	-	-	-	-	-	-
	Sp	-	-	-	-	-	-
cnorB2F/cnorB6R	Pg	-	-	-	-	-	-
	Ce	nsa	nsa	-	-	-	-
	Pv	nsa	nsa	-	-	-	-
	Sp	-	-	-	-	-	-
nosZ-F/nosZ-R	Pg	nsa	nsa	nsa	nsa	nsa	nsa
	Ce	nsa	nsa	nsa	nsa	nsa	-
	Pv	nsa	nsa	nsa	nsa	nsa	nsa
	Sp	nsa	nsa	-	-	-	-
nosZ-F/nosZ1622R	Pg	nsa	nsa	-	-	-	-
	Ce	nsa	nsa	nsa	nsa	nsa	-
	Pv	nsa	nsa	nsa	nsa	nsa	-
	Sp	nsa	nsa	-	-	-	-

^a Symbols: Amplicon of the correct size (+); no amplicon (-); multiple amplicons or single amplicon of the wrong size, i.e. no specific amplification (nsa)

^b Corals are abbreviated as follows: *Plenractus granulosa* (Pg); *Ctenactis echinata* (Ce); *Pocillopora verrucosa* (Pv); *Stylophora pistillata* (Sp)

Results

In the first batch of tested corals, amplicons of the correct size (425 bp) were found in *S. pistillata* and *P. granulosa* with the primer pair cd3aF/R3cd (Fig. S4.2 and Table S4.2). Clearest amplicons (as qualified with gel electrophoresis) were found with an annealing temperature of 51 °C (Fig. S4.2 and Table S4.2). Results of subsequent qPCRs mirrored results obtained from conventional PCRs. For the second batch of corals the primer pair cd3aF/R3cd was used with an annealing temperature of 51 °C. In addition to *S. pistillata* and *P. granulosa*, amplicons of the correct size were found in *A. hemprichii* and *M. dichotoma* (Fig. S4.3 and Table S4.3). Amplification products of subsequent qPCRs mirrored products obtained from conventional PCRs for each sample.

Table S4.3 | Amplification results^a of PCR using a range of primers for the denitrification pathway on nine Red Sea corals^b.

Primer pair ^c	Amplicon length ^d	Pg	Ce	Pv	Sp	Ah	Ap	P l	Ef	M d	Contro l
narGW9F/narGT38 R	500 bp	–	–	–	–						–
narG–F/narG–R	173 bp	–	nsa	–	nsa						–
nirK1F/nirK5R	514 – 515 bp	nsa	nsa	nsa	nsa						–
nirK1F/nirK127R	127 bp	nsa	nsa	nsa	nsa						–
nirS1F/nirS6R	890 bp	–	nsa	nsa	nsa						–
cd3aF/R3cd	425 bp	+	nsa	nsa	+	+	nsa	–	nsa	+	–
qnorB2F/qnorB5R	224 – 262 bp	–	–	–	–						–
cnorB2F/cnorB6R	389 bp	–	nsa	nsa	–						–
nosZ–F/nosZ–R	453 bp	nsa	nsa	nsa	nsa						–
nosZ–F/nosZ1622 R	415 – 453 bp	nsa	nsa	nsa	nsa						–

^a Symbols: Amplicon of the correct size (+); no amplicon (–); multiple amplicons or single amplicon of the wrong size, i.e. no specific amplification (nsa), empty cells indicate that the assessment was not performed.

^b Corals are abbreviated as follows: *Pleuractis granulosa* (Pg); *Ctenactis echinata* (Ce); *Pocillopora verrucosa* (Pv); *Stylophora pistillata* (Sp); *Acropora hemprichii* (Ah); *Acropora pharaonis* (Ap); *Porites lutea* (Pl); *Echinopora fruticulosa* (Ef); *Millepora dichotoma* (Md); Negative control (Control).

^c Annealing temperature of 51 °C for every primer pair.

^d Basepairs (bp).

Primer Assessment

Here, we studied the performance of 10 primer pairs targeting five functional genes of the denitrification pathway and encoding for the involved main enzymes. Specifically, the selected primer pairs targeted the denitrification gene clusters *nar*, *nir*, *nor* and *nos*. Based on primer performance for DNA isolated from coral, we selected the primer pair cd3af/R3cd which targets the *nirS* gene encoding for the cytochrome *cd₁* nitrite reductase. This primer pair was the only pair to give a dominant band of the correct size for several tested corals. Of note, this primer pair was previously found to perform well with DNA from other marine templates, such as coral rock²², marine sediments²³, as well as environmental samples from intertidal zones²⁴, and terrestrial ecosystems^{25–27}, highlighting its broad coverage.

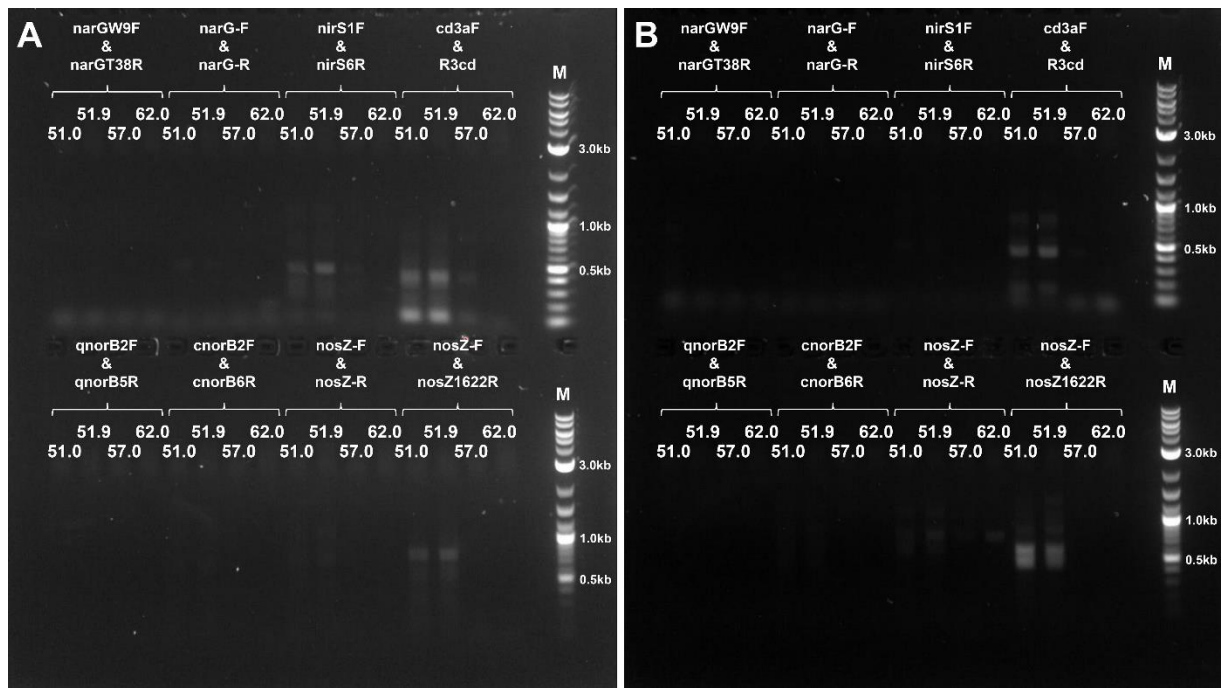


Figure S4.2 | PCR products from eight different primer pairs at four different annealing temperatures for (A) *Stylophora pistillata* and (B) *Pleuractis granulosa*. Annealing temperatures are 51.0, 51.9, 57.0 and 62.0 °C. M = Marker (2-log DNA ladder). Uncropped gel images originate from two separate gels.

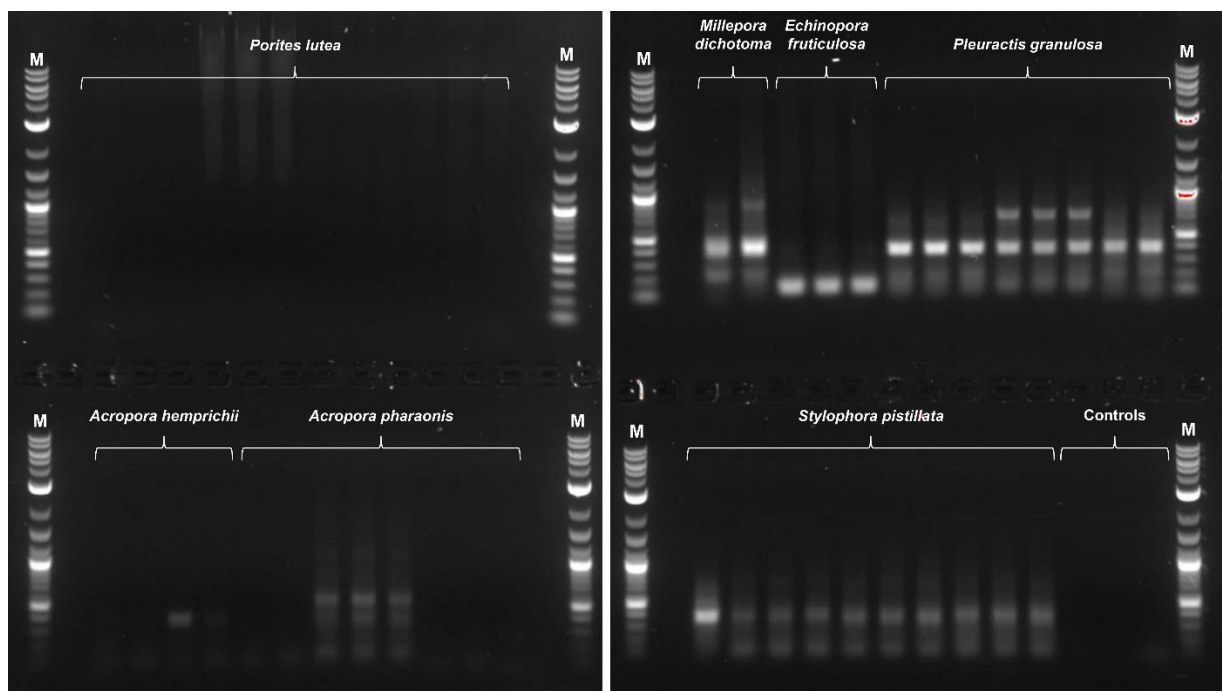


Figure S4.3 | PCR products using the primer pair cd3aF/R3cd at the optimal annealing temperature of 51 °C using 7 different Red Sea corals. M = Marker (2-log DNA ladder). Uncropped gel images originate from two separate gels.

Supplementary Material to Chapter 5:

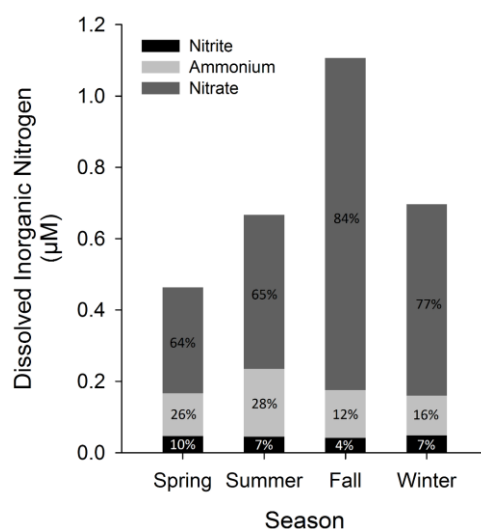
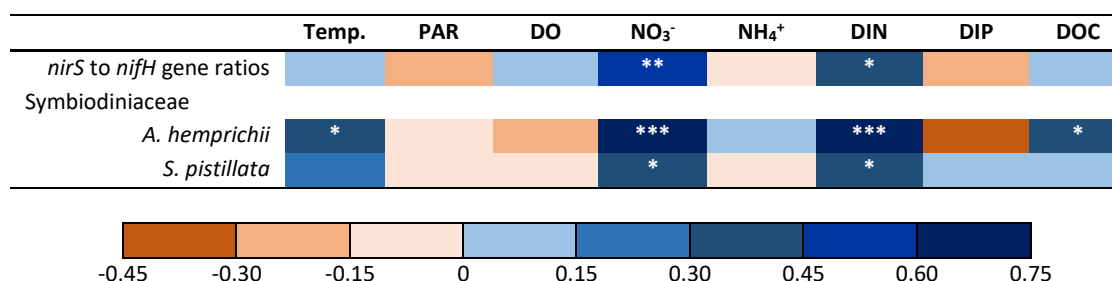


Figure S5.1 | Proportions of dissolved nitrogenous compounds. Data taken from Fig. 5.2. Numbers in the bars represent the total percentage of the nitrogenous compound pertaining to total DIN per season.

Table S5.1 | Summary of significant main effects and interactions based on permutational multivariate analysis of variance (PERMANOVA) for *nirS* to *nifH* gene ratios and Symbiodiniaceae cell densities.

<i>nirS</i> to <i>nifH</i> gene ratios			
	df	Pseudo-F	<i>p</i>
Season	3	3.04	0.039
Species	1	6.11	0.019
Season x Species	2	0.14	0.877
Symbiodiniaceae cell densities			
	df	Pseudo-F	<i>p</i>
Season	3	10.16	0.001
Species	1	0.52	0.473
Season x Species	3	3.19	0.037

Table S5.2 | Correlation coefficients for *nirS* to *nifH* gene ratios and Symbiodiniaceae cell density with eight environmental parameters (based on Pearson Product-Moment Correlation analysis).



Temp. = temperature, PAR = photosynthetically active radiation, NO₃⁻ = nitrate, NH₄⁺ = ammonium, DIN = dissolved inorganic nitrogen, DIP = dissolved inorganic phosphorus, DOC = dissolved organic carbon. The correlation coefficient is indicated by the colour chart below the table. Asterisks indicate significant correlations. **p* < 0.05, ** *p* < 0.01, ****p* < 0.001.

Supplementary Material to Chapter 6:

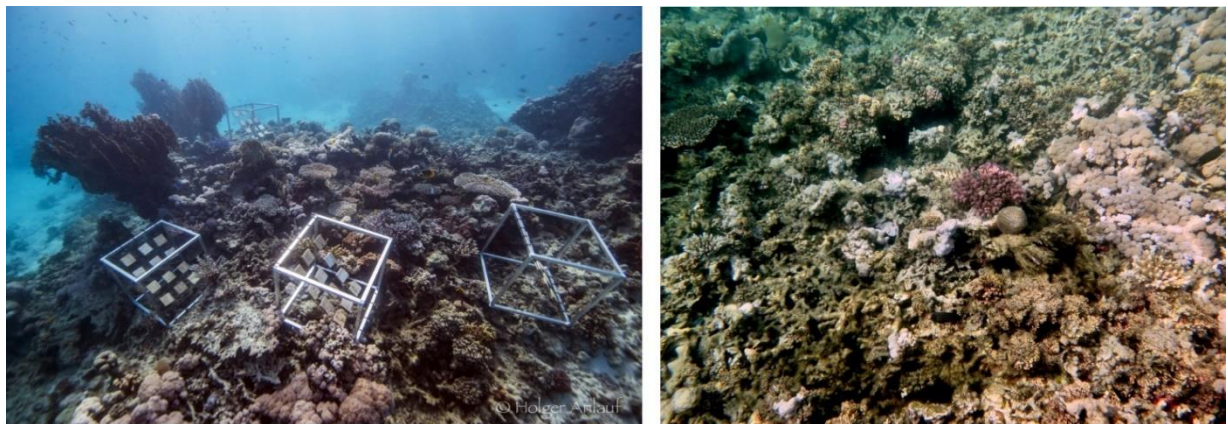


Figure S6.2 | Photos of investigated reef areas showing distinct coral-dominated (left) and algae-dominated reef areas (right). Right picture was taken by Holger Anlauf and was initially published in Roth and others (2018)²⁸, right photo was taken by Florian Roth.

Table S6.1 | Relative benthic cover in coral- and algae-dominated reef areas. Presented are mean proportional cover in % \pm standard error of major benthic categories assessed by photo quadrats ($n = 10$ in coral-dominated areas, $n = 12$ in algae-dominated areas).

Benthic category	Relative cover [%] in coral-dominated area	Relative cover [%] in algae-dominated area
Hard Coral	43.55 \pm 5.67	13.96 \pm 2.33
Soft Coral (<i>Xenia</i> sp.)	8.85 \pm 3.78	8.13 \pm 1.68
Turf Algae	26.15 \pm 5.02	47.50 \pm 7.15
Biogenic Rock	16.11 \pm 3.05	1.25 \pm 0.71
Coral Rubble	3.30 \pm 3.11	12.08 \pm 5.75
Reef Sands	0.52 \pm 0.27	11.46 \pm 3.66
<i>Tridacna</i>	1.34 \pm 0.82	0.00 \pm 0.00
Macro Algae	0.17 \pm 0.00	0.63 \pm 0.32
Sponges	0.00 \pm 0.00	0.00 \pm 0.00

Table S6.2 | Dinitrogen (N₂) fixation rates and denitrification potentials of investigated benthic categories. Rates are presented in mean \pm standard errors and in pmol N₂ cm⁻² h⁻¹. Data for hard corals consists of mean values of *P. verrucosa*, *A. hemprichii* and *S. pistillata*.

Benthic Category	Replicates	N ₂ fixation	Denitrification
Turf Algae	5	570.30 \pm 59.18	6.01 \pm 1.10
Coral Rubble	4	482.07 \pm 88.40	12.47 \pm 1.29
Soft Coral (<i>Xenia</i> sp.)	5	14.62 \pm 4.16	36.79 \pm 9.02
Biogenic Rock	5	97.77 \pm 15.99	13.64 \pm 1.52
Reef Sands	5	45.69 \pm 6.07	11.25 \pm 3.01
Hard Corals	13	5.11 \pm 1.89	6.47 \pm 2.27
<i>Pocillopora verrucosa</i>	5	2.52 \pm 0.42	3.71 \pm 0.77
<i>Acropora hemprichii</i>	4	6.57 \pm 3.23	15.80 \pm 4.56
<i>Stylophora pistillata</i>	4	6.88 \pm 4.86	0.59 \pm 0.25

Table S6.3 | Description of incubated benthic categories, and respective 2D to 3D conversion factor according to Cardini and others (2016)¹².

Benthic category	2D to 3D conversion factor	Description/incubated organism or substrate
Hard Corals	7.6	<i>Pocillopora, Acropora, Stylophora</i>
Soft Coral	6.5	Xeniidae
Biogenic Rock	2.5	Biogenic reef framework with visible carbonate structure (according to Bahartan and others (2010) ²⁹
Coral Rubble	5.2	Equal to coral rock, uncovered dead coral skeleton according to Rasser and Riegl (2002) ³⁰
Turf Algae	3.9	Dense mats composed of a heterogeneous assemblage of filamentous algae
Reef Sands	1.0	Surface layer with its associated microphytobenthos

Supplementary Material 6.1 | Nitrate Concentration Quantifications

Nitrate (NO_3^-) was added during the N cycling incubations serving as a substrate for denitrification, as the natural formulation pathway (nitrification) of NO_3^- is inhibited by acetylene^{31–33}. NO_3^- was added in form of a previously prepared sodium nitrate (NaNO_3) stock solution, prepared with MilliQ water and $\text{NaNO}_3 \geq 99.0\%$ (Sigma Aldrich). Water samples of incubation water were taken at the beginning of each incubation. Water samples were filtered immediately (Isopore™ GTTP membrane filters, 0.2 μm) and the filtrate was stored frozen at -50°C in the lab after collection. NO_3^- concentrations as well as further parameters (nitrite (NO_2^-) and phosphate (PO_4^{3-})) were determined using a continuous flow analyser (AA3, HR, SEAL, following colourimetric standard methods³⁴). Limits of quantification for NO_3^- , NO_2^- and PO_4^{3-} were 0.084, 0.011 and 0.043 $\mu\text{mol L}^{-1}$, respectively. Mean initial concentrations ($n = 4$) as well as seawater control concentrations of NO_3^- , NO_2^- and PO_4^{3-} are displayed in Table S6.4.

Table S6.4 | Mean \pm SE values ($n = 4$) of nitrate (NO_3^-), nitrite (NO_2^-) and phosphate (PO_4^{3-}) at the start of nitrogen cycling incubations (i.e., amended with 5 μM nitrate) and seawater controls

Parameter	$\mu\text{mol L}^{-1}$ incubation chamber	$\mu\text{mol L}^{-1}$ seawater control
NO_3^-	5.743 ± 0.17	1.056 ± 0.064
NO_2^-	0.071 ± 0.027	0.060 ± 0.008
PO_4^{3-}	0.116 ± 0.025	0.126 ± 0.009

Supplementary Material 6.2 | Quantification of Oxygen Concentrations During the Incubation Period

Oxygen fluxes were quantified for parallel studies with identical benthic categories (unpubl. data) that were sampled < 3 h before oxygen flux incubations. Incubation chambers (1L volume) were filled with ambient seawater that was collected from the same day. Specimens ($n = 5$ for reef sands, *Xenia* sp., turf algae, coral rubble, biogenic rock, and *P. verrucosa*; $n = 4$ for *Acropora damicornis*, and *Stylophora pistillata*; $n = 6$ control chambers to correct for background metabolism) were placed inside the incubation chambers. All chambers were sealed gastight and without any air enclosure. Incubation chambers were placed in a tempered water bath and constantly stirred (500 rpm) to ensure stable measurement conditions (27°C). A 2 h light ($\sim 200 \mu\text{M}$ quanta $\text{m}^{-2} \text{s}^{-1}$ photon flux) was performed prior a 2 h dark incubation with fresh ambient seawater. Oxygen levels were measured immediately before starting the respective incubation and after 2 h using a

WTW Multi 3430 which was equipped with a WTW DFO 925 oxygen sensor. Results were normalised to incubation time and surface area (surface areas of hard and soft corals, turf algae, biogenic rock, coral rubble were calculated using cloud-based 3-dimensional models of samples ^{7,8}, reef sands were mathematically calculated). Oxygen rates for each benthic category were then used to extrapolate the oxygen concentrations at respective time points during nitrogen incubations, considering the respective surface area of the specimens as well as the given headspace (200mL headspace – 20mL that was exchanged for acetylene addition). Results for extrapolated oxygen concentrations over time in the incubation chambers for N cycling quantifications are presented in Tab. S1. Our results show that thresholds for hypoxia (i.e., condition of low dissolved oxygen that becomes detrimental to aerobic organisms) and hyperoxia (i.e., condition where oxygen exceeds 100% air saturation) were not exceeded (see Hughes et al. (2020)³⁵). We, thus, believe that both N cycling pathways were assessed in representative scenarios.

Table S6.5 | Extrapolated range of hourly minimum and maximum oxygen (O₂) concentrations in the incubation water during nitrogen (N) cycling incubation

Benthic category	Range of mean O ₂ concentrations in incubation water [mg L ⁻¹] during N cycling incubation
Turf Algae	5.00 – 6.49*
Coral Rubble	5.37 – 6.43*
Soft Coral (<i>Xenia</i> sp.)	5.52 – 6.43*
Biogenic Rock	5.51 – 6.44
Reef Sands	5.85 – 6.50*
<i>Pocillopora verrucosa</i>	4.33 – 6.50*
<i>Acropora hemprichii</i>	5.52 – 6.50*
<i>Stylophora pistillata</i>	4.82 – 6.49*

* = indicates that the starting concentration was not exceeded during incubation

Supplementary Material 6.3 | Formulas of Extrapolated Fixed/Removed N per Benthos 3D Area

$$(A) \quad N_F = \sum \text{measured rate}_i * 2D \text{ to } 3D \text{ cf}_i * \text{benthic cover}_i$$

$$(B) \quad N_R = \sum \text{measured rate}_i * 2D \text{ to } 3D \text{ cf}_i * \text{benthic cover}_i$$

With: N _F	fixed nitrogen via dinitrogen fixation
N _R	removed nitrogen via denitrification
Measured rate _i	quantified N ₂ fixation/denitrification rate of respective benthic category according to table S6.2
2D to 3D cf _i	2D to 3D conversion factor of respective benthic category according to table S3
Benthic cover _i	benthic cover of respective benthic category according to table S6.1

Supplementary Material to Chapter 7:

Table S 7.1 | Nutrients released by the Osmocote® fertilizer bags around manipulated reef communities measured at different distances. Fertilizer: directly at the pin, Center: 25 cm towards the communities. *Indicates measurements from the reef water column.

Location	Time reference	Water-Temperature [°C]	Distance from fertilizer [cm]	NO ₂ [μM]	PO ₄ [μM]	NO ₃ [μM]	NH ₄ [μM]	DIN [μM N]	DIN/PO ₄
Background*	Start	24.90	---	0.04	0.06	0.34	0.13	0.51	8.37
Center	2 weeks		25	0.02	0.06	0.91	0.20	1.14	22.37
Fertilizer	2 weeks		0	0.03	0.44	5.68	1.34	7.06	17.00
Background	2 weeks	26.27	200	0.01	0.09	0.27	0.05	0.33	3.53
Center	4 weeks		25	0.06	0.12	1.07	0.24	1.37	11.68
Fertilizer	4 weeks		0	0.06	0.57	5.52	1.66	7.24	13.99
Background	4 weeks	26.48	200	0.07	0.15	0.33	0.09	0.49	3.36
Center	6.5 weeks		25	0.03	0.20	1.16	0.21	1.41	9.22
Fertilizer	6.5 weeks		0	0.05	0.30	5.04	1.49	6.59	40.79
Background	6.5 weeks	27.34	200	0.03	0.06	0.09	0.09	0.20	3.21
Background*	8 weeks	28.04	---	0.05	0.07	0.36	0.16	0.56	13.47

Table S 7.2 | Osmocote® fertilizer elemental and stable isotope composition. SD indicates the standard deviation (number of replicates: 4).

	δ ¹⁵ N	% N	δ ¹³ C	% C _{org}	C _{org} /N
Mean	16.326	7.722	-27.027	6.166	0.800
SD	0.513	0.416	0.859	0.328	0.046

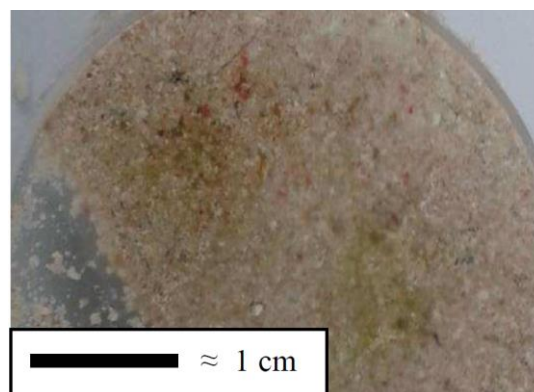


Figure S 7.1 | Sediment sample with epilithic algae after 8 weeks of in-situ eutrophication.

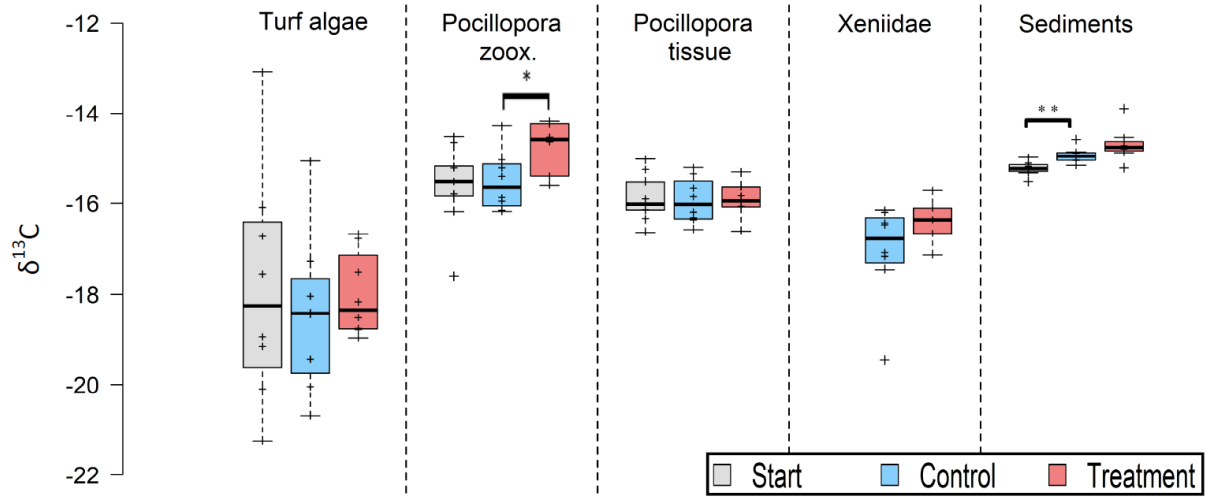


Figure S 7.2 | $\delta^{13}\text{C}$ in turf algae, *Pocillopora* cf. *verrucosa* zooxanthellae (“zoox.”) and tissue, *Xeniidae* and sediments before (grey), without (blue) and after 8 weeks in-situ eutrophication (red). Asterisks indicate significant differences (* $p < 0.05$, ** $p < 0.005$, *** $p < 0.001$).

Supplementary Material to Chapter 8:

Table S8.6 | Osmocote® Fertiliser composition

Coated Micronutrient	Amount
Ammoniacal Nitrogen*	8 %
Nitrate*	7 %
Phosphate (P ₂ O ₅)*	9 %
Soluble Potash (K ₂ O)*	12 %
Magnesium*	1.3 %
Sulfur*	5.9 %
Boron	0.02 %
Copper	0.05 %
Iron*	0.46 %
Manganese*	0.06 %
Molybdenum*	0.02 %
Zinc	0.05 %

* = micronutrients have been coated to provide 14.77 % coated slow-release nitrogen, 8.86 % coated slow-release available phosphate (P₂O₅), 11.81 % coated slow-release soluble potash (K₂O), 1.27 % coated slow-release magnesium, 5.85 % coated slow-release sulphur, 0.45 % coated slow-release iron, 0.059 % coated slow-release manganese, and 0.019 % coated slow-release molybdenum.

Table S8.2 | Differences (given as p-values) in gross primary production (P_{gross}), N₂ fixation and denitrification between functional groups of control and eutrophied communities, obtained via two-way permutational multivariate analysis of variance (PERMANOVA) with the factors “functional group” and “community” (i.e., control and eutrophied communities).

	P _{gross}	N ₂ fixation	Denitrification
Reef Sediment	0.002	0.001	0.081
Turf Algae	0.163	0.095	0.003
<i>P. verrucosa</i>	0.636	0.338	0.140

Table S8.3 | Results (p-values) of permutational multivariate analysis of variance (PERMANOVA) pair-wise tests for N₂ fixation and denitrification in all functional groups of control (Ctrl., blue) and eutrophied (Eutr, green) communities. Significant p-values in bold.

		Ctrl		Eutr			
		Turf Algae	<i>P. verrucosa</i>	Reef sediment	Turf Algae	<i>P. verrucosa</i>	
Ctrl	Reef Sediment	0.001	0.001	0.001	0.001	0.004	N ₂ -Fixation
	Turf Algae		0.001	0.019	0.095	0.001	
	<i>P. verrucosa</i>			0.001	0.001	0.338	
Eutr	Reef Sediment				0.017	0.001	
	Turf Algae					0.001	
Ctrl	Reef Sediment	0.536	0.170	0.081	0.068	0.923	
	Turf Algae		0.103	0.017	0.003	0.473	
	<i>P. verrucosa</i>			0.006	0.001	0.140	
Eutr	Reef Sediment				0.587	0.122	
	Turf Algae					0.098	

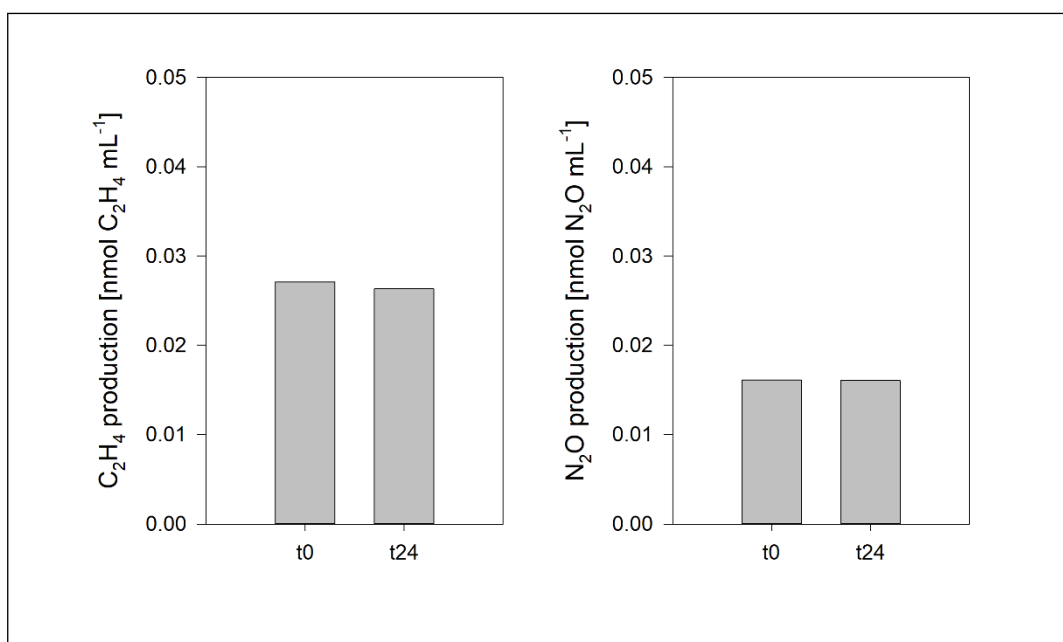


Figure S8.6 | Ethylene (C_2H_4 ; **left**) and nitrous oxide (N_2O ; **right**) production in control incubation chambers ($n = 2$; with $5\ \mu M$ nitrate addition) over the whole incubation time of 24 h with samplings at the beginning (t_0) and the end (t_{24}) of incubations.

Supplementary Material to Chapter 9:

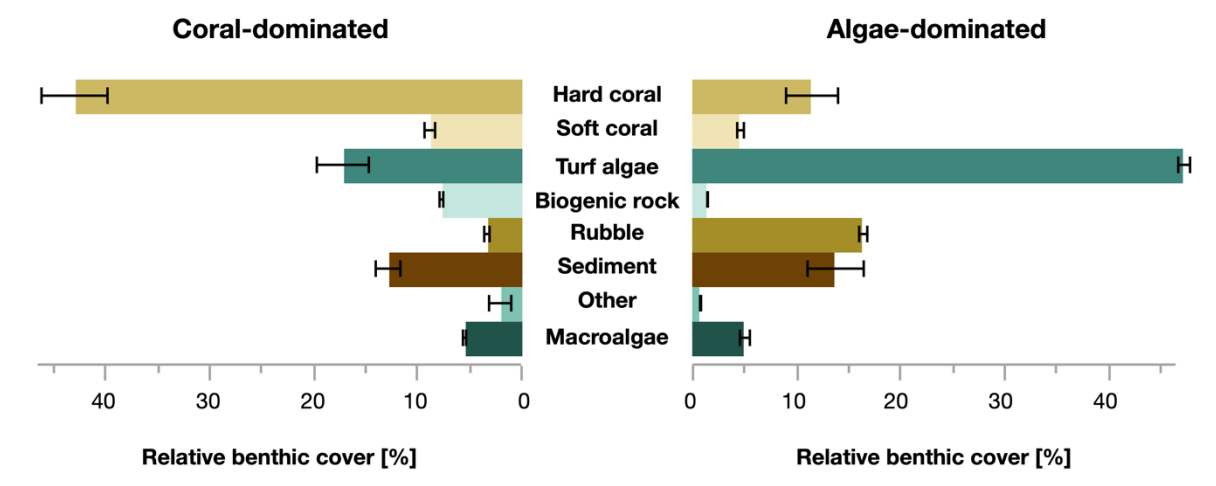


Figure S9.1 | Relative benthic cover of functional groups in the studied coral- and algae-dominated reef communities. The community composition at the level of major functional groups was assessed for each community ($n = 8$) at the onset of the experiments. This timepoint corresponds to the last timepoint of experiments from Roth et al. (2020)³⁶, where two-factor permutational multivariate analysis of variance (PERMANOVA) discriminated the communities according to coral and algal dominance. Details on the assessment and statistical evaluation of the community composition can be found in Appendix S1: Section S1 in Roth et al. (2020)³⁶. There were no visual indications that the community compositions changed in the short time (eight weeks) from before to after the nutrient enrichment.



Figure S9.2 | Exemplary pictures of (A) a coral-dominated community that has been surrounded by four pins with attached fertilizer bags, (B) a coral-dominated, and (C) an algae-dominated community during incubations with benthic chambers. For the incubations at the end of the experiments (i.e., after nutrient enrichment) fertilizer pins were removed from around the communities to deploy the benthic chambers. All photos: Florian Roth. Picture in (A) reproduced from Karcher et al. (2020)³⁷, pictures in (B) and (C) reproduced from Roth et al. (2020)³⁶, all under the CC-BY 4.0 License.

Supplementary Material SM9.1 | Water Sampling and Analysis

For the characterization of environmental background conditions, seawater samples for the determination of dissolved nitrate (NO_3^-), nitrite (NO_2^-), ammonium (NH_4^+), phosphate (PO_4^{3-}), and monomeric silicate ($\text{Si}(\text{OH})_4$) were taken in triplicates each month from 1 m above the seafloor with 60 mL acid-washed syringes. On the boat, samples were filtered immediately through syringe filters (Isopore™ membrane filters, 0.2 μm GTTP) into acid-washed 15 mL centrifuge tubes and stored dark and cool for transportation

to the laboratory (< 2 h). In the laboratory, samples were stored frozen at -50°C pending analysis using a continuous flow analyser (AA3 HR, SEAL, USA) following the designated colorimetric methods [121]. The limits of quantification (LOQ) were $0.084 \mu\text{mol NO}_3^- \text{L}^{-1}$, $0.011 \text{NO}_2^- \mu\text{mol L}^{-1}$, $0.043 \text{PO}_4^{3-} \mu\text{mol L}^{-1}$ and $0.191 \mu\text{mol Si(OH)}_4 \text{L}^{-1}$, respectively. From the syringes, 5 mL subsamples were filtered separately into acid-washed 15 mL centrifuge tubes for ammonium (NH_4^+) measurements underway using the ortho-phthalaldehyde (OPA) method. To the filtered sample, 1.2 mL OPA-solution was added and NH_4^+ was determined fluorometrically within 8 h after sampling (Trilogy® Laboratory Fluorometer with CDOM/ NH_4 module, Turner Designs Inc.) and following >4 h incubation with OPA in the dark (LOQ = $0.094 \mu\text{mol NH}_4^+ \text{L}^{-1}$).

For the calculation of fluxes within the benthic incubations chambers, discrete water samples for dissolved inorganic carbon (DIC), total alkalinity (TA), dissolved organic carbon (DOC), total dissolved nitrogen (TDN), and dissolved inorganic nitrogen (DIN) were withdrawn from the sampling ports with acid-washed syringes at the beginning and the end of each incubation. Subsamples for DIN were processed and measured according to the protocols outlined above and in Roth et al. (2018). Directly after sampling, subsamples for DIC and TA were transferred into 100 mL borosilicate bottles and immediately poisoned with saturated mercury chloride (HgCl_2) to inhibit biological activity. DIC was measured using an inorganic carbon analyser (Apollo SciTech, AS-C3) equipped with a non-dispersive infrared gas analyser (LI-COR, Li-7000 $\text{CO}_2/\text{H}_2\text{O}$). TA was measured by open-cell potentiometric acid-titration (Mettler Toledo, T50). Procedures for DIC and TA measurements were performed according to Dickson et al. (2007). Precision for both instruments was typically within $\pm 4 \mu\text{mol kg}^{-1}$. Subsamples for DOC and TDN were filtered through $0.2 \mu\text{m}$ Millipore® polycarbonate filters into pre-combusted (450°C , 4.5 h) acid-washed amber glass vials (Wheaton) with Teflon-lined lids, and samples were subsequently acidified with H_3PO_4 until reaching a pH 1 – 2. Samples were kept in the dark at 4°C until further analysis by high-temperature catalytic oxidation (HTCO) using a total organic carbon analyser (Shimadzu, TOC-L). To monitor the accuracy of DOC and TDN concentration measurements, we used reference material of deep-sea carbon ($42 - 45 \mu\text{mol C L}^{-1}$ and $31 - 33 \mu\text{mol N L}^{-1}$) and low carbon water ($1 - 143 \mu\text{mol C L}^{-1}$). DON concentrations were calculated after subtracting DIN from TDN ($\text{DON} = \text{TDN} - \text{DIN}$). Before sampling, all collection and sample processing devices for DOC (except the polycarbonate filters) were submerged in a 4% HCl bath to leach out any potential contamination of DOC samples.

Figure S9.3 | Daily gross primary production (GPP), net community production (NCP) and community respiration (CR) in coral- and algae-dominated reef communities, before and after nutrient enrichment. Data are means of replicates ($n = 4$) \pm SE.

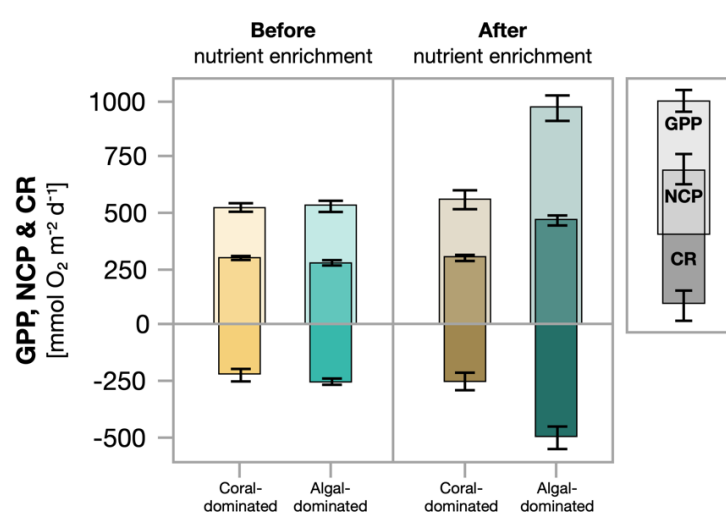


Table S9.1 | Hourly rates of major biogeochemical processes in coral- and algae-dominated reef communities. Fluxes are separated into measurements before and after nutrient enrichment, and into rates assessed during dark and light incubations. Values are presented as means (n = 4) ± standard error. Abbreviations: O₂ = dissolved oxygen; NCC = net community calcification; DOC = dissolved organic carbon; TDN = total dissolved nitrogen; DON = dissolved organic nitrogen; DIN = dissolved inorganic nitrogen; Std Err = standard error around the mean.

		<u>Before nutrient enrichment</u>				<u>After nutrient enrichment</u>			
		Dark incubations		Light incubations		Dark incubations		Light incubations	
		Algae-dominated	Coral-dominated	Algae-dominated	Coral-dominated	Algae-dominated	Coral-dominated	Algae-dominated	Coral-dominated
O₂ flux [mmol m ⁻² h ⁻¹]	Mean	-10.75	-9.30	24.34	26.35	-20.92	-10.69	37.86	24.36
	Std Err	0.58	1.16	1.06	0.80	2.09	1.63	1.81	1.10
NCC [mmol m ⁻² h ⁻¹]	Mean	0.35	3.10	0.48	9.93	-1.85	5.48	1.23	9.18
	Std Err	0.36	0.59	0.37	0.67	0.41	0.91	0.44	0.77
DOC flux [μmol m ⁻² h ⁻¹]	Mean	-285.05	344.22	572.07	412.26	-384.07	204.31	871.13	366.45
	Std Err	122.24	281.71	61.32	100.43	35.03	36.24	25.13	112.23
TDN flux [μmol m ⁻² h ⁻¹]	Mean	91.05	66.9	-18.47	18.73	228.28	167.55	201.85	207.38
	Std Err	48.67	41.43	48.31	37.51	20.73	29.95	29.41	25.02
DON flux [μmol m ⁻² h ⁻¹]	Mean	-40.78	12.30	-79.2	-77.88	138.6	69.65	156.68	136
	Std Err	13.14	57.23	43.68	58.34	53.79	38.65	10.73	32.28
DIN flux [μmol m ⁻² h ⁻¹]	Mean	131.83	54.6	60.78	96.63	89.73	97.83	45.13	71.35
	Std Err	44.16	20.10	33.04	21.78	42.63	28.54	26.22	18.04

Table S9.2 | Results of permutational multivariate analysis of variance (PERMANOVA) and subsequent pair-wise tests for all response parameters of coral- and algae-dominated reef communities, before and after nutrient enrichment. Top values: t-values; bottom values: p-values. Significant p-values ($p \leq 0.05$) in bold. Abbreviations: Coral = coral-dominated community; Algae = algae-dominated community; before = before nutrient enrichment; after = after nutrient enrichment; NCP = net community production; CR = community respiration; GPP = gross primary production; NCC = net community calcification; DOC = dissolved organic carbon; TDN = total dissolved nitrogen; DON = dissolved organic nitrogen; DIN = dissolved inorganic nitrogen; C:N = elemental carbon to nitrogen ratio of dissolved organic matter released by the communities.

	NCP	CR	GPP	NCC	DOC	TDN	DON	DIN	C:N	GPP:CR
Coral before vs algae before	1.5477 0.174	1.1328 0.282	0.3727 0.729	3.4999 0.005	0.73653 0.514	0.17983 0.933	0.43548 0.714	0.40067 0.723	1.077 0.315	1.4445 0.197
Coral before vs coral after	0.25179 0.828	0.61731 0.549	0.72675 0.49	1.1955 0.288	0.65264 0.563	2.0807 0.044	1.5011 0.191	0.81843 0.434	2.2669 0.066	0.50687 0.642
Coral before vs algae after	7.729 0.001	4.7804 0.005	9.126 0.002	5.1108 0.002	0.58748 0.596	2.3214 0.05	1.7339 0.149	0.79007 0.469	3.0674 0.029	1.7738 0.108
Algae before vs coral after	1.5282 0.161	0.26304 0.832	0.45277 0.672	3.6803 0.004	2.0809 0.101	2.8731 0.031	4.112 0.005	0.35607 0.785	2.1691 0.064	0.92615 0.388
Algae before vs algae after	8.0716 0.002	5.7803 0.002	8.1787 0.001	1.4693 0.081	1.5415 0.181	3.224 0.032	4.8189 0.006	0.83104 0.44	4.3528 0.011	1.0083 0.374
Coral after vs algae after	6.5333 0.002	3.6942 0.007	5.7029 0.002	5.2314 0.001	1.1007 0.306	1.2872 0.24	1.3383 0.264	1.154 0.289	1.0102 0.355	1.3481 0.22

Supplementary Material to Chapter 10:



Figure S10.3 | Representative turf algal fragment of approx. 10 cm length that was used in the present study. Picture was taken by Denis B. Karcher.

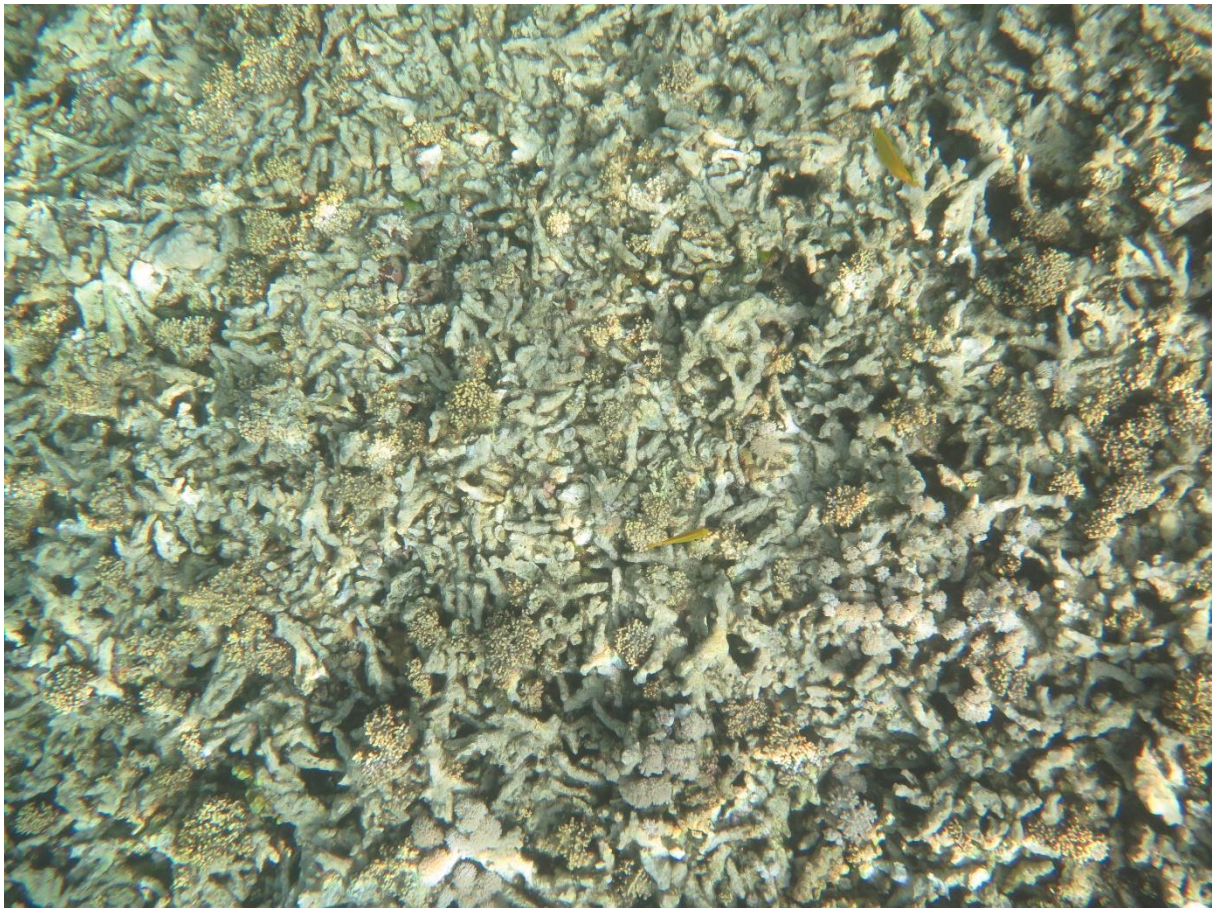


Figure S10.4 | Coral rubble-dominated area within the Abo Shosha reef in the central Red Sea. Picture was taken by Florian Roth.

References

1. Carpenter, E. J., Scranton, M. I., Novelli, P. C. & Michaels, A. Validity of N₂ fixation rate measurements in marine Oscillatoria (Trichodesmium). *J. Plankton Res.* **9**, 1047–1056 (1987).
2. Flett, R. J., Hamilton, R. D. & Campbell, N. E. R. Aquatic acetylene-reduction techniques: solutions to several problems. *Can. J. Microbiol.* **22**, 43–51 (1976).
3. Haines, J. R., Atlas, R. M., Griffiths, R. P. & Morita, R. Y. Denitrification and Nitrogen Fixation in Alaskan Continental Shelf Sediments. *Appl. Environ. Microbiol.* **41**, 412–421 (1981).
4. Wilson, S. T., Böttjer, D., Church, M. J. & Karl, D. M. Comparative assessment of nitrogen fixation methodologies, conducted in the oligotrophic north pacific ocean. *Appl. Environ. Microbiol.* **78**, 6516–6523 (2012).
5. Job, G. & Rüffler, R. Molecular-Kinetic View of Dilute Gases. in *Physical Chemistry from a Different Angle* 271–294 (Springer, Cham, 2016). doi:10.1007/978-3-319-15666-8
6. Breitbarth, E., Mills, M. M., Friedrichs, G. & Laroche, J. The Bunsen gas solubility coefficient of ethylene as a function of temperature and salinity and its importance for nitrogen fixation assays. *Limnol. Oceanogr. Methods* **2**, 282–288 (2004).
7. Lavy, A. *et al.* A quick, easy and non-intrusive method for underwater volume and surface area evaluation of benthic organisms by 3D computer modelling. *Methods Ecol. Evol.* **6**, 521–531 (2015).
8. Gutierrez-Heredia, L., Benzoni, F., Murphy, E. & Reynaud, E. G. End to End Digitisation and Analysis of Three-Dimensional Coral Models, from Communities to Corallites. *PLoS One* **11**, e0149641 (2016).
9. Mulholland, M. R., Bronk, D. A. & Capone, D. G. Dinitrogen fixation and release of ammonium and dissolved organic nitrogen by Trichodesmium IMS101. *Aquat. Microb. Ecol.* **37**, 85–94 (2004).
10. Charpy-Roubaud, C., Charpy, L. & Larkum, A. Atmospheric dinitrogen fixation by benthic communities of Tikehau lagoon (Tuamotu Archipelago, French Polynesia) and its contribution to benthic primary production. *Mar. Biol.* **139**, 991–997 (2001).
11. Weiss, R. F. & Price, B. A. Nitrous Oxide Solubility in Water and Seawater. *Mar. Chem.* **8**, 347–359 (1980).
12. Cardini, U. *et al.* Budget of Primary Production and Dinitrogen Fixation in a Highly Seasonal Red Sea Coral Reef. *Ecosystems* **19**, 771–785 (2016).
13. Pogoreutz, C. *et al.* Nitrogen fixation aligns with nifH abundance and expression in two coral trophic functional groups. *Front. Microbiol.* **8**, 1–7 (2017).
14. Gregory, L. G., Karakas-Sen, A., Richardson, D. J. & Spiro, S. Detection of genes for membrane-bound nitrate reductase in nitrate-respiring bacteria and in community DNA. *FEMS Microbiol. Lett.* **183**, 275–279 (2000).
15. Bru, D., Sarr, A. & Philippot, L. Relative abundances of proteobacterial membrane-bound and periplasmic nitrate reductases in selected environments. *Appl. Environ. Microbiol.* **73**, 5971–5974 (2007).
16. Braker, G., Fesefeldt, A. & Witzel, K. P. Development of PCR primer systems for amplification of nitrite reductase genes (nirK and nirS) to detect denitrifying bacteria in environmental samples. *Appl. Environ. Microbiol.* **64**, 3769–3775 (1998).
17. Zhang, X., He, L., Zhang, F., Sun, W. & Li, Z. The Different Potential of Sponge Bacterial Symbionts in N₂ Release Indicated by the Phylogenetic Diversity and Abundance Analyses of Denitrification Genes, nirK and nosZ. *PLoS One* **8**, 18–20 (2013).
18. Michotey, V., Méjean, V. & Bonin, P. Comparison of methods for quantification of cytochrome cd1-denitrifying bacteria in environmental marine samples. *Appl. Environ. Microbiol.* **66**, 1564–1571

- (2000).
19. Braker, G. & Tiedje, J. M. Nitric oxide reductase (*norB*) genes from pure cultures and environmental samples. *Appl. Environ. Microbiol.* **69**, 3476–3483 (2003).
 20. Kloos, K., Mergel, A., Rösch, C. & Bothe, H. Denitrification within the genus *Azospirillum* and other associative bacteria. *Aust. J. Plant Physiol.* **28**, 991–998 (2001).
 21. Throbäck, I. N., Enwall, K., Jarvis, Å. & Hallin, S. Reassessing PCR primers targeting *nirS*, *nirK* and *nosZ* genes for community surveys of denitrifying bacteria with DGGE. *FEMS Microbiol. Ecol.* **49**, 401–417 (2004).
 22. Yuen, Y. S., Yamazaki, S. S., Nakamura, T., Tokuda, G. & Yamasaki, H. Effects of live rock on the reef-building coral *Acropora digitifera* cultured with high levels of nitrogenous compounds. *Aquac. Eng.* **41**, 35–43 (2009).
 23. Nakano, M., Shimizu, Y., Okumura, H., Sugahara, I. & Maeda, H. Construction of a consortium comprising ammonia-oxidizing bacteria and denitrifying bacteria isolated from marine sediment. *Biocontrol Sci.* **13**, 73–89 (2008).
 24. Dini-Andreote, F., Brossi, M. J. de L., van Elsas, J. D. & Salles, J. F. Reconstructing the genetic potential of the microbially-mediated nitrogen cycle in a salt marsh ecosystem. *Front. Microbiol.* **7**, 1–13 (2016).
 25. Jung, J. *et al.* Change in gene abundance in the nitrogen biogeochemical cycle with temperature and nitrogen addition in Antarctic soils. *Res. Microbiol.* **162**, 1018–1026 (2011).
 26. Jung, J., Yeom, J., Han, J., Kim, J. & Park, W. Seasonal changes in nitrogen-cycle gene abundances and in bacterial communities in acidic forest soils. *J. Microbiol.* **50**, 365–373 (2012).
 27. Chen, S. *et al.* Organic carbon availability limiting microbial denitrification in the deep vadose zone. *Environ. Microbiol.* **20**, 980–992 (2018).
 28. Roth, F. *et al.* Coral reef degradation affects the potential for reef recovery after disturbance. *Mar. Environ. Res.* **142**, 48–58 (2018).
 29. Bahartan, K. *et al.* Macroalgae in the coral reefs of Eilat (Gulf of Aqaba, Red Sea) as a possible indicator of reef degradation. *Mar. Pollut. Bull.* **60**, 759–764 (2010).
 30. Rasser, M. W. & Riegl, B. Holocene coral reef rubble and its binding agents. *Coral Reefs* **21**, 57–72 (2002).
 31. Haines, J. R., Atlas, R. M., Griffiths, R. P., Morita, R. Y. & Sea, B. Denitrification and Nitrogen Fixation in Alaskan Continental Shelf Sediments. **41**, 412–421 (1981).
 32. Joye, S. B. & Paerl, H. W. Contemporaneous nitrogen fixation and denitrification in intertidal microbial mats: rapid response to runoff events. *Mar. Ecol. Prog. Ser.* **94**, 267–274 (1993).
 33. Miyajima, T., Suzumura, M., Umezawa, Y. & Koike, I. Microbiological nitrogen transformation in carbonate sediments of a coral-reef lagoon and associated seagrass beds. *Mar. Ecol. Prog. Ser.* **217**, 273–286 (2001).
 34. Grasshoff, K., Kremling, K. & Ehrhardt, M. *Methods of seawater analysis*. (Wiley-VCH, 1999).
 35. Hughes, D. J. *et al.* Coral reef survival under accelerating ocean deoxygenation. *Nat. Clim. Chang.* **10**, 296–307 (2020).
 36. Roth, F. *et al.* High summer temperatures amplify functional differences between coral- and algae-dominated reef communities. *Ecology* (2020). doi:10.1002/ecy.3226
 37. Karcher, D. B. *et al.* Nitrogen eutrophication particularly promotes turf algae in coral reefs of the central Red Sea. *PeerJ* **8**, e8737 (2020).

Versicherung an Eides Statt

Ich, Yusuf Christian El-Khaled, wohnhaft in der Hemmstraße 278, 28215 Bremen mit der Personalnummer 2869918, versichere an Eides Statt durch meine Unterschrift, dass ich die vorstehende Arbeit selbstständig und ohne fremde Hilfe angefertigt und alle Stellen, die ich wörtlich dem Sinne nach aus Veröffentlichungen entnommen habe, als solche kenntlich gemacht habe, mich auch keiner anderen als der angegebenen Literatur oder sonstiger Hilfsmittel bedient habe.

Ich versichere an Eides Statt, dass ich die vorgenannten Angaben nach bestem Wissen und Gewissen gemacht habe und dass die Angaben der Wahrheit entsprechen und ich nichts verschwiegen habe.

Die Strafbarkeit einer falschen eidesstattlichen Versicherung ist mir bekannt, namentlich die Strafandrohung gemäß § 156 StGB bis zu drei Jahren Freiheitsstrafe oder Geldstrafe bei vorsätzlicher Begehung der Tat bzw. gemäß § 161 Abs. 1 StGB bis zu einem Jahr Freiheitsstrafe oder Geldstrafe bei fahrlässiger Begehung.

Ort, Datum

Unterschrift

